

**Production of  
chiral amino alcohols and diamines  
in a biocatalytic (cascade) process**

Inaugural-Dissertation

zur Erlangung des Doktorgrades  
der Mathematisch-Naturwissenschaftlichen Fakultät  
der Heinrich-Heine-Universität Düsseldorf

vorgelegt von

**Selina Seide**

Aus Dinslaken

Jülich, Juli 2022

aus dem Institut für Bio- und Geowissenschaften 1:  
Biotechnologie des Forschungszentrum Jülich GmbH  
Der Heinrich-Heine-Universität Düsseldorf

Gedruckt mit der Genehmigung der  
Mathematisch-Naturwissenschaftlichen Fakultät der  
Heinrich-Heine-Universität Düsseldorf

Berichtersteller:

1. Prof. Dr. Martina Pohl
2. Prof. Dr. Jörg Pietruszka

Tag der mündlichen Prüfung:  
17.10.2022

## Publications

### Poster presentations

1. **Seide S., Torkler M., Zaparucha A., Rosenthal K., Lütz S., Pohl M.:** Production of valuable hydroxylated-L-lysine by novel  $\alpha$ -keto acid-dependent oxygenases. *Biotrans 2019*. Groningen, 07.-11.07.2019
2. **Seide S., Pohl M.:** HaloTag® immobilization of novel  $\alpha$ -keto acid-dependent dioxygenases increases initial rate activity and process stability. *Himmelfahrtstagung on Bioprocess Engineering 2021 - New Bioprocesses, New Bioproducts*. Online, 10.05.2021
3. **Seide S., Pohl M.:** Immobilization of novel  $\alpha$ -ketoacid-dependent dioxygenases enables catalyst recycling, and increases initial rate activity and process stability. *BioTrans 2021*. Online, 19.-22.07.2021
4. **Seide S., Pohl M.:** Immobilization of novel  $\alpha$ -ketoacid-dependent dioxygenases increases activity, enables catalyst recycling and application in preparative lab scale. *MECP2020+1*. Online, 13.-16.09.2021

### Publication in scientific journals

1. **Seide, S.; Arnold, L.; Wetzels, S.; Bregu, M.; Gätgens, J.; Pohl, M.** From Enzyme to Preparative Cascade Reactions with Immobilized Enzymes: Tuning Fe(II)/ $\alpha$ -Ketoglutarate-Dependent Lysine Hydroxylases for Application in Biotransformations. *Catalysts* **2022**, *12*, 354. <https://doi.org/10.3390/catal12040354>

*The only true wisdom is in knowing you know nothing*

- Socrates

# Table of contents

<b>Abstract</b> .....	<b>i</b>
<b>Kurzfassung</b> .....	<b>ii</b>
<b>Abbreviations</b> .....	<b>iii</b>
<b>1 Introduction</b> .....	<b>1</b>
1.1 <i>Bioeconomy and green chemistry</i> .....	1
1.2 <i>Biocatalysis – A general overview</i> .....	2
1.3 <i>C-H bond functionalization</i> .....	6
1.4 <i>Fe(II)/<math>\alpha</math>-ketoglutarate-dependent dioxygenase as a tool for C-H functionalization</i> .....	7
1.4.1 General overview .....	7
1.4.2 Structure of Fe(II)/ $\alpha$ -ketoglutarate-dependent oxygenases .....	8
1.4.3 Reaction mechanism .....	9
1.4.4 Application of KDOs in biotransformations .....	11
1.5 <i>Lysine decarboxylases as a tool to access bio-based polymers</i> .....	15
1.5.1 Biopolymers .....	15
1.5.2 Lysine decarboxylase from <i>Selenomonas ruminantium</i> .....	18
1.5.3 Structure of the lysine decarboxylase from <i>Selenomonas ruminantium</i> (SrLDC) .....	18
1.5.4 Reaction mechanism of PLP-dependent decarboxylases .....	19
1.6 <i>Biocatalytic process development/ process intensification</i> .....	20
1.6.1 Biocatalyst production .....	21
1.6.2 Biocatalyst formulation .....	23
1.6.3 Biotransformation .....	27
1.6.4 Product purification .....	29
1.6.5 Economic and ecologic benchmarks .....	29
1.7 <i>Aim of the thesis</i> .....	31
<b>2 Results</b> .....	<b>33</b>
2.1 <i>Publication: From Enzyme to Preparative Cascade Reactions with Immobilized Enzymes: Tuning Fe(II)/<math>\alpha</math>-Ketoglutarate-Dependent Lysine Hydroxylases for Application in Biotransformations</i> .....	33
2.2 <i>Supplementary Information</i> .....	59
<b>3 Discussion</b> .....	<b>121</b>
3.1 <i>Biocatalyst Production</i> .....	122
3.1.1 Soluble KDO production .....	122
3.1.2 Optimization of KDO purification .....	124
3.2 <i>KDO reaction system</i> .....	126
3.2.1 Evaluation of KDO activity assays .....	130
3.3 <i>Biocatalyst formulation - KDO immobilization studies</i> .....	132
3.3.1 EziG™ vs HaloTag® - Binding capacities and specific activities .....	132
3.3.2 Stability and activity of CaKDO under reaction conditions upon HaloTag® immobilization .....	133
3.3.3 Comparison of the stabilities of CaKDO, CpKDO, and FjKDO based on their structure .....	135
3.4 <i>Application of immobilized KDOs in biotransformations</i> .....	139

## Table of contents

3.4.1	Recyclability of immobilized KDOs .....	139
3.4.2	Application of immobilized KDOs in preparative lab scale.....	141
3.5	<i>Cascade Reaction towards (2S)-hydroxy-cadaverine</i> .....	143
3.6	<i>SrLDC as an alternative enzyme for the production of biopolymer precursors</i> .....	145
3.6.1	Process evaluation .....	145
3.6.2	Potential of <i>SrLDC</i> as a suitable enzyme for the production of polyamide precursors .....	149
3.7	<i>Downstream processing of hydroxy-L-lysine and hydroxy-cadaverine</i> .....	150
3.7.1	Purification of hydroxy-L-lysines and hydroxy-cadaverines from the reaction mixture .....	150
3.7.2	Alternative purification strategies for hydroxy-L-lysines .....	152
3.7.3	Alternative purification strategies for hydroxy-cadaverine.....	153
3.8	<i>Economic and ecologic process evaluation</i> .....	154
<b>4</b>	<b>Conclusion, summary, and outlook</b> .....	<b>160</b>
<b>5</b>	<b>References</b> .....	<b>163</b>
<b>6</b>	<b>Danksagung</b> .....	<b>174</b>
	<b>Eidesstattliche Erklärung</b> .....	<b>176</b>

## Abstract

Chemically, C-H functionalization is difficult because carbon-hydrogen bonds are relatively inert. Consequently, limitations in chemo-, regio- and stereo control occur, as conventional organic synthesis requires extensive protection group chemistry. Fe(II)/ $\alpha$ -ketoglutarate-dependent dioxygenases (KDOs) provide an excellent synthesis alternative, as they catalyze selective C-H oxidation reactions. However, recombinantly produced KDOs are predominantly formed as catalytically inactive inclusion bodies or precipitate upon purification. Further, they are unstable under oxidative conditions. As a result, their use is limited in preparative biotransformations.

Three different KDOs were evaluated in this study for their potential application in a preparative lab scale. They catalyze the stereoselective hydroxylation of the L-lysine side chain in 3-position (*Ca*KDO from *Catenulispora acidiphila*) and 4-position (*Cp*KDO from *Chitinophaga pinensis* or *Fj*KDO from *Flavobacterium johnsoniae*). This thesis aims to optimize process bottlenecks by increasing the soluble production of the enzymes and implementing an in-situ immobilization for improved enzyme stability and recyclability.

Covalent immobilization of the KDOs via the HaloTag® resulted in a strong increase in stability for *Ca*KDO. Upon immobilization of all three KDOs, the increase in stability enabled substrate conversion of > 200 mM L-lysine. Further, enzyme recycling was possible in an analytical scale for *Fj*KDO and *Cp*KDO for four batches with conversions of 100% and 84%, respectively, thereby effectively increasing the space-time yields. Further, immobilized *Ca*KDO-HaloTag® and *Fj*KDO-HaloTag® were applied in a preparative lab-scale (15 mL) with 16 g L<sup>-1</sup> product titers and specific space-time-yields of 73.4 g<sub>product</sub> L<sup>-1</sup> h<sup>-1</sup> per g<sub>immobilized CaKDO</sub> and 133.65 g<sub>product</sub> L<sup>-1</sup> h<sup>-1</sup> per g<sub>immobilized FjKDO</sub>, respectively. Using a HaloTag®-immobilized lysine decarboxylase from *Selenomonas ruminantium* (*Sr*LDC), the (3*S*)-hydroxy-L-lysine from the *Ca*KDO-catalyzed reaction was successfully decarboxylated to (2*S*)-hydroxy-cadaverine without intermediate product purification, yielding a product titer of 11.6 g L<sup>-1</sup> in a 15 mL consecutive batch reaction. The absence of metabolic background of whole cells or cell-free extracts enabled a successful product purification.

### Kurzfassung

Chemisch ist eine C-H-Funktionalisierung schwierig, da Kohlenstoff-Wasserstoffbindungen relativ träge sind. Dazu kommt es zu Einschränkungen bei der Chemo-, Regio- und Stereoselektivität mit Methoden der herkömmlichen organischen Synthese, die zumeist nur durch umfangreiche Schutzgruppenchemie realisiert werden kann. Fe(II)/ $\alpha$ -Ketoglutarat-abhängige Dioxygenasen (KDOs) bieten eine hervorragende Synthesealternative, da sie ein breites Spektrum selektiver C-H-Oxidationsreaktionen katalysieren. KDOs werden allerdings zum großen Teil als inaktive Einschlusskörper produziert, fallen bei der Reinigung aus und sind unter oxidativen Bedingungen instabil, sodass ihre Verwendung in präparativen Biotransformationen begrenzt ist.

In dieser Dissertation wurden drei verschiedene KDOs auf ihre mögliche Anwendung im präparativen Labormaßstab untersucht. Sie katalysieren die stereoselektive Hydroxylierung der L-Lysin Seitenketten in 3-Position (*CaKDO* aus *Catenulispora acidiphila*) und 4-Position (*CpKDO* aus *Chitinophaga pinensis* oder *FjKDO* aus *Flavobacterium johnsoniae*). Ziel dieser Arbeit war die Optimierung von Prozessengpässen durch die Steigerung der löslichen Enzym Produktion sowie die Immobilisierung der Enzyme direkt aus dem Rohzellextrakt zur Erhöhung der Enzymstabilität und zur Wiederverwendung.

Die kovalente HaloTag® -Immobilisierung der KDOs führte zu einer signifikanten Erhöhung der Stabilität der *CaKDO*. Nach der Immobilisierung aller drei KDOs ermöglichte die erhöhte Stabilität einen Substratumsatz von  $> 200$  mM L-Lysin. Darüber hinaus war das Enzymrecycling im analytischen Maßstab für *FjKDO* und *CpKDO* für 4 Reaktionszyklen mit Umsätzen von 100 % bzw. 84 % möglich, wodurch die Raumzeitausbeuten effektiv erhöht wurden. Dabei konnte die immobilisierte *CaKDO*-HaloTag® und *FjKDO*-HaloTag® im präparativen Labormaßstab (15 mL) mit 100 mM L-lysine mit 16 g L<sup>-1</sup> Produkttitel und Raumzeitausbeuten von 73,4 g<sub>Produkt</sub> L<sup>-1</sup> h<sup>-1</sup> pro g<sub>immobilisierter *CaKDO*</sub> bzw. 133,65 g<sub>Produkt</sub> L<sup>-1</sup> h<sup>-1</sup> pro g<sub>immobilisierter *FjKDO*</sub> eingesetzt werden. Unter Verwendung einer HaloTag®-immobilisierten Lysindecaboxylase aus *Selenomonas ruminantium* (*SrLDC*) wurde das (3*S*)-Hydroxy-L-Lysin aus der *CaKDO*-katalysierten Reaktion erfolgreich in (2*S*)-Hydroxy-Cadaverin decarboxyliert, ohne, dass das Zwischenprodukt aufgereinigt werden musste, wobei ein Produkttitel von 11,6 g L<sup>-1</sup> in einer 15-mL-Batch-Reaktion erreicht wurde.

Eine erfolgreiche Produkt Aufreinigung war möglich, da die Anwendung isolierter Enzyme, im Gegensatz zu ganzen Zellen oder Rohzellextrakten, sehr saubere Produktüberstände ermöglicht.

## Abbreviations

### Abbreviations

<b>BSA</b>	bovine serum albumin
<i>C. glutamicum</i>	<i>Corynebacterium glutamicum</i>
<b>CaKDO (KDO 1)</b>	KDO from <i>Catenulispora acidiphila</i>
<b>CatIBs</b>	catalytically active inclusion bodies
<b>CLEA</b>	cross-linked enzyme aggregates
<b>CpKDO (KDO 2)</b>	KDO from <i>Chitinophaga pinensis</i>
<b>Da</b>	Dalton
<b>DAD</b>	diode array detector
<b>DC</b>	decarboxylase
<i>E. coli</i>	<i>Escherichia coli</i>
<b>EcLDC</b>	lysine decarboxylase from <i>E. coli</i>
<b>FjKDO (KDO3)</b>	KDO from <i>Flavobacterium johnsoniae</i>
<b>FLD</b>	fluorescence detector
<b>FsKDO (KDO5)</b>	KDO from <i>Flavobacterium species</i>
<b>HEPES</b>	2-hydroxyethylpiperazine-N-a-ethanesulfonic acid
<b>HPLC</b>	high-pressure liquid chromatography
<b>IMAC</b>	immobilized metal ion affinity chromatography
<b>IPTG</b>	isopropyl- $\beta$ -D-thiogalactopyranoside
<b>KDO</b>	$\alpha$ -ketoglutarate-dependent dioxygenase
<b>LB</b>	<i>lysogenic broth</i>
<b>LDC</b>	lysine decarboxylase
<b>NTA</b>	nitrilotriacetic acid
<b>OPA</b>	O-phthaldialdehyde
<b>PAGE</b>	polyacrylamide gel electrophoresis
<b>PDB</b>	protein data bank
<b>PLP</b>	pyridoxal-5-phosphate
<b>rpm</b>	revolutions per minute
<b>SDS</b>	sodiumdodecylsulfate
<b>SrLDC</b>	LDC from <i>Selenomonas ruminantium</i>
<b>sSTY</b>	specific space-time-yield
<b>STY</b>	space-time-yield
<b>TB</b>	<i>terrific broth</i>
<b>TRIS</b>	Tris(hydroxymethyl)aminomethane

# 1 Introduction

## 1.1 Bioeconomy and Green Chemistry

Fossil resources, like coal, natural gas, and especially petroleum, are vital to many processes including the generation of energy or the production of technical products. As a source of raw materials and chemicals, fossil fuels are essential to our industrial processes. Petroleum is one of the key players in our industrial market economy: it is used in gasoline, diesel, or kerosene in the transportation sector, in the chemical sector for the production of bulk and fine chemicals, or as a precursor for active pharmaceutical ingredients. The use of petroleum, however, is highly problematic given that it contributes substantially to climate change due to the release of greenhouse gases during its extraction, refining, and burning. In addition, it has the potential to cause political conflicts, not to mention its inherent limitation and the inevitable need to substitute it.

To slow down the rapid consumption of non-renewable resources, the only alternative is the increased use of biomass [1]. Therefore, there is an urgent need to develop strategies that enable the use of natural resources in environmentally friendly, but at the same time economic industrial processes. These ideas are summarized under the concept of bioeconomy. Bioeconomy is a politically motivated concept with the objective of a transformation from a petroleum-based market economy to a market economy based on sustainable and renewable resources. More precisely, it is defined as: “the knowledge-based production and utilization of renewable resources, to provide products, processes, and services in all economic sectors within the context of a future-capable economic system” [2]. Petrochemistry is based on the principle of producing easy-to-handle and defined, chemically pure basic materials from crude oil in refineries. In efficient product lines, a system has been established in which basic chemicals, intermediate products, and refined products are manufactured. Many of these petroleum-based products can be replaced by value-added chemicals produced from biomass resources [1,3]. Such bio-based products thus represent a crucial new market opportunity. However, the challenge is to transfer the efficient product lines from oil refineries to biorefineries [1].

Major feedstocks for biorefineries include starch crops, sugar crops, perennial grasses and legumes, lignocellulosic crops, lignocellulosic residues, oil crops, aquatic biomass, and organic residues. A biorefinery typically processes feedstocks into several key intermediate products. Many processes have been developed to replace petroleum-based products and process routes

## Introduction

during the last decade. Consequently, a platform of bio-based chemicals was constructed including L-lysine, succinic acid, ethanol, glycerol, and many more. Platform chemicals are petroleum-based or bio-based intermediates, which act as building blocks to generate several industrial relevant products, like (bio-)polymers or active pharmaceutical ingredients [4,5].

Strongly connected to the concept of bioeconomy is also the concept of Green Chemistry. Green Chemistry finds application in the design of processes to reduce or eliminate the use and generation of hazardous substances while maximizing efficiency and sustainability. The ultimate goal is to reduce waste to conserve natural resources, limit environmental pollution, improve public health, and ensure work safety. The concept of Green Chemistry was originally published by Paul Anastas in 1998 [6,7] and is summarized by 12 principles. In 2005 a modification of these principles was published by Tang et al [8] and in 2008 the concept was extended by the 12 principles of green engineering (Figure 1) [9]. Together these principles serve to facilitate the design of more sustainable and less hazardous processes.

<b>Principles of Green Chemistry</b>	<b>Principles of Green Engineering</b>
<b>P</b> revent wastes	<b>I</b> nherently non-hazardous and safe
<b>R</b> enewable material	<b>M</b> inimize material diversity
<b>O</b> mit derivatization steps	<b>P</b> revention instead of treatment
<b>D</b> egradable chemical products	<b>R</b> enewable material and energy inputs
<b>U</b> se safe synthetic methods	<b>O</b> utput-led design
<b>C</b> atalytic reagents	<b>V</b> ery simple
<b>T</b> emperature, pressure ambient	<b>E</b> fficient use of mass, energy, space & time
<b>I</b> n-process monitoring	<b>M</b> eet the need
<b>V</b> ery few auxiliary substances	<b>E</b> asy to separate by design
<b>E</b> -factor, maximize feed in product	<b>N</b> etworks for exchange of local mass & energy
<b>L</b> ow toxicity of chemical products	<b>T</b> est the life cycle of the design
<b>Y</b> es, it's safe!	<b>S</b> ustainability throughout product life cycle

Figure 1: Overview of the principles of green chemistry and green engineering adapted from Tang et al. 2008 [9].

### 1.2 Biocatalysis – A general overview

One way to realize concepts of Green Chemistry and bioeconomy is by using biocatalysis. Generally, biocatalysis is defined as the conversion of organic compounds by organisms, cell extracts, or isolated enzymes. For many years humankind has used biocatalysis for the production of wine, beer, cheese, and bread, without knowing the underlying molecular

## Introduction

mechanisms [10,11]. Within the last decades, the development in genetic engineering, industrial microbiology, and process engineering lead to the development of improved and industrially relevant biotechnological processes. In the industrial biotechnology sector, enzymes are used to generate technical valuable products or precursors, like fine chemicals, pharmaceuticals, or biopolymers in a biocatalysis process [12,13]. One possibility of using enzymes in industrial multistep processes is fermentation, where living cells are used to generate relevant products using their own metabolism for the production of e.g. amino acids, vitamins, or antibiotics [14]. Carbon sources, like sugars or starch, are used for cell growth [15].

Another way to apply enzyme-based catalysis is called biotransformation. Here, isolated free enzymes, immobilized enzymes, or metabolically inactive resting whole cells are employed. During biotransformation reactions, the catalyzed reaction is mostly unlinked to the cell's metabolism and substrates are only used for the production of the desired product [14,15]. Using only one enzyme makes the reaction usually more specific and can avoid the formation of side products. The use of enzymes for biocatalysis often has several advantages compared to conventional chemical synthesis:

### ***Environmental impact***

Enzymes are renewable and biodegradable; they naturally occur in living organisms and catalyze a broad reaction range. Therefore, many enzymes optimally operate at mild pH, moderate temperature, and atmospheric pressure. Concerning energy use, reactions based on enzymatic catalysis therefore mostly work under environmentally friendly conditions [16–18]. In addition, by inherently being non-toxic, degradable catalysts from renewable feedstock, enzymes directly address the demands of Green Chemistry (Chapter 1.1). Compared to many toxic and hazardous chemical processes, this might be true. However, it must be kept in mind that biocatalytic processes are not per se environmentally friendly or green and an individual assessment of the environmental impact is necessary for every process. Biocatalytic processes require a high amount of water for the production of the enzyme and as a solvent for the process. In many studies, water as a solvent is considered inheritable green since it is non-hazardous and does not present problems of flammability or explosion risks as associated with organic solvents. Therefore, water is often not included in the environmental impact [19]. Nevertheless, water is contaminated during the process and most likely needs to be treated, which consequently leads to higher energy consumption. Since the product is often diluted in the aqueous solvent, the E-factor, a measure to describe the amount of waste generated in a process

## Introduction

[19–21] (Chapter 1.6.5), is negatively affected when water is considered as waste. Further, downstream processing of the product can be hard with water as a solvent. However, the environmental impact of biocatalysis, also including waste water, is often still better than conventional process routes, as synthesis routes can be shortened, the higher selectivity increases the atom economy and less toxic waste is formed relative to many conventional chemical processes [21–23]. Besides, concepts have been developed that enable the application of biocatalysts also in micro-aqueous reaction systems [24].

### *Selectivity*

Chemical reactions often yield a mixture of different stereoisomers. In contrast, enzymatic reactions often score with their high stereo-, regio- and chemoselectivity [18,25]. High stereoselectivity is often required for the production of bioactive compounds, like active pharmaceutical ingredients, since different stereoisomers can have significantly different effects [26]. There are various methods for the stereoselective chemical synthesis of molecules, including using chiral pools, racemic resolution, and asymmetric synthesis. Each of these methods has its drawbacks [25,27]. Often the stereoselective synthesis requires the extensive use of protection group chemistry, which negatively affects the step economy and atom economy of the process (Chapter 1.6.5) [28,29]. By contrast, regio- and stereoselectivity is often much easier to achieve by biocatalysis, due to the steric requirements in the enzyme's active site, which makes protection group chemistry redundant. As a result, biocatalytic processes often require fewer process steps and achieve a better atom economy. Additionally, many enzymes have a broad substrate range, which enables the use of a single enzyme for the synthesis of a broad product scope [25,30].

### *Cascade reactions*

The production of complex organic compounds usually requires the combination of several reaction steps toward the final product. In organic chemistry these steps are traditionally performed by consecutive batch reactions, often including the purification of intermediates, which is time-consuming and can result in additional waste [31]. Enzymatic cascade reactions describe reactions where at least two enzymes are used in two different reaction steps without intermediate product isolation [32]. The implementation of cascade reactions in industry can have several benefits: The number of intermediate steps can be reduced and a decrease of waste due to the elimination of downstream processing can be reached, resulting in a better step- and

## Introduction

atom economy and higher space-time-yields (Chapter 1.6.5), which is economically and environmentally favorable [33]. Furthermore, the reaction equilibrium can be actively shifted to the site of the desired product. Figure 2 shows the different modes of cascade reactions: simultaneous, sequential, or multi-step reactions [33]. The easiest way is a simultaneous cascade in a one-pot system, including all enzymes and reaction components in one reaction vessel at the same time [34]. To avoid cross-reactivity or the generation of undesired side products, enzymes can be applied in a sequential mode, by spatial or temporal separation [35]. When one or more isolation steps are needed, for instance, to get rid of one of the enzymes from the previous steps, the reaction is referred to as a multi-step reaction [33]. Yet, different enzymes often have different reaction rates, pH- and temperature optima. Therefore, optimization of these cascade reactions via reaction engineering is a crucial step. Complex reactions and a high number of reaction steps can also lead to mixed cascade modes [33].

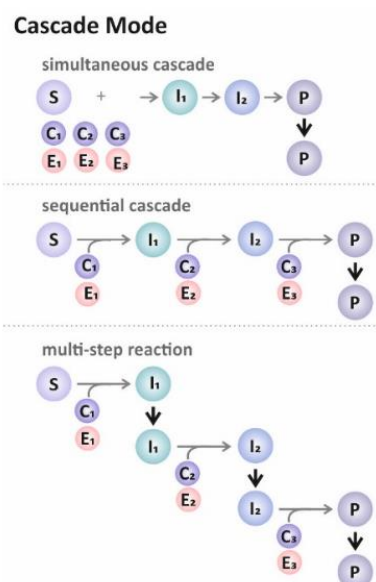


Figure 2: Definition of cascade modes. Simultaneous cascade: all reaction components are added at the same time. Sequential cascade: reaction components are added in a sequential mode. Multi-step reactions: if isolations are needed in between the reaction steps. S: substrate, I: intermediate, P: product, C: cosubstrate, E: enzyme. Figure adapted from Siedentop et al. [33].

However, the use of enzymes in industrial processes also faces some challenges: Enzymes are often unstable beyond their optimal pH, temperature range, or the cellular environment [36]. Furthermore, the production and application of isolated enzymes require several process steps, which often include time-consuming and cost-intensive purification steps and immobilization techniques. The use of chromatographic purification methods increases the process costs extensively and further immobilization e.g. by adsorption results in a fourfold increase in production costs [37]. For this reason, immobilized enzymes are often too expensive for application in industry and are mostly used when they can contribute to a process by

significantly improving it or enhancing its productivity, specifically for the production of valuable fine chemicals [37]. Therefore, different strategies exist for the enzyme and process design of enzymatic reactions, which can help to effectively optimize or plan the process at an early stage of development (Chapter 1.6). [19,38–40]

### 1.3 C-H bond functionalization

Hydrocarbons derived from fossil and renewable resources serve as precursors for a wide range of fine chemicals. However, C-H bonds are relatively inert; consequently, their activation remains challenging. Especially stereo- and regioselective C-H bond functionalization is highly desirable, but chemically hard to achieve, especially when “more activated” C-H bonds than the position of interest are present [41]. Furthermore, chemical C-H bond functionalization often suffers from low yields. However, there are numerous oxidoreductases effectively catalyzing different kinds of oxidation reactions, which can be divided into two mechanistic families: dehydrogenation and oxyfunctionalization. Dehydrogenases work by abstracting an H atom via an acceptor molecule (nicotinamide or flavin cofactor) and do not require an active oxygen intermediate [41,42]. Dehydrogenases generally catalyze reversible reactions and can therefore be used for oxidation as well as reductive reactions [43]. Here, key enzymes are alcohol dehydrogenases, flavin-dependent oxidases, copper-dependent oxidases, and laccases. The second group involves enzymes catalyzing oxyfunctionalization that activate molecular oxygen or peroxide for subsequent electrophilic substitution into the substrates. Since this allows the insertion of oxygen into C-H, C-C, and C=C bonds, and thereby the generation of new functional groups, oxyfunctionalization enzymes are becoming increasingly interesting. Enzymes catalyzing these reactions are flavin-dependent monooxygenases, heme-dependent monooxygenase, non-heme iron-dependent mono- and dioxygenases, as well as peroxygenases [41]. Three enzyme classes are especially interesting for the oxidation of C-H to C-OH bonds or the hydroxylation of C(sp<sup>3</sup>)-H bonds. Most commonly used are P450 monooxygenases, which use oxygen species, bound to an iron atom, which is coordinated within a heme prosthetic group. Since one oxygen atom is incorporated into the substrate and the other is reduced to water, two electrons are required to reduce the iron cofactor during the catalytic cycle. Therefore, P450 monooxygenases use nicotinamide/flavin cofactors or specific reductases as electron donors [44]. Protein engineering and directed evolution yielded a lot of P450 variants for new-to-nature C-H transformations [45]. Still, the preparative use of P450 monooxygenases

is limited, due to low specific activities, inefficient electron transfer, uncoupling effects, and low stability [42]. Another enzyme class catalyzing C-H hydroxylation are peroxygenases, which use H<sub>2</sub>O<sub>2</sub> instead of O<sub>2</sub> in a so-called peroxide shunt pathway with a broad range of substrates [46]. Peroxygenases are structurally related to P450 monooxygenases and contain a heme group in the active site [41,47]. They show high turnover numbers and previous studies have shown their application in non-aqueous and even neat organic reaction systems [41,47]. However, this enzyme class oxidizes its substrates unspecifically and H<sub>2</sub>O<sub>2</sub> is a strong inactivator of heme-dependent enzymes. Therefore, in situ H<sub>2</sub>O<sub>2</sub> regeneration systems are needed to enable peroxygenase reactions but simultaneously minimize oxidative inactivation [41,42]. Another interesting enzyme class for the oxidation of C-H bonds are Fe(II)/ $\alpha$ -ketoacid-dependent (di-) oxygenases, which will be described in detail in the following chapters (Chapter 1.4). While biocatalytic C-H oxyfunctionalizations are interesting reactions, many publications report processes only in an analytical scale, which leaves questions about enzyme expression levels, stability, overall process robustness, and feasibility of scale-up [48].

### **1.4 Fe(II)/ $\alpha$ -ketoglutarate-dependent dioxygenase as a tool for C-H functionalization**

#### **1.4.1 General overview**

Among the superfamily of Fe(II)/ $\alpha$ -ketoglutarate-dependent oxygenase,  $\alpha$ -ketoglutarate dependent dioxygenases (KDOs, EC 1.14.11.) catalyze the regio- and stereoselective hydroxylation of C(sp<sup>3</sup>)-H bonds [49]. Besides, this enzyme class catalyzes halogenation, ring closure, desaturation, epimerization, ring expansion, and epoxidations, making them an interesting target for biotransformations [42,50–53] (Figure 3). The first members of this family that were identified were prolyl and lysyl hydroxylases (C5 hydroxylation), which are involved in collagen biosynthesis [49]. Since then, these enzymes have been identified in several plants, microorganisms, and humans. KDOs have versatile functions and were found to be involved in nucleic acid repair mechanisms [54], transcriptional regulations, and hypoxic response to oxygen [55–58], which makes them especially interesting as a target for inhibition or activation in anti-ischemic therapies or antitumor therapies [54,59]. In plants and microorganisms, KDOs have been found in pathways leading to medically important antibiotics [49,60–62].

Enzymatic C-H hydroxylation has mainly focused on P450 monooxygenases, while KDOs have remained largely unexplored [63]. KDOs are self-sufficient and do not need specific reductases

## Introduction

or expensive biological nicotinamide or flavin cofactors, they utilize iron as a cofactor to activate  $O_2$ . The electrons required for oxyfunctionalization come from the cheap cosubstrate  $\alpha$ -ketoglutarate [42]. In hydroxylation reactions, one respective oxygen molecule is transferred to the cosubstrate  $\alpha$ -ketoglutarate and the main substrate; thereby they catalyze the oxidative decarboxylation of  $\alpha$ -ketoglutarate toward succinate and  $CO_2$ . However, in reactions like epoxidation, ring closure, ring expansion, epimerization, and halogenation, the second oxygen atom is reduced to water (Figure 3). To keep the iron (II) in its reduced state, ascorbic acid is added to the reaction. However, some KDOs are barely active without ascorbic acid. In these cases it is believed that iron reduction might not be the only role of ascorbic acid and investigation of its overall function is the subject of ongoing research [64].

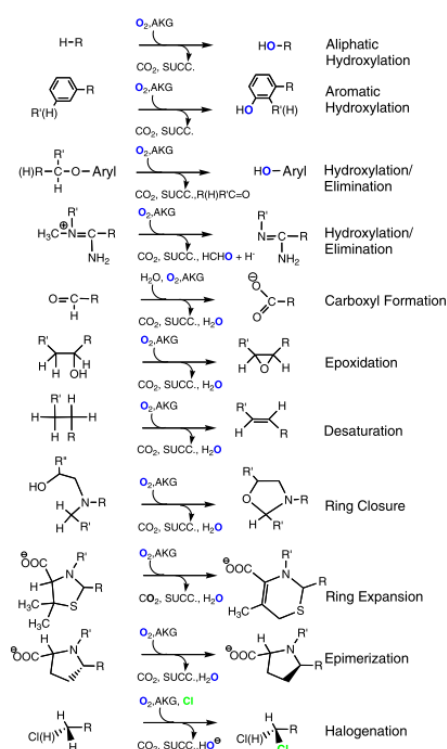


Figure 3: Diversity of reactions catalyzed by Fe(II)/ $\alpha$ -ketoglutarate-dependent oxygenases. AKG=  $\alpha$ -ketoglutarate, SUCC= succinate. Taken from Purpero and Moran, 2007 [65]. Reprinted with permission from Springer Nature.

### 1.4.2 Structure of Fe(II)/ $\alpha$ -ketoglutarate-dependent oxygenases

The substrate specificities of the members of this enzyme family are as diverse as their amino acid sequences [49]. Crystallographic studies have revealed two structural features, which are shared among this enzyme family. The Fe(II) is bound by a highly, but not universally,

## Introduction

conserved HXD/E...H triad, including two His residues and one Asp or Glu residue, resulting in a 2-His-1-carboxylate motif. Reasons for the occasional presence of glutamate instead of aspartate are yet unclear [64]. The 2-His-1-carboxylate motif is located within a double-stranded helix fold (DSBH), also called jellyroll, cupin, or jumonji C fold. It is composed of eight antiparallel strands forming a structure of two (minor and major) four-stranded antiparallel sheets (Figure 4) that form a squashed barrel. The more open-end contains the Fe(II) and  $\alpha$ -ketoglutarate binding elements. The DSBH is stabilized by internal hydrophobic interactions and by conserved  $\alpha$ -helices [49].  $\alpha$ -Helices at the N-terminus are assumed to play a role in fold stabilization and sometimes dimerization, while  $\alpha$ -helices at the C-terminus are involved in substrate recognition and dimerization. Loops with extensive secondary structure are often subfamily characteristics and play key structural and catalytic roles. For some enzymes of this family, it was not possible to obtain crystals for the holo enzyme under aerobic conditions, which lead to the development of anaerobic crystallization methods [49].

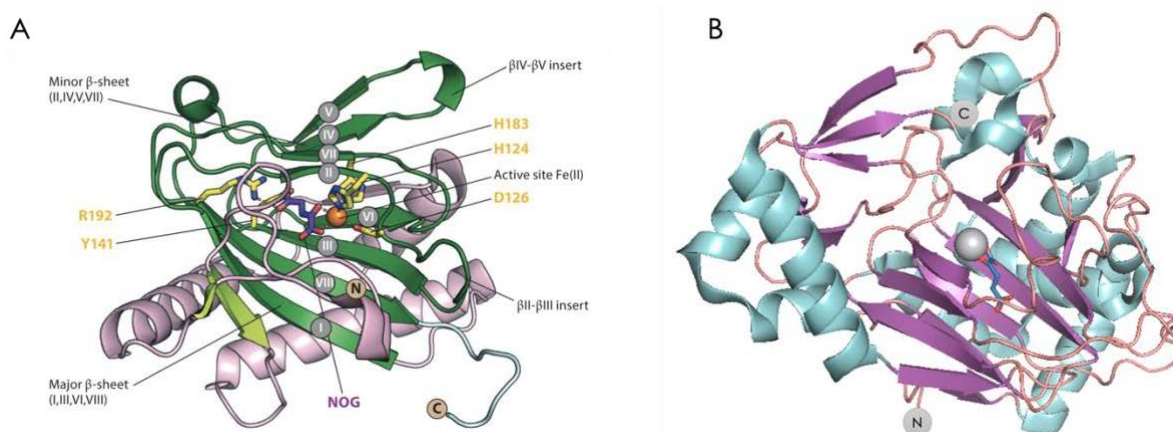


Figure 4: Structure of single monomers of prolyl hydroxylase from *Pseudomonas putida* and lysyl hydroxylase from *Catenulispora acidiphila* (KDO1, CaKDO) for comparison. A) View of a PPHD structure (PDB ID: 4IW3) showing Fe (orange sphere) and  $\alpha$ -ketoglutarate (purple); core DSBH (green) (I-VIII), N-terminal region, and C-terminal region are indicated and 2OG- (yellow ovals) binding residues. Abbreviations: 2OG, 2-oxoglutarate; 2OGX, 2OG-dependent oxygenase; DSBH, double-stranded  $\beta$ -helix; NOG, N-oxalylglycine; PDB, Protein Data Bank; PPHD, *Pseudomonas prolyl hydroxylase* domain. Taken from Islam *et al.* [64]. B) View of KDO1 (CaKDO) structure (PDB ID: 6F2B) showing Fe (grey sphere) and  $\alpha$ -ketoglutarate (blue); DSBH (magenta), N-terminal region and C-terminal region are indicated. Representation was done in PyMOL based on PDB code 6F2B [66].

### 1.4.3 Reaction mechanism

Kinetic, spectroscopic, and crystallographic analyses show that the Fe(II) cofactor binds to the active site before the substrate or the cosubstrate (1, Figure 5) [49]. When  $\alpha$ -ketoglutarate is absent, the Fe(II) is bound on one face by the three amino acid residues (2-His-1-Asp/Glu) and

## Introduction

three additional coordination sites are occupied by water molecules (1, Figure 5). In some cases, Fe(II) binds closely to the active site but can be removed using metal ion chelators or dialysis [49]. The processes by which Fe(II) is introduced to and maintained at the active site are not well understood [64]. Upon binding of  $\alpha$ -ketoglutarate, two water molecules are displaced, and the formation of a bidentate configuration with the keto group opposite the Asp and the carboxylate group opposite one of the His residues is generated (2, Figure 5). Next, the primary substrate is bound to the active site, but not to the metal ion (3, Figure 5). Binding to the active site triggers the displacement of the third water molecule and the binding of O<sub>2</sub> to the metal ion, producing a Fe(III)-superoxo intermediate (4, Figure 5). Also, the position of the initial binding of O<sub>2</sub> to the metal in *trans* to either the proximal or distal histidine is unclear and might vary [64]. The distal oxygen atom attacks the C2 of the Fe(III)-superoxo intermediate, generating a peroxohemiketal bicyclic intermediate (5, Figure 5). Next, oxidative decarboxylation of  $\alpha$ -ketoglutarate is initiated by the release of CO<sub>2</sub>, yielding a spectroscopically characterized Fe(IV)-oxo species, known as ferryl intermediate, to which succinate is bound (6, Figure 5) [64]. The ferryl species abstracts a hydrogen atom from the primary substrate, generating a substrate radical (7, Figure 5). Product formation and succinate release takes place in one of two ways: Either by a hydroxyl radical rebound (8.1, Figure 5), which yields the hydroxylated product, or by deprotonation of the Fe(III)-OH (7, Figure 5), yielding a Fe(III)-oxo intermediate (8.2, Figure 5), which is followed by the formation of a Fe(II) alkoxo species (9.2, Figure 5) and the dissociation to the products (Figure 5) [51,67,68]. Different steps of the reaction mechanism are not known in detail yet, including the activation of O<sub>2</sub>, how the Fe(IV)-oxo intermediate (5, Figure 5) is generated, and details about how the more exotic KDO reactions, like oxidative rearrangements (Figure 3), occur [64]. For some KDOs the enzyme:Fe(II): $\alpha$ -ketoglutarate complex seems to be stable and in some cases, the holo enzyme can even be purified as such. For some enzymes, the enzyme:Fe(II): $\alpha$ -ketoglutarate complex can undergo substrate uncoupled reactions, meaning the conversion of  $\alpha$ -ketoglutarate to succinate and CO<sub>2</sub> without the main substrate being present [49].

## Introduction

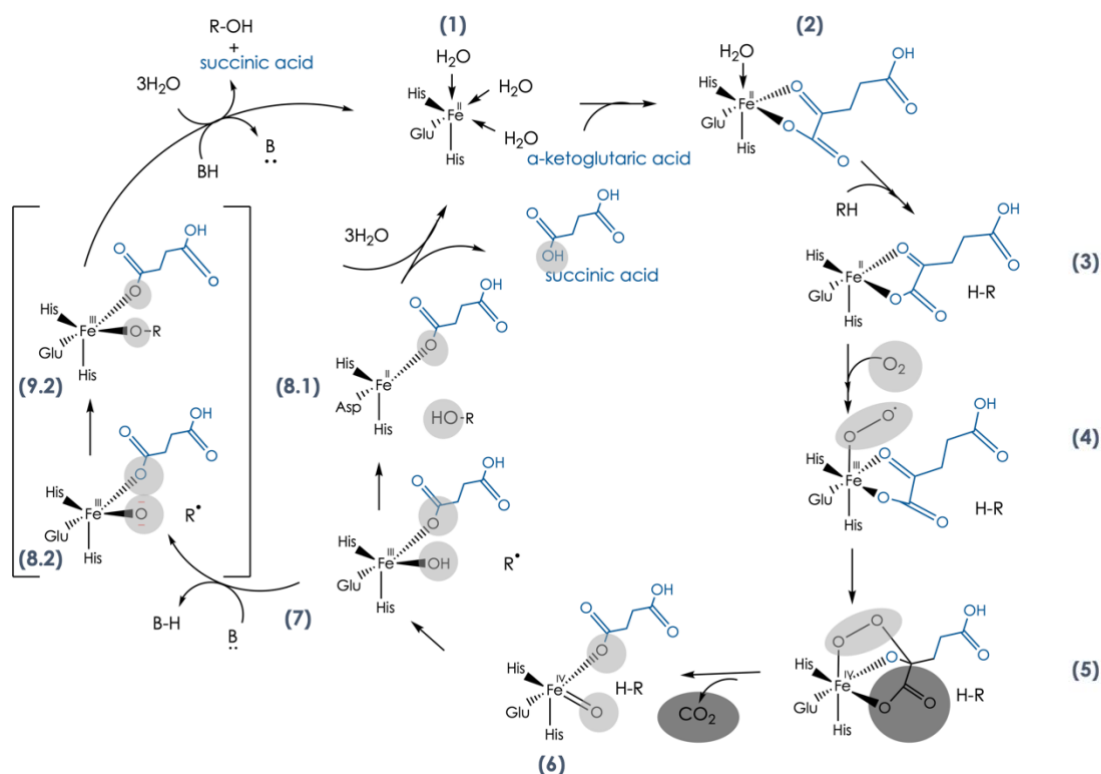


Figure 5: Common reaction mechanism postulated for hydroxylation reactions catalyzed by Fe(II)/ $\alpha$ -ketoglutarate-dependent oxygenases [51,67].

### 1.4.4 Application of KDOs in biotransformations

Next to their application in antibiotic synthesis, the application of KDOs in biocatalytic reactions has mainly focused on the hydroxylation of amino acids (Figure 6) [42]. As hydroxylated amino acids possess two to three stereocenters, they are potential chiral building blocks for asymmetric synthesis, pharmaceutical agents, and natural product synthesis, and respective enzymes are highly interesting [48,66]. While primary  $\beta$ -amino acids can easily be accessed from the corresponding  $\alpha$ -amino acids by conventional chemical synthesis, access to chiral amino alcohols needs tedious synthetic pathways and sensitive control of stereochemistry [48,69,70]. Several patents prove KDOs' potential for the biocatalytic production of functionalized amino acids [71–77].

However, the use of isolated KDOs at a larger scale remains challenging due to issues with the generation of reactive oxygen species leading to enzyme damage [64]. Up to now the number of preparative applications of KDOs in the literature is negligible, which is most likely due to their tendency to be produced in the form of insoluble inclusion bodies [78–81], their fast precipitation upon chromatographic purification [78], and their general instability under

## Introduction

oxidative conditions [81], making sufficient enzyme production and instability the bottlenecks for biotransformations. In most preparative applications KDOs are therefore applied as whole cells or as cell-free extracts [42,80,82,83]. Apart from the enzyme SadA, which was applied immobilized on controlled porosity glass (EziG™) [81], preparative applications of either isolated or immobilized KDOs are hardly known. When isolated enzymes are used, substrate concentrations or the scale of the reaction are usually low [42,63,74,84]. Since many of such applications concern the hydroxylation of amino acids [42], the use of *E. coli* whole cells or cell-free extracts can complicate the overall process by e.g. side reactions due to the cellular background and mass transfer issues. Downstream processing of products can be severely hampered by the large amounts of whole cells or cell-free extract that are necessary to achieve full conversion [81]. Further, whole cells and cell-free extract cannot be recycled, and separation of the biocatalyst is more difficult than for instance, using an immobilized enzyme (Chapter 1.6.2 and 1.6.2.1). Especially, oxygen transfer can be difficult, leading to low conversions. For increasing the oxygen transfer rate, often Triton-X is added to the mixture to permeabilize the cell wall [80,85].

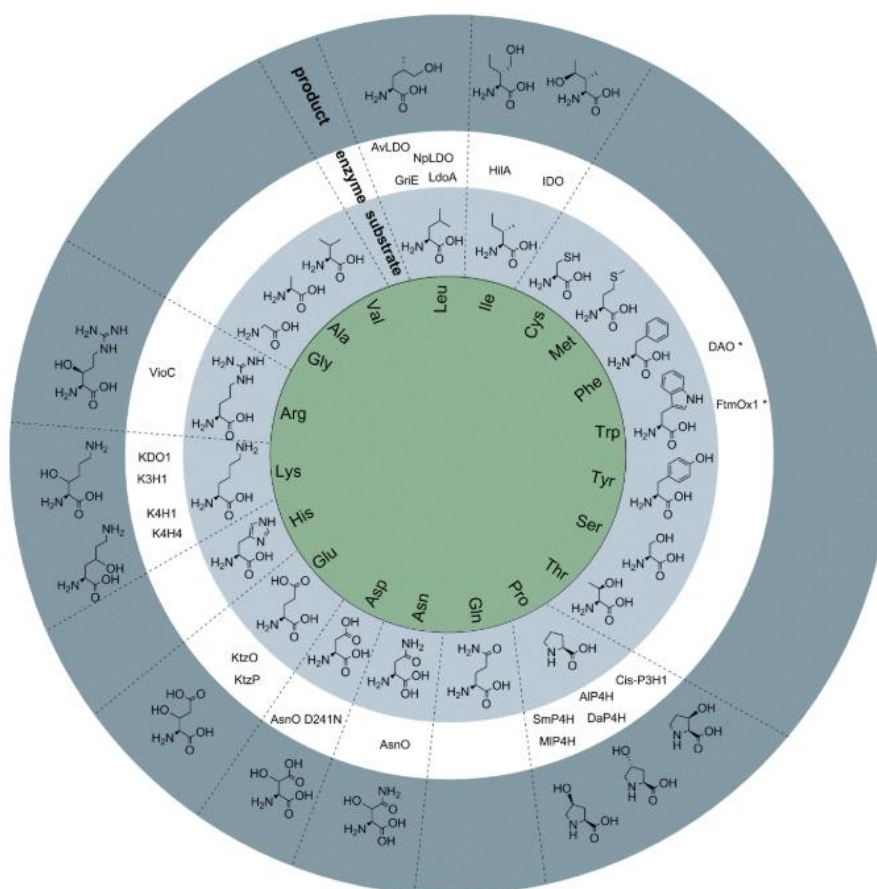


Figure 6: Overview of selected amino acid hydroxylations. The figure is taken from Peters and Buller [42] <https://creativecommons.org/licenses/by/4.0/>.

## Introduction

### 1.4.4.1 Lysine hydroxylases

Chiral hydroxy-L-lysines are used as chiral auxiliaries [42], as precursors for active pharmaceutical ingredients, such as the HIV protease inhibitor palinavir [86,87], for potential novel anticancer drugs such as tambromycin [82], the protein kinase c inhibitor (-) balanol [88], and the proteasome inhibitors cepafungin I or glidobactin A [79,89].

KDOs from *Catenulispora acidiphila* (*CaKDO*, KDO1: 3-hydroxylation), *Chitinophaga pinensis* (*CpKDO*, KDO2: 4-hydroxylation), and *Flavobacterium johnsoniae* (*FjKDO*, KDO3: 4-hydroxylation) have recently been discovered by Baud et al. [69,90] (Figure 8 and Figure 7) and are highly stereoselective [66]. K4H-2 and K4H-1, which correspond to *CpKDO* and *FjKDO*, respectively, were independently discovered by Hara et al. [83]. Crystal structures of *CaKDO* and another KDO from *Flavobacterium species* (*FsKDO*, KDO5) have been determined, demonstrating the typical double-stranded  $\beta$ -helix core structure of the  $\alpha$ -ketoglutarate-dependent oxygenase structural superfamily (Figure 7) [66,91]. For both enzymes, the crystal structures show tetramers formed by two dimers per asymmetric unit, while their quaternary structures in solution are different: dimeric for *CaKDO* and tetrameric for *FsKDO*. The catalytic site of both enzymes is accessible through a flexible loop that controls the opening to the catalytic site and is meant to shield the substrate from bulk solvents. The conserved HXD/E...H triad, shows the typical two His residues and one Glu residue [66].

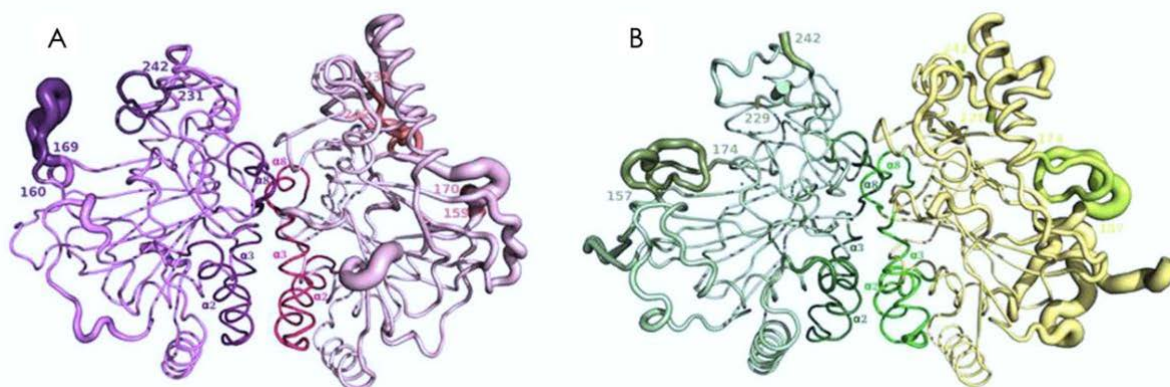


Figure 7: B-factor putty representation of the dimeric interface of *CaKDO* and *FsKDO*. Helix  $\alpha_2$ ,  $\alpha_3$ , and  $\alpha_8$  at the dimeric interface, lid, and adjacent loop are highlighted. The figure was taken from Bastard et al. [66] <https://creativecommons.org/licenses/by/4.0/>.

## Introduction

### 1.4.4.2 Lysine hydroxylases in cascade reactions

Baud et al. used the above described Fe(II)/ $\alpha$ -ketoglutarate-dependent dioxygenases (KDOs) and PLP-dependent decarboxylases from *Selenomonas ruminantium* (SrLDC), *Chitinophaga pinensis* (CpDC) and *Flavobacterium johnsoniae* (FjDC) for cascade reactions toward the synthesis of hydroxylated alpha-omega diamines via the hydroxylated-L-lysines from the KDO reaction. For the first cascade step, KDOs from different organisms were used to catalyze the stereoselective enzymatic hydroxylation for the synthesis of the corresponding hydroxy-L-lysines (Figure 8). The second cascade step is the decarboxylation of the (3*S*)-hydroxy-L-lysine to access the corresponding (2*S*)-hydroxy-cadaverine and (4*R*)-hydroxy-L-lysine to the corresponding 3-hydroxy-cadaverine. Isolated yields of 11-12 mg (93-98%) from the corresponding (2*S*)-hydroxy-cadaverine or 3-hydroxy-cadaverine HCl salt could be obtained by a preparative cascade reaction starting from 10 mM L-lysine on a 10 mL scale with enzymes applied in form of cell-free extract within total reaction times of about 36 h [69]. Since both substrates, L-lysine and  $\alpha$ -ketoglutarate, as well as L-ascorbic acid can be obtained by fermentation, this cascade can, in principle, be based fully on renewable resources.

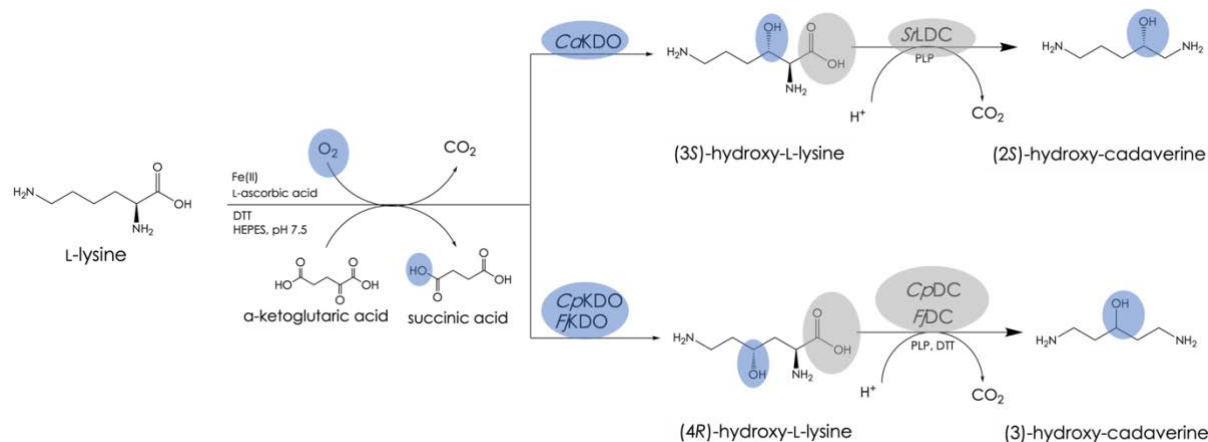


Figure 8: Single-step KDO reactions towards hydroxylated L-lysine derivatives and cascade reaction employing SrLDC, CpDC, and FjDC towards (2*S*)-hydroxy-cadaverine or (3)-hydroxy-cadaverine. Cascade reaction was first published by Baud et al. [69].

## 1.5 Lysine decarboxylases as a tool to access bio-based polymers

### 1.5.1 Biopolymers

The worldwide demand for plastics and chemical fibers is about 500 million tons per year. Most of these products rely on fossil resources like petroleum [92]. However, in the last years, the bio-based production of biopolymers was intensively studied. The global market size for bioplastics is considered to increase from currently \$9.2 billion to \$20 billion by 2026 and the global production capacity of bioplastics is supposed to expand to 2.9 million tons by 2025. In addition, biopolymers are considered to be superior polymers, due to their biocompatibility and biodegradability [93]. Among these, especially bio-based polyamides are interesting. Polyamides usually consist of a diamine monomer and a dicarboxylic acid, as shown in Figure 9. The diamine monomer can be derived from amino acids like L-lysine and L-ornithine and is an excellent basis for the production of biopolymer moieties from renewable materials. However, it should be noted that bio-based polyamides are not per se biodegradable [93].

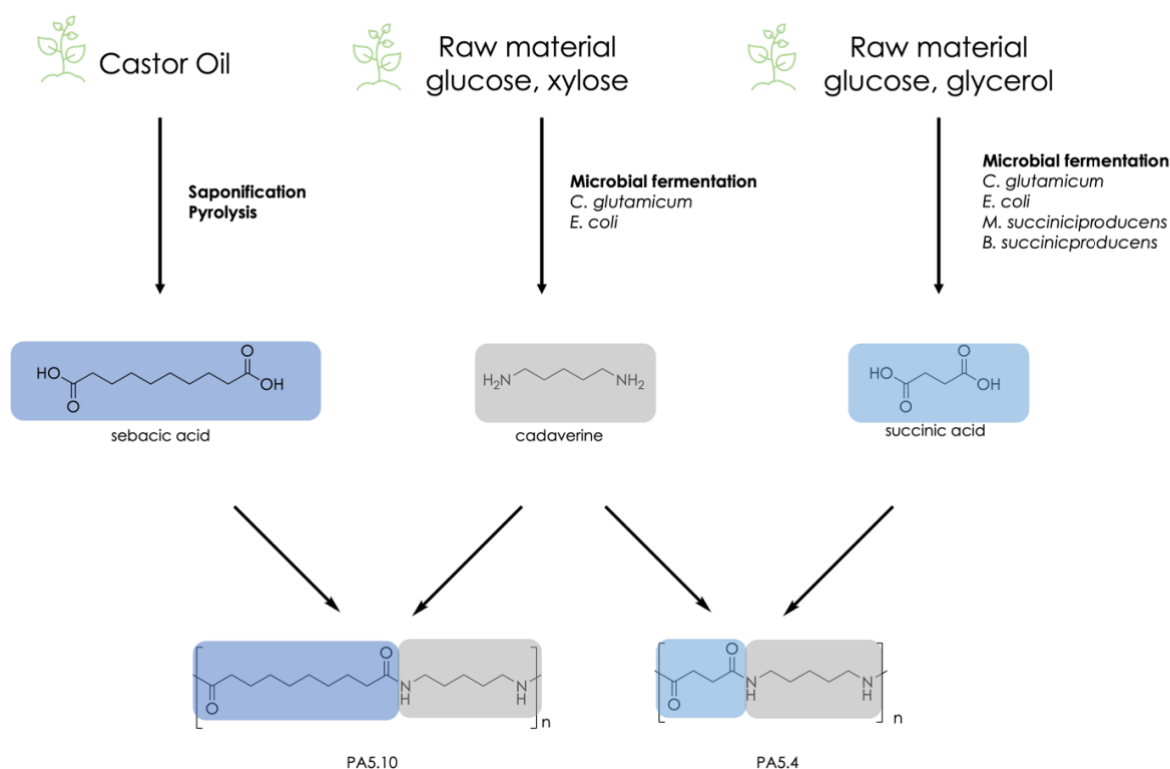


Figure 9: PA 5.10 and PA 5.4 as an example of fully bio-based nylon 5X materials from the diamine monomer cadaverine (1,5-diaminopentane) and dicarboxylic acid monomer (sebacic acid or succinic acid). Figure adapted from Kind et al. [94]

Especially the bio-based production of cadaverine (1,5-diaminopentane) (C5) has gained significant attention. It can replace the petrochemically produced hexamethylenediamine (C6)

## Introduction

as a building block for polyamides, polyurethane, and polyurea but also as a precursor for active pharmaceutical ingredients or applications in the agricultural sector (Figure 10). The resulting bio-polyamide nylon 5X materials have excellent properties, even superior to petroleum-based nylon 6.6. However, up to now, bulk cadaverine is commercially not available and there is no petrochemical route for the production of cadaverine [95]. Chemical cadaverine synthesis does not only have a significant impact on the environment, but it also suffers from serious equipment corrosion, low target product selectivity, poor catalyst stability, and incapability of continuous and stable production [92].

A lot of research has been invested in the biological production of cadaverine, which predominantly focuses on the production via fermentation using *E. coli* or *C. glutamicum* strains, mainly utilizing lysine decarboxylases to catalyze the reaction from L-lysine towards cadaverine. The most commonly used lysine decarboxylases originate from *E. coli*: the constitutive lysine decarboxylase *EcLDCc* and the inducible lysine decarboxylase *EcLDCi* (also called CadA or LdcI) [96,97]. Lysine decarboxylases are industrially used for the production of cadaverine, where most research focuses on the construction of engineered strains with CadA from *E. coli*. The direct microbial fermentation for the production of cadaverine based on sugars like glucose, galactose, starch, and lignocellulose or methanol and mannitol suffers from unsuitable downstream processing on an industrial scale due to the low concentration of cadaverine, its cellular degradation, product inhibition, high metabolic background, and long fermentation processes. Recently different studies using lysine decarboxylases from *E. coli* in whole-cell processes or as immobilized enzymes have been investigated as extensively reviewed by Huang et al. [92]. To further intensify cadaverine production processes, the discovery of novel and efficient lysine decarboxylases is crucial [92].

## Introduction

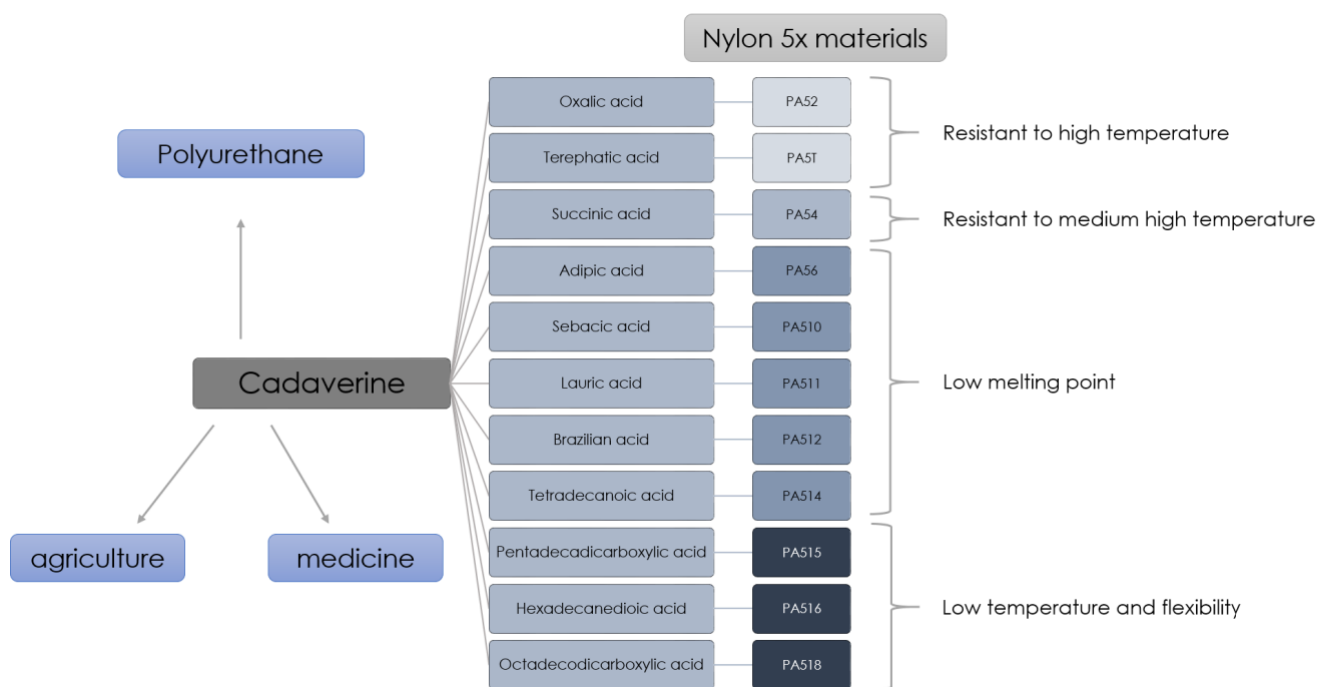


Figure 10: Application of cadaverine as a building block for nylon 5X materials. Figure adapted from Huang et al. [92]

Putrescin (tetramethylenediamin, 1,4-diaminobutan) is another biogenic amine that can be used as a building block for PA 4.6 or PA 4.4. PA 4.6 consists of putrescine and adipic acid, also known as Stanyl (nylon 4.6), produced by DMS N.V. Industrial production of putrescin is done by a petroleum-based chemical process using propylene, ammonia, and hydrocyanic acid [98]. Biotechnologically, putrescin can be produced via two routes, by decarboxylation of L-ornithine or L-arginine. Production of putrescin is mainly based on fermentation by *E. coli* or *C. glutamicum*, overexpressing the respective decarboxylase genes. However, the production via *C. glutamicum* is more productive, due to the higher tolerance toward putrescin [95].

The production of polyamines from amino acids has facilitated the production of novel functionalized compounds. Amino acid derivatives like hydroxy-L-lysines in a decarboxylation reaction could therefore result in respective hydroxylated cadaverine derivatives (Chapter 1.4.4.2). The additional hydroxyl groups can undergo various reactions like esterification, or they can act as initiation sites for ring-opening polymerizations of cyclic esters [99–102]. Thus, hydroxylated diamines could be attractive for polyamines with new properties and could enable access to the production of more complex polymers [101].

Cadaverine, various hydroxylated cadaverine derivatives, and putrescin can all be produced by a lysine decarboxylase from *Selenomonas ruminantium* (SrLDC).

### **1.5.2 Lysine decarboxylase from *Selenomonas ruminantium***

Lysine decarboxylases (LDCs) are Pyridoxal-5-phosphate (PLP)-dependent enzymes, which catalyze the decarboxylation of L-lysine to cadaverine under CO<sub>2</sub> release.

Inducible LDCs often play a role in maintaining pH homeostasis. Many bacteria use LDCs, whose expression is induced by acid stress from the environment and enables the organism to grow under acid stress. If the pH value is too low, the enzyme is induced, which subsequently consumes one proton from the enzymatic reaction at a time, thus increasing the pH inside the cell. Conversely, higher pH values lead to a decrease in enzyme activity. However, enzymes that are involved in biosynthesis pathways are constitutively expressed, regardless of the pH, and encompass L-ornithine, L-arginine, and L-lysine decarboxylases, which are responsible for the synthesis of polyamines such as putrescin, spermidine, and cadaverine [103].

Lysine decarboxylases are Non-homologous Isofunctional Enzymes (NISEs). NISEs are evolutionary unrelated enzymes that have evolved to catalyze the same reaction but with different primary and quaternary structures. There are three known structural families for LDCs: The alanine racemase (AR) superfamily, the 2,4-aminobutyric acid decarboxylase (DABA DC) superfamily, and the aspartate amino-transferase superfamily (AAT-fold). The *E. coli* LDCs belong to the aspartate amino-transferase superfamily. Whereas *Sr*LDC belongs to the alanine racemase family and represents a constitutive homodimeric bifunctional decarboxylase meaning that besides L-lysine also L-ornithine is accepted as a substrate with similar kinetic parameters [96,104–106]. Decarboxylation of L-ornithine is hereby possible due to a water molecule present between the key active site residue and the shorter L-ornithine molecule. As shown by Baud et al. *Sr*LDC is also able to decarboxylate (3*S*)-hydroxy-L-lysine, (4*R*)-hydroxy-L-lysine, and (5*R*)-hydroxy-L-lysine, although with different activities [69]. Furthermore, the predominant function of *Sr*LDC seems to be the biosynthesis of cadaverine for its use in the cell wall's peptidoglycan layer of *Selenomonas ruminantium*, and not necessarily as a pH control system [107,108].

### **1.5.3 Structure of the lysine decarboxylase from *Selenomonas ruminantium* (*Sr*LDC)**

The PLP-dependent L-lysine decarboxylase from *Sr*LDC is a dimer consisting of two monomers with a size of 44 kDa, respectively. Each of these monomers is composed of a barrel domain and a sheet domain (Figure 11). The barrel domain (Leu27-Cys261) consists of eight

## Introduction

$\alpha$ -helices ( $\alpha 2$ - $\alpha 9$ ) and eight parallel  $\beta$ -strands ( $\beta 2$ - $\beta 9$ ). The eight-stranded- $\beta$ -sheet core acts as a cofactor-binding site, which is wrapped by the  $\alpha$ -helices. A seven-stranded antiparallel  $\beta$ -sheet ( $\beta 1$ ,  $\beta 10$ - $\beta 15$ ) surrounded by three short  $\alpha$ -helices forms the sheet domain (Met1 Ser26, Gly262 Val393). The barrel domain of one monomer and the sheet domain of another monomer forms a dimer via a head-to-tail contact (Figure 11). This arrangement forms identical active sites at the dimer interface. PLP binds to a pocket formed in the barrel domain and the catalytic residue Lys51 interacts with the aldehyde group of the pyridoxal ring [103].

SrLDC shows a lower affinity towards PLP ( $K_d = 72 \mu\text{M}$  [109]) than other PLP-dependent enzymes, which might be due to the highly flexible active site. Upon introduction of internal disulfide bonds, Sagong et al. [109] were able to increase the PLP affinity threefold compared to the wildtype enzyme. Also, the introduction of additional disulfide bonds leads to a higher enzymatic activity and resistance to pH and temperature [109].

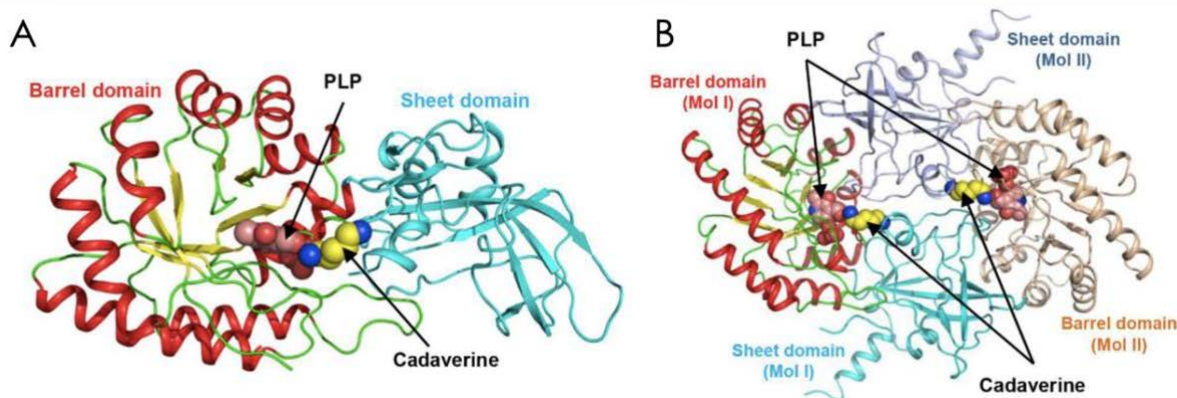


Figure 11: Crystal structure of SrLDC represented as a cartoon diagram. A) Monomer B) Dimer. Taken from Sagong et al. [103] <https://creativecommons.org/licenses/by/4.0/>.

### 1.5.4 Reaction mechanism of PLP-dependent decarboxylases

Pyridoxal-5-phosphate (PLP) is the active form of vitamin B6. It catalyzes reactions like transamination, racemization, and decarboxylation at the  $C\alpha$  of an amino acid substrate [110]. As for LDCs the reaction mechanism is not yet described in the literature but is thought to be similar to other decarboxylases [110]. Therefore, the following mechanism is based on the one described for histidine decarboxylase [111], which is presumed to occur in two steps: the first step being the decarboxylation of the substrate (L-lysine), followed by protonation (Figure 12). PLP-dependent enzymes exist in their resting state as a Schiff base, where the aldehyde group of PLP forms an internal aldimine bond with a lysine residue in the active site of the enzyme (1). L-lysine (substrate) binds to the PLP by forming an external aldimine (2). The

## Introduction

decarboxylation of L-lysine takes place by forming a carbanion intermediate (also called quinoid intermediate), which is resonance stabilized (3). By taking a proton from the medium, the carbanion is protonated (4). Upon release of the final product (cadaverine) the internal aldimine is re-established (1) (Figure 12) [110–113].

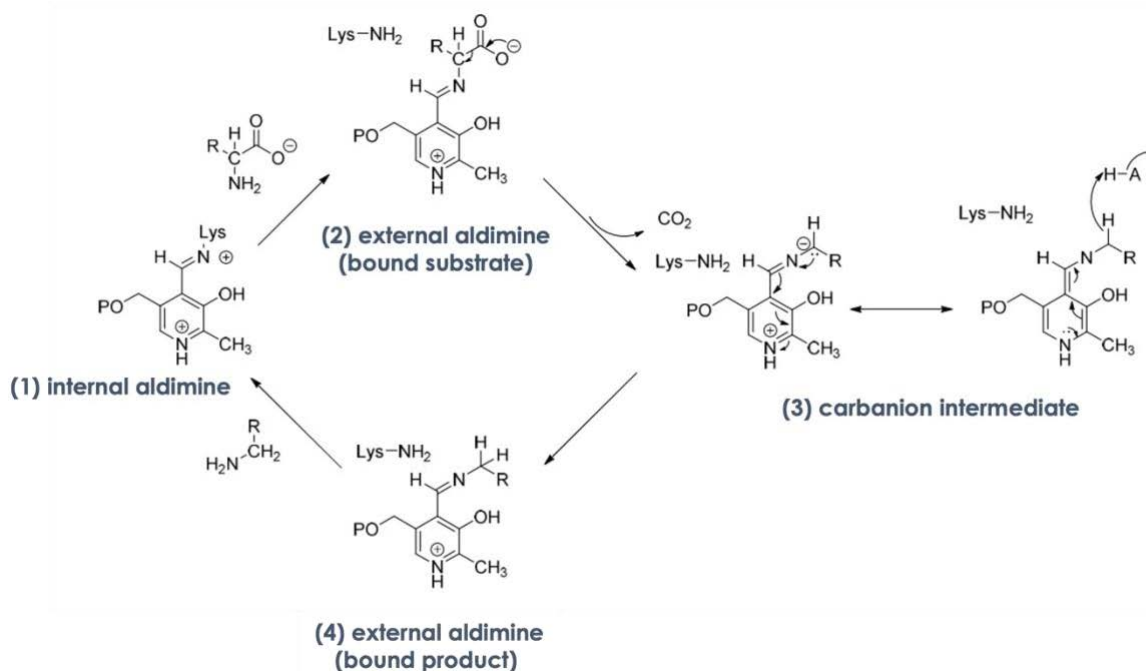


Figure 12: Reaction mechanism of PLP-dependent decarboxylases for the decarboxylation of L-lysine. Adapted from Joran and Patel [114].

## 1.6 Biocatalytic process development/ process intensification

An overall biocatalytic process consists of the production of the biocatalyst, the catalyst formulation, the actual biotransformation/reaction as well as isolation and purification of the product, potentially accompanied by recovery or recycling of coproduct and enzyme, respectively (Figure 13). For an industrial application of enzymes, certain demands concerning the enzyme, but also the process must be fulfilled. While research in academia is often focused on the development and the improvement of the enzyme, product titers, suitable production processes, and downstream processing strongly affect the performance of industrial biocatalytic processes [40]. Ideally, enzyme engineering and process intensification should go hand in hand [39].

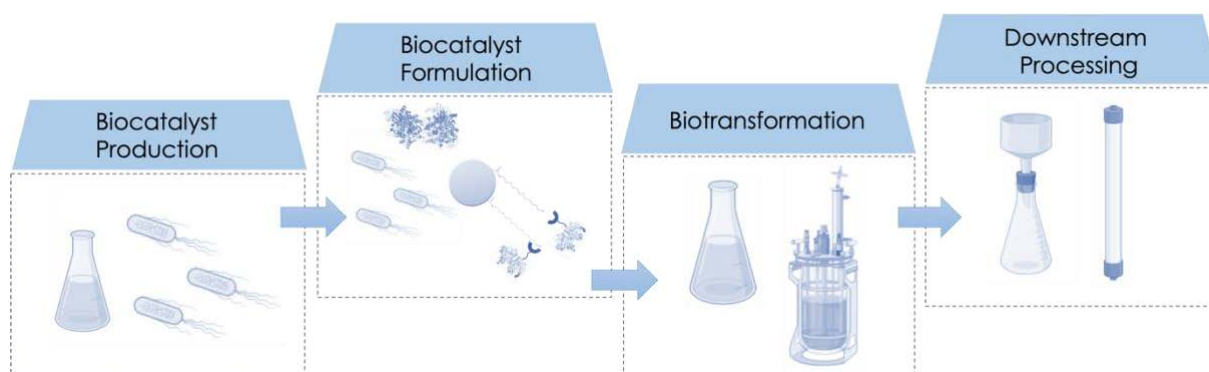


Figure 13: Process steps to be considered for biocatalytic process development. Figure created with BioRender.com.

### 1.6.1 Biocatalyst production

After the identification of appropriate enzymes for the desired reaction, their efficient production is mandatory. Without a robust production system, yielding high titers of the soluble active enzyme, the enzyme production process will always remain the bottleneck, no matter how advanced further process intensification strategies are. While recombinant protein production is best studied in *E. coli* and many strategies for soluble protein production have been identified, many heterologously expressed enzymes are produced in the form of catalytically inactive inclusion bodies [115]. In general, the expression of a recombinant protein induces an additional metabolic burden for the host organism. Meaning that a certain amount of resources is withdrawn from the host's metabolism for the expression of the foreign DNA. Metabolic burden and inclusion body formation are not directly linked; however, inclusion bodies occur as a response to the accumulation of not correctly folded recombinant proteins. A host organism that is not designed for the production of a large number of additional proteins will not be able to keep up with protein folding, and as a consequence, incorrectly folded proteins will accumulate. To enhance soluble protein production, different strategies have been developed, also including modification of the target sequence of the enzyme [115,116]. The strategies for improving soluble protein expression are numerous [115]. In the following sections, only the ones relevant to this thesis are considered.

During gene expression, cells may suffer from metabolic stress due to limitations in oxygen, nutrients, or pH shifts. If the recombinant protein requires cofactors (e.g. metal ions, vitamin derivatives) for activity, the limitation of such cofactors could influence proper protein folding and stability of the recombinant enzyme. Therefore, the composition of the cultivation medium is important and a screening of different media (components) can aid to enhance the soluble

## Introduction

protein production [117]. Other important parameters are the induction temperature and the inductor (e.g. isopropyl- $\beta$ -D-thiogalactopyranoside (IPTG)) concentration. Lower temperatures (16-25 °C) during the production of the recombinant protein can enhance the soluble protein production, probably due to a slower translation rate, and thus improve correct folding [117]. Further, hydrophobic interactions, the main forces in undesired aggregates, are reduced at lower temperatures [118]. However, a reduction in temperature can also lead to lower overall biomass [117]. Likewise, the translation rate can be influenced by the IPTG concentration. While a high IPTG concentration enables a high gene expression, it can also decrease correct protein folding [118]. Additionally, each typical *E. coli* cell exposes a different number of lactose permeases (encoded by *lacZY*) on its surface. Therefore, the actual amount of IPTG entering the cell can differ from cell to cell, making the adjustment of an optimal IPTG concentration difficult and not reproducible. Tuner BL21 (DE3) *E. coli* strains, are *lacZY* deletion mutants of the *E. coli* BL21(DE3) strain and allow for a uniform intake of IPTG into the cells of the population [119]. Another strategy is the activation or coexpression of molecular chaperones. Chaperones are proteins also encoded by *E. coli*, which actively drive folding attempts or prevent protein aggregation [116]. One strategy is to coexpress additional chaperones via a second plasmid. Different plasmids are available, for example from Takara Bio coding for different chaperones, or combinations thereof [120]. Another strategy is to overcome *E. coli*'s codon bias. Each amino acid is encoded by more than one codon; every organism has its own bias in its usage of the 61 available codons, meaning that the frequency in which different codons are used varies significantly between different organisms. In recombinant protein production, the host organism is often forced to express genes for which it does not have abundant tRNAs, also called rare codons. The expression of genes encoded by rare codons can lead to translational malfunctions and consequently to misfolded or truncated proteins. To overcome these problems, Rosetta2 BL21 (DE3) strains [119] are co-transformed with plasmids encoding for tRNAs of rare codons, also called pRARE. [118,121–123]

There are many more strategies, which can be used to enhance the soluble production of enzymes, however, no generic approach exists [115]. For every enzyme, an individual, optimal expression system must be found.

### 1.6.2 Biocatalyst formulation

For improved enzyme performance, a variety of strategies including classical enzyme engineering strategies and enzyme formulation strategies are available. While enzyme engineering pioneered by Arnold, Stemmer, and Reetz [40,124] has contributed a great deal to the application of enzymes in biotransformations, it is not relevant for this thesis and will thereby not be considered in the following. Another tool for enzyme optimization is their effective formulation. Enzymes can be formulated as a cell-free extract, in the form of resting whole cells, as free purified enzymes, or as immobilized enzymes. All formulations have advantages and disadvantages, which highly depend on the enzyme and the overall biocatalytic process.

A whole-cell biocatalyst, either used as proliferating cells or as resting cells, is by far the cheapest formulation of a biocatalyst. In their natural microenvironment, enzymes usually show inherent stability and benefit from the intrinsic availability of cofactors [125]. On the other hand, the mass transport of substrates and co-substrates via the cell membrane can be limited, requiring the addition of solvents, surfactants, or chelating agents, thereby potentially increasing the E-factor (Chapter 1.6.5) of the process [125]. Additionally, endogenous enzymes in the cell can lead to the formation of undesired side products, which could potentially lower the product yield or complicate downstream processing [126,127]. To compete with the enzymes in the cellular background, the target enzyme must be present in higher concentration and should transform the substrate with higher activity (compared to competing activities) to the target product. Furthermore, reactions, where a tight control of the reaction parameters is required, are difficult to perform with whole cells, because the environment inside the cell is less affected by the reaction conditions inside the reaction vessel [127].

Enzymes formulated as cell-free extract are similarly cheap to produce as whole cells, but require additional cell lysis and removal of cell debris, e.g., by centrifugation. Since the enzyme is available in its free form, there is no mass transfer limitation due to a cell wall, and control of reaction parameters is easier [127]. However, the missing cell environment and cell envelope can also result in a loss of enzyme stability. In addition, the soluble metabolic background of the cells is present in the cell-free extract, which can impair the atom economy due to the formation of side products and may complicate downstream processes.

The latter problem can be solved by using isolated enzymes that can be obtained after (chromatographic) purification from the cell-free extract. Pure enzymes are beneficial in

## Introduction

reactions where high reaction control is needed or high purity of the product stream is necessary [37,128]. However, the use of isolated enzymes faces some challenges: purification increases the catalyst costs immensely, especially if chromatography is required [37]. Purified enzymes often suffer from a lack of stability when used *in vitro* and, as holds for whole cells or cell-free extracts, they cannot be recycled. This makes them expensive, which is the reason why purified enzymes are often only used to generate high-value-added products [129]. One possibility to deal with the instability and the high production costs of purified enzymes is immobilizing the enzyme to the carrier directly from the crude cell extract [36,126,130].

### 1.6.2.1 Enzyme immobilization

The reaction conditions in a technical environment are often entirely different from the natural environment of enzymes in terms of pH, organic solvents, temperature, mechanical stress through shaking or pumping, non-physiological high substrate- and product concentrations or contact to different surfaces. Consequently, stabilization of the enzyme is required to improve the long-term operational stability. Besides optimizing the molecular structure of the enzyme, an increase in operational stability can also be achieved by enzyme immobilization. Purified enzymes as well as cell-free extracts are soluble in water, and hence are difficult to recover from an aqueous solution. Therefore, they are mainly employed on a single-use basis, which is neither cost-efficient nor in line with a circular economy [131]. Additionally, immobilized enzymes are often easier to handle as a solid than in solubilized form. An immobilisate can easily be separated from a liquid reaction mixture, which minimizes or eliminates protein contamination of the product and improves downstream processing. Furthermore, immobilization enables the efficient recovery and reuse of enzymes, which results in a decrease in process cost [126].

Depending on the enzyme, the reaction, and the process, there are three principal ways for immobilization: binding to a carrier, cross-linking of enzymes, and entrapment in matrices (Figure 14) [36]. Furthermore, immobilization can be applied to all kinds of enzyme formulations including whole cells or cell-free extracts, though, the application of genetically modified bacteria in processes requires administrative approval. However, the focus in the following Chapter will lay on immobilization based on covalent and non-covalent bonds for enzymes directly from the cell-free extract.

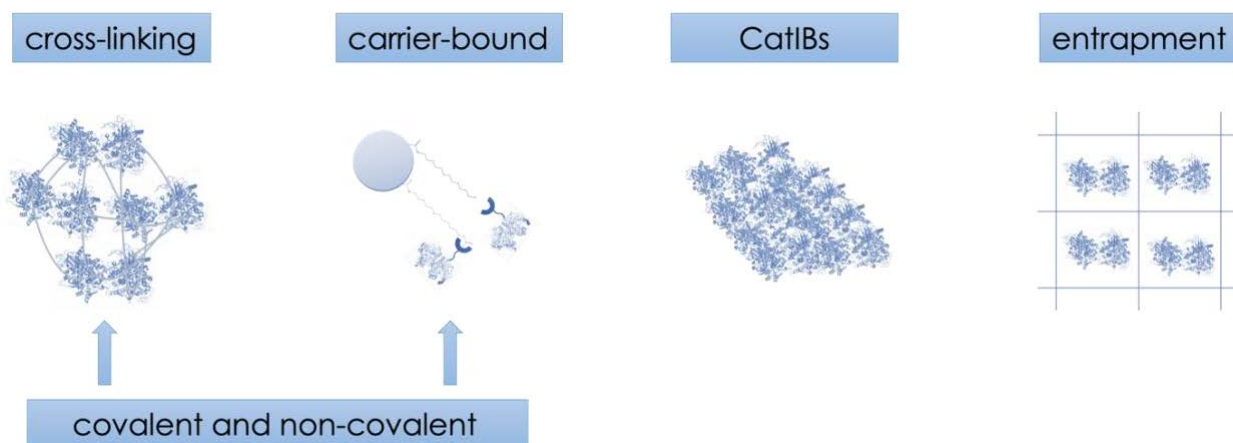


Figure 14: Enzyme immobilization strategies based on Sheldon and van Pelt [36]. Enzymes can be covalently or non-covalently immobilized by cross-linking, via binding to a carrier, by entrapment into a carrier material, or by targeted oligomerization for the formation of catalytically active inclusion bodies (CatIBs).

Immobilization via covalent or non-covalent bonds usually involves carriers. However, there are also immobilization strategies, where the catalyst is cross-linked to itself (Figure 14). One example are cross-linked enzyme aggregates (CLEAS), where crosslinking of the usually purified enzyme is induced by a cross-linking agent, like glutaraldehyde, to form intermolecular links between different functional groups found on the enzyme surface [132]. Another way to use carrier-free immobilization based on non-covalent interactions without the need for chemical cross-linkers and purified enzymes are catalytically active inclusion bodies (CatIBs), which can directly be produced in the organism using respective fusion peptides and proteins [133]. CatIBs can be produced by the genetic fusion of an aggregation-prone part, which leads to the formation of inter- and intramolecular interactions of the coiled-coil domains to each other and the enzymes. As they are basically inclusion bodies, which are fully biocompatible and mechanically stable [133–135]. There already exists a large toolbox of different CatIBs including different enzymes with different aggregation tags [136,137] and CatIBs have also already been successfully applied in biotransformations and cascade reactions [138,139]. One immense advantage compared to other immobilization techniques is that CatIBs of different enzymes can be produced via a standard protocol, without the need for laborious and expensive purification or additional immobilization steps [135]. However, through the induced aggregation of the enzymes, the resulting inclusion bodies often show greatly reduced residual activities and thus are mainly suitable for inherently active enzymes.

For carrier-based immobilization, the enzyme can be bound to the carrier by adsorption through non-covalent interactions, like van-der-Waals-, ionic-, metal chelate- or hydrophobic

## Introduction

interactions. Suitable carrier materials are inorganic materials, synthetic polymers as well as biopolymers. Binding via affinity adsorption is another way to bind an enzyme to a carrier and is usually realized by a matrix-bound ligand with affinity to a peptide or protein genetically fused to the enzyme. These fusion tag-based approaches are generally used to purify proteins. However, they can also be used to couple purification and enzyme immobilization in a single step [126]. A common tag is the poly-histidine (His)-tag, which is the most widespread and versatile technology relying on a chelate complex between histidine and divalent transition metal ions [140]. Recently, the Swedish company EnginZyme AB has developed an effective immobilization system by binding His-tagged proteins to beads of controlled porosity glass covered with different organic polymers and functionalized with Fe(III) ions for metal affinity binding (Figure 15A) [140]. The advantage of this non-covalent immobilization technique is the recycling of the carrier by removing inactive enzymes with imidazole. On the other hand, a clear disadvantage is possible enzyme leakage. In aqueous systems, immobilization by adsorption can be too weak leading to a loss of the enzyme. Therefore, immobilization by adsorption is often more advantageous in processes working in organic and unconventional media [141]. Another fusion tag-based approach is the Strep-tag I/II system, which is a peptide sequence with a strong binding affinity toward streptavidin-coated beads [142,143].

Covalent immobilization to a carrier is a promising alternative represented mainly by the HaloTag® (Promega) [144], SNAP-tag (New England Biolabs) [145], CLIP-tag (New England Biolabs) [146] and SpyTag/SpyCatcher [147] systems. These systems are based on fusion-tag enzymes/proteins/peptides that promote their covalent attachment to specific ligands [126]. Fusion tags can easily be introduced to the target enzyme by genetic fusion and enable a distinction and separation from other proteins in the host cell. This facilitates highly selective immobilization from the crude cell extract and circumvents laborious and expensive enzyme purification. Another advantage is the site-specific binding interaction through the fusion tag, which is ideally positioned such that active site residues are not impaired. Thus, enzymes are ideally all oriented in the same manner on the carrier surface, which supports the reproducibility of the immobilization. Additionally, the immobilization from crude cell extracts lowers the risk of enzyme inactivation. Therefore, it is especially interesting for enzymes, which suffer from instability during or after chromatographic purification or inherently only show low specific activities. Among these technologies, the HaloTag® system is the most commonly used for protein immobilization [148]. The HaloTag® is a mutated dehalogenase, which recognizes terminal chloroalkane residues on any respectively modified carrier material and instantly

## Introduction

forms a covalent ester bond between the carrier, e.g., commercially available HaloLink™ resin, and an aspartate residue in the active site of the HaloTag® (Figure 15B) [130,144]. The advantage of this covalent immobilization technique is the prevention of enzyme leakage and the high residual activity of 35–65% relative to the soluble enzyme [130,149,150]. In addition, the HaloTag® can enhance protein solubility, which is specifically advantageous to preventing inclusion body formation of respective fusion proteins [151].

Overall, there are many more immobilization approaches, although there is no common immobilization strategy available. Rather a case-to-case optimization for each enzyme is required [152].

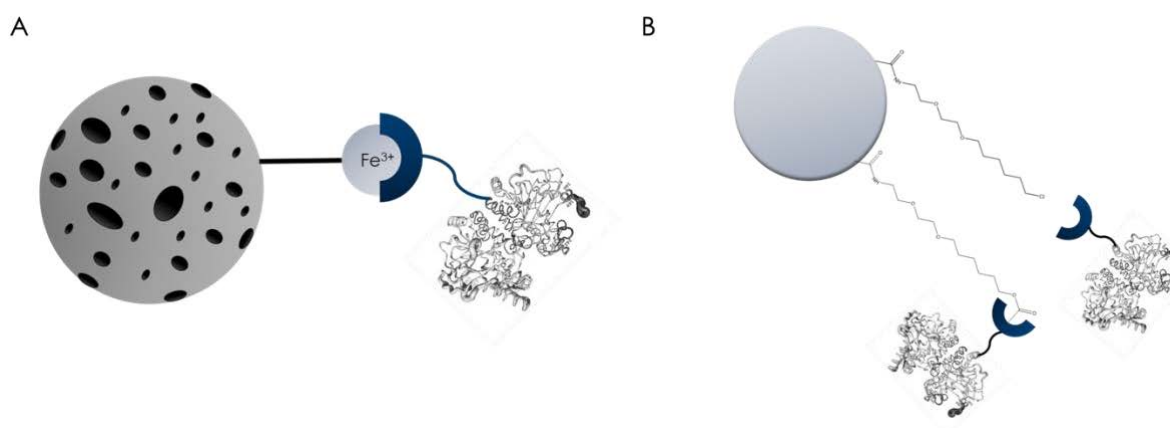


Figure 15: Two carrier-based immobilization methods. A) EziG immobilization: binding of His-tagged proteins to beads of controlled porosity glass coated with different organic polymers and functionalized with Fe(III) ions for metal affinity binding. B) HaloTag® immobilization: HaloTag® is a mutated dehalogenase, fused to the target enzyme, which recognizes terminal chloroalkane residues on any respectively modified carrier material forming a covalent ester bond between the carrier and an aspartate residue in the active site of HaloTag®

### 1.6.3 Biotransformation

#### 1.6.3.1 Reaction modes

Choosing the appropriate mode of operation depends on the biocatalytic process, the enzyme formulation, enzyme stability, activity, reusability, substrate, and product load as well as kinetic and thermodynamic issues. Stirred tank reactors (STR) are most commonly used for batch reactions. All reaction components are added to the STR at the beginning and the reaction proceeds optimally until full conversion of the substrate(s) is reached. Temperature control and pH control can easily be realized e.g. by titration during the reaction. Nevertheless, temperature, pH, and especially substrate and product concentrations can vary during STR processes, and

## Introduction

they become more heterogeneous when the process is scaled up. Although increased mixing can reduce this heterogeneity, it may also increase shear forces, potentially inactivating the enzymes. The high substrate or product concentrations may also inhibit enzyme activity. Operating in a fed-batch mode, which feeds the substrate at distinct concentrations over time, can prevent substrate inhibition. Often, fed-batch processes perform better than simple batch processes, and in some cases, they can also perform as well as comparable continuous processes. In addition, STRs are much cheaper than more complex continuous reactors [153]. There is, however, a wide variety of applications of biocatalysis already done in continuous mode, since a continuous stream of reactants is attractive because enzyme inhibition might be avoided and downstream processing is straightforward [39]. One way to apply biocatalysis in a continuous mode is via enzyme membrane reactors. An Enzyme Membrane Reactor (EMR) is a special device for carrying out continuous processes in which the enzymes are retained by a selective membrane. Regardless of the EMR configuration, the main goal is to maintain full enzyme activity in the reaction volume by ensuring complete enzyme separation. In some cases, enzyme molecules may circulate freely or are immobilized on the membrane's surface [154]. Another possibility of a continuous reaction setup are plug-flow reactors, which require immobilized enzymes [155]. In comparison with batch reactors, continuous systems generally can have several advantages: They offer improved mixing because of a higher flow velocity, and they allow for better mass transfer since they have a larger surface area. However, more knowledge about process parameters is needed, therefore the establishment of continuous processes can be more time-consuming. In plug-flow reactors, for example, pH control is not possible and mass transport limitations can occur [156]. Nevertheless, the use of continuous systems for enzymatic cascade reactions can be beneficial, since many flow processes can be automated by thermal control, pressure control, technology for process analytics, and in-line purifications. This leads to the design of economically more efficient processes, due to less setup time and higher space-time yields with higher conversion and a reduced amount of catalyst [157].

### *1.6.3.2 Reaction conditions*

Optimal reaction parameters can significantly affect enzyme performance. Here the solvent system, concentration of the reaction components (substrate, cofactors, supplements), buffer, pH, temperature, and, where appropriate: cofactor regeneration, are the most important

parameters. In general, it is important to find a balance between enzyme activity and stability. Especially cascade reactions require an operating window where the reaction parameters of different enzymes overlap. This is much more complicated in a simultaneous mode than in a sequential mode (Chapter 1.2). Finding the operating window becomes more complicated with the number of reaction steps and enzymes [33].

### **1.6.4 Product purification**

When designing enzymatic processes often only the enzyme performance and process design are considered. However, also purification of the product is an important part and can contribute to the E-factor as well (Chapter 1.6.5) [128]. Here the degree of purity, as well as the product recovery, are key parameters [33]. Therefore processes should be designed to yield clean product streams, not only in terms of undesired byproducts but also regarding undesired protein contamination [128]. Hence, immobilized enzymes are especially interesting in terms of product purification, because they can easily be separated from the reaction mixture. The actual product purification is often performed by chromatographic methods because of its robustness, scalability, and costs [33]. However, if the reaction suffers from an unfavorable reaction equilibrium or product inhibition, in situ product removal strategies can be advantageous. In situ product removal aims for integrated (co-)product removal to prevent reductions in rate, conversion, yield, and titer, thereby shifting the reaction equilibrium to a thermodynamically favorable state. Typically, a nonpolar product is (continuously) extracted into an organic phase based on its high partition coefficient, and thereby can easily be obtained after phase separation and solvent evaporation. However, in situ product removal can also be done by crystallization, if the product possesses a very low solubility in the reaction solvent and crystallization/precipitation can either be obtained directly, spontaneously, or initiated with specifically chosen counter ions [158].

### **1.6.5 Economic and ecologic benchmarks**

All the above-discussed tools aim for an economically feasible process. A key goal of synthesis today is producing the target molecules in a realistic and environmentally friendly manner, if

## Introduction

not in an optimal manner. Among all the factors that influence the practicality of a synthesis, the step economy is the most important. Step economy targets the minimization of steps in multistep synthesis since the amount of steps needed for a target-oriented synthesis dictates the cost, scope, timeline, waste stream, and many others. The step economy is highly dependent on the invention or discovery of new reactions. By using new reactions, an otherwise tedious and unfeasible synthesis can become a feasible and scalable synthesis [159–161].

Next to the step economy, process feasibility at a technical scale is determined by certain benchmarks, which will be described in the following. Depending on the industry, different values are tolerated, as summarized in Table 1.

- Product titer ( $\text{g L}^{-1}$ )
- Space-time-yield or volumetric productivity ( $\text{g}_{\text{product}} \text{L}^{-1} \text{h}^{-1}$  or  $\text{d}^{-1}$ )
- Specific space-time-yields ( $\text{g}_{\text{product}} \text{L}^{-1} \text{h}^{-1}$  or  $\text{d}^{-1} \text{g}_{\text{catalyst}}$ )
- Selectivity (%)

Table 1: Economic and ecologic benchmarks tolerated based on the industry. Values were taken from Tufvesson 2013, Straathof 2002, Pollard 2007, Sheldon 2016. [12,162–164]

Industry	Reaction yield [%]	Selectivity [%]	Product titers [ $\text{g L}^{-1}$ ]	STY [ $\text{g L}^{-1} \text{d}^{-1}$ ]	E-factor
pharma	> 90	> 98	50-100	> 0.1	25- > 100
fine	> 90	> 98	50-100	1-300	5-50
bulk	> 99	> 98	200-400	n.d	< 1-5

As already pointed out above, biocatalysis is not per se “green”. To evaluate the greenness of a process, several tools are available, as reviewed by Lima-Ramos [19]. However, in the relevance of this thesis, only the E-factor and atom economy are further considered.

The atom economy (Equation 1) evaluates the percentage of mol-% educt that is found in the desired product and is ideally at 100%.

Equation 1: Atom economy

$$\text{atom economy}[\%] = \frac{MW(\text{desired product})[\text{g mol}^{-1}]}{\sum MW(\text{educt})[\text{g mol}^{-1}]} \times 100$$

## Introduction

It should be noted that this calculation relies on theoretical values based on the reaction equation. Therefore, it neglects both the actual product and educt concentrations and yields. Especially enzymatic reactions often need further cofactors, co-substrates, and other additives, e.g. for the stabilization of the enzyme. Therefore, another important parameter to assess the greenness of a process is the E-factor (Equation 2), which shows the overall waste (kg) generated per product (kg) synthesized.

*Equation 2: E-factor*

$$E - factor = \frac{m(waste)[kg]}{m(desired\ product)[kg]}$$

Ideally, the E-factor should be at 1 or lower. Particularly, the production of biocatalysts consumes a large amount of water, which is further increased when biotransformations occur in aqueous media. The integration of wastewater leads to high E-factor values and can make a comparison of process parameters difficult. It should also be noted that the E-factor does not consider the environmental impact of the waste. Therefore, enzyme preparation itself and water are often not considered as waste, because enzymes per se are biodegradable and water is considered to be inherently sustainable [19]. Again, different industries tolerate different values (Table 1).

### 1.7 Aim of the thesis

This doctoral thesis is part of the CLIB Competence Center Biotechnology. A part of CLIB deals with the production of chemicals from renewable resources via biocatalytic processes.

In this context, this thesis is aimed at the development and process intensification of an enzymatic cascade process for the production of hydroxylated L-lysines and cadaverine derivatives in preparative lab-scale using three literature known Fe(II)/ $\alpha$ -ketoglutarate-dependent dioxygenases (KDOs) and three respective (hydroxy-lysine) decarboxylases ((L)DCs) [69].

The two-step catalytic cascade involves the hydroxylation of L-lysine via a KDO-catalyzed reaction towards the derivatives of L-lysine hydroxylated in 3- and 4-position, followed by the decarboxylation catalyzed by lysine decarboxylases toward (2S)-hydroxy-cadaverine or 3-hydroxy-cadaverine (Figure 8). The main substrate, L-lysine, as well as the cosubstrate

## Introduction

$\alpha$ -ketoglutarate, can be produced by fermentation, therefore the process could generally be based on renewable resources.

The relevant enzymes should be characterized regarding their use in the preparative laboratory scale and suitable candidates should be combined in appropriate cascades.

Especially the KDO-catalyzed first step of the reaction is challenging because these enzymes generally suffer from low soluble production, difficult purification, and instability in biotransformations. The aim of this thesis is therefore to find suitable approaches to produce, purify, and stabilize these enzymes for their application in preparative lab scale. Furthermore, a suitable enzyme formulation of KDOs and LDCs should be evaluated to enable a two-step cascade, including respective process intensification and downstream processing.

## 2 Results

### 2.1 Publication: From Enzyme to Preparative Cascade Reactions with Immobilized Enzymes: Tuning Fe(II)/ $\alpha$ -Ketoglutarate-Dependent Lysine Hydroxylases for Application in Biotransformations

Selina Seide, Lilia Arnold, Solange Wetzels, Mariela Bregu, Jochem Gätgens and Martina Pohl\*

\*Corresponding author

Published in *Catalysts*, 2022, 12, 354

<https://doi.org/10.3390/catal12040354>

Context:

In this publication, three KDOs (*Ca*KDO, *Cp*KDO, *Fj*KDO) were immobilized via EziG™ and the HaloTag®. The application of KDO-HaloTag® immobilized to HaloLink™ resin was tested in repetitive batch experiments and applied in preparative lab-scale biotransformations toward the production of (3*S*)-hydroxy-L-lysine and (4*R*)-hydroxy-L-lysine. After immobilization studies of a second enzyme, a lysine decarboxylase from *Selenomonas ruminantium* (*Sr*LDC), *Ca*KDO, and *Sr*LDC were combined in a preparative lab-scale cascade reaction toward (2*S*)-hydroxy-cadaverine.

Contributions:

Solange Wetzels, Mariela Bregu, and Lilia Arnold worked on the immobilization, reaction optimization, and application of *Sr*LDC under the supervision of Selina Seide. Lilia Arnold and Selina Seide worked on the enzyme production, purification, and the implementation of amino acid HPLC analytics. Furthermore, Lilia Arnolds worked on the immobilization of *Sr*LDC towards putrescine in a preparative lab-scale. Application studies of immobilized KDOs, the reaction in preparative lab-scale, set up of the cascade reactions, and product purification were performed by Selina Seide. GC-MS-ToF analysis was performed by Jochem Gätgens. GC-MS-ToF data analysis was done by Jochem Gätgens and Martina Pohl. The work was coordinated and supervised by Martina Pohl. Selina Seide and Martina Pohl wrote the manuscript.

Article

# From Enzyme to Preparative Cascade Reactions with Immobilized Enzymes: Tuning Fe(II)/ $\alpha$ -Ketoglutarate-Dependent Lysine Hydroxylases for Application in Biotransformations

Selina Seide, Lilia Arnold, Solange Wetzels, Mariela Bregu, Jochem Gätgens and Martina Pohl \*

IBG-1: Biotechnology, Forschungszentrum Jülich GmbH, 52425 Jülich, Germany; s.seide@fz-juelich.de (S.S.); li.arnold@fz-juelich.de (L.A.); s.wetzels@mediaexclusive.nl (S.W.); bregu.mariela@gmail.com (M.B.); j.gaetgens@fz-juelich.de (J.G.)

\* Correspondence: ma.pohl@fz-juelich.de; Tel.: +49-246-161-4388

**Abstract:** Fe(II)/ $\alpha$ -ketoglutarate-dependent dioxygenases (KDOs) catalyze a broad range of selective C–H oxidation reactions. However, the difficult production of KDOs in recombinant *E. coli* strains and their instability in purified form have so far limited their application in preparative biotransformations. Here, we investigated the immobilization of three KDOs (*Ca*KDO, *Cp*KDO, *Fj*KDO) that catalyze the stereoselective hydroxylation of the L-lysine side chain using two one-step immobilization techniques (HaloTag<sup>®</sup>, EziG<sup>™</sup>). The HaloTag<sup>®</sup>-based immobilisates reached the best results with respect to residual activity and stability. In preparative lab-scale experiments, we achieved product titers of 16 g L<sup>-1</sup> (3*S*)-hydroxy-L-lysine (*Ca*KDO) and (4*R*)-hydroxy-L-lysine (*Fj*KDO), respectively, starting from 100 mM L-lysine. Using a HaloTag<sup>®</sup>-immobilized lysine decarboxylase from *Selenomonas ruminantium* (*Sr*LDC), the (3*S*)-hydroxy-L-lysine from the *Ca*KDO-catalyzed reaction was successfully converted to (2*S*)-hydroxy-cadaverine without intermediate product purification, yielding a product titer of 11.6 g L<sup>-1</sup> in a 15 mL consecutive batch reaction. We propose that covalent in situ immobilization is an appropriate tool to access the preparative potential of many other KDOs.

**Keywords:** 2-oxoglutarate-dependent oxygenases; hydroxylation; amino acid modification;

1,5-diamino pentane; 1,5-diaminopentane-(2*S*)-ol; L-ornithine; 1,4-diaminobutan; OPA derivatization; repetitive batch; cascade reaction

---

## 1. Introduction

C–H functionalization is a chemically challenging reaction because carbon hydrogen bonds are relatively inert, making chemo-, regio-, and stereo-selectivity hard to control with conventional chemical catalysts [1]. The most commonly used enzyme class for such reactions up to now is P450 monooxygenases. However, the application of these enzymes on a preparative scale is often limited due to issues with inefficient electron transfer, uncoupling reactions, low activity and stability, and the requirement of expensive redox cofactors [2,3]. Another promising enzyme class for C–H functionalization are non-heme Fe(II)/ $\alpha$ -ketoglutarate-dependent dioxygenases (KDOs, EC 1.14.11.), which make

## Results

up a large superfamily of enzymes utilizing Fe(II) as a cofactor. KDOs catalyze the oxidative decarboxylation of their cosubstrate  $\alpha$ -ketoglutarate ( $\alpha$ -KG) towards succinate and CO<sub>2</sub>. The enzymatic reaction activates O<sub>2</sub>, which then can be used in a set of different oxidation reactions including hydroxylation, halogenation, ring closure, desaturation, epimerization, ring expansion, and epoxidation [4–8]. A great advantage of KDOs is that they are self-sufficient, as they do not need specific reductases or expensive biological redox cofactors. Many KDOs are associated with natural product biosynthesis pathways in bacteria, fungi, plants, and vertebrates, where the most studied pathways include the biosynthesis of antibiotics such as penicillin, cephalosporin, cephamycin, and clavam [4,8]. The number of different chemically challenging reactions that this enzyme class is able to catalyze makes them an interesting target for biocatalytic applications [7].

The most common industrial application of KDOs is the stereoselective hydroxylation of amino acids. The resulting products serve as precursors for the chemical and pharmaceutical industry, as was recently extensively reviewed by Peters and Buller [7].

Chiral hydroxy-L-lysines are used as chiral auxiliaries [7], as precursors for active pharmaceutical ingredients, such as the HIV protease inhibitor palinavir [9,10], for potential novel anticancer drugs such as tambromycin [11], the protein kinase c inhibitor (-) balanol [12], and the proteasome inhibitors cepafungin I or glidobactin A [13,14]. Lysine, ornithine and its hydroxylated derivatives are also precursors for polyamides, as their decarboxylation yields the respective terminal diamines, such as putrescine, cadaverine, and hydroxylated derivatives thereof, which can be used for the production of novel (fully) bio-based polyamides. The resulting bio-polyamide nylon 5X materials have excellent properties, even superior to petroleum-based nylon 6.6 [15–17]. Additional hydroxyl groups can undergo various reactions, such as esterification, or they can act as initiation sites for ring opening polymerizations of cyclic esters [18–20]. Thus, hydroxylated diamines could provide access to functionalized polymers [21].

Meanwhile, several L-lysine hydroxylases for the stereoselective hydroxylation of the L-lysine side chain in either the 3- or 4-position are known. KDOs from *Catenulispora acidiphila* (CaKDO, KDO1: 3-hydroxylation), *Chitinophaga pinensis* (CpKDO, KDO2: 4-hydroxylation), and *Flavobacterium johnsoniae* (FjKDO, KDO3: 4-hydroxylation) have recently been discovered by Baud et al. [22,23] (Figure 16). At the same time, Hara et al. independently discovered K4H-2 and K4H-1, which correspond to CpKDO and FjKDO, respectively [24]. The crystal structures of CaKDO and another KDO from *Flavobacterium species* (FsKDO, KDO5) were solved, demonstrating the typical double-stranded  $\beta$ -helix core structure of the  $\alpha$ -KG-dependent oxygenase structural superfamily [25,26]. In the crystal structure, both enzymes show two dimers per asymmetric unit, whereas their quaternary structure in solution is different: dimeric in the case of CaKDO and tetrameric for FsKDO [25].

Three major problems tend to occur when working with KDOs in general:

1. The enzyme yield from recombinant *E. coli* hosts is often low with a large fraction of insoluble non-active inclusion bodies, which can be partly prevented by coexpression of chaperones [11,13,27–29];

## Results

- Purification and storage of these enzymes is challenging, due to the requirement of Fe(II) as a cofactor, which must be prevented from oxidation and dissociation from the active site [25,29];
- Precipitation occurs under oxidative conditions due to the instability of the enzyme [28,29].

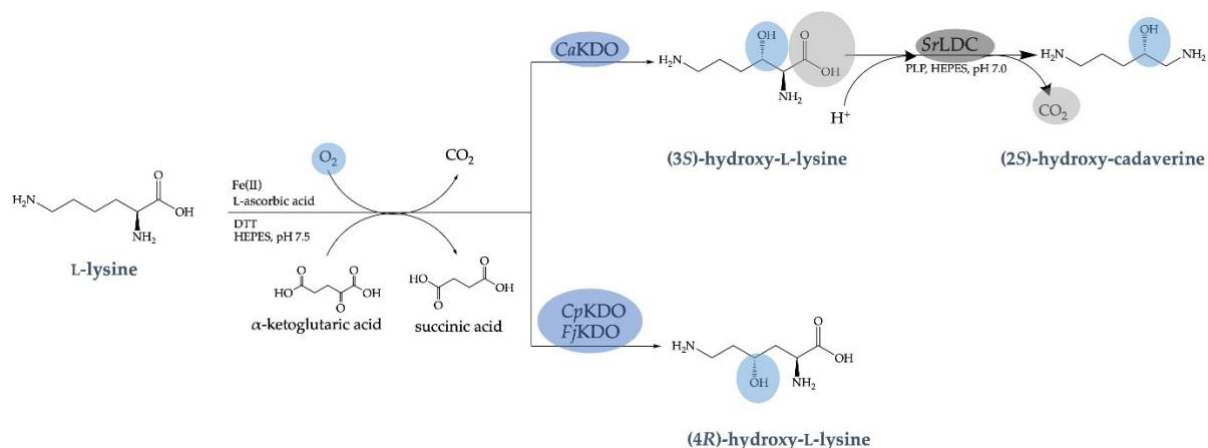


**Figure 16:** Reaction scheme of the stereoselective hydroxylation of the L-lysine side chain in the 4-position catalyzed by KDO from *Chitinophaga pinensis* (CpKDO) and KDO from *Flavobacterium johnsoniae* (FjKDO) or in the 3-position catalyzed by KDO from *Catenulispora acidiphila* (CaKDO) followed by decarboxylation to (2S)-hydroxy cadaverine catalyzed by SrLDC from *Selenomonas ruminantium*.

Therefore, most applications of KDOs in biotransformation employ whole recombinant cells or respective cell-free extracts [11,13,14,24,27]. Since some KDOs, such as CaKDO, CpKDO, and FjKDO, show very low specific activities [23], high concentrations of whole cells [24] or cell-free extracts [11] are required. In both cases, side reactions may occur due to the (potentially higher) activity of other enzymes. Mass transfer, oxygen transfer, and product separation are also often hampered by the high concentration of cellular components. In comparison, working with isolated enzymes allows a much more flexible process optimization [28,30]. On the other hand, enzyme purification is expensive; soluble enzymes often have low stability; they cannot be recycled and might complicate reaction engineering and product purification, as in the case of whole cells and cell-free extracts. Furthermore, the enzyme is usually the biggest cost factor in enzyme-catalyzed syntheses [31]. Thus, efficient immobilization techniques are crucial to increase process economy specifically for complex enzymes such as KDOs that are difficult to produce and show only low activity [23]. Thus, we tested two different one-step immobilization techniques to concentrate the biocatalyst directly from crude-cell extracts, increase its stability, and enable recycling.

There is hardly any application of immobilized KDOs in the literature, probably because many immobilization techniques require purified enzymes beforehand. During the course of this study, the Kourist group published the application of immobilized N-succinyl-L-amino acid dioxygenase SadA on EziG™ Amber for the production of N-succinyl-β-hydroxy-L-valine on a preparative lab scale [28]. EziG™ consists of a specific controlled pore glass (CPG), coated with an organic polymer layer, and was recently developed as a one-step immobilization from cell-free extracts for proteins with a poly-histidine tag [32]. Instead of nickel or cobalt ions, iron is chelated on the surface of the respectively modified

## Results

carriers. EziG™ beads are available with three surface modifications with different hydrophobicity: Amber, Coral, and Opal. The advantage of this non-covalent immobilization technique is the recycling of the carrier by removing inactive enzyme with imidazole. On the other hand, a clear disadvantage is possible enzyme leakage. Here, covalent immobilization using HaloTag® represents a good alternative. HaloTag® is a mutated dehalogenase, which recognizes terminal chloroalkane residues on any respectively modified carrier material and instantly forms a covalent ester bond between the carrier, e.g., commercially available HaloLink™ resin, and an aspartate residue in the active site of HaloTag® [33,34]. The advantage of this covalent immobilization technique is the prevention of enzyme leakage and the high residual activity of 35–65% relative to the soluble enzyme [34–36]. In addition, HaloTag® can enhance protein solubility, which is specifically advantageous to prevent the inclusion body formation of respective fusion proteins [37].

In this study, three different KDOs, which catalyze the stereoselective hydroxylation of the L-lysine side chain in the 3-position (*Ca*KDO from *Catenulispora acidiphila*) and the 4-position (*Cp*KDO from *Chitinophaga pinensis* or *Fj*KDO from *Flavobacterium johnsoniae*) [22,23], were investigated for their potential application in a preparative lab scale. First, KDO production and purification were optimized in order to increase the soluble protein production and enzyme stability during purification. Then, we tested two one-step immobilization techniques (HaloTag®, EziG™), followed by application of all three KDO-HaloTag® variants immobilized on HaloLink™ resin in repetitive batch experiments. HaloTag®-immobilized *Ca*KDO and *Fj*KDO were then selected for preparative-scale biotransformations.

Finally, *Ca*KDO and a lysine decarboxylase from *Selenomonas ruminantium* (*Sr*LDC) [23], both immobilized on HaloLink™ resin, were combined in a cascade reaction for the production of (2*S*)-hydroxy cadaverine (Figure 16).

## 2. Results

### 2.1. KDO Production and Purification

In the present study, a previously described protocol for *Ca*KDO production using coexpressed chaperones (GroEL/GroES) [11] was successfully applied to enhance the soluble production of *Ca*KDO, *Cp*KDO, and especially, *Fj*KDO, as well as for their HaloTag® fusions (Supplementary Materials, Figure S24). Without coexpression of chaperones, these enzymes were barely active and rapidly precipitated already from the cell-free extracts (data not shown). As can be seen by SDS-PAGE analysis, chaperones are still present even after purification and immobilization (Supplementary Materials, Figure S24, Figure S25, Figure S31) due to obviously strong binding to the target enzyme, which was described for several proteins before [38].

Initial tests demonstrated that freeze-drying is the best option to maintain the activity of KDOs after immobilized metal affinity chromatography (IMAC), which prevents using HEPES buffer or the addition of 10vol% glycerin, which both stabilize the enzymes in solution for a short time (data not shown). As earlier reported [29], we also observed the loss of activity after elution from IMAC when we tried to purify *Cp*KDO in TRIS buffer (Supplementary Materials, Figure S29B). Since *Ca*KDO and *Fs*KDO showed a higher degree of ordered structure in

## Results

structural investigations upon binding of Fe(II) and  $\alpha$ -KG [25], we presumed a positive effect on the enzyme stability upon addition of these cofactors and optimized the IMAC purification protocol, respectively. We used a combination of sodium phosphate buffer with low concentrations of the cosubstrate  $\alpha$ -KG, as well as L-ascorbic acid and dithiothreitol (DTT) as reducing agents. Precipitation and inactivation of all three KDOs was successfully prevented by the addition of the Fe(II) cofactor immediately after IMAC, and the desalting step took place in the presence of  $\alpha$ -KG, Fe(II) and the reducing agents, followed by lyophilization of the enzyme from the same mixture (Supplementary Materials, Section 2.2.1.1).

While we were able to improve the soluble KDO production and purification, purification of these enzymes is laborious and costly, and the enzyme yield is low. Furthermore, all components applied during the desalting step contaminate the lyophilizate, decreasing the protein content to 10–35%. This and the low enzyme yield consequently lead to problems when utilizing the lyophilizate for reactions. Furthermore, precipitation due to the instability of purified *Ca*KDO during biotransformation remains an issue (Supplementary Materials, Figure S30).

### 2.2. Immobilization and Reaction Optimization with KDOs

We tested the immobilization of KDOs as a suitable reaction engineering approach to increase enzyme stability and avoid enzyme purification, simultaneously, and compared two simple one-step immobilization techniques that allow immobilization directly from the cell-free extract: HaloTag<sup>®</sup> and EziG<sup>™</sup>.

In order to investigate the binding capacities of the different carriers, we quantified the enzyme concentration on the beads using the BCA assay (Supplementary Materials, Section S2.2.3.1.1.) and confirmed the enzyme immobilization qualitatively by SDS PAGE (Supplementary Materials, Figure S31). Loading of the HaloLink<sup>™</sup> resin reached 4.8 mg mL<sup>-1</sup>resin for *Ca*KDO-HaloTag<sup>®</sup>, 7.0 mg mL<sup>-1</sup>resin *Cp*KDO-HaloTag<sup>®</sup>, and 5.6 mg mL<sup>-1</sup>resin *Fj*KDO-HaloTag<sup>®</sup>, which is in line with the manufacturer's information of 7 mg of enzyme per mL HaloLink<sup>™</sup> resin (Supplementary Materials, Table S6). For the three different EziG<sup>™</sup> beads, only 0.11–0.16 mg *Ca*KDO, 0.03–0.05 mg *Cp*KDO, and 0.03–0.06 mg *Fj*KDO were bound per mg of beads (Supplementary Materials, Table S6), representing 3–16% *w/w* of the binding capacity. This is lower or in the lower range of the binding capacities specified in the manufacturer's information (15–60% *w/w*) [32,39].

Both immobilization techniques were compared by measuring the specific activities of the immobilisates relative to the free purified enzymes with His-Tag (Figure 17). Immobilization of *Ca*KDO via HaloTag<sup>®</sup>, EziG<sup>™</sup> Amber, and Opal increased the specific activities, with the HaloTag<sup>®</sup> immobilisate showing the highest residual activity (280 ± 39%) compared to the free enzyme without HaloTag<sup>®</sup>. The EziG<sup>™</sup> Coral immobilisate showed similar specific activity compared to the free enzyme (95 ± 0.9%). For *Cp*KDO, all immobilized variants were less active compared to the free enzyme. The highest residual activity was measured with the HaloTag<sup>®</sup> immobilisate (70 ± 1.5%). Likewise, all immobilized *Fj*KDO preparations were less active than the free variant, with the highest residual activity (62 ± 7.6%) for the EziG<sup>™</sup> Opal variant. Here, the

## Results

HaloTag<sup>®</sup> immobilization resulted in only moderate residual activities of about  $43 \pm 0.3\%$  (Figure 17). These results demonstrate again the different performance of immobilization strategies even with highly similar enzymes.

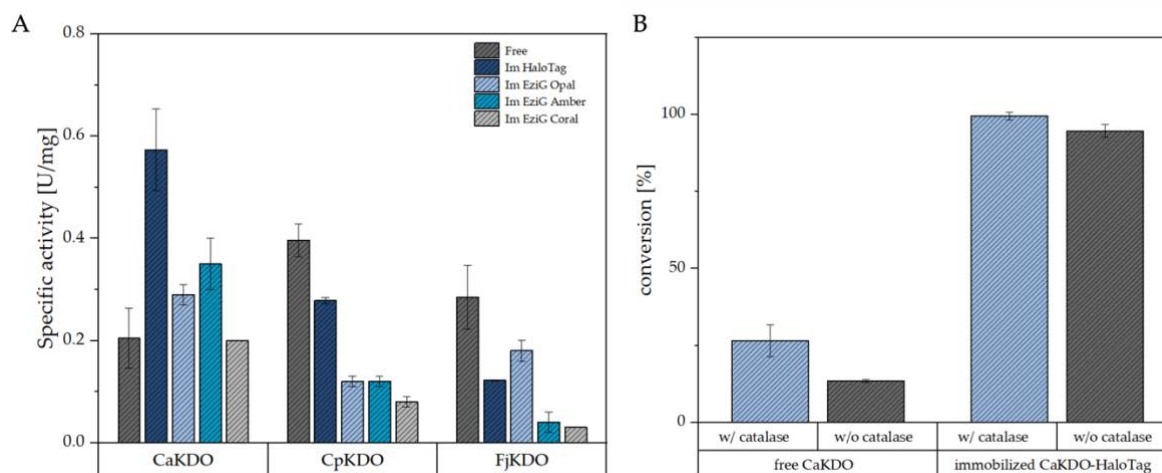


**Figure 17:** (A) Specific activities for L-lysine hydroxylation catalyzed by immobilized KDOs and the respective purified (free) variants with His-Tag. Assays were performed in 1 mL with 200 mM HEPES, pH 7.5, with 0.5 mg mL<sup>-1</sup> immobilized or free enzyme, 100 mM L-lysine, 150 mM  $\alpha$ -KG, 2.5 mM L-ascorbic acid, 0.01 mM DTT, and 1 mM (NH<sub>4</sub>)<sub>2</sub>Fe(SO<sub>4</sub>)<sub>2</sub> for 1 h at 25 °C in an overhead shaker. (B) Conversion of free CaKDO (with His-Tag) and HaloTag<sup>®</sup>-immobilized CaKDO with and without 1 mg mL<sup>-1</sup> catalase after a 24 h reaction time. Assays were performed in 1 mL with the same mixture (see A) on a thermo shaker for 24 h at 21 °C, 750 rpm. Error bars are the result of two technical replicates or, in case of the immobilized variants, of two independent immobilizations.

Since the HaloLink<sup>™</sup> resin is commercially available, shows better binding capacities, and for two of the three KDOs, the HaloTag<sup>®</sup> immobilization worked best, we decided to continue our work with HaloTag<sup>®</sup>-immobilized KDOs.

While phosphate buffer was used for the purification of the enzymes, HEPES buffer was found to be better suited for biotransformations (data not shown). This is most likely, because the Fe(II) present in the reaction mixture tends to oxidize in aqueous systems. This reaction triggers a reaction called the Fenton reaction, leading to the generation of reactive oxygen species (ROS), which can attack the enzyme and impair its stability. It was shown in previous studies that the amount of formed ROS correlates with the buffer and the pH used and is lower for HEPES buffer in comparison to other buffers [40–42]. Furthermore, buffers such as HEPES and MOPS are more suitable for reaction systems incorporating metal ions due to their lower metal-binding constants compared to other buffers, such as TRIS or phosphate buffers [43]. One way to deal with the generated ROS is to add catalase to the reaction [44]. We tested the addition of catalase exemplarily with both CaKDO preparations, as this enzyme showed the highest activity, but the lowest stability in the free form among the tested L-lysine hydroxylases (see below). As demonstrated in Figure 17B, catalase was beneficial for the biotransformation with free CaKDO, whereas there was only a negligibly

## Results

higher conversion for the reaction with HaloTag<sup>®</sup>-immobilized *Ca*KDO, which does not justify the application of catalase.

Next, we compared the free KDOs with His-Tag to their respective HaloTag<sup>®</sup> variants immobilized on the HaloLink<sup>™</sup> resin in terms of productivity and stability under the reaction conditions (Figure 18). The stabilizing effect of immobilization was most pronounced for *Ca*KDO, where the *Ca*KDO-HaloTag<sup>®</sup> immobilisate outperformed the free variant already after 1 h of reaction time. While conversion with the free variant stopped after 10%, *Ca*KDO-HaloTag<sup>®</sup> fully converted 100 mM L-lysine to (3S)-hydroxy-L-lysine in 24 h. We could demonstrate that the higher stability was a result of the immobilization and not of the HaloTag<sup>®</sup> fusion (Supplementary Materials, Figure S32). For *Cp*KDO and *Fj*KDO, both variants, the free and the HaloTag<sup>®</sup> immobilisate, were stable over the reaction time of 24 h, but reached only 53–79% conversion until the reaction was stopped, which is in line with the lower specific activity of both immobilized enzymes compared to *Ca*KDO-HaloTag<sup>®</sup> (Figure 17A). As these enzymes are still active after 24 h, full conversion could easily be achieved by a higher enzyme concentration or a prolonged reaction time. The slightly faster conversion observed with free *Cp*KDO and *Fj*KDO relative to the immobilized variants was due to the higher molecular mass of 35 kDa of the HaloTag<sup>®</sup>-fusions (Figure 18B,C).

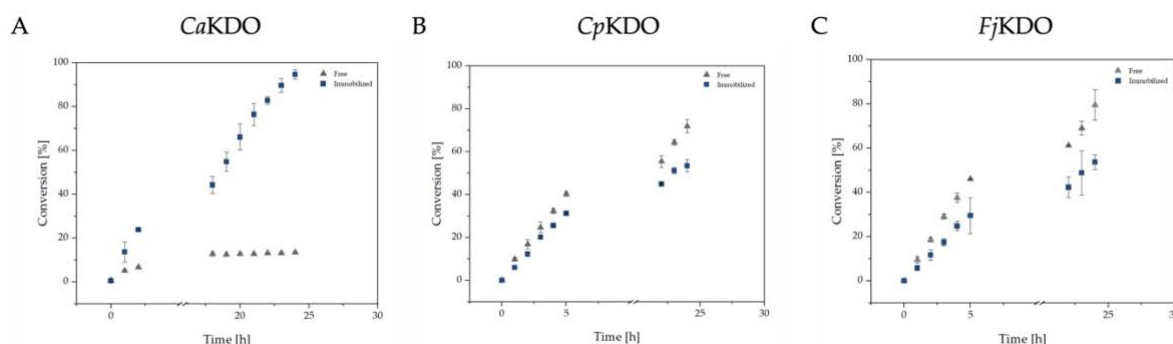


**Figure 18:** Enzyme stabilities of HaloTag<sup>®</sup>-immobilized versus free (with His-Tag) KDO variants under the reaction conditions. (A) *Ca*KDO-HaloTag<sup>®</sup> vs free *Ca*KDO (B) *Cp*KDO-HaloTag<sup>®</sup> vs free *Cp*KDO (C) *Fj*KDO-HaloTag<sup>®</sup> vs free *Fj*KDO. Reaction conditions: 200 mM HEPES, pH 7.5, and 0.5 mg mL<sup>-1</sup> catalyst, 100 mM L-lysine, 150 mM  $\alpha$ -KG, 2.5 mM L-ascorbic acid, and 1 mM (NH<sub>4</sub>)<sub>2</sub>Fe(SO<sub>4</sub>)<sub>2</sub> for 24 h at 25 °C in an overhead shaker. Reaction volume 1 mL. For further information, see Section 3.3. Error bars are a result of the reaction carried out with two independently immobilized batches.

To maximize the productivity, the L-lysine concentration was increased from 100 mM to 500 mM. Full conversion of 200 mM L-lysine to the corresponding hydroxy-L-lysines was possible with all three KDOs in a 3–4 h reaction time with respectively higher enzyme concentrations of 6.5–7.5 mg mL<sup>-1</sup> (Figure 19). It is obvious that reactions starting from 200 mM L-lysine proceeded slightly more slowly relative to those with 100 mM, which was probably caused by oxygen limitation, substrate inhibition, or other kinetic effects. The conversion of 500 mM L-lysine was tested with immobilized *Ca*KDO-HaloTag<sup>®</sup>, which yielded 82% conversion within 26 h (Figure 19A). Aeration in this simple reaction setup using a 5 mL reaction tube attached to an overhead shaker was achieved by opening of the tube every 15 min. The reaction stopped temporarily overnight, due to oxygen depletion, and started again the next day after

## Results

aeration with the same velocity, as can be deduced from the slope of the conversion curve (Figure 19A). Yet, full conversion of 500 mM L-lysine within about a 12 h reaction time is most probably possible in a reaction setup with continuous aeration, e.g., by performing the reaction in a shaking flask [11,24].

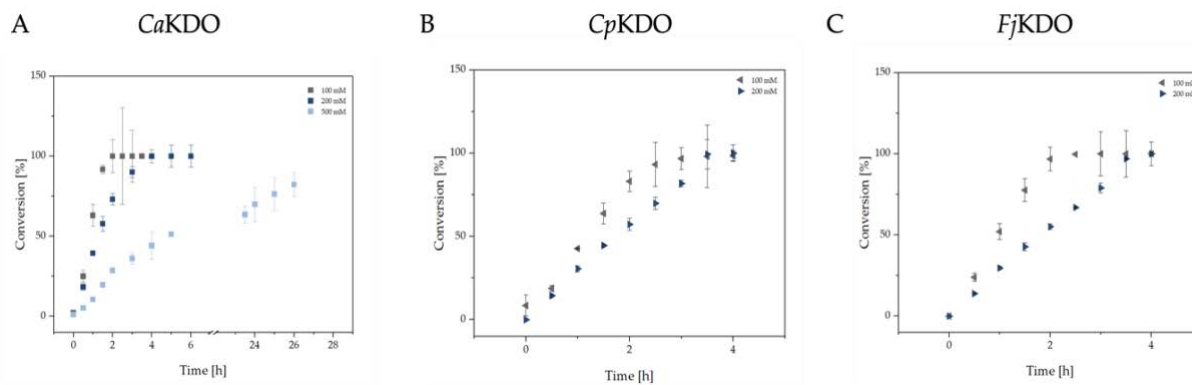


**Figure 19:** Conversion curves for different L-lysine concentrations (100 mM–500 mM). Reactions were performed in a 1 mL scale in 200 mM HEPES, pH 7.5 with 5 mg mL<sup>-1</sup> *CaKDO* (A), *CpKDO* (B), and *FjKDO* (C) for 100 mM L-lysine and 7.5 mg mL<sup>-1</sup> *CaKDO*, 6.5 mg mL<sup>-1</sup>, *CpKDO*, 6 mg mL<sup>-1</sup> *FjKDO* for 200 mM L-lysine, respectively. Conversions with 500 mM L-lysine were performed with 5 mg mL<sup>-1</sup> immobilized *CaKDO*. The reaction mix contained 100–500 mM L-lysine, 150–750 mM  $\alpha$ -KG (1.5 fold excess), 2.5 mM L-ascorbic acid, 0.01 mM DTT, and 1 mM (NH<sub>4</sub>)<sub>2</sub>Fe(SO<sub>4</sub>)<sub>2</sub>. The reaction was run for 4–26 h at 25 °C in an overhead shaker. Error bars are the result of two independent immobilizations.

## Results

### 2.3. Repetitive Batch Studies

In addition to the benefits immobilization offers on enzyme stabilization, it also enables recycling of the catalyst, which is decisive for the process economy. Recyclability of *Ca*KDO, *Cp*KDO, and *Fj*KDO immobilized via HaloTag<sup>®</sup> was tested in repetitive batch studies (Figure 20).

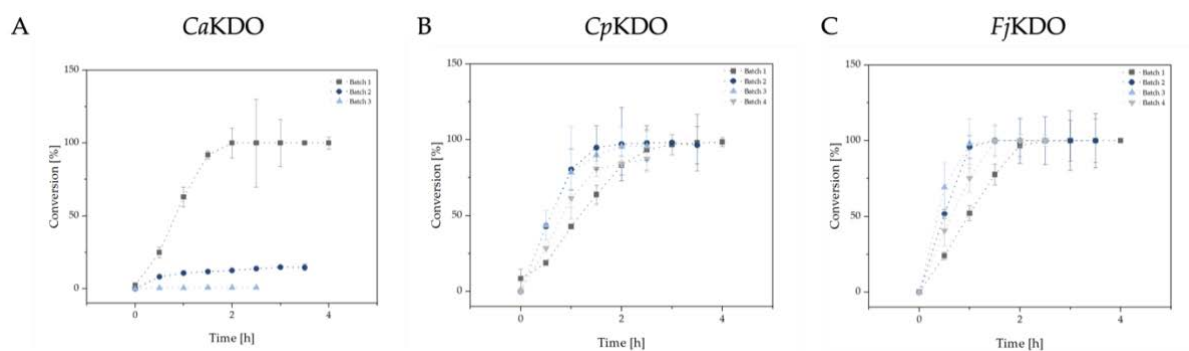


**Figure 20:** Repetitive batch studies with three HaloTag<sup>®</sup>-immobilized KDO (A) *Ca*KDO (B) *Cp*KDO (C) *Fj*KDO. Reactions were performed in a 1 mL scale in 200 mM HEPES, pH 7.5, with 5 mg mL<sup>-1</sup> immobilized enzyme, 100 mM L-lysine, 150 mM  $\alpha$ -KG, 2.5 mM L-ascorbic acid, 0.01 mM DTT, and 1 mM (NH<sub>4</sub>)<sub>2</sub>Fe(SO<sub>4</sub>)<sub>2</sub> for 24 h at 25 °C in an overhead shaker. After each batch, the immobilized catalyst was precipitated by centrifugation, washed 4 times with 50 mM HEPES, pH 7.5, and stored over night at 4 °C until the next reaction was started with a freshly prepared reaction mixture. Error bars are the result of two independent immobilizations.

After four batches, *Cp*KDO-HaloTag<sup>®</sup> still gave 84% conversion in 4 h, while *Fj*KDO-HaloTag<sup>®</sup> converted 100% in 3 h (Figure 20B,C). Even after seven batches, *Fj*KDO-HaloTag<sup>®</sup> catalyzed the conversion by 27% in 4 h (data not shown). This corresponds to a specific space-time yield of 2333 g<sub>product</sub> L<sup>-1</sup> h<sup>-1</sup> per g<sub>immobilized</sub> *Cp*KDO and 4803 g<sub>product</sub> L<sup>-1</sup> h<sup>-1</sup> per g<sub>immobilized</sub> *Fj*KDO. By contrast the single batch reactions gave a space-time yield of 795 g<sub>product</sub> L<sup>-1</sup> h<sup>-1</sup> per g<sub>immobilized</sub> *Cp*KDO and 1081 g<sub>product</sub> L<sup>-1</sup> h<sup>-1</sup> per g<sub>immobilized</sub> *Fj*KDO, showing that a recycling approach can effectively increase the reaction efficiency. Factors such as constant shaking, which can lead to friction between the beads and enzyme inactivation, as well as the partial loss of the immobilisate during the washing steps between batches might lead to the loss of active enzyme. Since the stability of KDOs is a major concern anyway, the little loss of activity after four batches for *Cp*KDO-HaloTag<sup>®</sup> and after seven batches for *Fj*KDO-HaloTag<sup>®</sup> exceeded our expectations, especially since previous experiments with SadA immobilized on EziG Amber showed only 10% of the initial reaction rate after the first reaction cycle [28].

Unfortunately, recycling of *Ca*KDO-HaloTag<sup>®</sup> was not that easy, as the catalyst was already almost inactive after the first batch (Figure 20A). Remarkably, the reaction mix showed a blue color after the first reaction, which occurred after L-lysine was fully consumed (Supplementary Materials, Figure S34). Similar findings were already reported for the 2,4-dichlorophenoxyacetate oxygenase (TfdA) [29,45]. MS-analyses suggested that hydroxylation of a tryptophan residue close to the iron binding site of TfdA occurs in absence of the primary substrate. The tryptophan residue can then chelate the Fe(III) ion located in the active

## Results

site, which was assumed to be the origin of the blue color. Upon treatment with dithionite, dialysis with EDTA, and reconstitution of Fe(II) in the active site, 81% activity could be restored, most likely due to a displacement of the Fe(III) from the oxidized tryptophan [29,45]. However, in the case of *CaKDO*, no aromatic residue is close enough to the active site to explain the blue color by an analogous mechanism (Supplementary Materials, Figure S36). Furthermore, in our case, only the reaction mix, not the immobilisate, appeared blue. Since the goal of this work was the application of KDOs in a preparative lab scale, this aspect was not further investigated, but we tested if treatment with dithionite and EDTA could regenerate the activity of the immobilized *CaKDO* after the first batch. Indeed, it was possible to regain activity, and the regenerated immobilisate was only slightly less active compared to the first batch (Supplementary Materials, Figure S35). These results represent a good basis to regenerate immobilized *CaKDO* more frequently.

### *2.4. Preparative Lab-Scale Reactions with CaKDO-HaloTag® and FjKDO-HaloTag®*

Next, *CaKDO-HaloTag®* and *FjKDO-HaloTag®* were chosen for a reaction on a preparative lab scale for the synthesis of (3*S*)-hydroxy-L-lysine and (4*R*)-hydroxy-L-lysine, respectively. Reaction optimization with free *CaKDO* at a small scale (1 mL) yielded the optimal reaction parameters (pH, temperature, Fe(II) concentration, use of additives), which were mostly in line with the results already published by Baud et al. [23], for the analytical scale. Only the optimal reaction temperature of the *CaKDO* reaction was found at 20 °C, whereas the optimal reaction temperature of *FjKDO* was at 25 °C (data not shown). The optimal reaction parameters were used for both immobilized enzymes to convert 100 mM L-lysine in a 15 mL reaction in non-baffled shaking flasks (Figure 21).

## Results

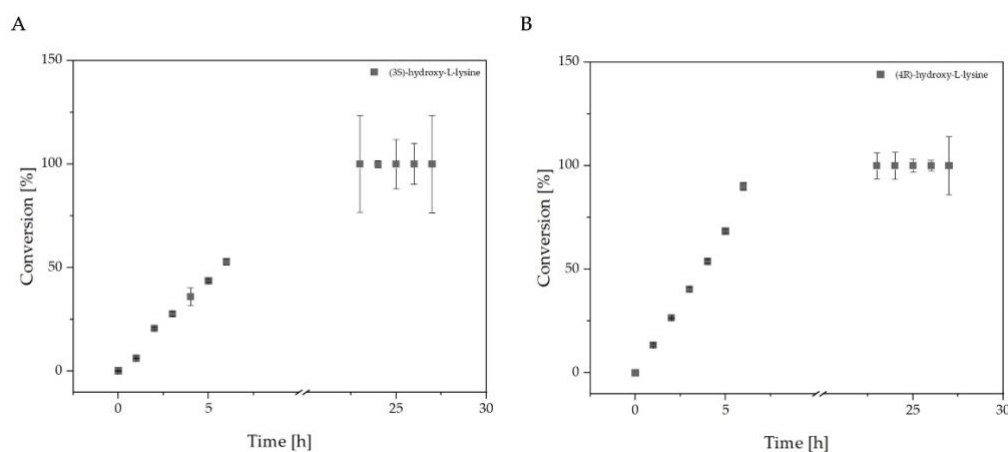


**Figure 21:** Conversion curves for the synthesis of (3S)-hydroxy-L-lysine by *Ca*KDO (A) and (4R)-hydroxy-L-lysine (*Fj*KDO) (B), respectively. Reactions were performed in a 50 mL shaking flask without baffles in a reaction volume of 15 mL, (A) 1.3 mg mL<sup>-1</sup> immobilized *Ca*KDO-HaloTag®, 20 °C, and (B) 1.2 mg mL<sup>-1</sup> immobilized *Fj*KDO-HaloTag®, 25 °C. Reaction mixture: 100 mM L-lysine, 150 mM  $\alpha$ -KG, 2.5 mM L-ascorbic acid, 0.01 mM DTT, and 1 mM (NH<sub>4</sub>)<sub>2</sub>Fe(SO<sub>4</sub>)<sub>2</sub> for 27 h, at 150 rpm orbital shaking. Error bars are the result of two independent immobilizations.

For both reactions, full conversion was reached in less than 24 h, with product titers of 16 g L<sup>-1</sup> and a total product amount of 240 mg (Figure 21), corresponding to specific space-time yields of 73.4 g<sub>product</sub> L<sup>-1</sup> h<sup>-1</sup> per g<sub>immobilized *Ca*KDO} and 133.65 g<sub>product</sub> L<sup>-1</sup> h<sup>-1</sup> per g<sub>immobilized *Fj*KDO}.</sub></sub>

In order to increase the scale further, different reaction setups were tested with the immobilized *Ca*KDO-HaloTag®. In a 10 mL shaking flask reaction, full conversion of 200 mM L-lysine was reached in 20 h (Supplementary Materials, Figure S38A) corresponding to a product titer of 32.4 g L<sup>-1</sup> and a specific space-time yield of 100 g L<sup>-1</sup> h<sup>-1</sup> per g<sub>immobilized *Ca*KDO}. Continuous aeration was also tested using a synthesis workstation at a 50 mL scale, where full conversion of 100 mM L-lysine was successfully achieved in 70 h (Supplementary Materials, Figure S38B). This corresponds to a product titer of 16.2 g L<sup>-1</sup>, but a specific space-time yield of only 4.63 g L<sup>-1</sup> h<sup>-1</sup> per g<sub>immobilized *Ca*KDO} due to the longer reaction time compared to the shaking flask experiments. Since the aeration rate could not be controlled in our synthesis workstation, we suspected that not only the increased scale, but also an oxygen limitation prolonged the reaction time. We figured out that when working with isolated and immobilized KDOs, the aeration must be carefully balanced. Too little oxygen limits the reaction, but too much oxygen can increase the oxidation of the Fe(II) cofactor, making it either unavailable for the enzyme and/or decreasing the enzyme stability due to the presence of ROS. Often, a simpler setup in shaking flasks can already be sufficient [11,24]. Here, the filling volume and mixing speed must be assessed to provide adequate oxygen supply. Our results demonstrate that an increase in scale and substrate concentration for KDOs is in general possible using immobilized enzymes in combination with an open reaction system for oxygen supply.</sub></sub>

Different other groups have already worked on the production of hydroxy-L-lysines via a KDO-catalyzed reaction, as summarized in Table 2. Apart from Baud et al. [22,23], who used IMAC-purified enzymes, most

## Results

groups applied cell-free extracts or whole cells. Working with isolated enzymes resulted in low product titers and total yields (1.6 g L<sup>-1</sup> or 0.016 g total yields) [22,23]. We were able to increase these titers 10–20-times by increasing the substrate concentration, which was possible due to the optimized production, increased stability, and recyclability by immobilization. Remarkably, our product titers of 32 g L<sup>-1</sup> (3S)-hydroxy-L-lysine are comparable to the product titers of 32.43–43 g L<sup>-1</sup> obtained with whole cells on a 40 mL scale, as reported by Hara et al. [24].

**Table 2:** Comparison of process parameters of previously published KDO-catalyzed biotransformations towards hydroxy-L-lysines in a preparative lab scale.

Enzymes	Enzyme Formulation	Product	Reaction Scale (mL)	L-Lysine (mM)	Highest Product Titers (g L <sup>-1</sup> )	Product Titers at full conv. (g L <sup>-1</sup> )	Total Yield (g)	Ref.
<i>Ca</i> KDO, <i>Cp</i> KDO, <i>Fj</i> KDO	Isolated enzymes or cell-free extract	(3S)-hydroxy-L-lysine (4R)-hydroxy-L-lysine	10	10	1.6	1.6	0.016	[22,23]
<i>Ca</i> KDO	Cell-free extract	(3S)-hydroxy-L-lysine	1000	35	4	4	4	[11]
K3H1 K4H4	Whole cells	(3S)-hydroxy-L-lysine (4R)-hydroxy-L-lysine	40	500–600 200–400	43 (88% conv.) 86 (88% conv.)	32.43 81.09	3.2–3.44 1.3–1.72	[24]
GlbB	Cell-free extract	(4R)-hydroxy-L-lysine	1000	40	6–7 (95% conv.)		6–7	[14]
<i>Plum</i> KDO	Whole cells	(4R)-hydroxy-L-lysine	50	25–50	4.8 (60% conv.)	4.05	0.20–0.24	[27]
<i>Ca</i> KDO <i>Fj</i> KDO	HaloTag®-immobilized	(3S)-hydroxy-L-lysine (4R)-hydroxy-L-lysine	10–50	100–200	16–32 (100% conv.)	16–32	0.24–0.32	This study

In the context of the preparative synthesis of hydroxy-L-lysines, product isolation must also be considered. The isolation of the target product is easier from less-complex reaction mixtures, which preferably only contain the target product without residual substrate or side products. The heterogeneity of reaction mixtures is definitely lower in reactions with isolated enzymes instead of cell-free extracts or whole-cell biocatalysts. For the present lysine hydroxylation, separation of hydroxy-L-lysines from residual L-lysine is specifically challenging due to their chemical and physical similarity. Thus, for integrated processes aiming for isolated hydroxy-L-lysines, only processes with full conversion can be considered. In our case, HPLC and GC-ToF-MS analyses demonstrated that the L-lysine was completely converted to the respective hydroxy-L-lysines and contained, besides  $\alpha$ -KG, succinate, and HEPES, no further side products (Supplementary Materials, Section 2.2.11). With a two-step chromatographic purification [46], the organic acids were fully removed, although traces of HEPES buffer remained, as can be deduced from the NMR-spectra (Supplementary Materials, Figure S50, Figure S51, Figure S56 and Figure S57).

## Results

### 2.5. Cascade Reaction towards (2S)-Hydroxy-Cadaverine

As previously shown by Baud et al. [22], coupling of the KDO reaction with a second step incorporating a (lysine) decarboxylase provides access to valuable hydroxy-cadaverines hydroxylated in the 2- and 3-position depending on the combination of the respective KDOs and lysine decarboxylases (Figure 16). However, the reaction was performed with cell-free extract and limited to a substrate concentration of 10 mM at a 10 mL scale, with the KDO reaction being the limiting step [22]. Because (2S)-hydroxy-cadaverine is harder to produce chemically than 3-hydroxy-cadaverine, due to its chiral center, we concentrated on this cascade starting from 100 mM L-lysine in a 15 mL scale with immobilized *Ca*KDO-HaloTag® in the first step and a lysine decarboxylase from *Selenomonas ruminantium* (*Sr*LDC) [22,47,48] in the second reaction step. This pyridoxal phosphate-(PLP)-dependent enzyme accepts besides L-lysine and L-ornithine [49] also (3S)-hydroxy-L-lysine as a substrate [22].

Likewise, for *Sr*LDC, we compared the two immobilization techniques: HaloTag® and EziG™, also with the goal of enzyme recycling. Since (3S)-hydroxy-L-lysine is not commercially available, all experiments concerning the immobilization, optimization of the reaction conditions, and repetitive batch experiments were carried out with L-lysine as a substrate.

As demonstrated in Figure 22 soluble and HaloTag®-immobilized *Sr*LDC showed the same performance in the conversion of L-lysine to cadaverine, whereas respective immobilisates on EziG™ beads were less active. The enzyme load of the carrier was higher for the HaloLink™ resin (7.14 mg *Sr*LDC-HaloTag® per mL resin), while the enzyme load of the EziG™ beads was between 0.082 mg per mg EziG™ Opal beads and 0.126 mg per mg EziG™ Coral beads. Similar to the KDOs, *Sr*LDC binds better to the HaloLink™ resin, showing a similar specific activity as the free enzyme, as can be deduced from the conversion curve (Figure 22A).

## Results

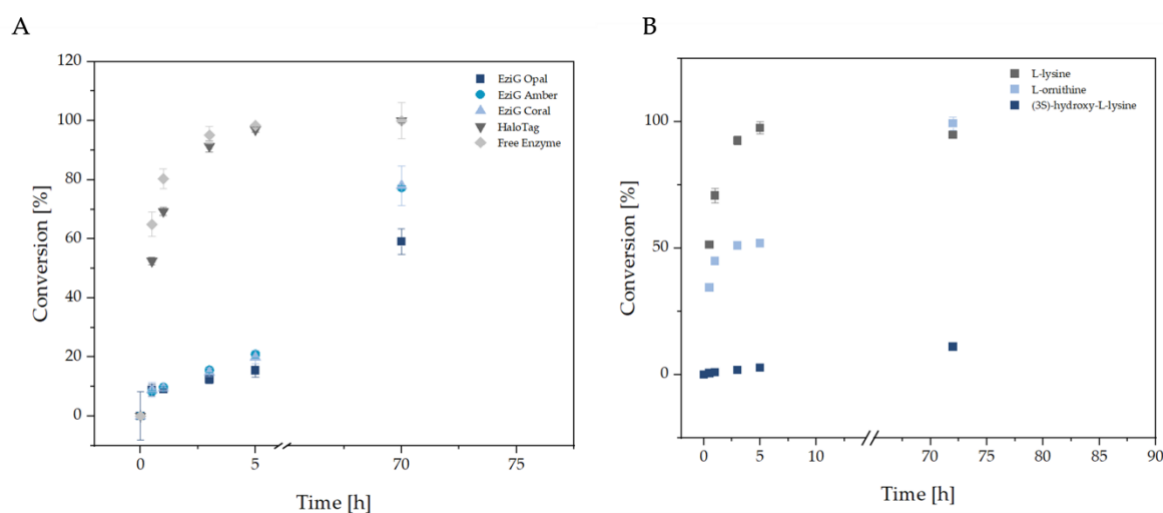


**Figure 22:** (A) Comparison of the conversion of free *SrLDC* (with His-Tag), *SrLDC* HaloTag®-immobilized to HaloLink™ resin, and *SrLDC* immobilized to EziG™ Opal, Amber, and Coral. (B) Comparison of the conversion of L-lysine, L-ornithine, and (3S)-hydroxy-L-lysine with immobilized *SrLDC*-HaloTag® (0.1 mg mL<sup>-1</sup>). Reaction conditions: volume: 1 mL, 100 mM L-lysine or L-ornithine, 2 mM PLP in 100 mM HEPES, pH 7.0, in an overhead shaker at 35 °C under the exclusion of light. For (3S)-hydroxy-L-lysine, the supernatant of the *CaKDO* reaction was used (Figure 6A). Error bars are a result of two technical replicates or, in the case of the immobilized variants, of two independent immobilizations.

Next, the HaloTag®-immobilized *SrLDC* was tested for its activity towards the different substrates (L-lysine, L-ornithine, (3S)-hydroxy-L-lysine). After a 5 h reaction time, almost full conversion of the substrate L-lysine (100 mM) was achieved, whereas the conversion of L-ornithine and (3S)-hydroxy-L-lysine occurred significantly more slowly (Figure 22A). Yet, full conversion of L-ornithine to putrescin was achieved after 72 h. At this point, only 11% of (3S)-hydroxy-L-lysine was converted to (2S)-hydroxy-cadaverine, showing the low activity of *SrLDC* for this substrate. However, it has to be considered that (3S)-hydroxy-L-lysine was applied in the form of a supernatant taken from a previous KDO reaction. Therefore, other components in the reaction mixture might also lead to a decrease in activity.

Simultaneously, important reaction parameters for the *SrLDC*-HaloTag® reaction from L-lysine to cadaverine were investigated. The influence of pH, substrate concentration, temperature, and the concentration of the cofactor PLP on the reaction was tested (Supplementary Materials, Section 2.2.7).

The highest cadaverine concentration after 5 h ( $67.87 \pm 2.72\%$ ) was obtained starting from 100 mM L-lysine, whereas L-lysine concentrations > 100 mM resulted in lower conversion, which could be explained by possible substrate inhibition of the enzyme (Supplementary Materials, Figure S39). In short-term experiments (20 min), the tested PLP concentrations in the range of 0.05–2 mM gave identical results (Supplementary Materials, Figure S39B). Since supplementation of PLP is known to be beneficial for LDCs and the cofactor is unstable at room temperature and towards light exposure [50], 1 mM PLP was used for further experiments. Additionally, a pH of 7 and a reaction temperature of 35 °C were found to be optimal (Supplementary Materials, Section 2.2.7, Figure S39A,D).

## Results

Under optimized reaction conditions, the sequential cascade reaction was performed without intermediate purification (Figure 23). Full conversion of 100 mM L-lysine in the first reaction step was achieved after approximately a 10 h reaction time in a shaking flask. After 25 h, the supernatant containing the (3S)-hydroxy-L-lysine was transferred to a falcon tube, and 2.5 mg mL<sup>-1</sup> of immobilized *SrLDC* was added. After 47 h, a conversion of 97% was reached, corresponding to a specific space-time yield of 6.5 g L<sup>-1</sup> h<sup>-1</sup> per g<sub>immobilized *SrLDC*</sub> and a product titer of 11.6 g L<sup>-1</sup> (2S)-hydroxy cadaverine. The results demonstrate that the *SrLDC* reaction is not impaired by components from the KDO-catalyzed step, since increasing the enzyme concentration from 0.1 mg mL<sup>-1</sup> to 2.5 mg mL<sup>-1</sup> led to full conversion of (3S)-hydroxy-L-lysine to (2S)-hydroxy-cadaverine. Increased enzyme concentrations could principally decrease the reaction time for both steps further.

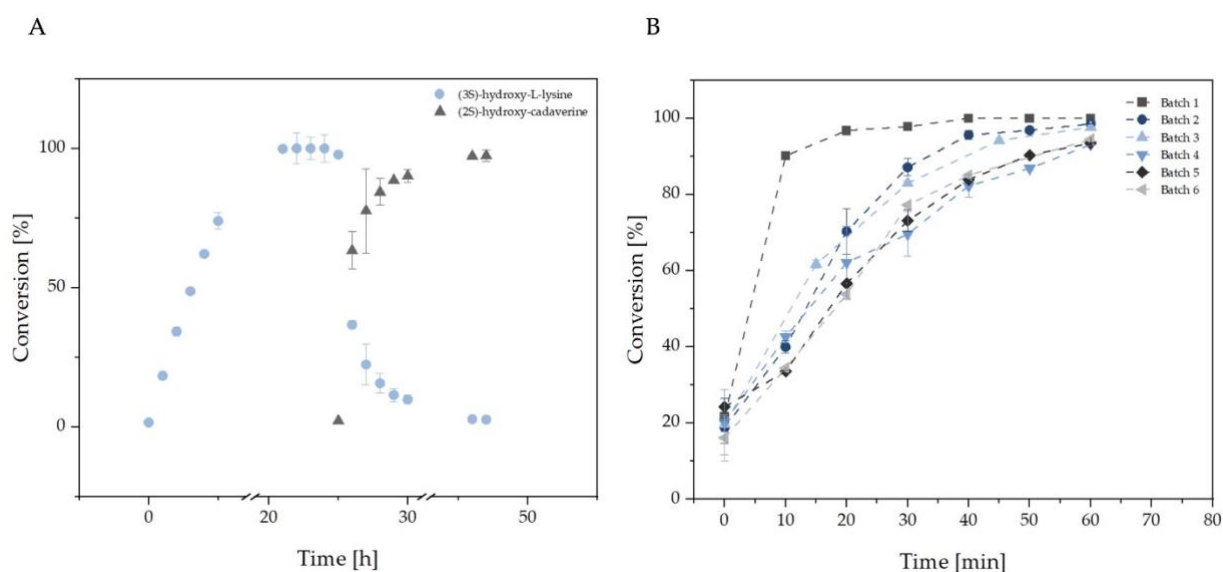


**Figure 23:** *CaKDO*-HaloTag<sup>®</sup> and *SrLDC*-HaloTag<sup>®</sup> cascade reaction for the production of 2-hydroxy-cadaverine and repetitive batch experiments of *SrLDC*-HaloTag<sup>®</sup> for the production of cadaverine. (A) Conversion curves of the sequential cascade reaction of immobilized *CaKDO* and *SrLDC* in preparative scale. The KDO reaction was performed in a 50 mL shaking flask without baffles in a reaction volume of 15 mL, at 20 °C, and 1.3 mg mL<sup>-1</sup> HaloTag<sup>®</sup>-immobilized *CaKDO*. Reaction conditions: 100 mM L-lysine, 150 mM  $\alpha$ -KG, 2.5 mM L-ascorbic acid, 0.01 mM DTT, and 1 mM (NH<sub>4</sub>)<sub>2</sub>Fe(SO<sub>4</sub>)<sub>2</sub> for 25 h, at 150 rpm orbital shaking. Afterwards, the reaction supernatant was transferred to a 50 mL falcon tube; the pH was titrated to 7.0; 1 mM PLP was added. The second reaction was started with 2.5 mg mL<sup>-1</sup> HaloTag<sup>®</sup>-immobilized *SrLDC*. The reaction was run for another 22 h in an overhead shaker at 35 °C under the exclusion of light. (B) Repetitive batch reactions of HaloTag<sup>®</sup>-immobilized *SrLDC*. Reaction was performed in a 50 mL falcon tube, in a reaction volume of 15 mL and 1 mg mL<sup>-1</sup> HaloTag<sup>®</sup>-immobilized *SrLDC* starting from 100 mM L-lysine, in 100 mM HEPES, pH 7.0, with 1 mM PLP in an overhead shaker at 35 °C under exclusion of light. After each batch, the immobilized catalyst was separated by centrifugation, washed 4 times with 100 mM HEPES, pH 7.0, and used for the next reaction. Error bars are the result of two independent immobilizations.

HPLC and GC-ToF-MS analyses demonstrated full conversion of the (3S)-hydroxy-L-lysine to (2S)-hydroxy-cadaverine (Supplementary Materials, Section 2.2.12.4), which enabled us to successfully purify the (2S)-hydroxy-cadaverine by a protocol from Fossey-Jouenne et al. [46] for

## Results

NMR analysis (Supplementary Materials, Section 2.2.12.4) without any remaining impurities (Supplementary Materials Figure S66 and Figure S67). This is in contrast to in vivo approaches with a *Corynebacterium glutamicum* strain overexpressing recombinant KDO genes and three different LDC genes for the production of (4*R*)-hydroxy-L-lysine and 3-hydroxy-cadaverine from L-lysine [21].

Similar product titers for 3-hydroxy-cadaverine (11.4 g L<sup>-1</sup>) to our approach for the production of (2*S*)-hydroxy-cadaverine could be achieved, with a strain containing *Fj*KDO and LDCc. However, the amount of by-product (cadaverine titer 39 g L<sup>-1</sup>) and intermediates ((4*R*)-hydroxy-L-lysine titer 4.1 g L<sup>-1</sup>) was high, most likely due to the substrate preference of the lysine decarboxylases for L-lysine and the generally lower activity of LDCs towards the hydroxy-L-lysines. While the constant supply of L-lysine and  $\alpha$ -KG provided by the cellular metabolism in vivo is certainly advantageous, the pH inside living cells is hard to control relative to isolated enzymes, especially when pH-active compounds (lysine and cadaverine derivatives) are involved and cascade reactions include enzymes that are highly pH dependent [48,51]. Further, isolation of the target product 3-hydroxy-cadaverine from a mixture of substrate (L-lysine), intermediate ((4*R*)-hydroxy-L-lysine), by-product (cadaverine), and other cellular components is definitely challenging, due to the close physical and chemical properties of the molecules. Thus, in the case of cascades containing KDOs and LDCs, a sequential approach including isolated immobilized enzymes seems to be advantageous and simpler compared to in vivo approaches.

Next, we investigated if immobilized *Sr*LDC-HaloTag<sup>®</sup> could be recycled in repetitive batch experiments using L-lysine (100 mM) as a substrate (Figure 23B). It can be clearly seen that the first reaction is the fastest and the turnover rates decrease less between the second and the last reaction (cycles 2–6) than between cycle 1 and 2. Still, a conversion of  $\geq 94\%$  could be achieved in the last cycle after 1 h. So far, immobilized *Sr*LDC-HaloTag<sup>®</sup> showed a reusability of at least six cycles in a 15 mL scale with little loss of activity and potentially even a higher number of cycles. This is a good basis for further reaction engineering of the cascade towards (2*S*)-hydroxy cadaverine. Because the enzyme activity towards (3*S*)-hydroxy-L-lysine is much lower than towards L-lysine, prolonged reaction times are necessary to achieve full conversion.

Besides, the product of the decarboxylation of L-lysine, cadaverine, is also an interesting industrial compound for the production of fully biobased polymers [15,52]. Biological production of cadaverine is commonly performed by fermentative microbial production [52], (immobilized) whole recombinant *E. coli* cells [15,53], or immobilized LDCs. Immobilization of LDCs was previously performed on poly(3-hydroxybutyrate) (P(3HB) biopolymers [54], chitin [55], or via different carrier-free immobilization methods, such as catalytically active inclusion bodies (CatIBs) [56], or in the form of crosslinked enzyme aggregates (CLEASs) [57]. Currently, most processes using immobilized enzymes use the constitutive (*Ec*LDCc) or inducible (CadA) LDCs from *E. coli*. While CadA is active in a pH range between 5 and 6, it is rapidly inhibited at pH higher than 8.0 [58]. Furthermore, it is inhibited at higher concentrations of lysine [59] and cadaverine [60]. In contrast, the constitutive *Ec*LDCc has a broader pH range [51] and is hardly inhibited by L-lysine [61]. To our knowledge, an application of *Sr*LDC for the production of cadaverine has not yet been tested. As was recently extensively reviewed by Huang et al.

## Results

[15], biological cadaverine production using fermentation, whole cells, and biotransformations with immobilized enzymes led to space-time yields between  $10 \text{ g L}^{-1} \text{ h}^{-1}$  and  $204 \text{ g L}^{-1} \text{ h}^{-1}$ . With HaloTag<sup>®</sup>-immobilized *SrLDC*, we achieved a product titer of  $58.4 \text{ g L}^{-1}$ , corresponding to a specific space-time yield of  $655 \text{ g L}^{-1} \text{ h}^{-1}$  per  $\text{g}_{\text{immobilized } SrLDC}$ . Furthermore, HaloTag<sup>®</sup>-immobilized *SrLDC* was able to catalyze the full conversion of  $100 \text{ mM}$  L-ornithine on a  $15 \text{ mL}$  preparative lab reaction (Supplementary Materials, Figure S40), giving access to  $8.8 \text{ g L}^{-1}$  1,4-diaminobutane (putrescine), which is another interesting building block for the production of biobased polyamides [16].

Considering all these factors, *SrLDC* is an interesting enzyme for further investigation of its potential for the synthesis of cadaverine, putrescine, and respective hydroxylated derivatives.

### 3. Materials and Methods

#### 3.1. Materials

All chemicals were purchased from Sigma-Aldrich, Roth, Merck, VWR International (Radnor, PA, USA), Merck KGaA (Darmstadt, Germany), Sigma-Aldrich Chemie GmbH (Steinheim, Germany), AppliChem GmbH (Darmstadt, Germany), and Thermo Fisher Scientific (Waltham, MA, USA). Plasmid pGro7 (GroEL/GroES) was obtained from Takara Holdings. The strains used were *Escherichia coli* DH5 $\alpha$  and *Escherichia coli* BL21 (DE3). The plasmids pET-22b(+)-CaKDO, pET-22b(+)-CpKDO, pET-22b(+)-FjKDO, and pET-22b(+)-*SrLDC* were a kind gift from Prof. Anne Zaparucha and were described previously [22,23].

HaloLink<sup>™</sup> resin was purchased from Promega. EziG<sup>™</sup> immobilization particles were kindly provided by Dr. Karim Engelmark Cassimjee.

#### 3.2. Immobilization of KDOs and *SrLDC* on HaloTag<sup>®</sup> and EziG<sup>™</sup>

A 15% (*w/v*) (*SrLDC*) or 30% (*w/v*) (KDO) cell suspension consisting of the produced pellet and HaloTag<sup>®</sup> immobilization buffer (KDOs:  $50 \text{ mM}$  HEPES, pH 7.5 with 10% glycerol, *SrLDC*:  $100 \text{ mM}$  HEPES, pH 7.0 with 10% glycerol) or EziG<sup>™</sup> immobilization buffer ( $20 \text{ mM}$  HEPES, pH 7.5 (KDOs) or pH 7.0 (*SrLDC*), with  $500 \text{ mM}$  NaCl) was prepared from the frozen *E. coli* cell pellets. The mixture was suspended in an ice bath for 30 min under constant magnetic stirring. Cells were lysed by sonication and debris removed by centrifugation. Afterwards,  $1 \text{ mL}$  of the cell-free extract was added to  $1 \text{ mL}$  washed (with HaloTag<sup>®</sup> buffer) HaloLink<sup>™</sup> slurry (25% beads) or  $10 \text{ mg}$  EziG<sup>™</sup> beads (Amber, Coral, Opal) and incubated at  $25 \text{ }^\circ\text{C}$  for 30 min in an overhead shaker. After incubation, the immobilisates were washed 4 times with  $50 \text{ mM}$  HEPES, pH 7.5 (KDOs), or  $100 \text{ mM}$  HEPES, pH 7.0 (*SrLDC*), and the amount of bound protein was quantified by the BCA assay (Supplementary Materials, Section S2.2.3.1.1) and confirmed by SDS PAGE (Supplementary Materials, Section S2.2.3.1.2).

#### 3.3. Biotransformation with KDOs

All reactions were performed as technical duplicates (same enzyme batch). The  $10 \text{ }\mu\text{L}$  samples were diluted 1:50 with  $50 \text{ mM}$  HEPES buffer, and the reaction was stopped by incubation at  $80 \text{ }^\circ\text{C}$  for 5 min in a thermo shaker (Eppendorf). Substrate and product concentrations were

## Results

determined by HPLC (3.6). Reaction mix: 100–500 mM L-lysine, 150–1000 mM  $\alpha$ -KG (1.5 molar excess), 1 mM ammonium iron(II)sulfate, 2.5 mM L-ascorbic acid, 0.01 mM DTT in 200 mM HEPES buffer, pH 7.5.

### 3.3.1. Initial Rate Activity

For initial activity measurements, enzyme concentrations of 0.5–1 mg mL<sup>-1</sup> for the free and immobilized variants of *CaKDO*, *CpKDO*, and *FjKDO* were used. Conversions were measured up to a maximum of 10% to ensure initial rate conditions. Due to the different residual activities of the immobilized enzymes, the assay conditions were respectively adapted to the enzyme preparation (Table 3).

**Table 3:** Assay conditions for respective enzymes and formulations.

Enzyme Formulation	Reaction Time	Sampling (10 $\mu$ L)
<i>CaKDO</i> EziG™	60 min	every 10 min
<i>CaKDO</i> HaloTag®	20 min	every 4 min
<i>CpKDO</i> HaloTag® & EziG™	50 min	every 10 min
<i>FjKDO</i> HaloTag® & EziG	30 min	every 5 min
Free enzymes	30 min	every 5 min

The reaction was mixed at 25 °C in an overhead shaker for sufficient mixing of the beads and the reaction mixture

### 3.3.2. Analytical Scale Reactions

For analytical-scale reactions and initial rate activity measurements, the reaction was started by adding 1 mL reaction mix (3.3) to a 2 mL reaction tube containing either the lyophilized free enzyme or the immobilized enzyme. The reaction was mixed at 25 °C in an overhead shaker or vertically attached on a thermomixer to guarantee sufficient mixing of the beads and the reaction mixture.

Enzyme formulations and concentrations for different experiments:

Stability under reaction conditions: 0.5 mg mL<sup>-1</sup> for the free and immobilized variants.

Different substrate concentrations:

HaloTag® variants immobilized on HaloLink™ resin:

- 5 mg mL<sup>-1</sup> *CaKDO*, *CpKDO*, *FjKDO* for 100 mM L-lysine;
- 7.5 mg mL<sup>-1</sup> *CaKDO* 6.5 mg mL<sup>-1</sup> *CpKDO* 6 mg mL<sup>-1</sup> *FjKDO* for 200 mM L-lysine;
- 5 mg mL<sup>-1</sup> *CaKDO* for 500 mM L-lysine.

### 3.3.3. Repetitive Batch Experiments

For repetitive experiments, 1 mL of the reaction mixture (3.3) was added to the immobilized enzyme (5 mg mL<sup>-1</sup> *CaKDO*-HaloTag®, *CpKDO*-HaloTag®, *FjKDO*-HaloTag®) using 5 mL reaction tubes. In order to guarantee sufficient oxygen supply, the tubes were opened every 15 min. Samples (10  $\mu$ L) were taken every 30 min over a period of 4 h for subsequent HPLC analysis. Afterwards the tubes were centrifuged, the beads were washed 4 times with 1 mL 50 mM HEPES buffer, pH 7.5, and stored overnight at 4 °C. The next day, the beads were washed once with 200 mM HEPES buffer, pH 7.5, before the reaction was started again with a freshly prepared reaction mixture. The procedure was repeated for three to seven batches, depending on the enzyme.

## Results

### 3.3.4. Regeneration of Immobilized *Ca*KDO-HaloTag®

After the first batch (3.3, 3.3.3), the beads were washed 4 times with 50 mM HEPES buffer, pH 7.5. After the addition of different concentrations of dithionite (1 or 10 mM) and 100 mM EDTA, the beads were shaken in an overhead shaker for 1 h at room temperature. Afterwards, the tubes were centrifuged; the beads were washed 4 times with 50 mM HEPES buffer, pH 7.5, to remove EDTA and dithionite and stored overnight at 4 °C. The next day, the beads were washed once with 200 mM HEPES buffer, pH 7.5, and the reaction was started again with a freshly prepared reaction mixture including 1 mM  $\text{Fe}(\text{NH}_4)_2(\text{SO}_4)_2$ , thereby restoring the cofactor for the reaction. As a control, one of the reactions was incubated only with 50 mM HEPES (Supplementary Materials, Figure S35).

### 3.3.5. Reactions in Preparative Lab Scale

Conversion of 100 mM L-lysine in 15 mL: The reaction was started by adding 15 mL of reaction mix (3.3) with 100 mM L-lysine to a 50 mL Erlenmeyer flask without baffles containing 1.2 mg mL<sup>-1</sup> and 1.3 mg mL<sup>-1</sup> HaloTag®-immobilized *Ca*KDO and *Fj*KDO, respectively. The reaction was mixed by orbital shaking at 150 rpm at 20 °C and 25 °C for *Ca*KDO and *Fj*KDO, respectively. Each reaction was performed as a technical duplicate. Samples (10 µL) were taken every hour over a period of 24 h. The reaction was quenched by heat inactivation at 80 °C for 5 min. Substrate and product concentrations were measured by HPLC (3.6).

Conversion of 200 mM L-lysine in 10 mL: The reaction was started by adding 10 mL of reaction mix (3.3) with 200 mM L-lysine and 1 mg mL<sup>-1</sup> catalase (Sigma Aldrich) to a 25 mL Erlenmeyer flask without baffles containing 1.35 mg mL<sup>-1</sup> HaloTag®-immobilized *Ca*KDO. The reaction was mixed by orbital shaking at 150 rpm at 20 °C. Samples were taken every hour over a period of 52 h, excluding night hours. For sample workup and analysis, see above.

Conversion of 100 mM L-lysine in 50 mL using an EasyMax 402 Thermostat system (Mettler Toledo): The reaction was started by adding 30 mL of reaction mix (3.3) to the EasyMax reaction vessel (100 mL) containing 20 mL immobilized *Ca*KDO HaloTag® slurry (1 mg mL<sup>-1</sup> enzyme) in 200 mM HEPES, pH 7.5. The reaction was stirred at 150 rpm, 20 °C, and the pH was continuously controlled with 0.5 M NaOH, while filtered purge gas was introduced to the surface of the reaction and incorporated into the reaction mixture by stirring (the aeration rate cannot be controlled with this device). Samples were taken every hour over a period of 70 h, excluding night hours. For sample workup and analysis, see above.

### 3.4. Biotransformations with SrLDC

All reactions were mixed at 35 °C in an overhead shaker to guarantee sufficient mixing of the beads and the reaction mixture. Reactions were performed as technical duplicates (same enzyme batch). The 10 µL samples were diluted 1:50 with 50 mM HEPES buffer, and the reaction was stopped by incubation at 80 °C for 5 min in a thermo shaker (Eppendorf). Substrate and product concentrations were determined by HPLC (3.6).

## Results

### 3.4.1. Analytical Scale

The reaction was started by adding 1 mL reaction mix containing 100 mM L-lysine, 1 mM PLP, and 100 mM HEPES buffer, pH 7.0, to a 2 mL reaction tube containing either the lyophilized free enzyme or immobilized enzyme. In the case of experiments with (3*S*)-hydroxy-L-lysine, the reaction supernatant from the previous KDO reaction was taken, and 1 mM PLP was added and titrated to pH 7.0.

### 3.4.2. Repetitive Batch Experiments in a Preparative Lab Scale

For repetitive experiments, 15 mL of the reaction mixture (100 mM L-lysine, 1 mM PLP in 100 mM HEPES, pH 7.0) was added to the 1 mg mL<sup>-1</sup> immobilized enzyme. The reaction was performed in 50 mL falcon tubes. Samples were taken every 10 min over a period of 1 h. Afterwards, the tubes were centrifuged, washed 2× with 100 mM HEPES buffer, pH 7.0, and used for the next batch. The procedure was repeated for 6 batches.

### 3.4.3. CaKDO and SrLDC Cascade Reaction

The CaKDO-HaloTag<sup>®</sup> reaction was performed in a 50 mL shaking flask without baffles in a reaction volume of 15 mL, at 20 °C, and 1.3 mg mL<sup>-1</sup> CaKDO-HaloTag<sup>®</sup> immobilized on HaloLink<sup>™</sup> resin. The reaction mix contained 100 mM L-lysine, 150 mM α-KG, 2.5 mM L-ascorbic acid, 0.01 mM DTT, 1 mM (NH<sub>4</sub>)<sub>2</sub>Fe(SO<sub>4</sub>)<sub>2</sub>, and 200 mM HEPES, pH 7.5. The reaction was performed for 27 h, at 150 rpm orbital shaking. Afterwards, the reaction supernatant (consisting of approximately 100 mM (3*S*)-hydroxy-L-lysine, 50 mM α-KG, 100 mM succinate, 2.5 mM L-ascorbic acid, 0.01 mM DTT, 1 mM (NH<sub>4</sub>)<sub>2</sub>Fe(SO<sub>4</sub>)<sub>2</sub>, 200 mM HEPES, pH 7.5) was transferred to a 50 mL falcon tube; the pH was titrated to 7.0, and 1 mM PLP was added. The second reaction was started by adding 2.5 mg mL<sup>-1</sup> SrLDC-HaloTag<sup>®</sup> immobilized on HaloLink<sup>™</sup> resin and run for another 21 h in an overhead shaker at 35 °C under the exclusion of light. Samples (10 μL) were taken every hour (excluding night hours) and analyzed by HPLC (3.6).

### 3.5. Product Purification

Hydroxy-L-lysines and (2*S*)-hydroxy-cadaverine were purified as previously described by Fossey-Jouenne et al. [46].

### 3.6. HPLC Analyses

All biotransformations were monitored by HPLC using a diode array detector (DAD) or a fluorescence detector (FLD), with the DAD detector giving the best results. For the analysis of amino acid derivatives, diamines, and (2*S*)-hydroxy-cadaverine, a pre-column derivatization step with *ortho*-phthaldialdehyde (OPA, Sigma-Aldrich) was performed. Approximate retention times were 5.6 min for L-histidine (internal standard), 8.8 min for 5-hydroxy-(*D,L*)-lysine, 8.9 min for (4*S*)-hydroxy-L-lysine, 9.0 min for (3*S*)-hydroxy-L-lysine, 9.1 min for L-lysine, 9.4 min for (2*S*)-hydroxy-cadaverine, and 10.0 min for cadaverine. Concentrations were derived from the linear calibration of five reference solutions (0.1-2.5 mM) containing L-histidine, 5-hydroxy-(*D,L*)-lysine, L-lysine, and cadaverine. Calibration was performed at least once per week or prior to every HPLC run. For details and chromatograms, see Supplementary Materials, Sections 2.2.9 and 2.2.12.

## Results

### 3.7. GC-ToF-MS Analysis

Components of the reaction mixture and mass information to identify the different hydroxy-L-lysines and the (2*S*)-hydroxy-cadaverine were analyzed by GC-ToF-MS according to a previously described protocol [63]. For details, see Supplementary Materials, Section S11.

(3*S*)-hydroxy-L-lysine, (4*R*)-hydroxy-L-lysine, and 5-hydroxy-(*D,L*)-lysine gave two trimethyl-silyl (TMS) derivatives modified with four and five TMS groups, respectively. On the GC chromatogram (Supplementary Materials, Figure S43), we can clearly identify these derivatives by retention times and masses (Supplementary Materials, Figure S43, Table S9). GC-ToF-MS analytics was also able to discriminate between the two possible diastereomers. As can be seen in the GC-chromatogram (Supplementary Materials Figure S43), both TMS species of 5-hydroxy-(*D,L*)-lysine, which was bought as a diastereomeric mixture, showed double peaks, indicating the presence of diastereomers, while the respective TMS derivatives of (3*S*)-hydroxy-L-lysine, (4*R*)-hydroxy-L-lysine, and (2*S*)-hydroxy-cadaverine only showed single peaks, indicating the presence of only one diastereomer.

### 3.8. NMR Analysis

After product purification (3.5) of the respective hydroxy-L-lysines and the (2*S*)-hydroxy-cadaverine, the 1D and 2D NMR spectra were recorded. For both components, the NMR signals were successfully assigned to the molecular structure (Supplementary Materials, Section 2.2.12). While no major impurities were visible in the (2*S*)-cadaverine spectrum (Supplementary Materials, Figure S66 and Figure S67), some impurities remained in the hydroxyl-lysine samples, probably due to the high concentration of HEPES buffer present in the reaction supernatant (Supplementary Materials, Figure S50, Figure S51, Figure S56 and Figure S57). For both hydroxyl-L-lysine derivatives, the position of the hydroxyl group was assigned indirectly through the CH-group, as hydroxyl groups are not visible in the NMR spectrum in deuterated water (Supplementary Materials, Figure S50, Figure S51, Figure S56 and Figure S57).

## 4. Conclusions

Here, we demonstrate that covalent in situ immobilization is an appropriate tool to access the preparative potential of KDOs. Immobilization via the HaloTag<sup>®</sup> solved almost all the problems that hamper the application of KDOs besides the analytical scale. The one-step immobilization rapidly concentrated the enzyme from cell-free extracts on the carrier with high residual activity and improved stability, specifically in the case of *Ca*KDO, which showed the lowest stability among the tested KDOs. Upon KDO immobilization, the increase in the stability enabled a substrate conversion of > 200 mM L-lysine, without the generation of any side products. Further, enzyme recycling was demonstrated, which was simple for immobilized *Cp*KDO-HaloTag<sup>®</sup> and *Fj*KDO-HaloTag<sup>®</sup> but required treatment with dithionite and EDTA in the case of *Ca*KDO. We were able to apply the immobilized *Ca*KDO-HaloTag<sup>®</sup> and *Fj*KDO-HaloTag<sup>®</sup> in a preparative lab scale (15 mL) and could show that a further increase in scale (up to 50 mL) or substrate concentration (200 mM L-lysine) was in general possible.

## Results

This generally led to a decrease in process costs and an increase in process sustainability, meeting the requirements of processes that will become increasingly important within the next few years.

Especially in the cascade reactions of KDOs and LDCs towards hydroxy-cadaverine derivatives, the immobilization approach seems to be superior to systems using in vivo two-phase fermentation approaches [21]. In the case of cascade reactions where the second enzyme has a higher activity towards the substrate of the first reaction (L-lysine) than the intermediate (hydroxyl-L-lysine), full conversion in the KDO-catalyzed step is mandatory, before the LDC comes into play to avoid the loss of L-lysine by the production of cadaverine as a main side product and related purification problems. Using immobilized enzymes allows for an easy separation of the enzyme in a simple sequential reaction setup, where the reaction parameters of the different reaction steps can easily be adjusted to the respective optimal parameters (temperature, pH, reactor design, aeration, and mixing of immobilized enzymes) and successful product purification.

We propose that covalent in situ immobilization is an appropriate tool to access the preparative potential of many other KDOs.

**Supplementary Materials:** The following supporting information can be downloaded at: <https://www.mdpi.com/2073-4344/12/4/354#supplementary>. [63,64]

**Author Contributions:** Conceptualization, S.S. and M.P.; methodology, S.S., L.A., J.G., M.B., S.W., and M.P.; validation, S.S., L.A., J.G., M.B., S.W., and M.P.; formal analysis, S.S., L.A., J.G., M.B., S.W., and M.P.; investigation, S.S., L.A., J.G., M.B., and S.W.; resources, M.P.; data curation, M.P.; writing—original draft preparation, S.S.; writing—review and editing, M.P.; visualization, S.S.; supervision, M.P.; project administration, M.P.; funding acquisition, M.P. All authors have read and agreed to the published version of the manuscript.

**Funding:** This research was supported by the CLIB-Competence Center Biotechnology (CKB) funded by the European Regional Development Fund (EFRE) and the North-Rhine Westphalian Ministry of Economic Affairs, Innovation, Digitalization and Energy (MWIDE) (grant number: EFRE-0300097). Funded by the Deutsche Forschungsgemeinschaft (DFG, German Research Foundation): 491111487.

**Data Availability Statement:** The data are contained within the article or Supplementary Material.

**Acknowledgments:** The plasmids pET-22b(+)-CaKDO, pET-22b(+)-CpKDO, pET-22b(+)-FjKDO, and pET-22b(+)-SrLDC and the standards of (3S)-hydroxy-L-lysine and (4R)-hydroxy-L-lysine were a kind gift from Anne Zapparucha. We further thank Anne for many fruitful discussions and helpful advice. Furthermore, we thank Christiane Claaßen for the analysis of the NMR spectra, Philipp Nerke for scientific advice and fruitful discussions, and Astrid Wirtz for her help concerning HPLC analytics. Many thanks also go to members of the IBOC team for performing NMR measurements and Karim Engelmark Cassimjee for providing the EziG™ immobilization particles.

**Conflicts of Interest:** The authors declare no conflict of interest.

## Results

### References

1. Turner, N.J.; Humphreys, L. *Biocatalysis in Organic Synthesis: The Retrosynthesis Approach*; The Royal Society of Chemistry: London, UK, 2018; ISBN 978-1-78262-530-8.
2. Bernhardt, R.; Urlacher, V.B. Cytochromes P450 as promising catalysts for biotechnological application: Chances and limitations. *Appl. Microbiol. Biotechnol.* **2014**, *98*, 6185–6203, <https://doi.org/10.1007/s00253-014-5767-7>.
3. O'Reilly, E.; Köhler, V.; Flitsch, S.L. Cytochromes P450 as useful biocatalysts: Addressing the limitations. *Chem. Commun.* **2011**, *47*, 2490–2501, <https://doi.org/10.1039/c0cc03165h>.
4. Gao, S.S.; Naowarajna, N.; Cheng, R.; Liu, X.; Liu, P. Recent examples of  $\alpha$ -ketoglutarate-dependent mononuclear non-haem iron enzymes in natural product biosyntheses. *Nat. Prod. Rep.* **2018**, *35*, 792–837, <https://doi.org/10.1039/c7np00067g>.
5. Martinez, S.; Hausinger, R.P. Catalytic mechanisms of Fe(II)- and 2-Oxoglutarate-dependent oxygenases. *J. Biol. Chem.* **2015**, *290*, 20702–20711, <https://doi.org/10.1074/jbc.R115.648691>.
6. Schofield, C.; Hausinger, R. 2-Oxoglutarate-Dependent Oxygenases. In *Metallobiology*; Schofield, C., Hausinger, R., Eds.; The Royal Society of Chemistry: London, UK, 2015; ISBN 978-1-84973-950-4.
7. Peters, C.; Buller, R.M. Industrial application of 2-oxoglutarate-dependent oxygenases. *Catalysts* **2019**, *9*, 221.
8. Hibi, M.; Ogawa, J. Characteristics and biotechnology applications of aliphatic amino acid hydroxylases belonging to the Fe(II)/ $\alpha$ -ketoglutarate-dependent dioxygenase superfamily. *Appl. Microbiol. Biotechnol.* **2014**, *98*, 3869–3876, <https://doi.org/10.1007/s00253-014-5620-z>.
9. Wang, F.; Zhu, M.; Song, Z.; Li, C.; Wang, Y.; Zhu, Z.; Sun, D.; Lu, F.; Qin, H.M. Reshaping the Binding Pocket of Lysine Hydroxylase for Enhanced Activity. *ACS Catal.* **2020**, *10*, 13946–13956, <https://doi.org/10.1021/acscatal.0c03841>.
10. Marin, J.; Didierjean, C.; Aubry, A.; Casimir, J.; Briand, J.; Guichard, G.; Poincare, H. Synthesis of Enantiopure 4-Hydroxypipercolate and 4-Hydroxylysine Derivatives from a Common 4,6-Dioxopiperidinecarboxylate Precursor. *J. Org. Chem.* **2004**, *69*, 130–141, <https://doi.org/10.1021/jo0353886>.
11. Zhang, X.; King-Smith, E.; Renata, H. Total Synthesis of Tambromycin by Combining Chemocatalytic and Biocatalytic C–H Functionalization. *Angew. Chemie Int. Ed.* **2018**, *57*, 5037–5041, <https://doi.org/10.1002/anie.201801165>.
12. Lampe, J.W.; Hughes, P.F.; Biggers, C.K.; Smith, S.H.; Hu, H. Total Synthesis of (–)- and (+) Balanol. *Synthesis* **1996**, 3263, 4572–4581.
13. Amatuni, A.; Renata, H. Identification of a lysine 4-hydroxylase from the glidobactin biosynthesis and evaluation of its biocatalytic potential. *Org. Biomol. Chem.* **2019**, *17*, 1736–1739, <https://doi.org/10.1039/c8ob02054j>.
14. Amatuni, A.; Shuster, A.; Adibekian, A.; Renata, H. Concise Chemoenzymatic Total Synthesis and Identification of Cellular Targets of Cepafungin, I. *Cell Chem. Biol.* **2020**, *27*, 1318–1326.e18, <https://doi.org/10.1016/j.chembiol.2020.07.012>.
15. Huang, Y.; Ji, X.; Ma, Z.; Łężyk, M.; Huang, Y.; Zhao, H. Green chemical and biological synthesis of cadaverine: Recent development and challenges. *RSC Adv.* **2021**, *11*, 23922–23942, <https://doi.org/10.1039/d1ra02764f>.
16. Becker, J.; Wittmann, C. Diamines for bio-based materials. *Ind. Biotechnol. Prod. Process.* **2017**, 393–409, <https://doi.org/10.1002/9783527807833>.
17. Kind, S.; Neubauer, S.; Becker, J.; Yamamoto, M.; Völkert, M.; von Abendroth, G.; Zelder, O.; Wittmann, C. From zero to hero—Production of bio-based nylon from renewable resources using engineered *Corynebacterium glutamicum*. *Metab. Eng.* **2014**, *25*, 113–123, <https://doi.org/10.1016/j.ymben.2014.05.007>.
18. Gómez, R.V.; Varela, O. Synthesis of regioisomeric, stereoregular AABB-type polyamides from chiral diamines and diacids derived from natural amino acids. *Tetrahedron Asymmetry* **2007**, *18*, 2190–2196, <https://doi.org/10.1016/j.tetasy.2007.09.010>.
19. Kakwere, H.; Perrier, S. Design of complex polymeric architectures and nanostructured materials/hybrids by living radical polymerization of hydroxylated monomers. *Polym. Chem.* **2011**, *2*, 270–288, <https://doi.org/10.1039/c0py00160k>.
20. Orgueira, H.A.; Erra-Balsells, R.; Nonami, H.; Varela, O. Synthesis of chiral polyhydroxy polyamides having chains of defined regio and stereoregularity. *Macromolecules* **2001**, *34*, 687–695, <https://doi.org/10.1021/ma000016+>.
21. Prell, C.; Vonderbank, S.-A.; Meyer, F.; Pérez-García, F.; Wendisch, V.F. Metabolic engineering of *Corynebacterium glutamicum* for de novo production of 3-hydroxycadaverine. *Curr. Res. Biotechnol.* **2021**, *4*, 32–46, <https://doi.org/10.1016/j.crbiot.2021.12.004>.
22. Baud, D.; Peruch, O.; Saaidi, P.L.; Fossey, A.; Mariage, A.; Petit, J.L.; Salanoubat, M.; Vergne-Vaxelaire, C.; de Berardinis, V.; Zapparucha, A. Biocatalytic Approaches towards the Synthesis of Chiral Amino Alcohols from Lysine: Cascade Reactions Combining  $\alpha$ -Keto Acid Oxygenase Hydroxylation with Pyridoxal Phosphate-Dependent Decarboxylation. *Adv. Synth. Catal.* **2017**, *359*, 1563–1569.

## Results

23. Baud, D.; Saaidi, P.-L.L.; Monfleur, A.; Harari, M.; Cuccaro, J.; Fossey, A.A.; Besnard, M.; Debard, A.; Mariage, A.; Pellouin, V.; et al. Synthesis of Mono- and Dihydroxylated Amino Acids with New  $\alpha$ -Ketoglutarate-Dependent Dioxygenases: Biocatalytic Oxidation of C–H Bonds. *ChemCatChem* **2014**, *6*, 3012–3017, <https://doi.org/10.1002/cctc.201402498>.
24. Hara, R.; Yamagata, K.; Miyake, R.; Kawabata, H.; Uehara, H.; Kino, K.; Baud, D.; Saaidi, P.L.; Monfleur, A.; Harari, M.; et al. Discovery of Lysine Hydroxylases in the Clavaminate Synthase-Like Superfamily for Efficient Hydroxylysine Bioproduction. *Appl. Environ. Microbiol.* **2017**, *83*, e00693-17, <https://doi.org/10.1128/AEM.00693-17>.
25. Bastard, K.; Isabet, T.; Stura, E.A.; Legrand, P.; Zaparucha, A. Structural Studies based on two Lysine Dioxygenases with Distinct Regioselectivity Brings Insights into Enzyme Specificity within the Clavaminate Synthase-Like Family. *Sci. Rep.* **2018**, *8*, 16587, <https://doi.org/10.1038/s41598-018-34795-9>.
26. McDonough, M.A.; Loenarz, C.; Chowdhury, R.; Clifton, I.J.; Schofield, C.J. Structural studies on human 2-oxoglutarate dependent oxygenases. *Curr. Opin. Struct. Biol.* **2010**, *20*, 659–672, <https://doi.org/10.1016/j.sbi.2010.08.006>.
27. Rolf, J.; Nerke, P.; Britner, A.; Krick, S.; Lütz, S.; Rosenthal, K. From cell-free protein synthesis to whole-cell biotransformation: Screening and identification of novel  $\alpha$ -ketoglutarate-dependent dioxygenases for preparative-scale synthesis of hydroxy-L-lysine. *Catalysis* **2021**, *11*, 1038, <https://doi.org/10.3390/catal11091038>.
28. Busch, F.; Busch, F.; Brummund, J.; Calderini, E.; Schürmann, M.; Kourist, R. Cofactor Generation Cascade for  $\alpha$ -Ketoglutarate and Fe(II)-Dependent Dioxygenases. *ACS Sustain. Chem. Eng.* **2020**, *8*, 8604–8612, <https://doi.org/10.1021/acssuschemeng.0c01122>.
29. Mantri, M.; Zhang, Z.; McDonough, M.A.; Schofield, C.J. Autocatalyzed oxidative modifications to 2-oxoglutarate dependent oxygenases. *FEBS J.* **2012**, *279*, 1563–1575, <https://doi.org/10.1111/j.1742-4658.2012.08496.x>.
30. Fessner, W.D. Systems Biocatalysis: Development and engineering of cell-free “artificial metabolisms” for preparative multi-enzymatic synthesis. *New Biotechnol.* **2015**, *32*, 658–664, <https://doi.org/10.1016/j.nbt.2014.11.007>.
31. Tufvesson, P.; Lima-Ramos, J.; Nordblad, M.; Woodley, J.M. Guidelines and Cost Analysis for Catalyst Production in Biocatalytic Processes. *Org. Process Res. Dev.* **2011**, *15*, 266–274, <https://doi.org/10.1021/op1002165>.
32. Cassimjee, K.E.; Federsel, H.J. Chapter 13: EziG: A Universal Platform for Enzyme Immobilization. *RSC Catal. Ser.* **2018**, *29*, 345–362, <https://doi.org/10.1039/9781782629993-00345>.
33. Encell, L.P. Development of a Dehalogenase-Based Protein Fusion Tag Capable of Rapid, Selective and Covalent Attachment to Customizable Ligands. *Curr. Chem. Genom.* **2013**, *6*, 55–71, <https://doi.org/10.2174/1875397301206010055>.
34. Döbbber, J.; Pohl, M. HaloTag<sup>TM</sup>: Evaluation of a covalent one-step immobilization for biocatalysis. *J. Biotechnol.* **2017**, *241*, 170–174, <https://doi.org/10.1016/j.jbiotec.2016.12.004>.
35. Döbbber, J.; Pohl, M.; Ley, S.V.; Musio, B. Reaction Chemistry & Engineering immobilization directly from crude cell extract for alcohols and epoxides. *React. Chem. Eng.* **2017**, *3*, 8–12, <https://doi.org/10.1039/C7RE00173H>.
36. Döbbber, J.; Gerlach, T.; Offermann, H.; Rother, D.; Pohl, M. Closing the gap for efficient immobilization of biocatalysts in continuous processes: HaloTag<sup>TM</sup> fusion enzymes for a continuous enzymatic cascade towards vicinal chiral diols. *Green Chem.* **2018**, *20*, 544–552, <https://doi.org/10.1039/c7gc03225k>.
37. Sun, C.; Li, Y.; Taylor, S.E.; Mao, X.; Wilkinson, M.C.; Fernig, D.G. HaloTag is an effective expression and solubilisation fusion partner for a range of fibroblast growth factors. *PeerJ* **2015**, *2015*, 1–24, <https://doi.org/10.7717/peerj.1060>.
38. Rohman, M.; Harrison-Lavoie, K.J. Separation of copurifying GroEL from glutathione-S-transferase fusion proteins. *Protein Expr. Purif.* **2000**, *20*, 45–47, <https://doi.org/10.1006/prep.2000.1271>.
39. EnginZyme EziG<sup>TM</sup> Product Data Sheet. 2014, 9137. Available online: <https://enginzyme.com/wp-content/uploads/2017/03/EziG-Product-Data-Sheet.pdf> (accessed on 19.03.2022)
40. Grady, J.K.; Chasteen, N.D.; Harris, D.C. Radicals from “Good’s” buffers. *Anal. Biochem.* **1988**, *173*, 111–115, [https://doi.org/10.1016/0003-2697\(88\)90167-4](https://doi.org/10.1016/0003-2697(88)90167-4).
41. Welch, K.D.; Davis, T.Z.; Aust, S.D. Iron autoxidation and free radical generation: Effects of buffers, ligands, and chelators. *Arch. Biochem. Biophys.* **2002**, *397*, 360–369, <https://doi.org/10.1006/abbi.2001.2694>.
42. Tadolini, B. Iron autoxidation in mops and hepes buffers. *Free Radic. Res.* **1987**, *4*, 149–160, <https://doi.org/10.3109/10715768709088100>.
43. Ferreira, C.M.H.; Pinto, I.S.S.; Soares, E.V.; Soares, H.M.V.M. (Un)suitability of the use of pH buffers in biological, biochemical and environmental studies and their interaction with metal ions-a review. *RSC Adv.* **2015**, *5*, 30989–31003, <https://doi.org/10.1039/c4ra15453c>.

## Results

44. Kivirikko, K.I.; Prockop, D.J. Partial purification and characterization of procollagen lysine hydroxylase from chick embryos. *Biochem. Biophys. Acta Enzymol.* **1972**, *258*, 366–379, [https://doi.org/10.1016/0005-2744\(72\)90228-8](https://doi.org/10.1016/0005-2744(72)90228-8).
45. Liu, A.; Ho, R.Y.N.; Que L., J. Alternative reactivity of an  $\alpha$ -ketoglutarate-dependent iron(II) oxygenase: Enzyme self-hydroxylation. *J. Am. Chem. Soc.* **2001**, *123*, 5126–5127, <https://doi.org/10.1021/ja005879x>.
46. Fossey-Jouenne, A.; Vergne-Vaxelaire, C.; Zaparucha, A. Enzymatic Cascade Reactions for the Synthesis of Chiral Amino Alcohols from L-lysine. 2018, 1–9, <https://doi.org/10.3791/56926>.
47. Sagong, H.; Son, H.F.; Kim, S.; Kim, Y.; Kim, K.; Kim, K. Crystal Structure and Pyridoxal 5-Phosphate Binding Property of Lysine Decarboxylase from *Selenomonas ruminantium*. *PLoS ONE* **2016**, *11*, e0166667, <https://doi.org/10.1371/journal.pone.0166667>.
48. Jeong, S.; Yeon, Y.J.; Choi, E.; Byun, S.; Cho, D.; Kim, I.K.; Kim, Y.H. Alkaliphilic lysine decarboxylases for effective synthesis of cadaverine from L-lysine. *Korean J. Chem. Eng.* **2016**, *33*, 1530–1533, <https://doi.org/10.1007/s11814-016-0079-5>.
49. Takatsuka, Y.; Yamaguchi, Y.; Ono, M.; Kamio, Y. Gene Cloning and Molecular Characterization of Lysine Decarboxylase from *Selenomonas ruminantium* Delineate Its Evolutionary Relationship to Ornithine Decarboxylases from Eukaryotes. *J. Bacteriol.* **2000**, *182*, 6732–6741.
50. Gerlach, T.; Nugroho, D.L.; Rother, D. The Effect of Visible Light on the Catalytic Activity of PLP-Dependent Enzymes. *ChemCatChem* **2021**, *13*, 2398–2406, <https://doi.org/10.1002/cctc.202100163>.
51. Kind, S.; Jeong, W.K.; Schröder, H.; Zelder, O.; Wittmann, C. Identification and elimination of the competing N-acetyldiaminopentane pathway for improved production of diaminopentane by *Corynebacterium glutamicum*. *Appl. Environ. Microbiol.* **2010**, *76*, 5175–5180, <https://doi.org/10.1128/AEM.00834-10>.
52. Mi, J.; Liu, S.; Qi, H.; Huang, J.; Lan, X.; Zhang, L. Cellular Engineering and Biocatalysis Strategies toward Sustainable Cadaverine Production: State of the Art and Perspectives. *ACS Sustain. Chem. Eng.* **2021**, *9*, 1061–1072, <https://doi.org/10.1021/acssuschemeng.0c07414>.
53. Bhatia, S.K.; Kim, Y.H.; Kim, H.J.; Seo, H.M.; Kim, J.H.; Song, H.S.; Sathiyarayanan, G.; Park, S.H.; Park, K.; Yang, Y.H. Biotransformation of lysine into cadaverine using barium alginate-immobilized *Escherichia coli* overexpressing CadA. *Bioprocess Biosyst. Eng.* **2015**, *38*, 2315–2322, <https://doi.org/10.1007/s00449-015-1465-9>.
54. Seo, H.M.; Kim, J.H.; Jeon, J.M.; Song, H.S.; Bhatia, S.K.; Sathiyarayanan, G.; Park, K.; Kim, K.J.; Lee, S.H.; Kim, H.J.; et al. In situ immobilization of lysine decarboxylase on a biopolymer by fusion with phasin: Immobilization of CadA on intracellular PHA. *Process Biochem.* **2016**, *51*, 1413–1419, <https://doi.org/10.1016/j.procbio.2016.07.019>.
55. Zhou, N.; Zhang, A.; Wei, G.; Yang, S.; Xu, S.; Chen, K.; Ouyang, P. Cadaverine Production From L-Lysine with Chitin-Binding Protein-Mediated Lysine Decarboxylase Immobilization. *Front. Bioeng. Biotechnol.* **2020**, *8*, 103, <https://doi.org/10.3389/fbioe.2020.00103>.
56. Kloss, R.; Limberg, M.H.; Mackfeld, U.; Hahn, D.; Grünberger, A.; Jäger, V.D.; Krauss, U.; Oldiges, M.; Pohl, M. Catalytically active inclusion bodies of L-lysine decarboxylase from *E. coli* for 1,5-diaminopentane production. *Sci. Rep.* **2018**, *8*, 5856, <https://doi.org/10.1038/s41598-018-24070-2>.
57. Park, S.H.; Soetyono, F.; Kim, H.K. Cadaverine production by using cross-linked enzyme aggregate of *Escherichia coli* lysine decarboxylase. *J. Microbiol. Biotechnol.* **2017**, *27*, 289–296, <https://doi.org/10.4014/jmb.1608.08033>.
58. Lemonnier, M.; Lane, D. Expression of the second lysine decarboxylase gene of *Escherichia coli*. *Microbiology* **1998**, *144*, 751–760, <https://doi.org/10.1099/00221287-144-3-751>.
59. Kim, H.J.; Kim, Y.H.; Shin, J.H.; Bhatia, S.K.; Sathiyarayanan, G.; Seo, H.M.; Choi, K.Y.; Yang, Y.H.; Park, K. Optimization of direct lysine decarboxylase biotransformation for cadaverine production with whole-cell biocatalysts at high lysine concentration. *J. Microbiol. Biotechnol.* **2015**, *25*, 1108–1113, <https://doi.org/10.4014/jmb.1412.12052>.
60. Sabo, D.L.; Boeker, E.A.; Byers, J.B.; Waron, H.; Fischer, E.H. Purification and Physical Properties of Inducible *Escherichia coli* Lysine Decarboxylase. *Biochemistry* **1974**, *13*, 662–670.
61. Shin, J.; Joo, J.C.; Lee, E.; Hyun, S.M.; Kim, H.J.; Park, S.J.; Yang, Y.H.; Park, K. Characterization of a Whole-Cell Biotransformation Using a Constitutive Lysine Decarboxylase from *Escherichia coli* for the High-Level Production of Cadaverine from Industrial Grade L-Lysine. *Appl. Biochem. Biotechnol.* **2018**, *185*, 909–924, <https://doi.org/10.1007/s12010-018-2696-4>.
62. Paczia, N.; Nilgen, A.; Lehmann, T.; Gätgens, J.; Wiechert, W.; Noack, S. Extensive exometabolome analysis reveals extended overflow metabolism in various microorganisms. *Microb. Cell Fact.* **2012**, *11*, 1–14, <https://doi.org/10.1186/1475-2859-11-122>.
63. Bradford, M.M. A Rapid and Sensitive Method for the Quantitation Microgram Quantities of Protein Utilizing the Principle of Protein-Dye Binding. *Anal. Biochem.* **1976**, 248–254, doi:10.1016/j.cj.2017.04.003.
64. Chen, R.F.; Scott, C.; Trepman, E. Fluorescence properties of o-phthalaldehyde derivatives of amino acids. *BBA - Protein Struct.* **1979**, *576*, 440–455, doi:10.1016/0005-2795(79)90419-7.

## 2.2 Supplementary Information

### **Supplementary Information: From enzyme production to preparative cascade reactions with immobilized enzymes: Tuning Fe(II)/ $\alpha$ -ketoglutarate-dependent lysine hydroxylases for application in biotransformation**

Selina Seide, Lilia Arnold, Solange Wetzels, Mariela Bregu, Jochem Gätgens, Martina Pohl

IBG-1: Biotechnology, Forschungszentrum Jülich GmbH, 52425 Jülich, Germany

Correspondence: ma.pohl@fz-juelich.de

### 2.2.1 Enzyme production

#### 2.2.1.1 *Optimized KDO production protocol*

Soluble and HaloTag® KDOs were produced according to a protocol from Zhang et al. [1]. For the production of soluble and HaloTag®-KDOs, competent *E. coli* BL21 cells were transformed with pET-28a(+)-KDO or pRSETA-KDO-HaloTag® and the pGro7 plasmids. An overnight culture was used to inoculate 10x 200 mL TB-medium in 1 L non-baffled Erlenmeyer flasks containing 25  $\mu\text{g mL}^{-1}$  chloramphenicol and 50  $\mu\text{g mL}^{-1}$  ampicillin. The cultures were shaken at 150 rpm at 37 °C until an OD<sub>600</sub> of approximately 1.5 was reached, and gene expression was induced by adding IPTG and L-arabinose at final concentrations of 0.025 mM and 1 mg mL<sup>-1</sup>, respectively. Cultivation was continued for another 20-24 hours at 23 °C and shaking at 250 rpm. Cell were harvested by centrifugation (4 °C, 15 min, 3,000 x g), and the cell pellets were stored at -20 °C until further use.

Production and solubility of free KDOs and HaloTag®- KDOs was analyzed by SDS-PAGE (Chapter 2.2.1.3).

## Results

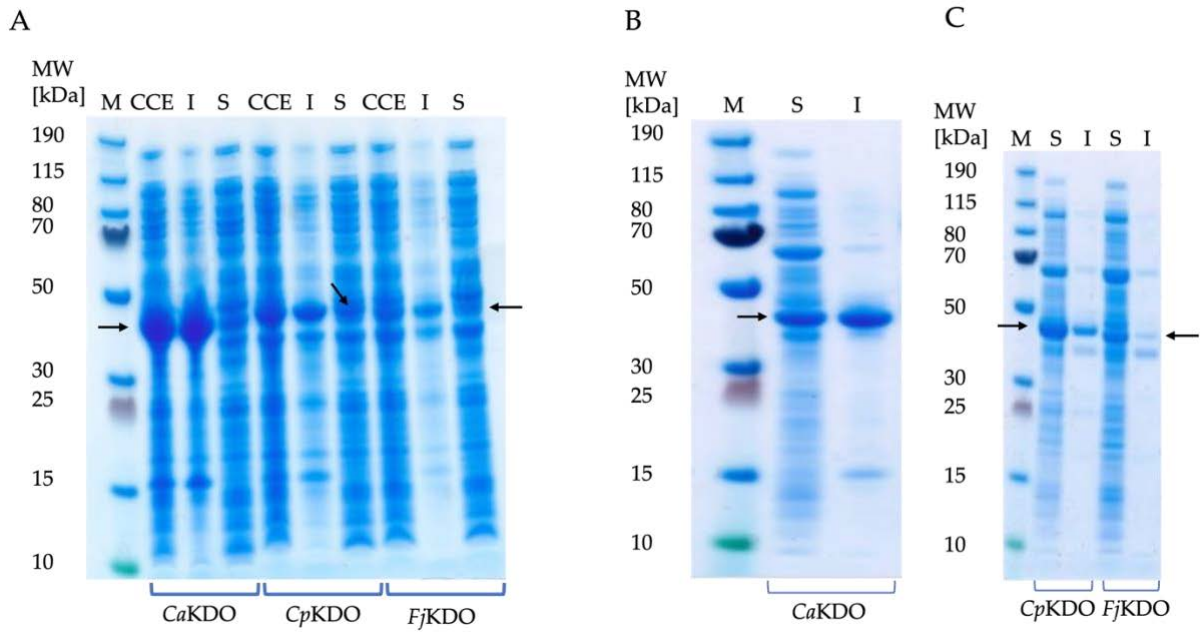


Figure S24: KDO production in *E. coli* BL21(DE3) A) KDO production according to the protocol from Baud et al. [2,3]. B) CaKDO production according to the protocol from Zhang et al. [1]. C) CpKDO and FjKDO production according to the protocol from Zhang et al. CCE= crude cell extract, M= marker, I= Insoluble fraction, S= soluble fraction. Enzyme masses: free variants with HisTag. Enzyme masses with hexahistidine tag indicated by arrows: CaKDO = 40 kDa, CpKDO = 44 kDa, FjKDO = 42 kDa. Chaperones: GroEL = 60 kDa, GroES = 10 kDa.

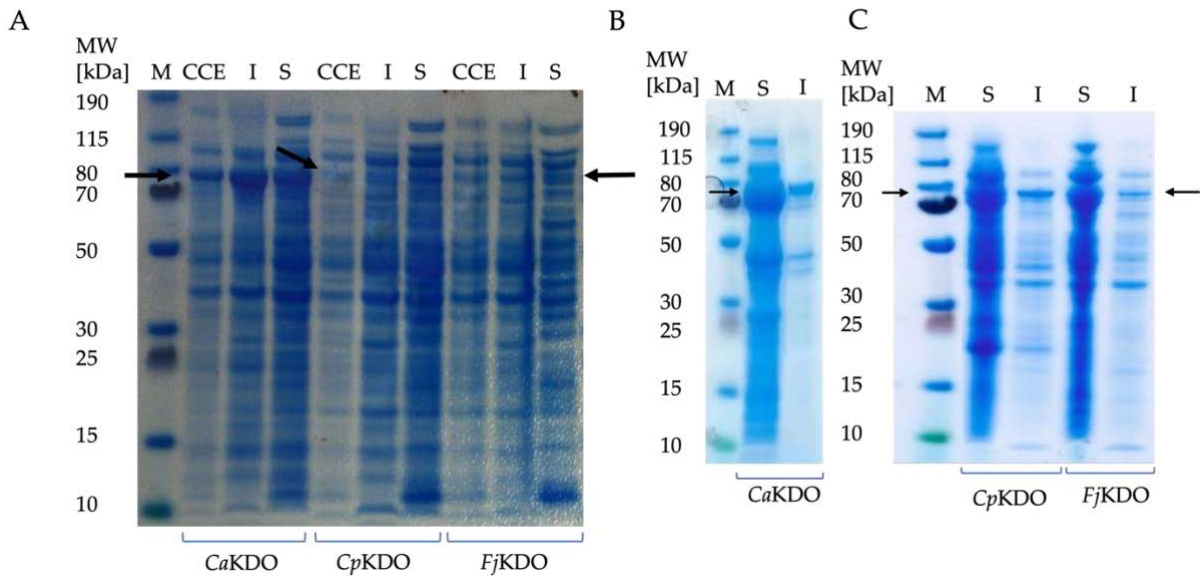


Figure S25: KDO-HaloTag® production in *E. coli* BL21(DE3) A) Protocol in LB medium w/o chaperone B) CaKDO-HaloTag® and C) CpKDO-HaloTag® and FjKDO-HaloTag® produced with chaperones [1]. M = marker, CCE = crude cell extract, I = insoluble fraction, S = soluble fraction. Enzyme masses of HaloTag® variants indicated by arrows: CaKDO= 75 kDa, CpKDO= 79 kDa, FjKDO= 77 kDa. Chaperones: GroEL= 60 kDa, GroES= 10 kDa.

## Results

### 2.2.1.2 *SrLDC production protocol*

For the production of the *SrLDC* with hexahistidine tag and the *SrLDC*-HaloTag®-fusion, competent *E. coli* BL21(DE3) cells were transformed with either pET-28a(+)-*SrLDC* or pRSETA-*SrLDC*-HaloTag® and pGro7 plasmids, respectively. An overnight culture was used to inoculate 10x 200 mL TB-media in 1 L non-baffled Erlenmeyer flasks containing 25 µg mL<sup>-1</sup> chloramphenicol and 50 µg mL<sup>-1</sup> ampicillin. Cultures were shaken at 150 rpm at 37 °C until an OD<sub>600</sub> of approximately 0.7 - 0.9 was reached, and protein production was induced by adding IPTG and L-arabinose to a final concentration of 0.025 mM and 1 mg mL<sup>-1</sup>, respectively. Cultures were incubated for another 20-24 hours at 23 °C and shaking at 250 rpm. Cells were harvested by centrifugation (4 °C, 15 min, 3,000x g), and the cell pellets were stored at -20 °C until further use. Production and solubility of His-tagged *SrLDC* and the *SrLDC*-HaloTag® fusion was controlled by SDS-PAGE (Chapter 2.2.1.3).

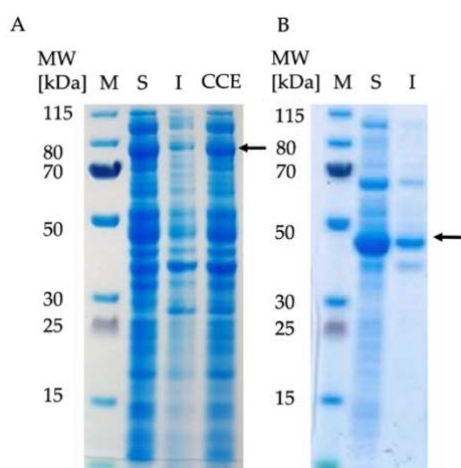


Figure S26: *SrLDC*-HisTag (A) and *SrLDC*-HaloTag® (B) production in *E. coli* BL21(DE3). Protocol from Zhang et al. [1]. CCE = crude cell extract, M = marker, I = insoluble fraction, S = soluble fraction. Arrows indicate: *SrLDC*-HaloTag® = 79 kDa, *SrLDC*-HisTag = 44 kDa. Chaperone masses: GroEL = 60 kDa, GroES = 10 kDa.

## Results

### 2.2.1.3 SDS-PAGE

If not stated otherwise, samples were prepared as followed:

Table S4: reagents used for SDS-PAGE sample preparation

Reagent	Volume [ $\mu$ l]
Sample	5-10 $\mu$ l
NuPAGE® LDS Sample Buffer (4x)	7.5 $\mu$ l
NuPAGE® Reducing Agent (10x)	3 $\mu$ l
Millipore-Water	Depending on sample concentration
Total Volume	30 $\mu$ l

Prepared samples were denatured at 98 °C for 10 minutes. For the experimental setup a NuPAGE® Novex® 4-12 % Bis-Tris gradient gel was put into a XCell Sure™ Mini-Cell gel chamber (Invitrogen), filled with NuPAGE® MES SDS Running Buffer (1 x). Marker (5  $\mu$ L, PageRuler Plus Prestained Protein ladder or PageRuler Unstained Protein ladder, ThermoFisher Scientific) and 10  $\mu$ l of each sample were transferred to the sample pockets. The gel ran at constant voltage of 200 V, a current of 100 mA and 15 watts for 45 minutes.

### 2.2.1.4 Bradford assay

Protein concentration of soluble KDOs was determined via Bradford assay [4], for which bovine serum albumin (BSA) was used as standard. Prior to sample measurements, a calibration curve with BSA was prepared. Therefore, samples of BSA with a concentration from 0.01 to 0.1 mg mL<sup>-1</sup> were measured.

100  $\mu$ l sample was added to 900  $\mu$ l Bradford reagent. Samples were incubated for 10 minutes and measured afterward photometrically at 595 nm (Shimadzu UV-1800/UV-1600) in a PMMA 1.5 mL semi-flat cuvette at 25°C. As a control, 100  $\mu$ l buffer was mixed with 900  $\mu$ l Bradford reagent and incubated in the same manner as described above.

The corresponding calibration curve was used to calculate the sample protein concentration.

## Results

Table S5: Composition of Bradford reagent used for determination of protein concentration via Bradford assay

Component	Mass [g L <sup>-1</sup> ]
Coomassie Brilliant Blue G-250	0.1
<i>ortho</i> -phosphoric acid 85 %	187
Abs. ethanol	40

### 2.2.2 Chromatographic enzyme purification

#### 2.2.2.1 KDO purification

##### 2.2.2.1.1 Typical protocol causing precipitation of KDOs

Cells were lysed by sonication in equilibration buffer (50 mM TRIS, 300 mM NaCl, pH 7.5) and cell free extracts were loaded onto an NiNTA column (Qiagen). After loading of the cell-free extract, the column was washed with washing buffer (50 mM TRIS, 300 mM NaCl, 40 mM imidazole, pH 7.5). The target enzyme was eluted with elution buffer (50 mM TRIS, 300 mM NaCl, 250 mM imidazole, pH 7.5). Fractions containing the target enzyme were desalted with a Sephadex G-25 column (GE Healthcare) and desalting buffer (10 mM TRIS, pH 7.5). The desalted fractions were lyophilized and stored at -20 °C. Protein concentrations were determined by Bradford assay (Chapter 2.2.1.4) and analyzed by SDS PAGE (Chapter 2.2.1.3).

##### 2.2.2.1.2 Optimized protocol

In order to purify the precipitation-prone soluble KDOs, an optimized purification protocol was applied. Cells were lysed by sonication in **equilibration buffer** (20 mM sodium phosphate buffer, 0.5 M NaCl, 0.1 mM DTT, 5 mM  $\alpha$ -ketoglutarate, adjusted to pH 7.4) and cell-free extracts were loaded onto an NiNTA column (Qiagen). After loading of the cell-free extract, the column was washed with **washing buffer** (20 mM sodium phosphate buffer, 0.5 M NaCl, 20 mM imidazole, 0.1 mM DTT, 5 mM  $\alpha$ -ketoglutarate, adjusted to pH 7.4). The target enzyme was eluted with **elution buffer** (20 mM sodium phosphate buffer, 0.5 M NaCl, 300 mM imidazole, 0.1 mM DTT, 5 mM  $\alpha$ -ketoglutarate, adjusted to pH 7.4). Directly after elution 100  $\mu$ l of a stock solution containing the iron (II) cofactor and L-ascorbic acid as a reducing agent (20 mM sodium phosphate buffer, 100 mM ammonium iron(II)sulfate, 250 mM L-ascorbic acid, adjusted to pH 7.4) were added per 10 mL elution fraction. Fractions containing the target enzyme were desalted by a PD-10 column (GE Healthcare) using a buffer

## Results

containing 10 mM sodium phosphate, 0.1 mM DTT, 1 mM ammonium iron(II)sulfate, 2.5 mM L-ascorbic acid, and 5 mM  $\alpha$ -ketoglutarate, adjusted to pH 7.4. The desalted fractions were lyophilized overnight (Christ ALPHA, 1-3 LD Plus) and stored at -20 °C. Sample purity was analyzed by SDS PAGE (Chapter 2.2.1.3). Protein concentration was determined by Bradford assay (Chapter 2.2.1.4).

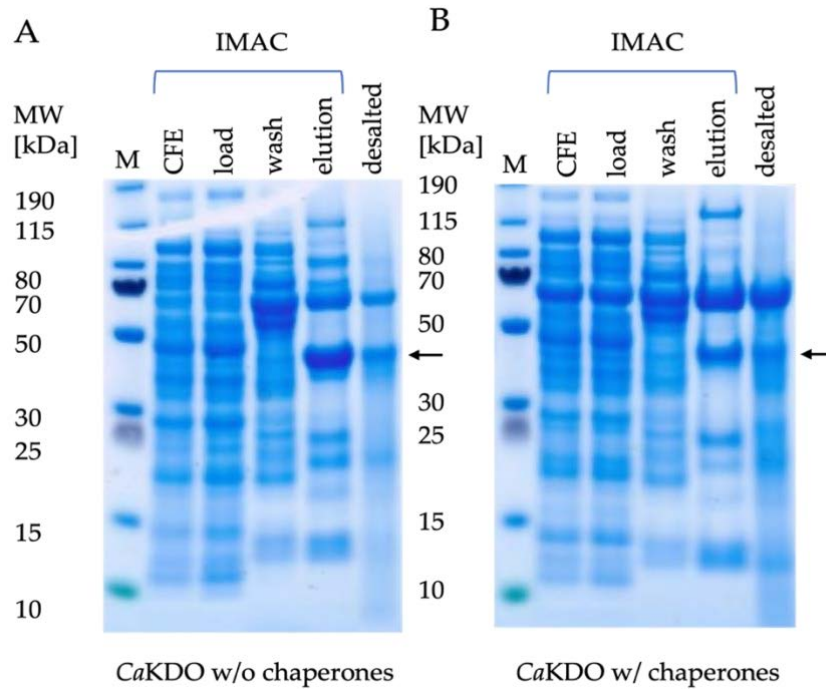


Figure S27: Optimized purification (Chapter 2.2.1.1) of CaKDO produced with (w/) and without (w/o) coexpression of chaperones GroEL/ES. M = marker, CFE = cell free extract, load = the flow through after elution. Arrow indicates CaKDO with HisTag = 40 kDa. Chaperones: GroEL= 60 kDa, GroES= 10 kDa.

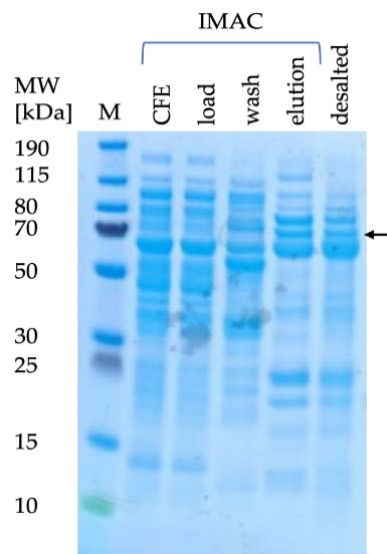


Figure S28: Optimized CaKDO-HaloTag® purification (Chapter 2.2.1.1). Arrow indicates: CaKDO-HaloTag® = 75 kDa. Chaperones: GroEL= 60 kDa, GroES= 10 kDa

## Results

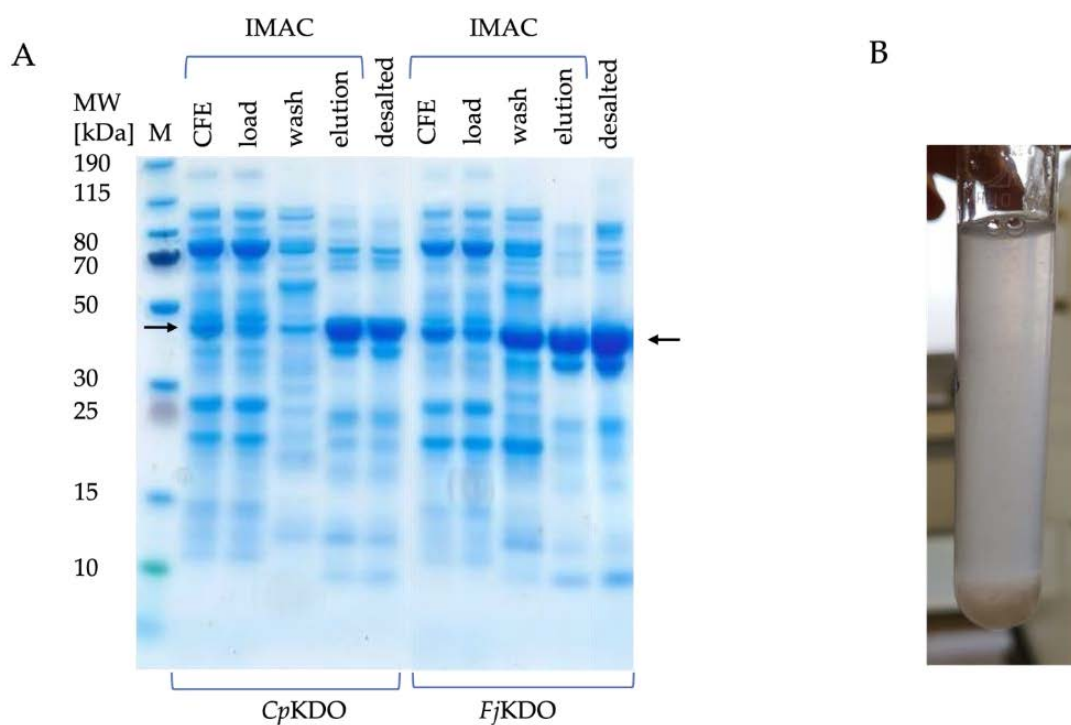


Figure S29: A) Optimized purification of CpKDO and FjKDO (Chapter 2.2.2.1.2), B) precipitated CpKDO after IMAC elution with non-optimized protocol in TRIS buffer (Chapter 2.2.2.1.1). Enzyme masses: free variants with HisTag: CpKDO= 44 kDa, FjKDO= 42 kDa. Chaperones: GroEL= 60 kDa, GroES= 10 kDa



Figure S30: Precipitated free CaKDO during reaction.

### 2.2.2.2 SrLDC purification

Cells were lysed by sonication in equilibration buffer (50 mM TRIS, 300 mM NaCl, 1 mM pyridoxal-5'-phosphate (PLP), pH 7.5) and the cell-free extract was loaded onto an NiNTA column. After loading, the column was washed with washing buffer (50 mM TRIS, 300 mM NaCl, 40 mM imidazole, 1 mM PLP, pH 7.5). SrLDC was eluted with elution buffer (50 mM TRIS, 300 mM NaCl, 250 mM imidazole, 1 mM PLP, pH 7.5). Fractions containing the target

## Results

enzyme were desalted with a Sephadex G-25 column and desalting buffer (10 mM TRIS, 1 mM PLP, pH 7.5). The desalted fractions were lyophilized and stored at -20 °C. Protein concentration was determined by Bradford assay (Chapter 2.2.1.4) and analyzed by SDS PAGE (Chapter 2.2.1.3).

### 2.2.3 Immobilization experiments

#### 2.2.3.1 Enzyme load and SDS PAGE

##### 2.2.3.1.1 Determination of enzyme concentration by BCA assay

For the determination of the protein concentration and binding capacities the interchim® Protein quantitation Kit for BCA assay was used and a BSA standard series of 0 - 2 mg mL<sup>-1</sup> was prepared before each measurement. 196 µL reagent A, 4 µL reagent B and 25 µL of each sample or standard were added to a 1.5 mL Eppendorf reaction tube and incubated for 30 min at 37 °C and 1200 rpm in a thermoshaker (Eppendorf). After incubation, the samples were centrifuged at 10,400 × g for 2 min. Afterward, 200 µL of the supernatant was added to a 96-well microtiter plate and measured at 562 nm using a TECAN Infinite® M200 reader. The protein concentration of the samples was determined using the calibration curve.

##### 2.2.3.1.2 SDS PAGE preparation for immobilized enzymes

**HaloTag®:** To release the covalently bound enzyme from the HaloLink™ resin a saponification with NaOH and SDS of the ester bond connecting HaloTag® and HaloLink™ resin was performed. Therefore, 30 µL of 200 mM NaOH and 1% SDS (w/v) were added to 15 µL of the HaloLink™ resin slurry, incubated for 15 min at room temperature and centrifuged (25 °C, 2 min, 20,000xg). For SDS PAGE 15 µL of the supernatant were used (Chapter 2.2.1.3).

**EziG™:** To release the target enzyme bound to the EziG™ beads, 1 mL of the slurry was centrifuged (25 °C, 2 min, 20,000x g), and the supernatant discarded. The beads were incubated for 15 min at room temperature in 30 µL 50 mM HEPES buffer, pH 7.5 containing 300 mM imidazole to detach the enzyme from the beads. After centrifugation (25 °C, 2 min, 20,000x g), 19.5 µL of the supernatant was used for SDS PAGE (Chapter 2.2.1.3).

## Results

### 2.2.3.2 KDO immobilization

#### 2.2.3.2.1 Determination of binding capacities of immobilized KDOs

Determination of enzyme concentration for the calculation of binding capacities was done as described in Chapter 2.2.3.2.1.

*Table S6: Binding capacities of EziG™ and HaloTag® immobilized KDOs measured by the BCA assay. Data from two independent immobilizations from the same enzyme batch.*

Enzyme	Immobilization method	Binding capacity
		(EziG™: mg enzyme/ mg beads) (HaloTag®: mg enzyme/ mL HaloLink™ resin)
CaKDO	HaloTag®	4.81± 0.075
	Opal	0.11± 0.002
	Amber	0.16± 0.028
	Coral	0.12± 0.071
CpKDO	HaloTag®	7.00± 0.868
	Opal	0.03± 0.005
	Amber	0.05± 0.009
	Coral	0.04± 0.015
FjKDO	HaloTag®	5.64± 0.623
	Opal	0.03± 0.005
	Amber	0.06± 0.013
	Coral	0.05± 0.031

## Results

### 2.2.3.2.2 Analysis of immobilized KDOs by SDS PAGE

SDS PAGE preparation as described in Chapter 2.2.3.1.2.

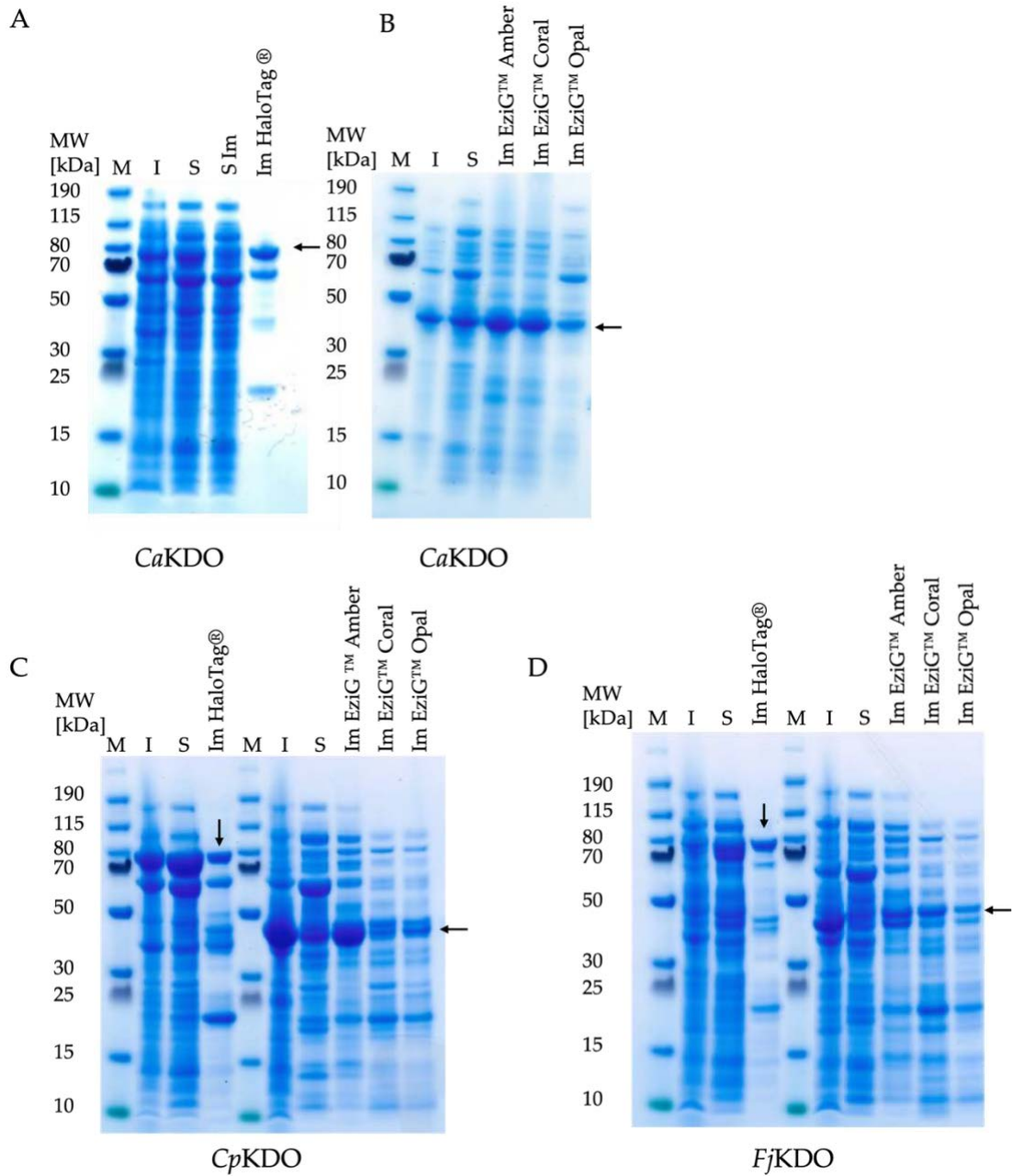


Figure S31: KDO immobilization on different carriers as indicated. M = marker, I = insoluble fraction, S = soluble fraction, IM= immobilized. Enzyme masses indicated by arrows: free variants with HisTag CaKDO = 40 kDa, CpKDO = 44 kDa, FjKDO = 42 kDa. HaloTag® variants: CaKDO = 75 kDa, CpKDO = 79 kDa, FjKDO = 77 kDa. Chaperones: GroEL = 60 kDa, GroES = 10 kDa.

## Results

### 2.2.3.2.3 Influence of the HaloTag® and immobilization on HaloLink™ resin on conversion and stability of CaKDO

The reaction was started by adding 1 mL reaction mix containing 10 mM L-lysine, 15 mM  $\alpha$ -ketoglutarate, 1 mM ammonium iron(II) sulfate, 2.5 mM L-ascorbic acid, 0.01 mM dithiothreitol (DTT) and 200 mM HEPES buffer, pH 7.5, to a 2 mL reaction tube containing either the lyophilized free CaKDO with His-Tag, the free HaloTagged – enzyme or the immobilized HaloTag®-enzyme, respectively. The reaction was mixed at 25 °C horizontally attached on a thermomixer to guarantee sufficient mixing of the beads and the reaction mixture.

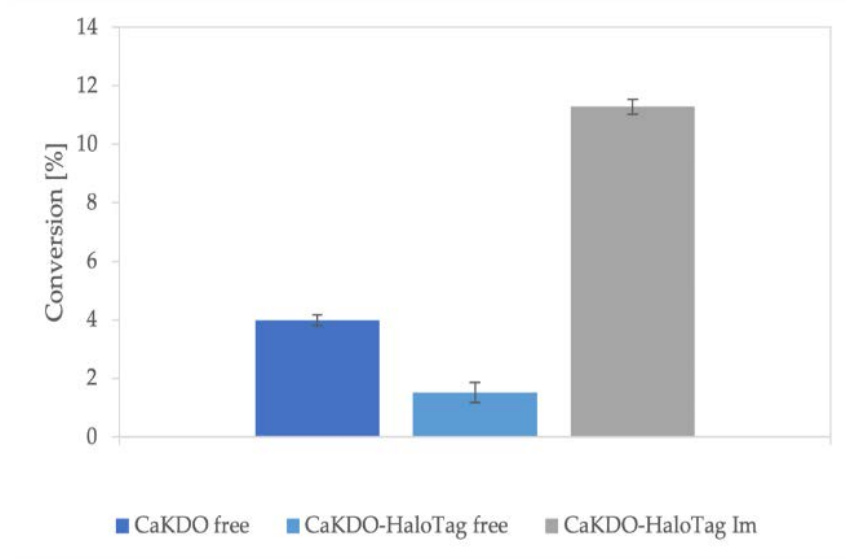


Figure S32: Stability under reaction conditions of free CaKDO with His-Tag, free CaKDO-HaloTag®, and CaKDO-HaloTag® immobilized on HaloLink™ resin: enzyme concentration 0.5 mg mL<sup>-1</sup>, reaction time 2 h.

## Results

### 2.2.3.3 SrLDC immobilization

#### 2.2.3.3.1 Determination of binding capacities of immobilized SrLDC

Binding capacities were determined as described in Chapter 2.2.3.1.1.

Table S7: Binding capacities of EziG™ and HaloLink resin loaded with SrLDC were measured by the BCA assay (Chapter 2.2.3.1.1). Data from two independent immobilizations from the same enzyme batch.

Enzyme	Immobilization method	enzyme load
		(EziG™: mg enzyme/ mg beads mg) (HaloTag®: mg enzyme/ mL HaloLink™ resin)
SrLDC	HaloTag®	7.14 ± 0.40
	Opal	0.082 ± 0.006
	Amber	0.105 ± 0.010
	Coral	0.126 ± 0.018

#### 2.2.3.3.2 Analysis of immobilized SrLDC by SDS PAGE

SDS PAGE was prepared as described in Chapter 2.2.3.1.2.

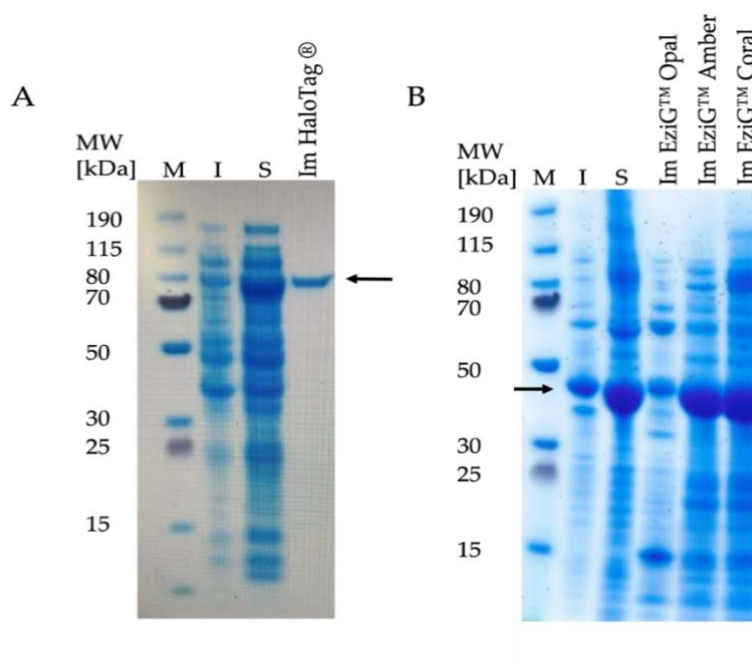


Figure S33: Analysis of SrLDC immobilisates. A) HaloTag®-immobilisate B) EziG™-immobilization on respective EziG™ Beads. M = marker, I = insoluble fraction, S = soluble fraction, IM= immobilized. Enzyme masses indicated by arrows: SrLDC-HisTag= 44 kDa, SrLDC-HaloTag® = 79 kDa. Chaperones: GroEL= 60 kDa, GroES= 10 kDa.

## Results

### 2.2.4 CaKDO-HaloTag® regeneration experiments upon repetitive batch studies

#### 2.2.4.1 Color change of CaKDO reaction after the first batch

Pictures were taken at the end of the repetitive batch experiments with the CaKDO-HaloTag® immobilisate as described in the main paper (Materials and Methods, Section 3.3.3.).

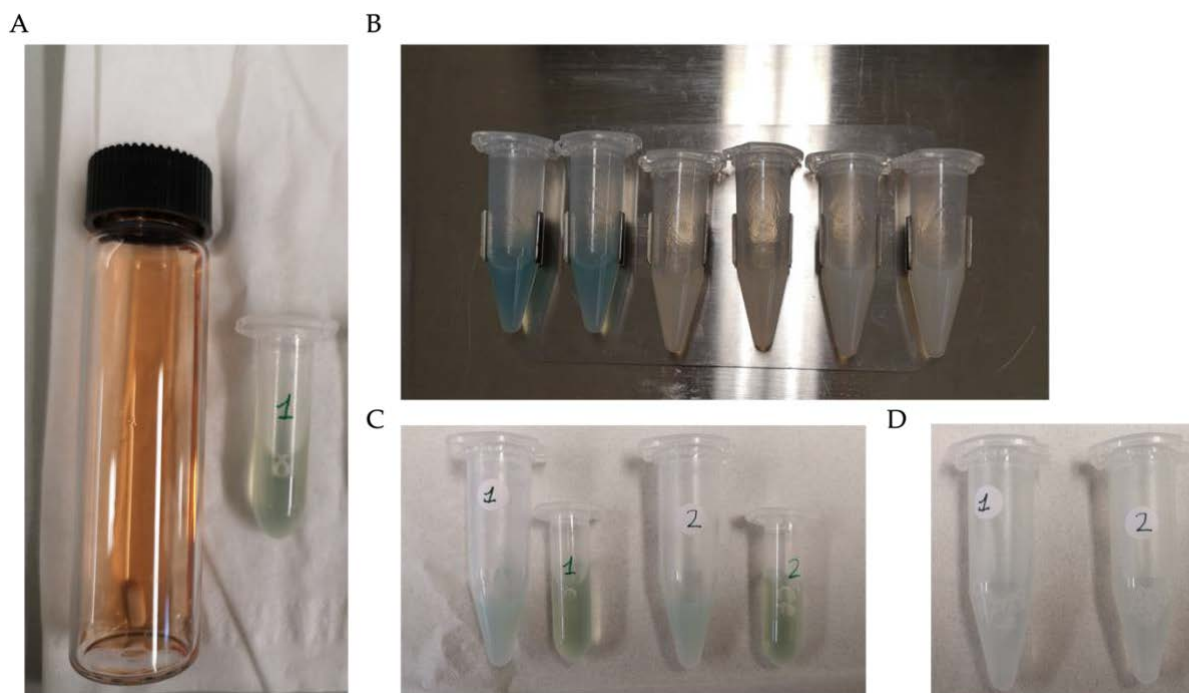


Figure S34: End of the first batch from repetitive batch experiments with CaKDO. A) Left: reaction mix before reaction (Main paper, Materials and Methods, Section 3.3.). Right: supernatant after first batch. B) Picture was directly taken after reaction. Left: Two reactions of CaKDO-HaloTag®, middle: two reactions of CpKDO-HaloTag®, right: FjKDO-HaloTag®, all immobilized on HaloLink™ resin. C) CaKDO-HaloTag® reaction after centrifugation. Large vessel with immobilisate, small vessel with supernatant D) CaKDO-HaloTag® immobilisate washed once with 50 mM HEPES, pH 7.5.

## Results

### 2.2.4.2 Regeneration of immobilized CaKDO-HaloTag®

The reaction took place as described (main paper, Materials and Methods, Section 3.3.3. and 3.3.4.). Samples were taken every 30 min for 2 h and after 24 h.

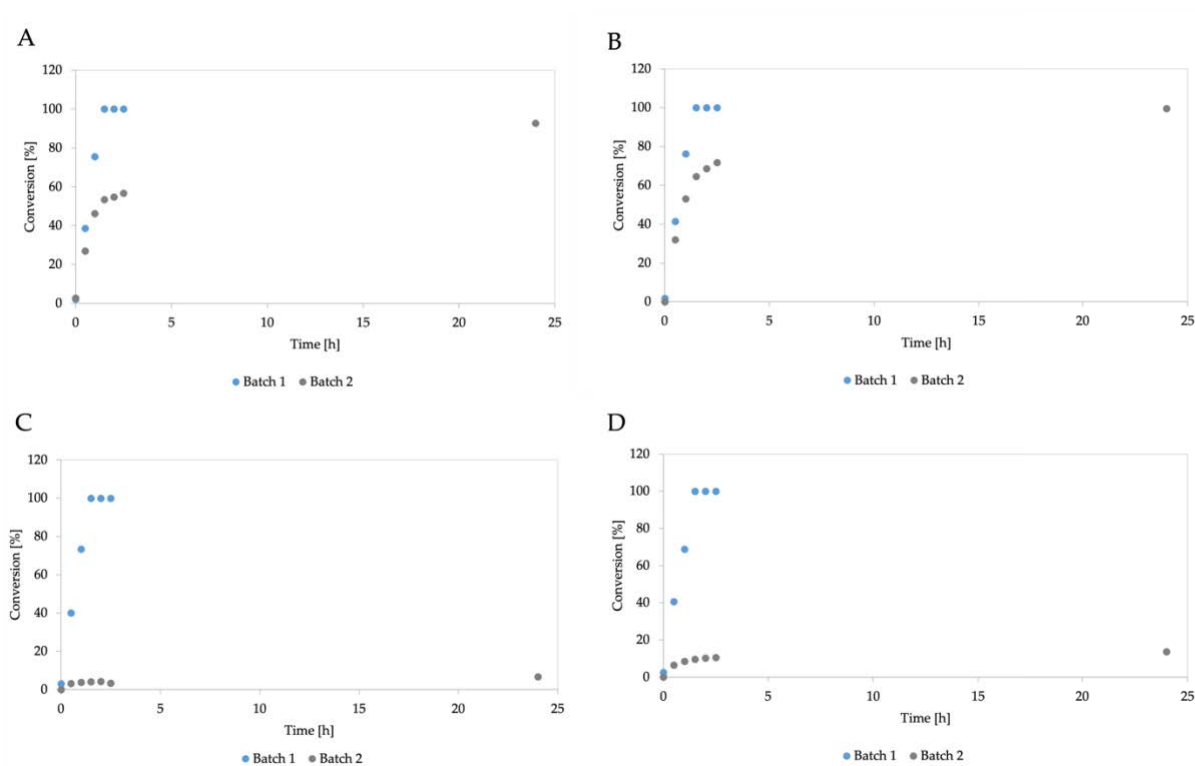
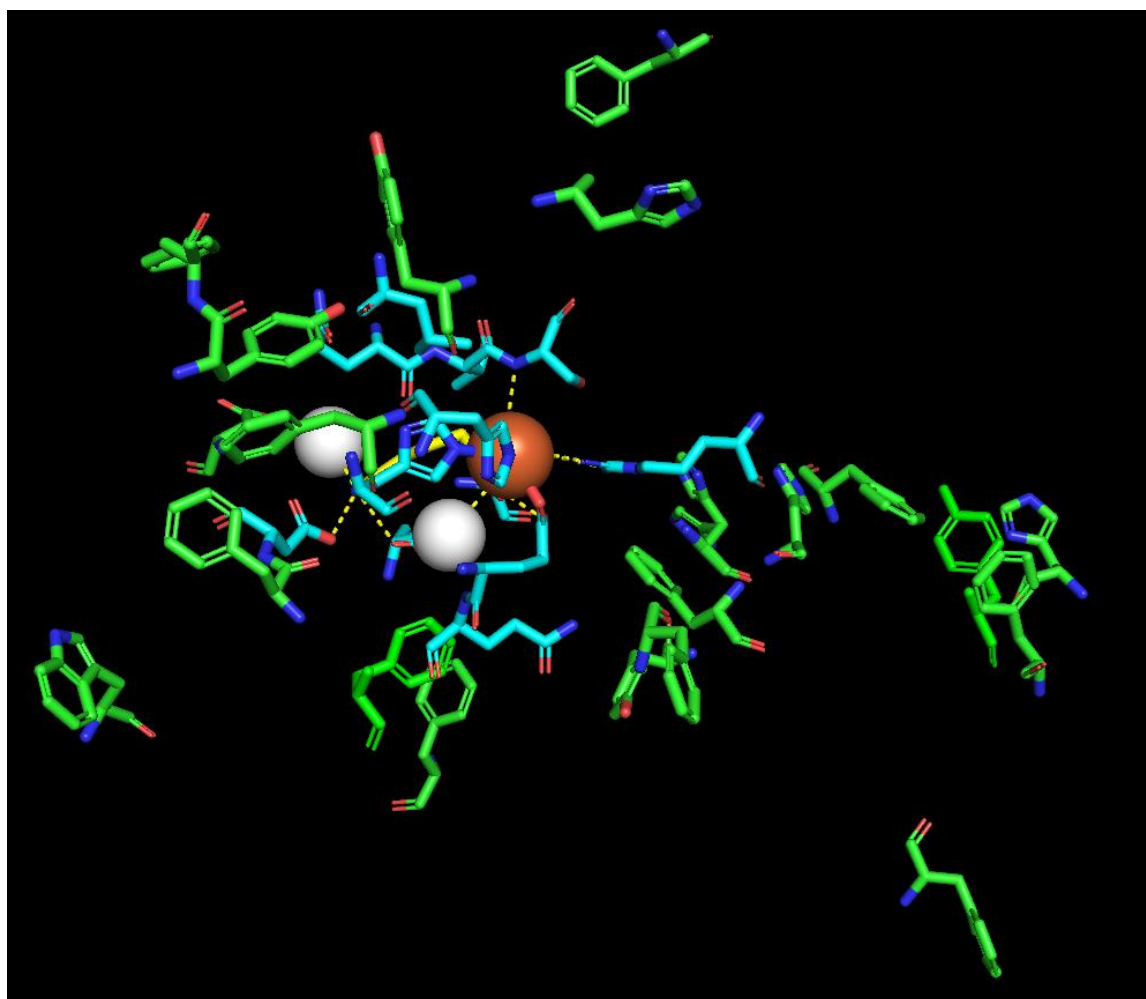


Figure S35: Regeneration studies for immobilized CaKDO-HaloTag®. A) Regeneration with 1 mM dithionite and 100 mM EDTA in 50 mM HEPES, pH 7.5. B) Regeneration with 10 mM dithionite and 100 mM EDTA in 50 mM HEPES, pH 7.5. C) Regeneration with 10 mM dithionite, 100 mM EDTA and 1 mM  $(\text{NH}_4)_2\text{Fe}(\text{SO}_4)_2$  in 50 mM HEPES, pH 7.5. Incubation over night at 4 °C. D) control. 50 mM HEPES, pH 7.5, no EDTA or dithionite added.

## Results

### 2.2.4.3 *CaKDO active site with aromatic residues*

The active site was presented with PyMOL based on PDB code 6F2A from Bastard et al. [5].



*Figure S36: CaKDO active site (blue) and close aromatic residues (green). L-lysine with polar interactions (yellow), Iron(II) (red sphere) and water (white sphere) bound to L-lysine.*



## Results

### 2.2.7 SrLDC reaction optimization

The reaction was started by adding 1 mL reaction mix containing 100-1500 mM L-lysine, 0.05-2 mM PLP and 100 mM HEPES buffer, pH 7.0-8.0, to a 2 mL reaction tube containing SrLDC-HaloTag® immobilized on HaloLink™ resin. The reaction was performed in an overhead shaker at 25 °C – 35 °C under exclusion of light.

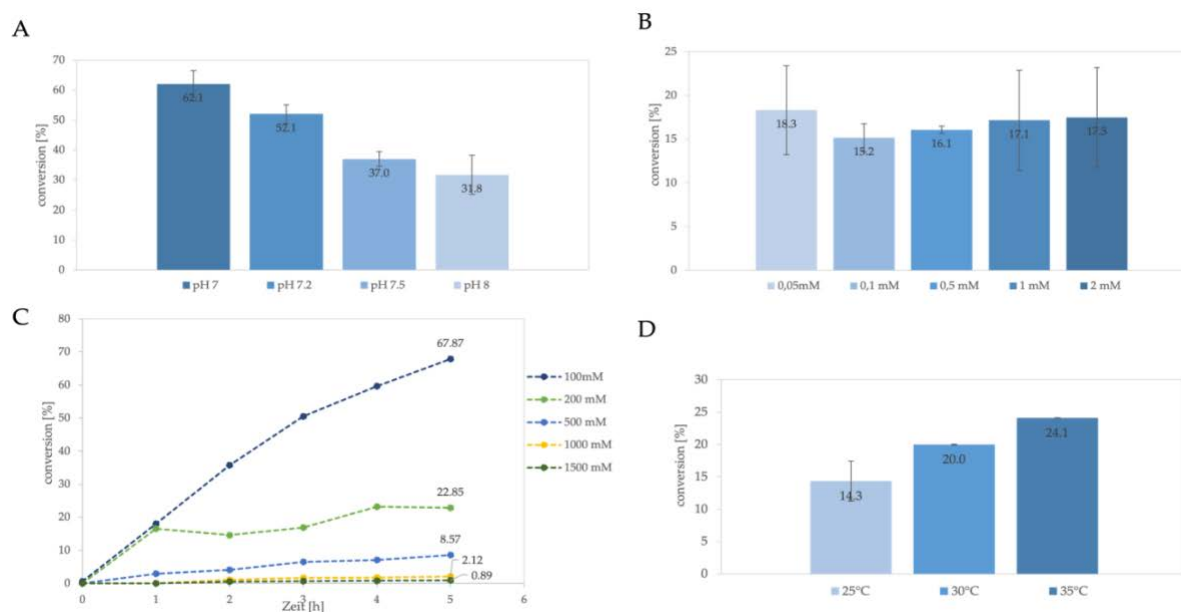


Figure S39: SrLDC-HaloTag® reaction optimization. A) Conversion at different pH values (7.0-8.0). B) Conversion with different PLP concentrations (0.05-2 mM). C) Different L-lysine concentrations (100-1500 mM). D) Different temperatures, 25 °C-35 °C. Reactions were done in the form of technical duplicates of the same enzyme batch but different immobilizations.

Table S8: Optimized reaction parameters tested for SrLDC-HaloTag reaction from L-lysine to cadaverine. Further information in SI Figure S39.

Parameter	range tested	optimal conditions
Buffer type	HEPES	HEPES
pH	7.0 - 8.0	7.0
Substrate concentration	0.1 M - 1.5M	0.1 M
PLP concentration	0.05 - 2 mM	2 mM
Temperature	25 °C – 35 °C	35 °C

## Results

### 2.2.8 Production of putrescin, cadaverine, and (2S)-hydroxy-cadaverine by HaloTag®-immobilized SrLDC

For preparative lab scale experiments 15 mL of the reaction mixture containing 100 mM of the respective substrate (L-lysine, L-ornithine, (3S)-hydroxy-L-lysine), 1 mM PLP and 100 mM HEPES buffer, pH 7.0, were added to the immobilized enzyme (1 mg mL<sup>-1</sup> for experiments with L-lysine, 1.5 mg mL<sup>-1</sup> for experiments with L-ornithine, 2.5 mg mL<sup>-1</sup> for experiments with (3S)-hydroxy-L-lysine). Reactions were performed in 50 mL falcon tubes in an overhead shaker at 35 °C under exclusion of light. Samples were taken every 10 min over a period of 1-2 h. The reaction was quenched by incubation for 5 min at 80 °C. Substrate and product concentrations were measured by HPLC (Main paper, Materials and Methods, Section 3.6.).

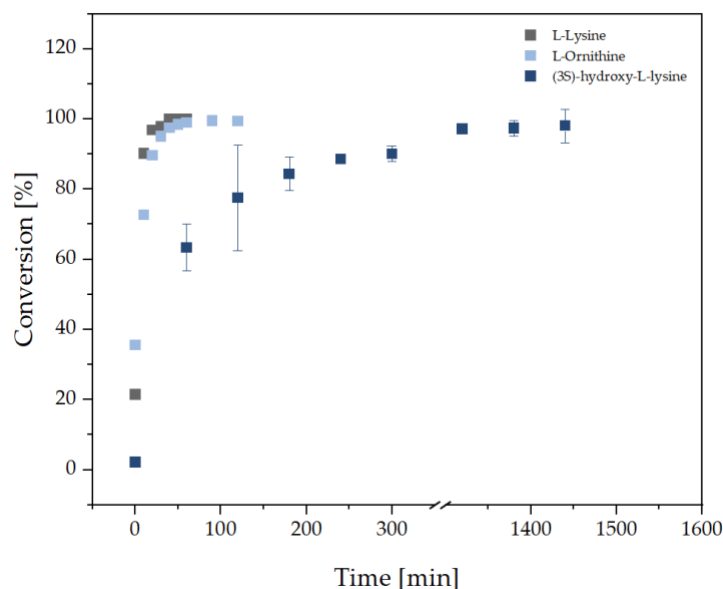


Figure S40: Preparative lab scale (15 mL) experiments with HaloTag® immobilized SrLDC and different substrates (L-lysine, L-Ornithine, (3S)-hydroxy-L-lysine).

## 2.2.9 HPLC

### 2.2.9.1 HPLC analysis with Diode Array Detector

All amino acid derivatives, diamines and (2*S*)-hydroxycadaverine were analyzed by amino acid HPLC on an Infinity Lab Poroshell HPH-C18, (4.6x100 mm, 2.7-micron) or Agilent Zorbax Eclipse Plus C18 (4.6x100 mm, 3.5 micron) and an UHPLC Guard Infinity lab Poroshell HPH-C18 (4.6x5 mm 2.7-micron) or ZORBAX RRHD Eclipse Plus C18 (2.1 mm, 1.8 μm) guard column using an Agilent 1260 Infinity Quaternary LC system (Agilent Technologies) equipped with a 1260 Diode Array Detector (detection wavelength 338 nm). Prior to injection, samples were diluted 1:100 (v/v) in 50 mM HEPES buffer, pH 7.5 and 1 mM L-histidine as internal standard was added. For analysis, a pre-column derivatization step with 9 μl *ortho*-phthaldialdehyde (OPA, Sigma-Aldrich) and 1 μl sample (6 mixing iterations) was performed. The mobile phase A was composed of 10 mM sodium borate buffer, pH 8.2, and the mobile phase B contained 45% (v/v) methanol, 45% (v/v) acetonitrile and 10% (v/v) water. For chromatographic separation, a gradient was applied with a flow of 1.5 mL min starting with 0% B, 1–6.8 min 0–47% B, 8.3-8.6 min 85% B, 8.8-10.5 min 100% B, 11.5-12 min 0% B.

Approximate retention times were 5.6 min for L-histidine (internal standard), 8.8 min for 5-hydroxy-D,L-lysine, 8.9 min for (4*S*)-hydroxy-L-lysine, 9.0 min for (3*S*)-hydroxy-L-lysine, 9.1 min for L-lysine, 9.4 min for (2*S*)-hydroxy-cadaverine and 10.0 min for cadaverine. Concentrations were derived from the linear calibration of five reference solutions (0.1 mM-2.5 mM) containing L-histidine, 5-hydroxy-D,L-lysine, L-lysine and cadaverine. Calibration was performed at least once per week or prior to every HPLC run. In order to correct possible effects of the derivatization efficiency due to the two amine groups present in L-lysine and its derivatives, conversions were calculated as followed:

$$\text{conversion}[\%] = \frac{100}{(\text{substrate conc.} + \text{product conc.})} \times \text{product conc.}$$

## Results

### Calibration

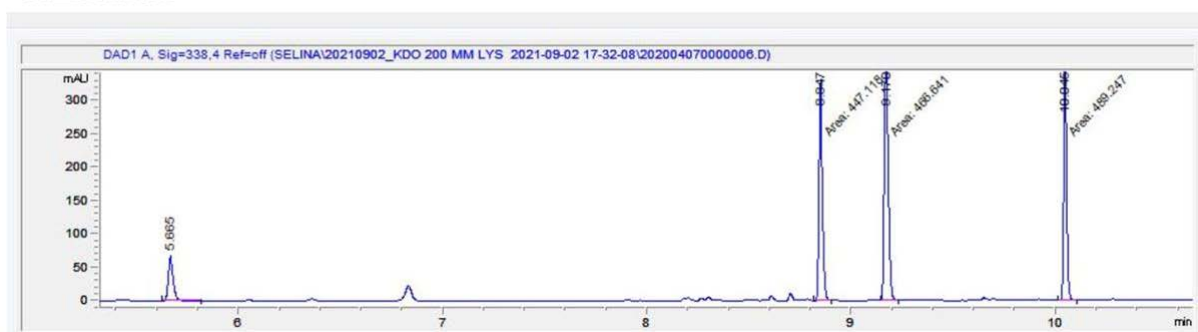


Figure S41: HPLC chromatograms of calibration. Approximate retention times were 5.6 min for L-histidine (internal standard), 8.8 min for (R,S)-5-hydroxy-D,L-lysine, 9.1 min for L-lysine, and 10.0 min for cadaverine.

An example of the conversion of L-lysine can be seen in Chapter 2.2.12.1.1 for (3*S*)-hydroxy-L-lysine and Chapter 2.2.12.2.1 for (4*R*)-hydroxy-L-lysine. The conversion of (3*S*)-hydroxy-L-lysine to (2*S*)-hydroxy-L-cadaverine in the cascade reaction with *Sr*LDC-HaloTag® is shown in Chapter 2.2.12.4.1

#### 2.2.9.2 HPLC analysis with fluorescence detector

The amino acids were separated and quantified as *ortho*-phthalaldehyde (OPA) derivatives by reverse phase chromatography using an Agilent 1290 Infinity I LC system Agilent Santa Clara USA© an ultra-high performance liquid chromatography system UHPLC© equipped with a fluorescence detector.

A gradient of sodium borate buffer A: 10 mM Na<sub>2</sub>HPO<sub>4</sub> 10 mM, Na<sub>2</sub>B<sub>4</sub>O<sub>7</sub> pH 8.2 and B: methanol was used as eluent for the Kinetex 2.6 μm EVO C18 100 Å, 100 x 2.1 mm, which was equipped with a SecurityGuard™ ULTRA cartridge protective column (Phenomenex, Aschaffenburg, Germany). The initial parameter for the gradient was set to 90% A and the gradient was changed in 1 minute to 80%. In the next 6 minutes solvent A was set to 30%. At 8 minutes the gradient was changed to 0% A and was hold for further 1.2 minutes. The re-equilibration started at 9.3 min and was carried out until 11.2 min were reached.

The derivatives were detected at 340 nm excitation and 450 emission wavelengths at a flow rate of 0.4 mL min. The temperature was at constant hold at 40 °C.

### **DAD versus FLD**

During method development, different detection strategies for amines and amino acids were tested, including measurement on an HPLC system with FLD detector and DAD detector. Since 3- and 4-hydroxy-L-lysine derivatives are not commercially available, the HPLCs were calibrated with 5-hydroxy-D,L-lysine, as explained in the materials and method section of the main paper. The DAD method (main paper, Materials and Methods, Section 3.6.) was compared to the method using an FLD detector (Chapter 2.2.9.2). In both cases, samples were derivatized with OPA. We found significant differences in the concentration of (3*S*)-hydroxy-L-lysine and (4*R*)-hydroxy-L-lysine with the different detectors (Figure S42). Using the DAD detector, we could follow the depletion of substrate (L-lysine) concomitant with an increase of the respective products ((4*R*)-hydroxy-L-lysine and (3*S*)-hydroxy-L-lysine) during the course of the reaction (Chapters 2.2.12.1.1, 2.2.12.2.1, 2.2.12.4.1). However, in analogous measurements with the FLD detector the areas for the hydroxy-L-lysines were smaller than expected regarding the conversion of the substrate (L-lysine) (data not shown). Since L-lysine contains two amino groups, their derivatization can lead to the generation of three different isoindol derivatives. The di-substituted OPA-derivates of both amino groups can thereby lead to an inner-molecular quenching of the fluorescence signal [6]. We figured out that the hydroxy group of hydroxy-L-lysines can enhance this quenching effect depending on the hydroxylation position (Figure 71). However, we do not know if this effect is concentration-dependent and if a calibration with the actual hydroxy-L-lysines can decrease this effect. Since the absorption of the OPA-derivatives is not impaired, we chose a DAD detector, although most previous publications dealing with the production of hydroxy-L-lysines analyzed the respective OPA-derivatives using an FLD detector [7,8].

## Results

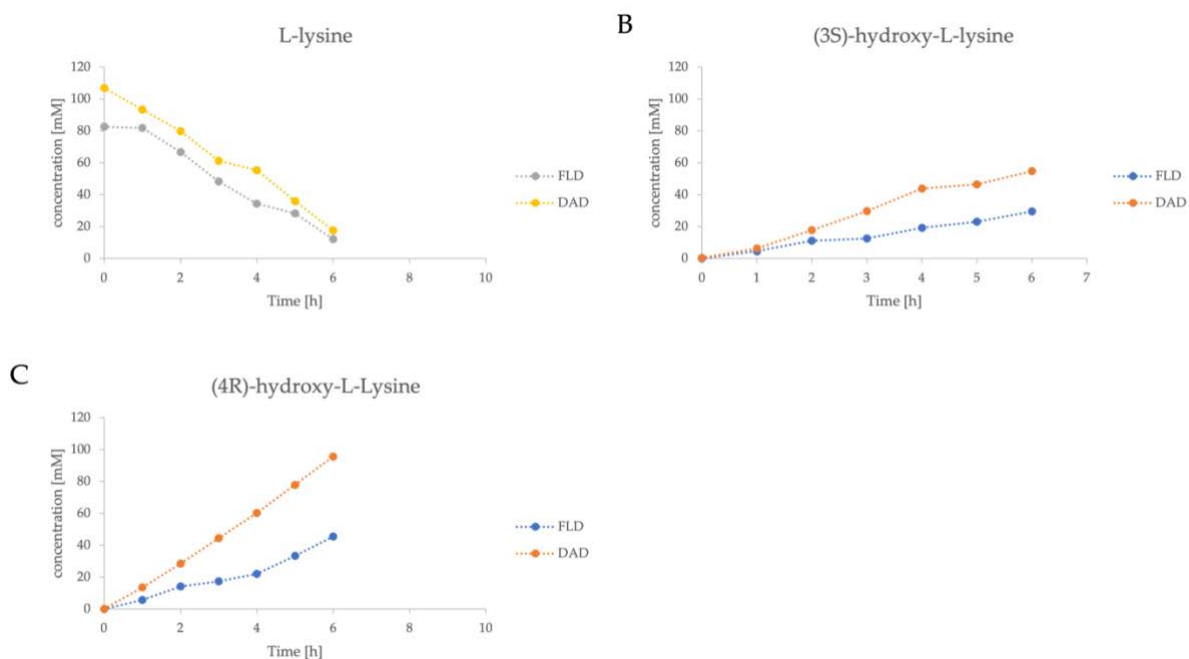


Figure S42: Comparison of respective substrate and product concentrations of samples following the conversion in preparative lab scale analyzed by HPLC with DAD detection and fluorescence detection, respectively.

### 2.2.10 NMR analysis

NMR spectra were measured on an Advance/DRX 600 MHz NMR Spektrometer (Bruker) with D<sub>2</sub>O (Eurisotop) at concentrations of approx. 30-55 mg mL<sup>-1</sup>.

After product purification of the respective hydroxy-L-lysines and the (2S)-hydroxy-cadaverine, 2D HSQC and COSY NMR spectra were recorded that can be found in Chapter 2.2.12.1.4 for (3S)-hydroxy-L-lysine, Chapter 2.2.12.2.3 for (4R)-hydroxy-L-lysine, and Chapter 2.2.12.4.3 for (2S)-hydroxy-cadaverine.

### 2.2.11 GC-ToF-MS analysis

Sample preparation as well as GC-TOF-MS measurements were carried out according to a previously described protocol [9].

#### Sample preparation

Prior to analysis 13  $\mu$ L aliquots of the samples were shock frozen in liquid nitrogen, stored at -20 °C and then lyophilized overnight in a Christ LT-105 freeze drier (Martin Christ Gefriertrocknungsanlagen, Osterode am Harz, Germany)

## Results

### Two step derivatization

The dried samples were consecutively derivatized with 50  $\mu\text{L}$  MeOX (20  $\text{mg mL}^{-1}$  O-methylhydroxylamine in pyridine) for 90 min at 30  $^{\circ}\text{C}$  and 600 rpm in an Eppendorf Thermomixer followed by incubation with additional 80  $\mu\text{L}$  of MSTFA (N-acetyl-N-(trimethylsilyl)-trifluoroacetamide) for 90 min at 40  $^{\circ}\text{C}$  and 600 rpm.

### MS Data Acquisition

For the determination of the derivatized metabolites an Agilent 8890N double SSL gas chromatograph (Agilent, Waldbronn, Germany) equipped with a L-PAL3-S15 liquid autosampler was used, coupled to a LECO GCxGC HRT+ 4D high resolution time of flight mass spectrometer (LECO, Mönchengladbach, Germany). The system was controlled by the LECO ChromaToF software.

1  $\mu\text{L}$  sample was injected into a split/splitless injector at 280  $^{\circ}\text{C}$  at varying split modes.

For 1D GC analysis the Back Injector was equipped with a 30 m Agilent EZ-Guard VF-5 ms + 10 m guard column (Agilent, Waldbronn, Germany).

For 2D GCxGC analysis the Front Injector was equipped with a 30 m HP 5-ms Ui column (HP) connected to a 2 m Rtxi17 (Restek) in a secondary oven. Constant helium flow was adjusted to 1  $\text{mL m}^{-1}$  in for the active injector and column and to 0.5  $\text{mL min}^{-1}$  for the passive injector. The GC temperature program started at 60  $^{\circ}\text{C}$  with a hold time of 2 min, followed by a temperature ramp of +12  $^{\circ}\text{C/min}$  up to the final temperature of 300  $^{\circ}\text{C}$ , hold time of 8 min. Total run time of 30 min. The secondary oven temperature offset was set to +15  $^{\circ}\text{C}$  above the first oven temperature. The transfer line temperature was set to 300  $^{\circ}\text{C}$ . The ToF MS was operated in positive electron impact [EI]<sup>+</sup> mode at an electron energy of 70 eV. Ion source temperature was set to 250  $^{\circ}\text{C}$ .

The MS was tuned and calibrated with the mass fragmentation pattern of PFTBA (Perfluoro-tri-n-butylamine, heptacosafuorotributylamine). During analysis the accurate masses were corrected to a single point lockmass of PFTBA as an external reference at  $m/z$  218,9856.

1D data acquisition was done in stick mode with a scan rate of 200 scans/sec.

### Peak Identification

For identification of known metabolites we used the comparison of the actual RI value (Retention time Index) and a baseline noise subtracted fragmentation pattern to our in house accurate  $m/z$  database JuPoD, and the commercial nominal database NIST20 (National Institute of Standards and Technology, USA).

## Results

Unknown peaks were identified by a comparison of actual fragmentation pattern and fragment elemental composition to known fragment masses from our in house JuPoD database and were verified by virtual derivatization and fragmentation of the predicted structure.

For GC spectra of all products and the standard 5-hydroxy-D,L-lysine see Chapter 2.2.11.

The mass fragment analyses and the product specific fragments can be found in Chapter 2.2.11

The mass spectra of the respective products can be found in Chapter 2.2.12.1.2 for (3*S*)-hydroxy-L-lysine, Chapter 2.2.12.2.2 for (4*R*)-hydroxy-L-lysine, Chapter 2.2.12.3.1 for the standard 5-hydroxy-D,L-lysine, and Chapter 2.2.12.4.2.2.2.12.4 for (2*S*)-hydroxy-cadaverine.

Comparison of the (3*S*)-hydroxy-L-lysine produced in this work and a sample produced by Baud et al. can be found in Chapter 2.2.12.1.3.

## Results

### 2.2.11.1 GC-ToF-MS GC chromatogram of all products

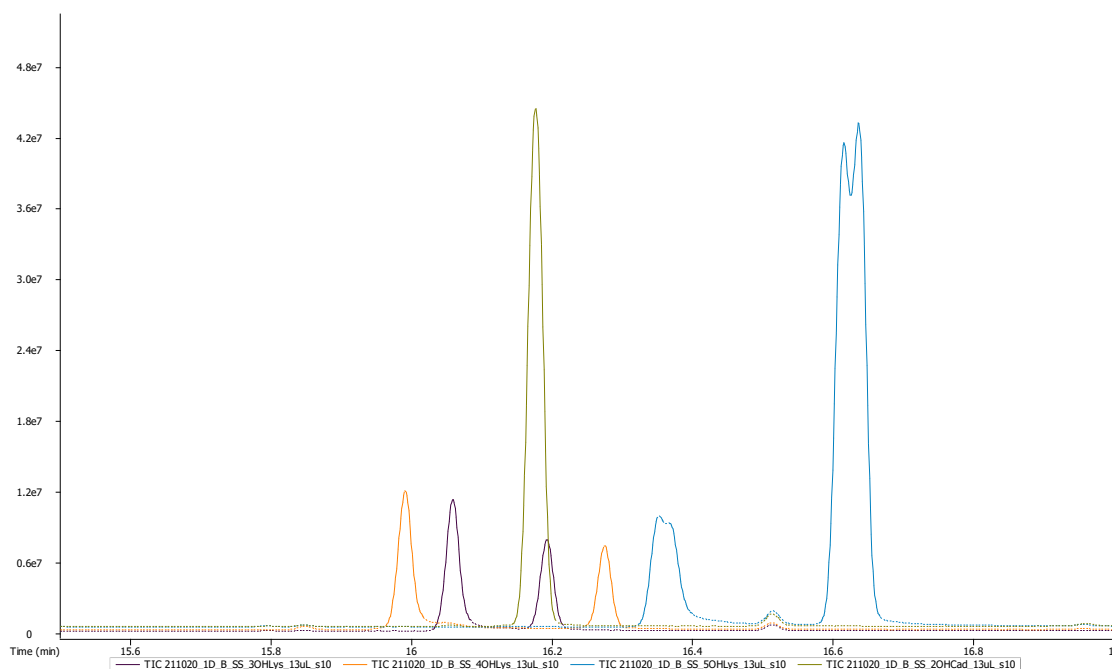


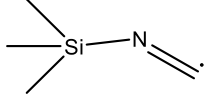
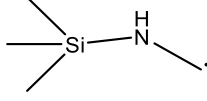
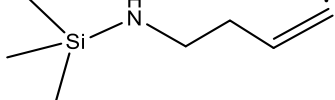
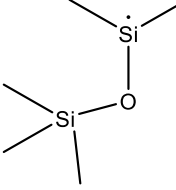
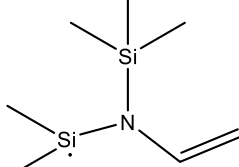
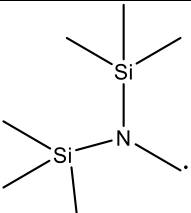
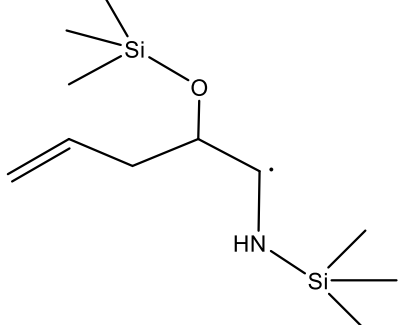
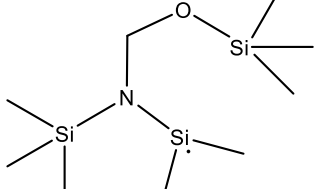
Figure S43: GC chromatogram of GC-ToF-MS analytics. blue: 5-hydroxy-D,L-lysine TMS species indicating the presence of diastereomers by double peaks, orange= (4R)-hydroxy-L-lysine TMS species, purple= (3S)-hydroxy-L-lysine TMS species, green= (2S)-hydroxy-cadaverine TMS species (second species more upstream of chromatogram).

### 2.2.11.2 GC-ToF-MS fragment analysis

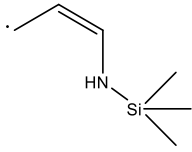
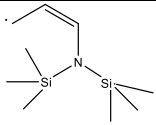
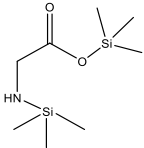
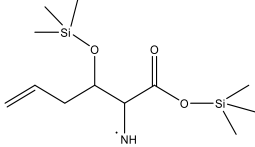
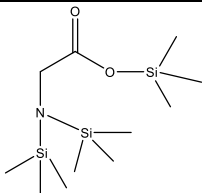
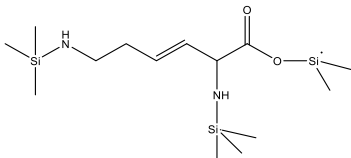
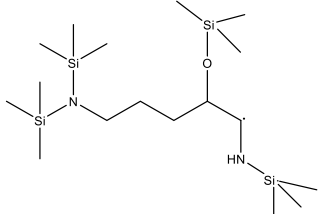
Table S9: Table of MS fragments showing the common fragments of all spectra and the product specific fragments.

common fragments (structure and formula)	[Mass] <sup>+</sup> u (Da) C = 12,0000
 C <sub>2</sub> H <sub>7</sub> Si•	59,031153
 C <sub>3</sub> H <sub>9</sub> Si•	73,046803
 C <sub>3</sub> H <sub>8</sub> NSi•	86,042052

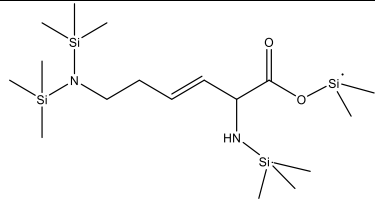
# Results

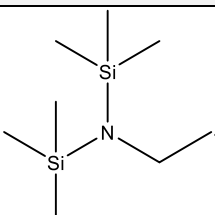
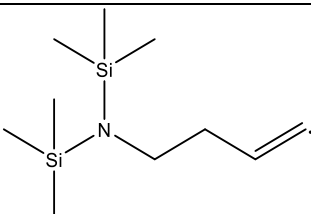
 <p style="text-align: center;"><math>C_4H_{10}NSi\bullet</math></p>	100,057702
 <p style="text-align: center;"><math>C_4H_{12}NSi\bullet</math></p>	102,073352
 <p style="text-align: center;"><math>C_7H_{16}NSi\bullet</math></p>	142,104652
 <p style="text-align: center;"><math>C_5H_{15}OSi_2\bullet</math></p>	147,065595
 <p style="text-align: center;"><math>C_7H_{18}NSi_2\bullet</math></p>	172,097229
 <p style="text-align: center;"><math>C_7H_{20}NSi_2\bullet</math></p>	174,112879
 <p style="text-align: center;"><math>C_{11}H_{26}NOSi_2\bullet</math></p>	244,154744
 <p style="text-align: center;"><math>C_9H_{26}NOSi_3\bullet</math></p>	248,131670

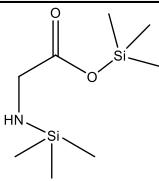
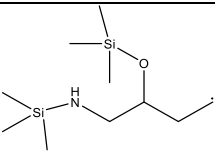
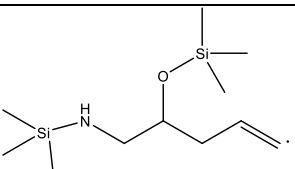
## Results

Specific fragments of 3-HO-Lysine	[Mass] <sup>+</sup> u (Da) C = 12,0000
 <p style="text-align: center;"><math>C_6H_{14}NSi\bullet</math></p>	128,089002
 <p style="text-align: center;"><math>C_9H_{22}NSi_2\bullet</math></p>	200,128529
 <p style="text-align: center;"><math>C_8H_{21}NO_2Si_2\bullet</math></p>	219,110533
 <p style="text-align: center;"><math>C_{12}H_{26}NO_3Si_2\bullet</math></p>	288,144573
 <p style="text-align: center;"><math>C_{11}H_{29}NO_2Si_3</math></p>	291,150060
 <p style="text-align: center;"><math>C_{14}H_{33}N_2O_2Si_3\bullet</math></p>	345,184434
 <p style="text-align: center;"><math>C_{17}H_{45}N_2OSi_4\bullet</math></p>	405,260347

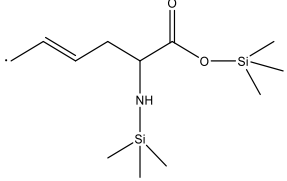
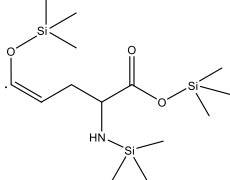
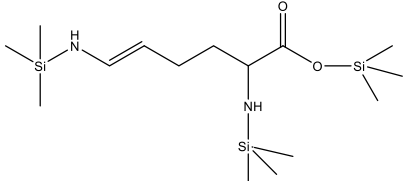
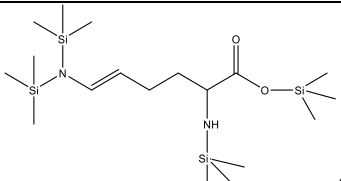
## Results

 <p><math>C_{17}H_{41}N_2O_2Si_4\bullet</math></p>	417,223961
---	------------

Specific fragments of 4-HO-Lysine	[Mass] <sup>+</sup> u (Da)
 <p><math>C_8H_{22}NSi_2\bullet</math></p>	188,128529
 <p><math>C_{10}H_{24}NSi_2\bullet</math></p>	214,144179

Specific fragments of 5-HO-Lysine	[Mass] <sup>+</sup> u (Da)
 <p><math>C_8H_{21}NO_2Si_2</math></p>	219,110533
 <p><math>C_{10}H_{26}NOSi_2\bullet</math></p>	232,154744
 <p><math>C_{11}H_{26}NOSi_2\bullet</math></p>	244,154744

# Results

 <p style="text-align: center;"><math>C_{12}H_{26}NO_2Si_2\bullet</math></p>	272,149659
 <p style="text-align: center;"><math>C_{14}H_{32}NO_3Si_3</math></p>	346,168450
 <p style="text-align: center;"><math>C_{15}H_{36}N_2O_2Si_3</math></p>	360,207909
 <p style="text-align: center;"><math>C_{18}H_{44}N_2O_2Si_4\bullet</math></p>	432,247436

## Results

### 2.2.12 Instrumental analytics of products

#### 2.2.12.1 Instrumental analysis of (3S)-hydroxy-L-lysine

##### 2.2.12.1.1 HPLC

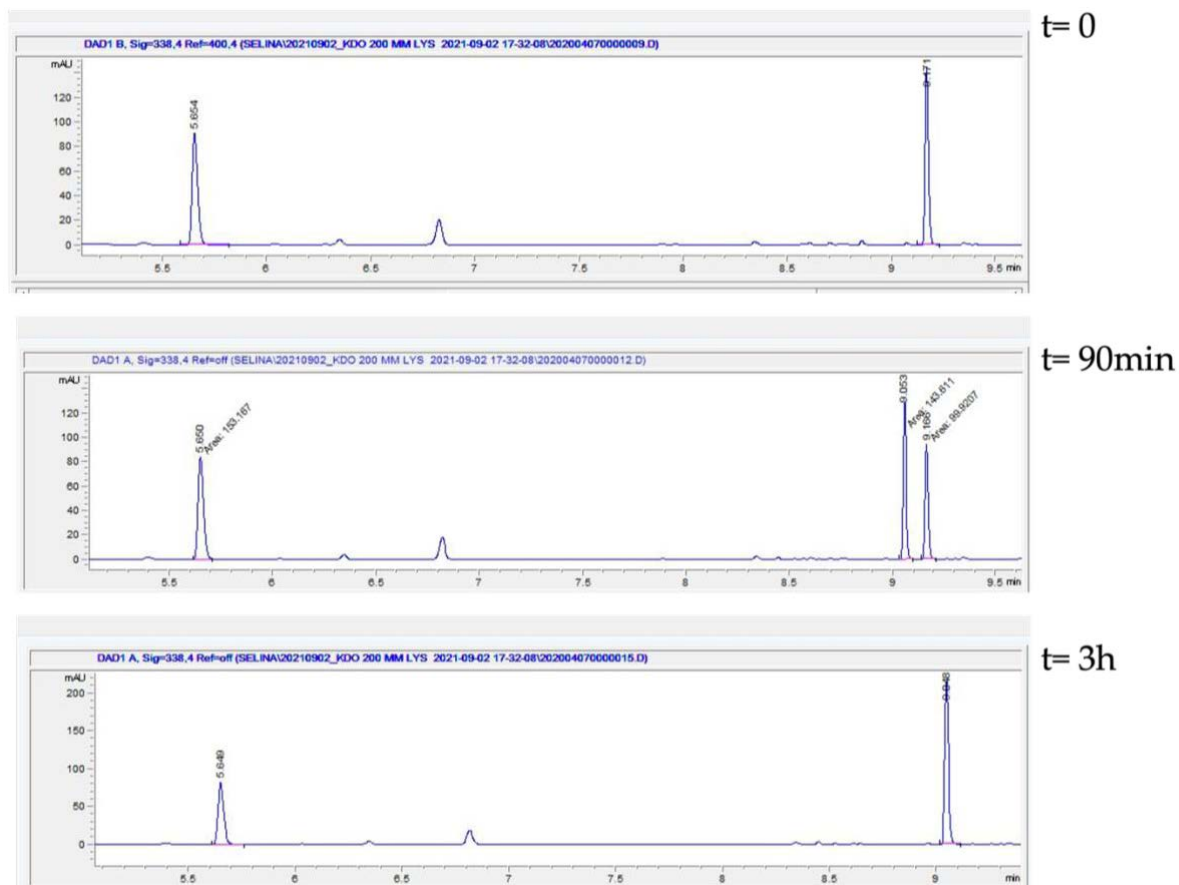


Figure S44: HPLC chromatograms of the monitoring of L-lysine hydroxylation by CaKDO-HaloTag®. Peaks: L-histidine (internal standard): 5.6 min, (3S)-hydroxy-L-lysine: 9.0 min, L-lysine: 9.1 min.

## Results

### 2.2.12.1.2 GC-ToF-MS

#### GC- Chromatogram

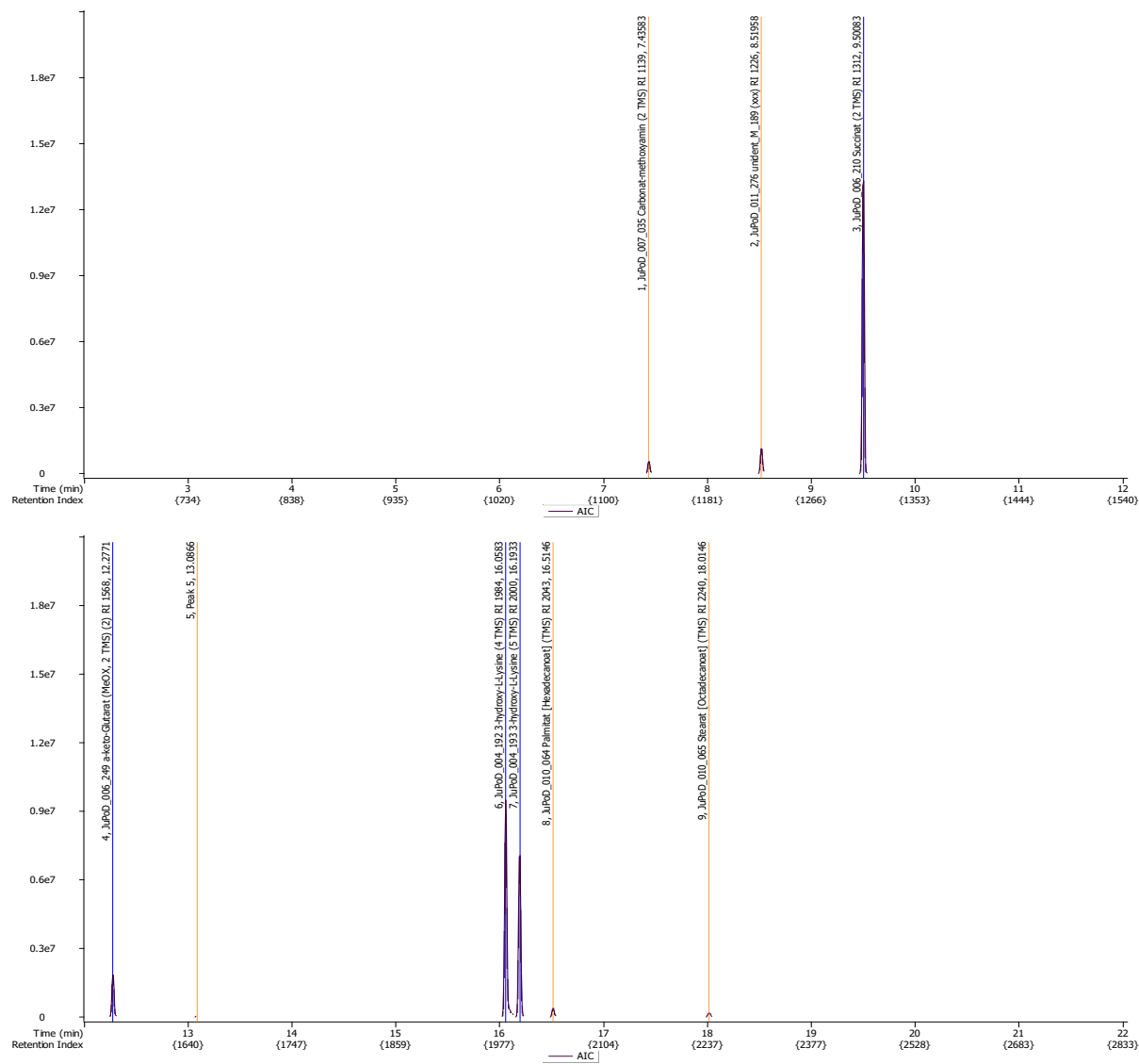


Figure S45: GC chromatogram of the supernatant of a biotransformation towards (3S)-hydroxy-L-lysine. Besides the target product, the supernatant contains  $\alpha$ -ketoglutarate, succinate, and traces of palmitate and stearate.

# Results

## MS-Spectra

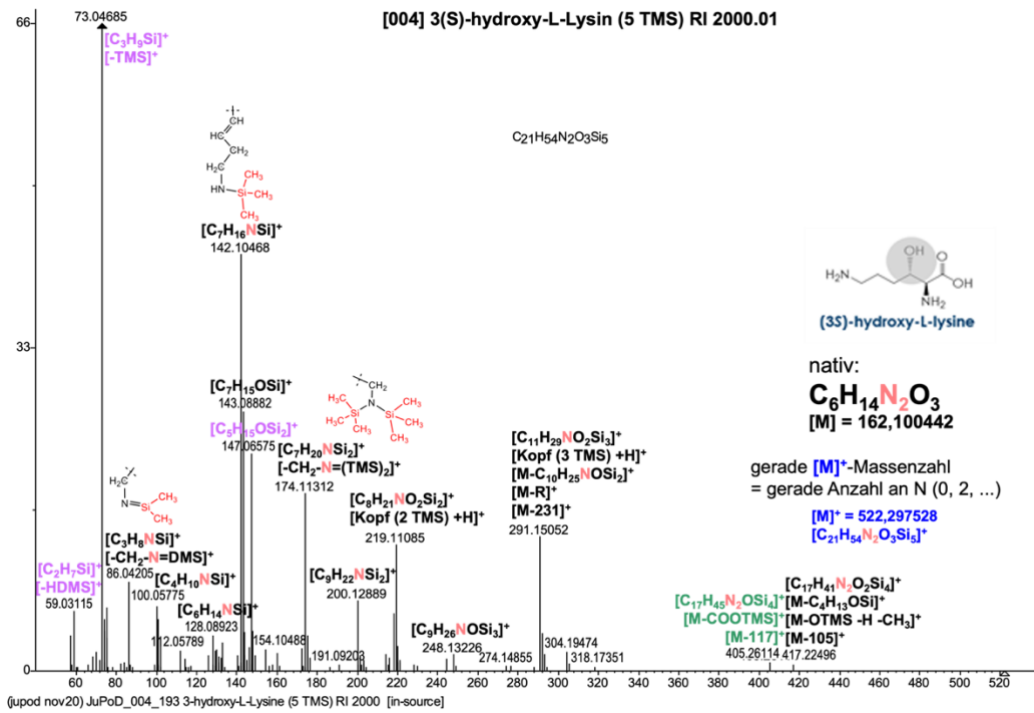


Figure S46: GC-ToF-MS spectrum of the (3S)-hydroxy-L-lysine-5 TMS derivative.

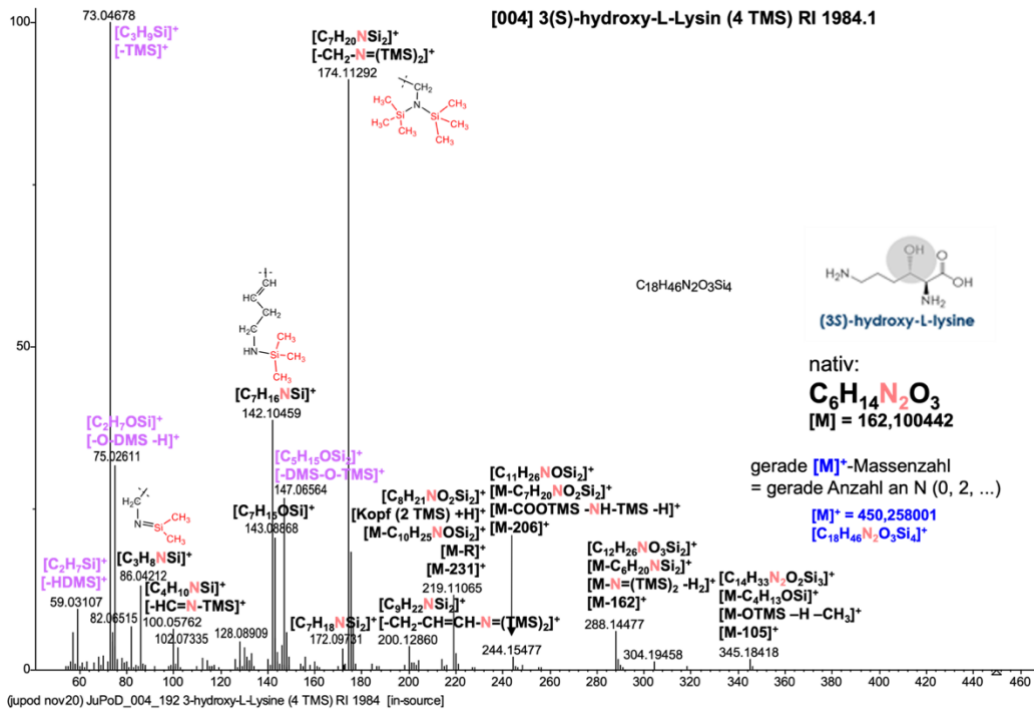


Figure S47: GC-ToF-MS spectrum of the (3S)-hydroxy-L-lysine-4 TMS derivative.

## Results

### 2.2.12.1.3 Comparison of (3S)-hydroxy-L-lysine from Baud et al. [2,3]

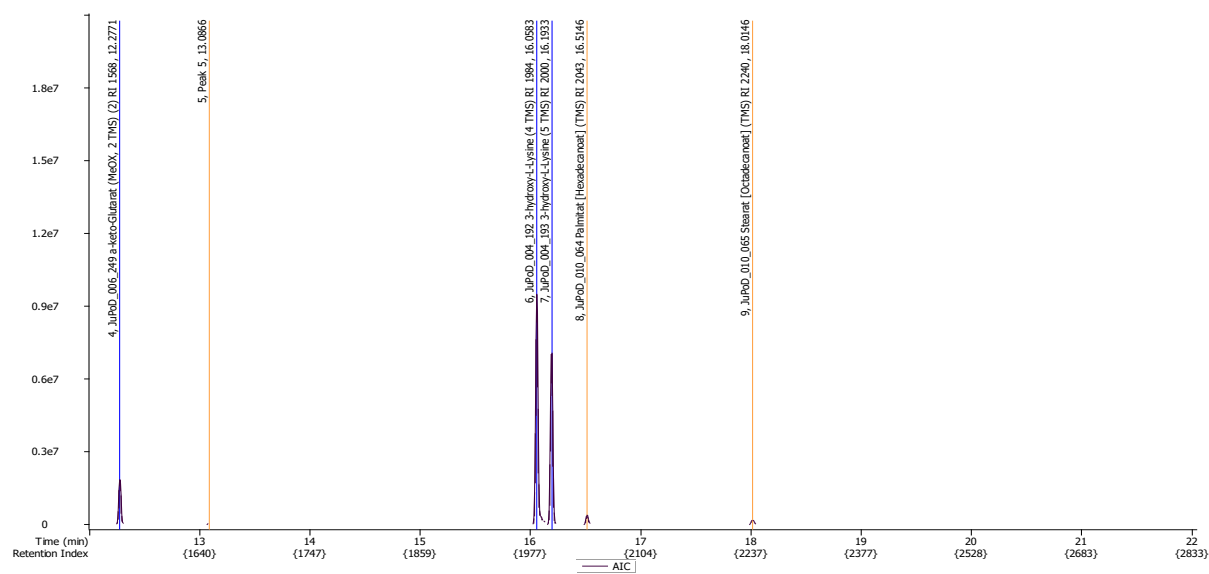


Figure S48: (3S)-hydroxy-L-lysine produced in this work. GC chromatogram from GC-ToF-MS analytics showing the two TMS species of the (3S)-hydroxy-L-lysine fragments.

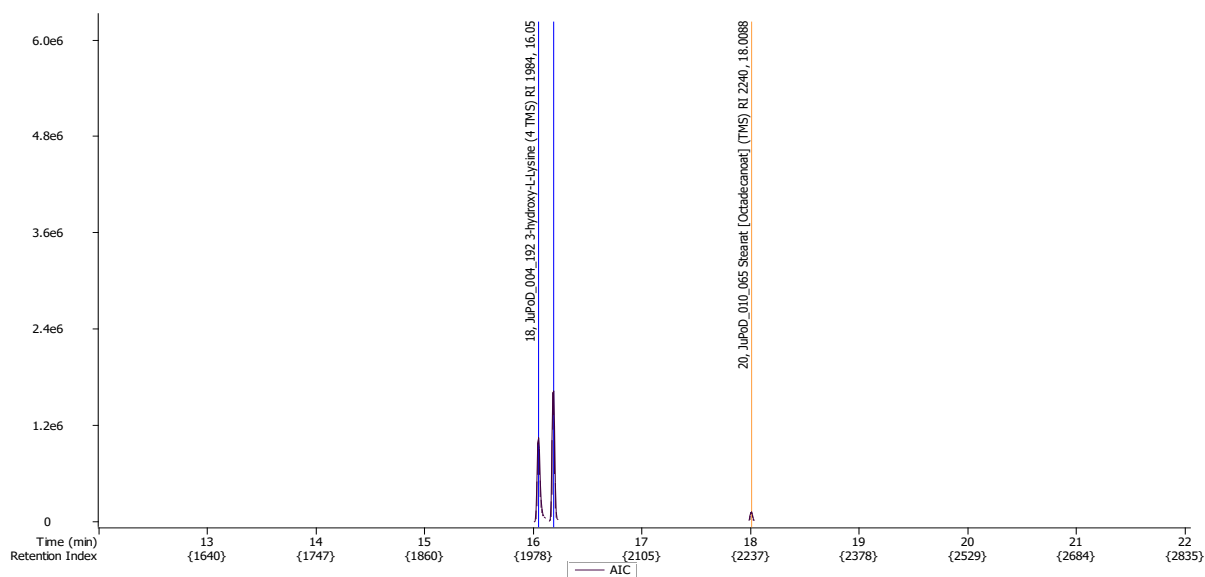


Figure S49: (3S)-hydroxy-L-lysine produced by Baud et al. [2,3]. GC chromatogram from GC-ToF-MS analytics showing the two TMS species of the (3S)-hydroxy-L-lysine fragments.

## Results

(3*S*)-hydroxy-L-lysine produced in this work:

Table S10: Table of (3*S*)-hydroxy-L-lysine specific fragments and properties.

fragment detected	formula	retention time (min)	Lib. RI	Expected Ion m/z	similarity
JuPoD_004_192 (3 <i>S</i> )-hydroxy-L-Lysine (4 TMS) RI 1984	C <sub>18</sub> H <sub>46</sub> N <sub>2</sub> O <sub>3</sub> Si <sub>4</sub>	16.06	1984.70(1)	450.258001	951
JuPoD_004_193 (3 <i>S</i> )-hydroxy-L-Lysine (5 TMS) RI 2000	C <sub>21</sub> H <sub>54</sub> N <sub>2</sub> O <sub>3</sub> Si <sub>5</sub>	16.19	2000.70(1)	522.297528	950

(3*S*)-hydroxy-L-lysine produced by Baud et al. [2,3]:

Table S11: Table of (3*S*)-hydroxy-L-lysine specific fragments and properties.

fragment detected	formula	retention time (min)	Lib. RI	Expected Ion m/z	similarity
JuPoD_004_192 3-hydroxy-L-Lysine (4 TMS) RI 1984	C <sub>18</sub> H <sub>46</sub> N <sub>2</sub> O <sub>3</sub> Si <sub>4</sub>	16.05	1984.70(1)	450.258001	919
JuPoD_004_193 3-hydroxy-L-Lysine (5 TMS) RI 2000	C <sub>21</sub> H <sub>54</sub> N <sub>2</sub> O <sub>3</sub> Si <sub>5</sub>	16.19	2000.70(1)	522.297528	921

## Results

### 2.2.12.1.4 NMR

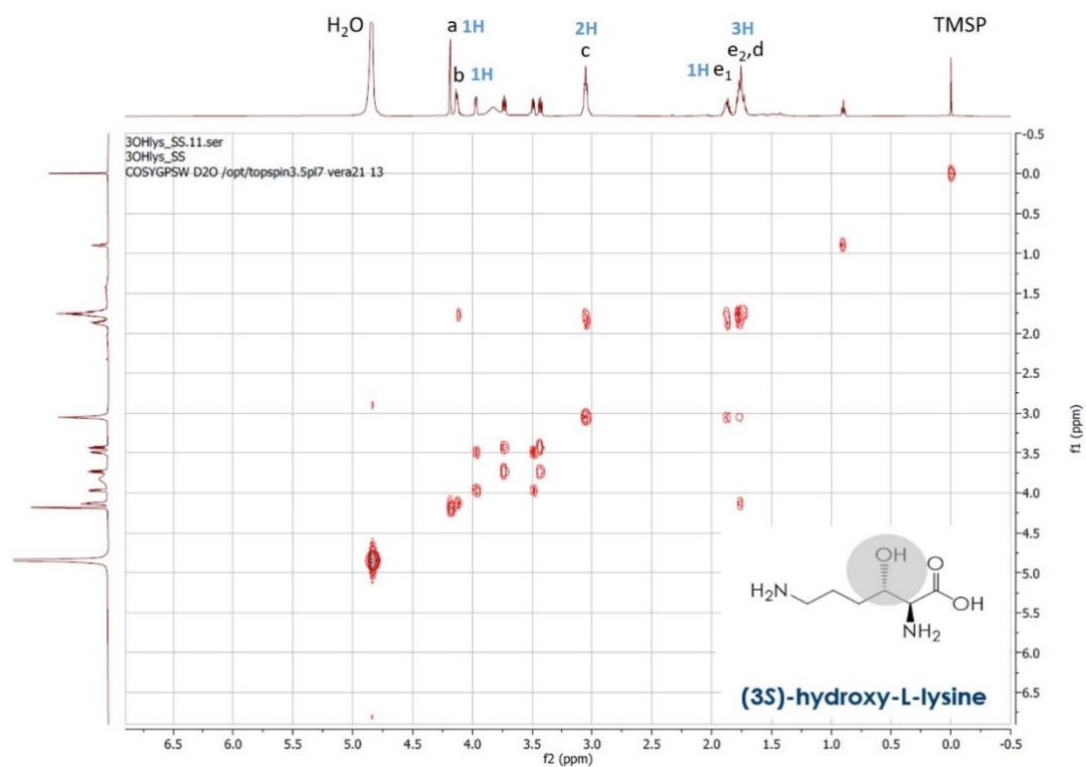


Figure S50: COSY NMR of (3S)-hydroxy-L-lysine. Yellow rectangles show impurities still present after purification.

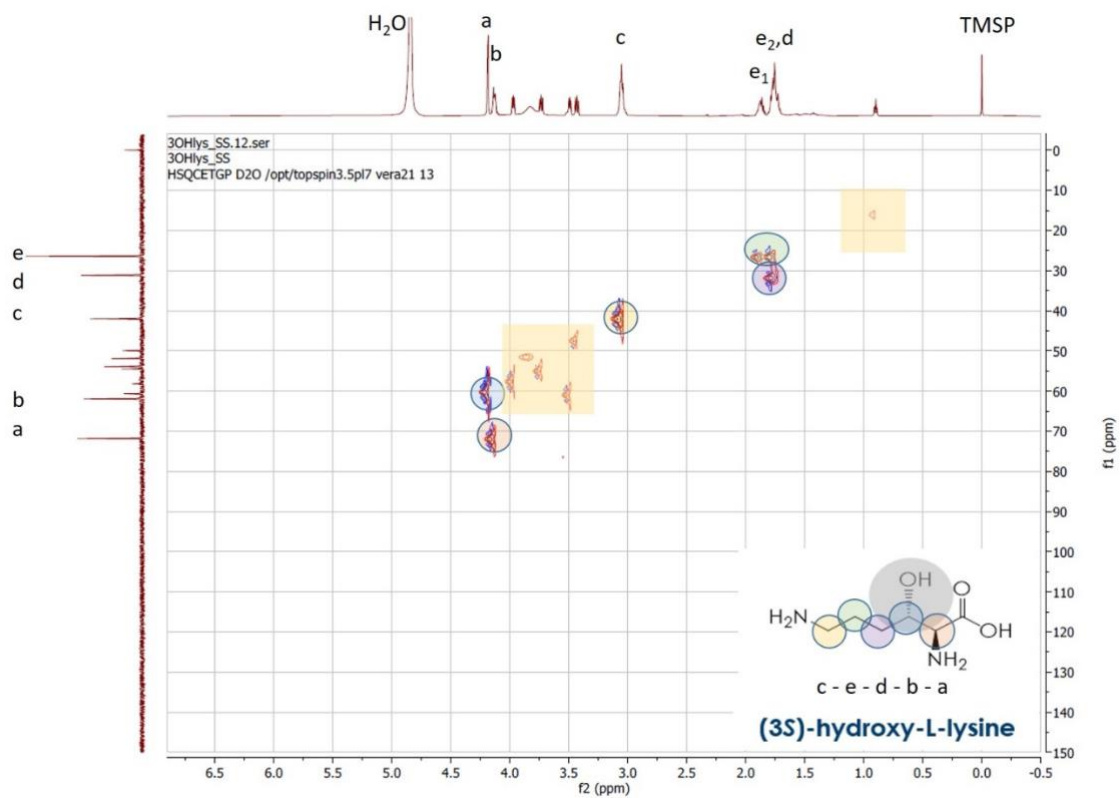


Figure S51: 2D HSQC NMR of (3S)-hydroxy-L-lysine. Yellow rectangles show impurities still present after purification.

## Results

### 2.2.12.2 Instrumental analysis of (4R)-hydroxy-L-lysine

#### 2.2.12.2.1 HPLC

#### (4R)-hydroxy-L-lysine

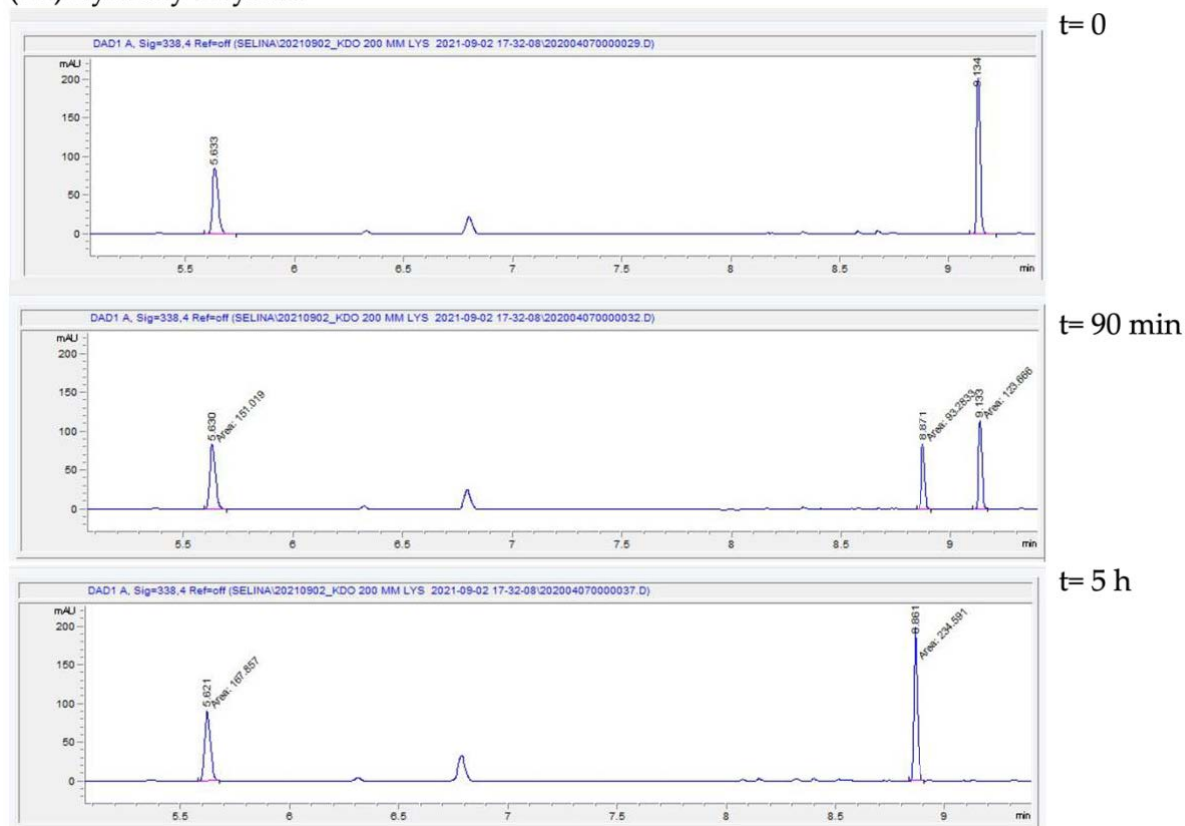


Figure S52: HPLC chromatograms of the monitoring of L-lysine hydroxylation by CpKDO- or FjKDO-HaloTag®. Peaks: L-histidine (internal standard): 5.6 min, (4R)-hydroxy-L-lysine: 8.9 min, L-lysine: 9.1 min.

## Results

### 2.2.12.2.2 GC-ToF-MS

#### GC-Chromatogram

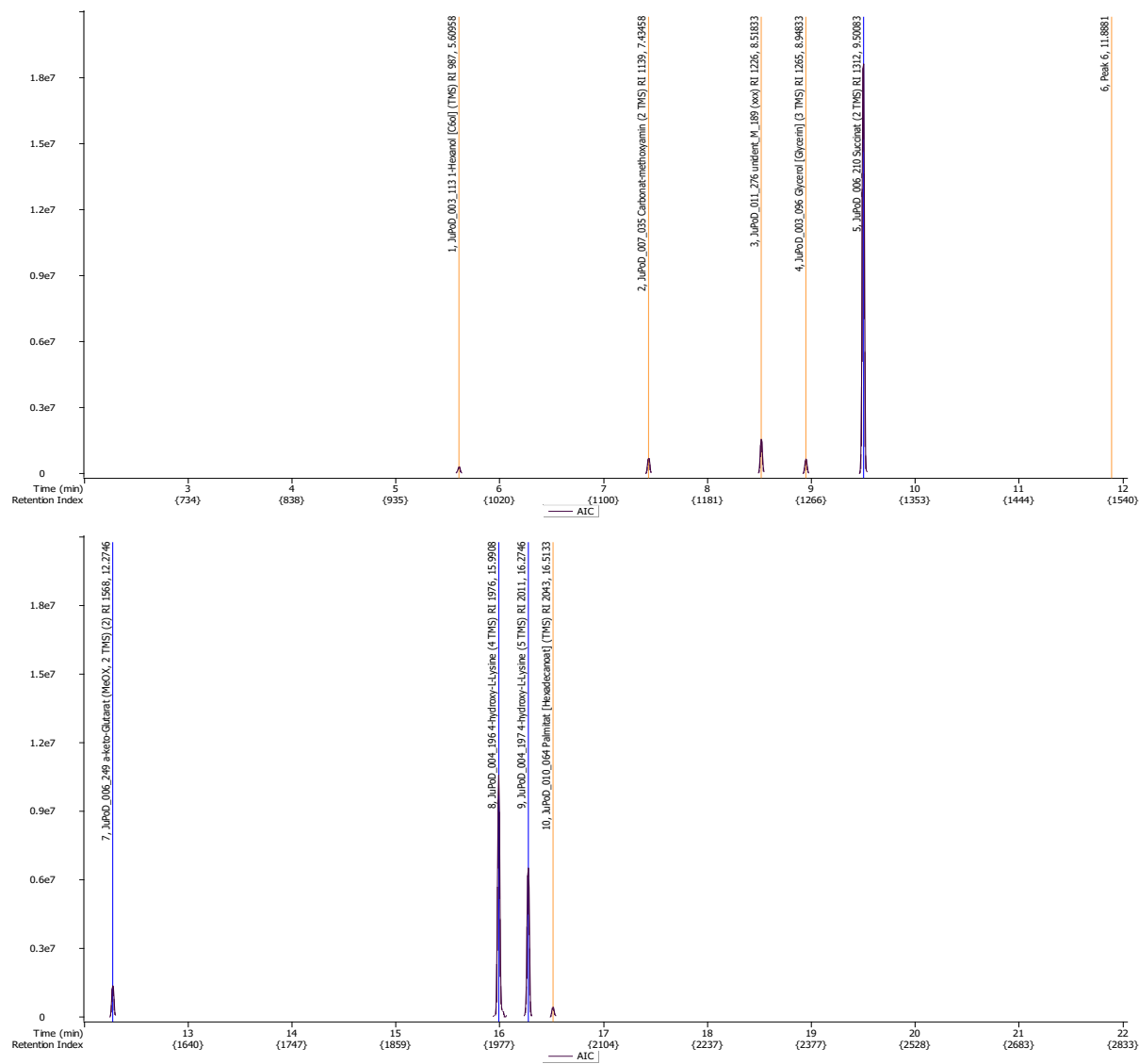


Figure S53: GC chromatogram of the supernatant of a biotransformation towards (4R)-hydroxy-L-lysine. Besides the target product, the supernatant contains  $\alpha$ -ketoglutarate, succinate and traces of palmitate and glycerol and hexanol.

# Results

## MS-Spectra

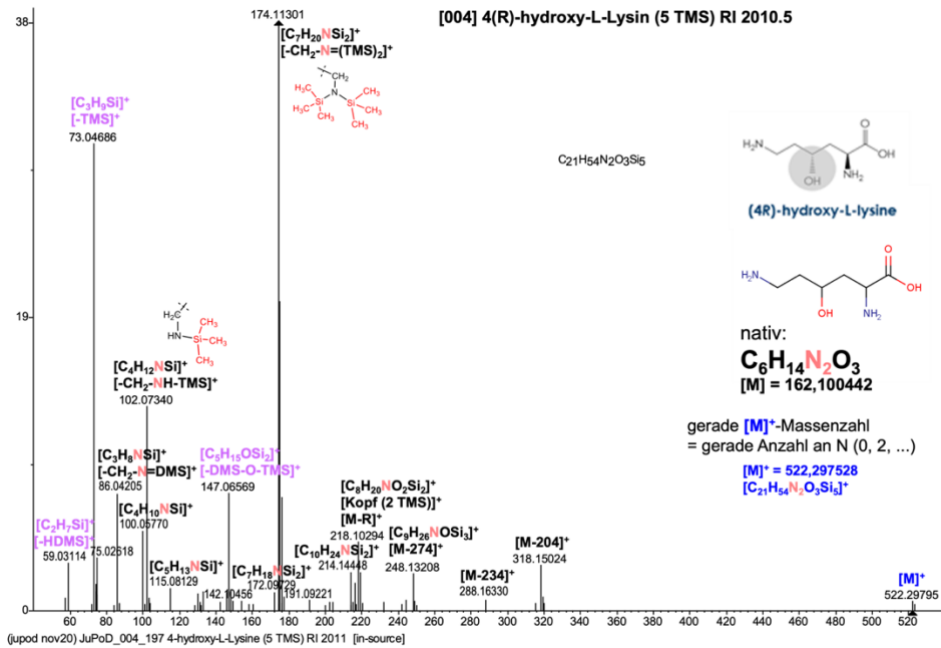


Figure S54: GC-ToF-MS spectrum of 5 TMS (4R)-hydroxy-L-lysine.

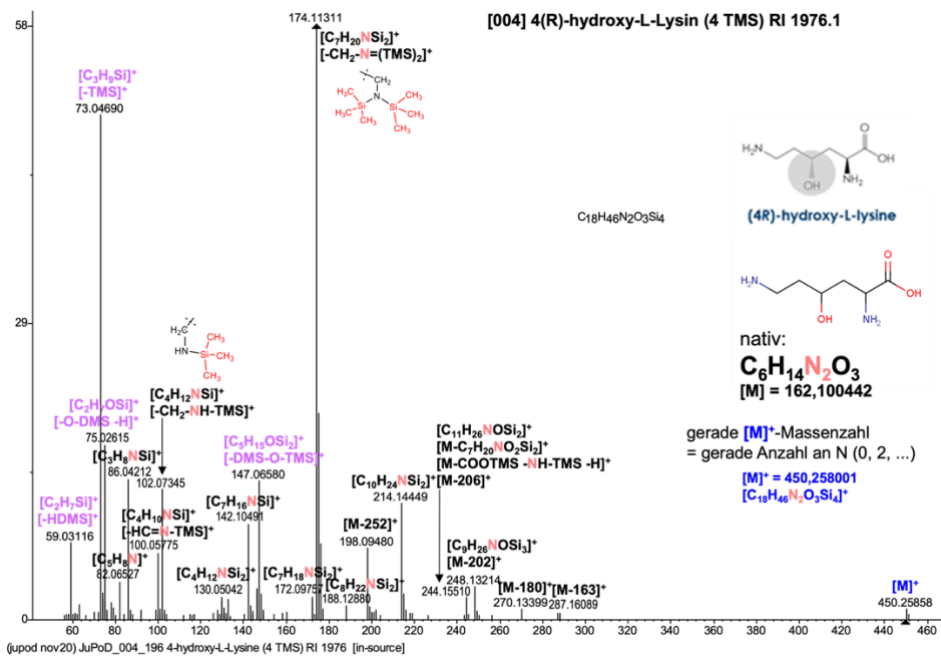


Figure S55: GC-ToF-MS spectrum of 4 TMS (4R)-hydroxy-L-lysine.

## Results

### 2.2.12.2.3 NMR

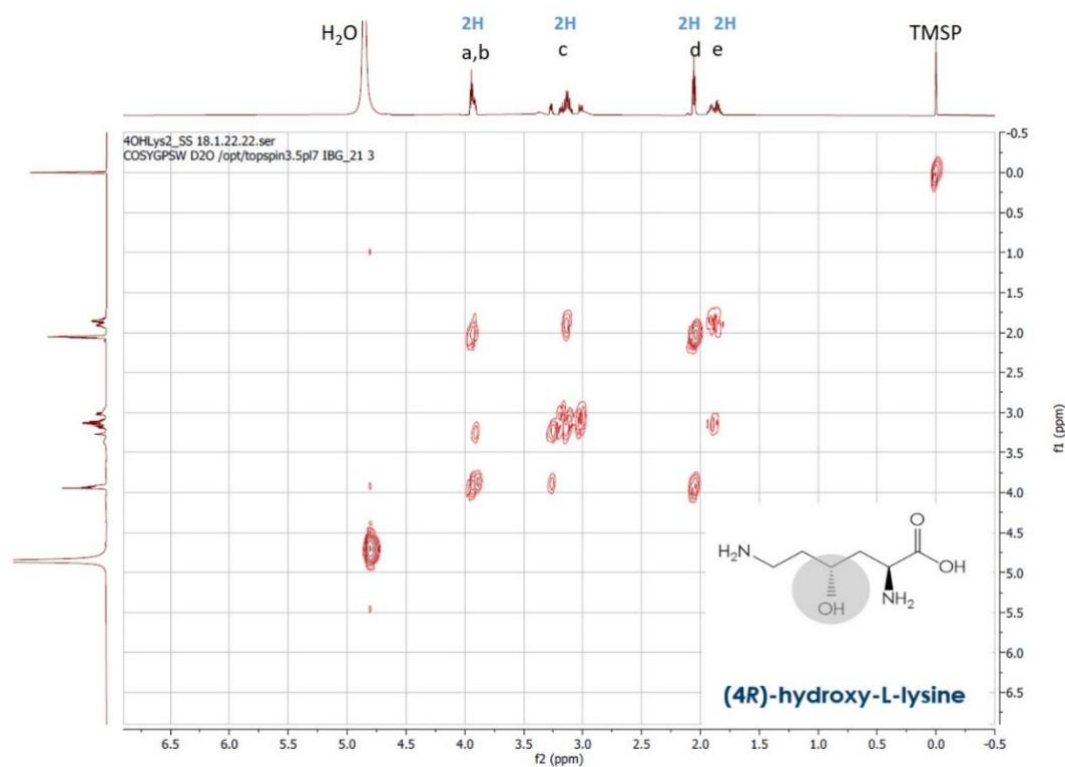


Figure S56: COSY NMR of (4R)-hydroxy-L-lysine. Yellow rectangles show impurities still present after purification.

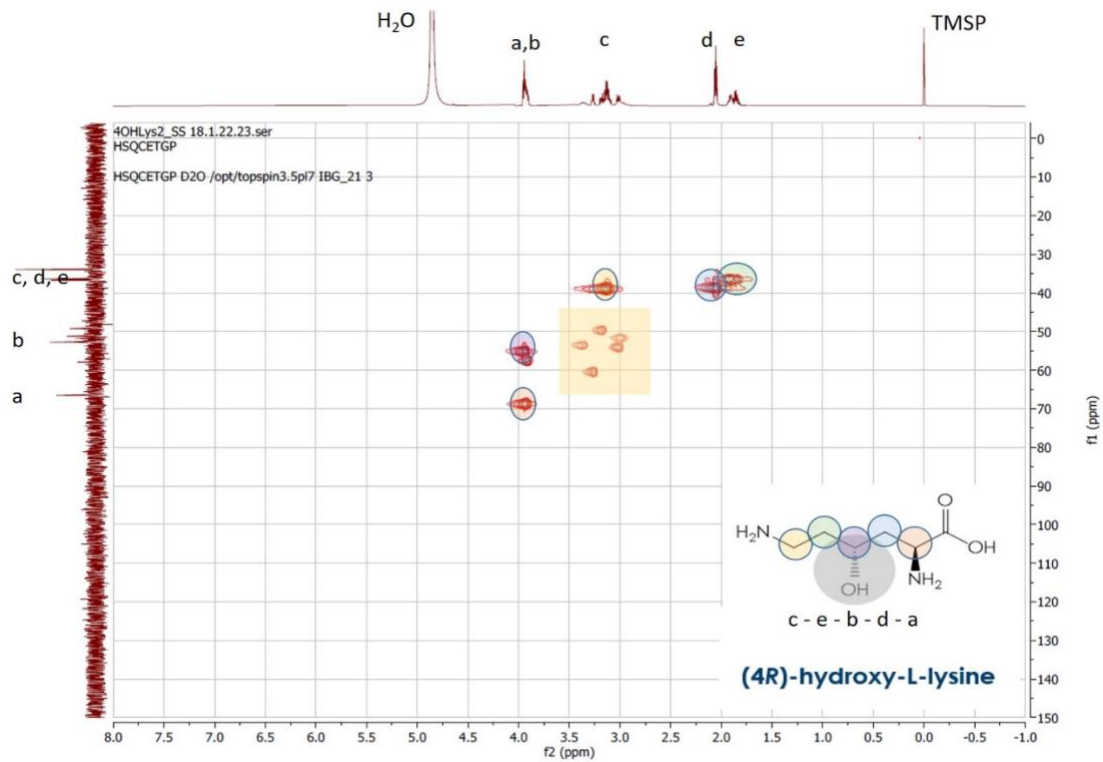


Figure S57: 2D HSQC NMR spectrum of (4R)-hydroxy-L-lysine.

## Results

### 2.2.12.3 Instrumental analysis of the standard 5-hydroxy-D,L-lysine

#### 2.2.12.3.1 GC-ToF-MS

#### GC-Chromatogram

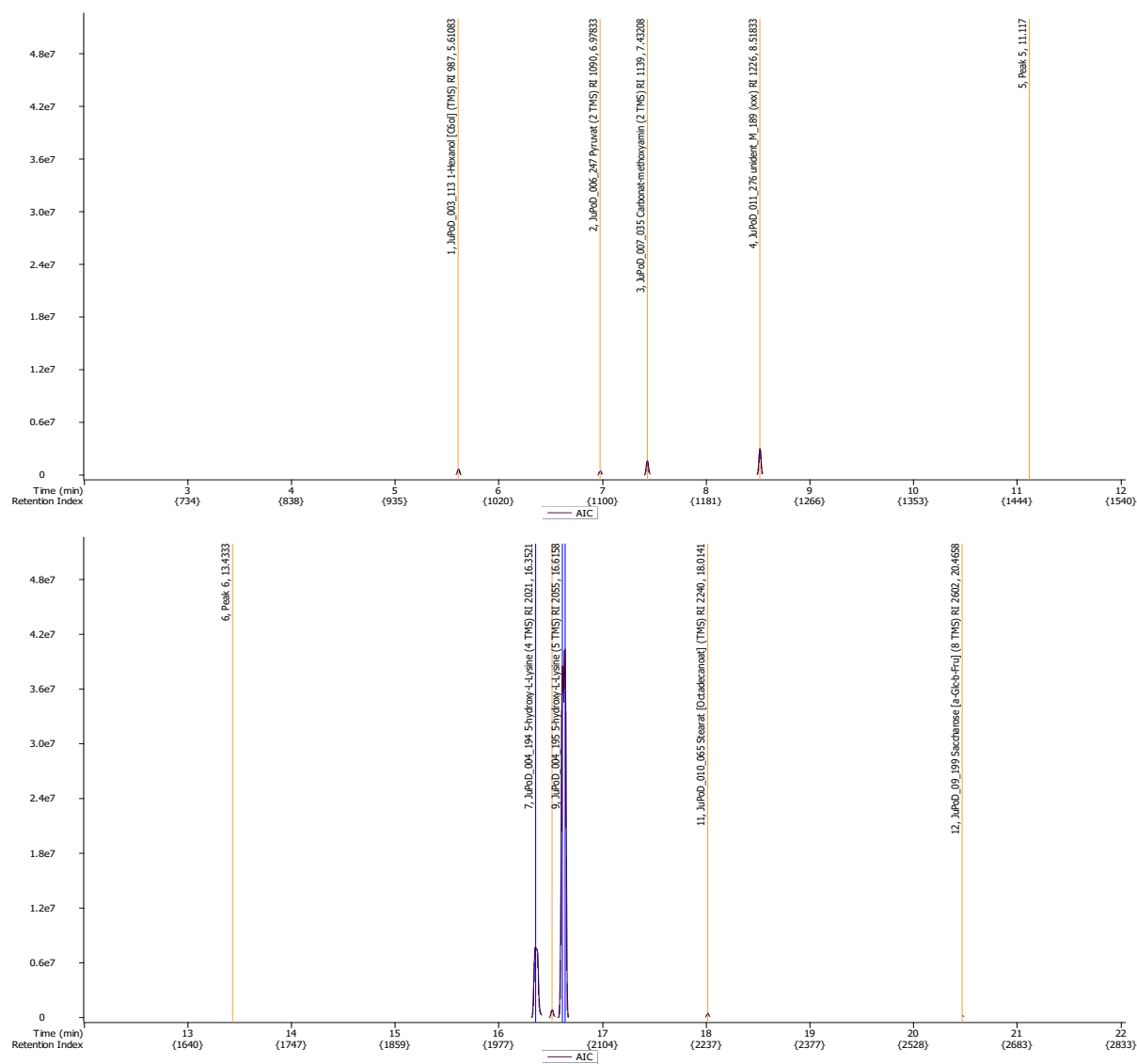


Figure S58: GC- chromatogram of 5-hydroxy-D,L-lysine.

# Results

## MS-Spectra

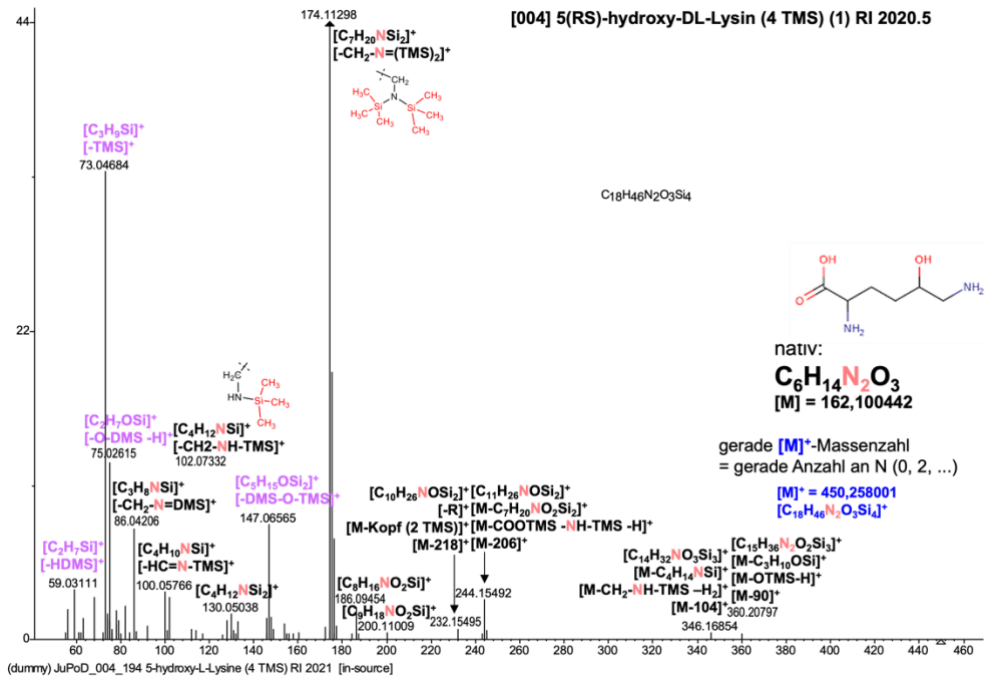


Figure S59: GC-ToF-MS spectrum of 4 TMS 5-hydroxy-D,L-lysine.

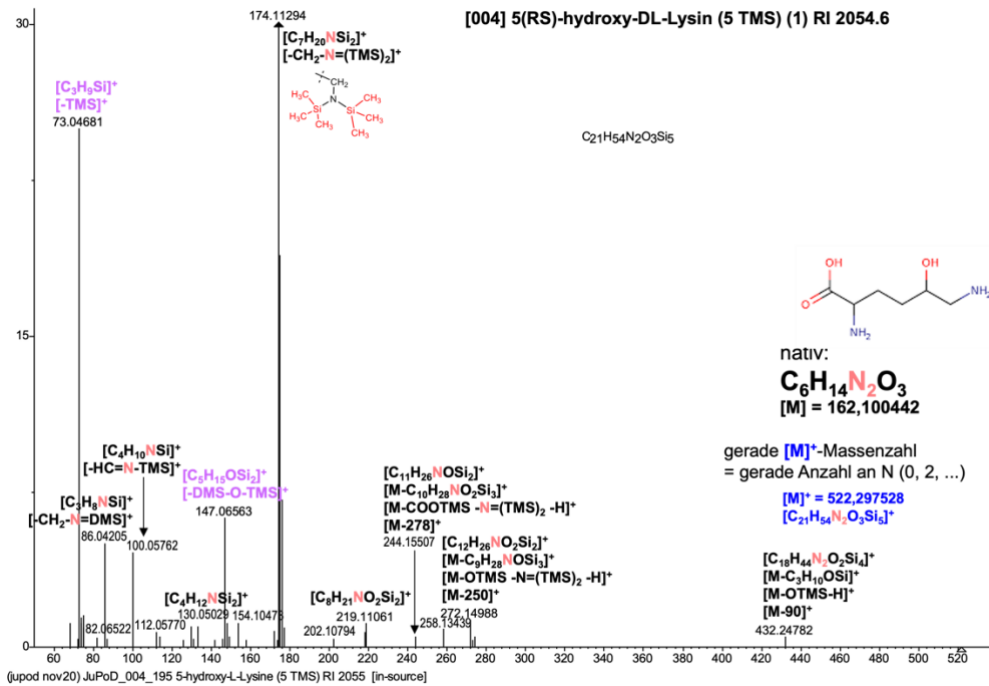


Figure S60: GC-ToF-MS spectrum of 5 TMS 5-hydroxy-D,L-lysine.

## Results

### 2.2.12.4 Instrumental analysis of (2S)-hydroxy-cadaverine

#### 2.2.12.4.1 HPLC

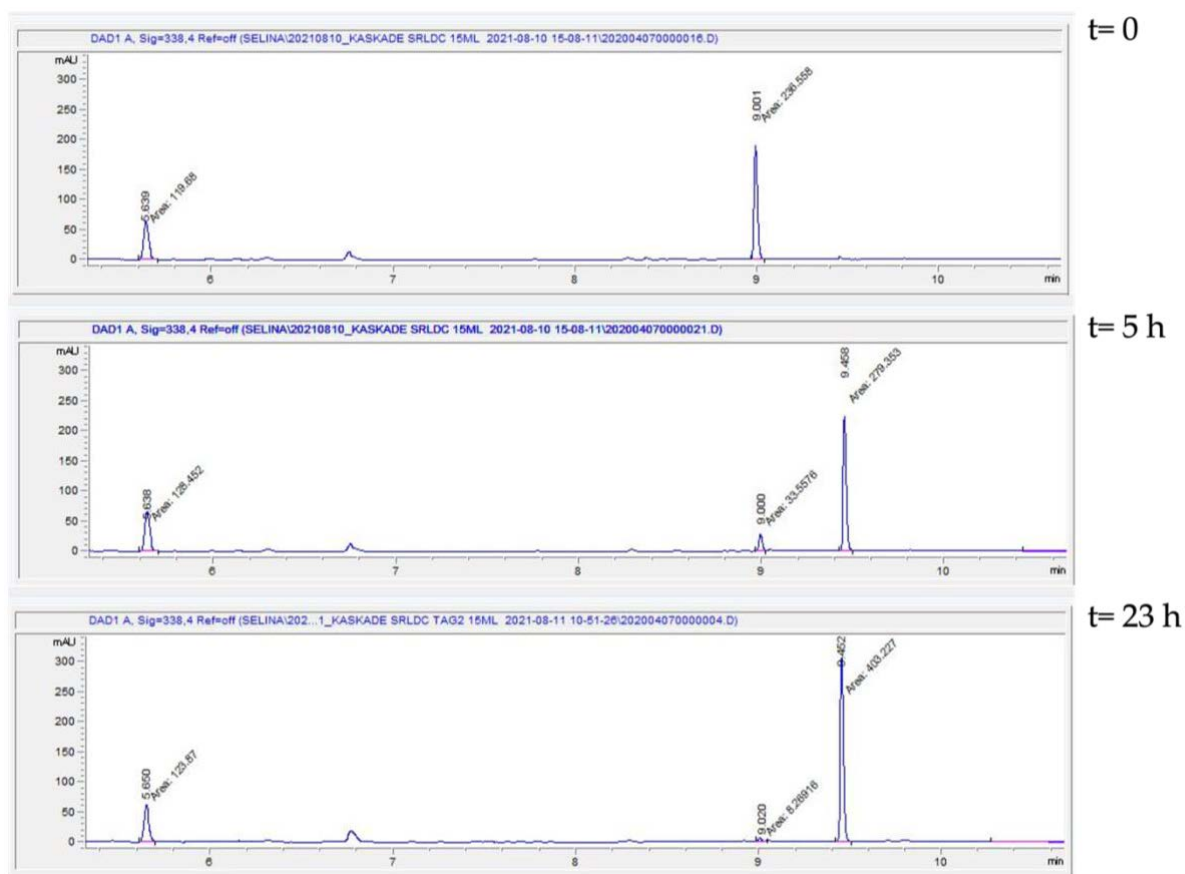


Figure S61: HPLC chromatograms of the monitoring of (3S)-hydroxy-L-lysine decarboxylation to (2S)-hydroxy cadaverine by StLDC-HaloTag®. Peaks: L-histidine (internal standard): 5.6 min, (3S)-hydroxy-L-lysine: 9.0 min, (2S)-hydroxy-cadaverine L-lysine: 9.4 min.

# Results

## 2.2.12.4.2 GC-ToF-MS

### GC-Chromatogram

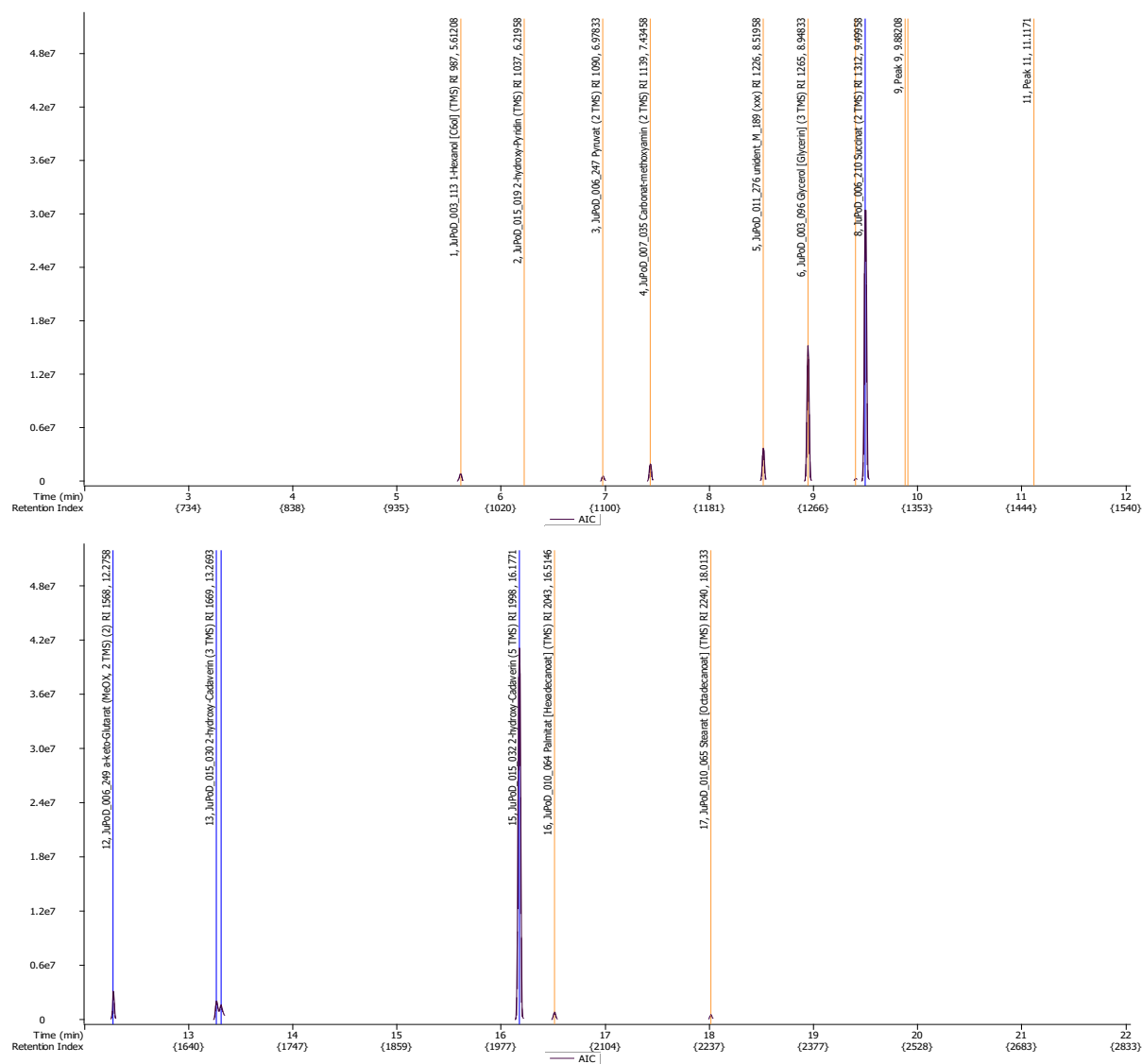


Figure S62: GC-chromatogram of (2S)-hydroxy-cadaverine.



## Results

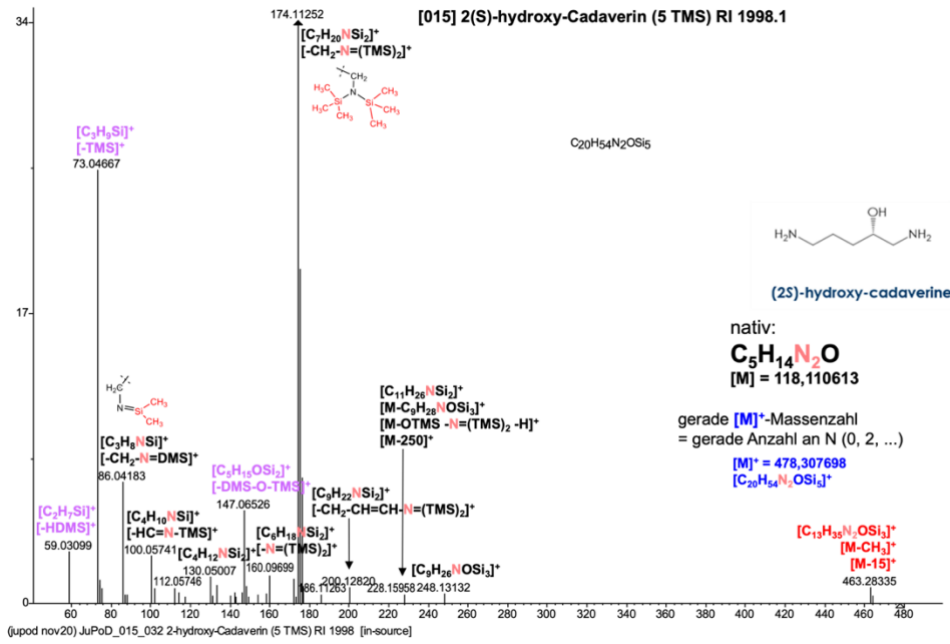


Figure S65: GC-ToF-MS spectrum of 5 TMS (2S)-hydroxy-cadaverine.

### 2.2.12.4.3 NMR

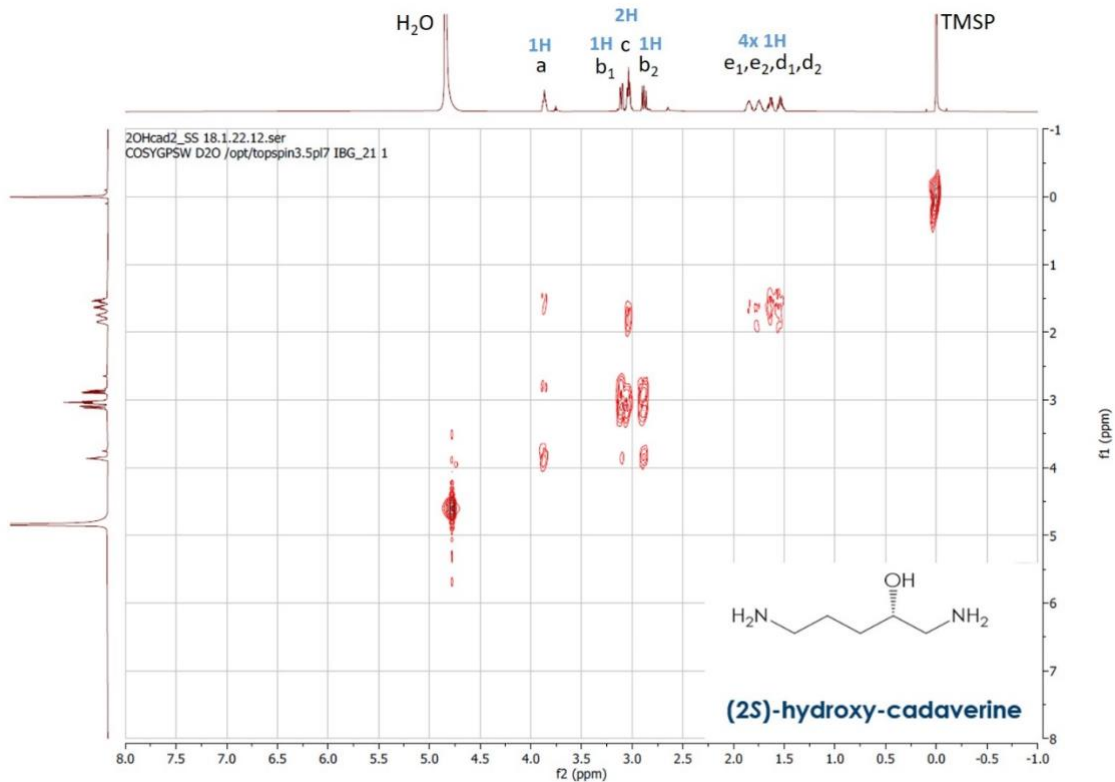


Figure S66: COSY NMR of (2S)-hydroxy-cadaverine.

## Results

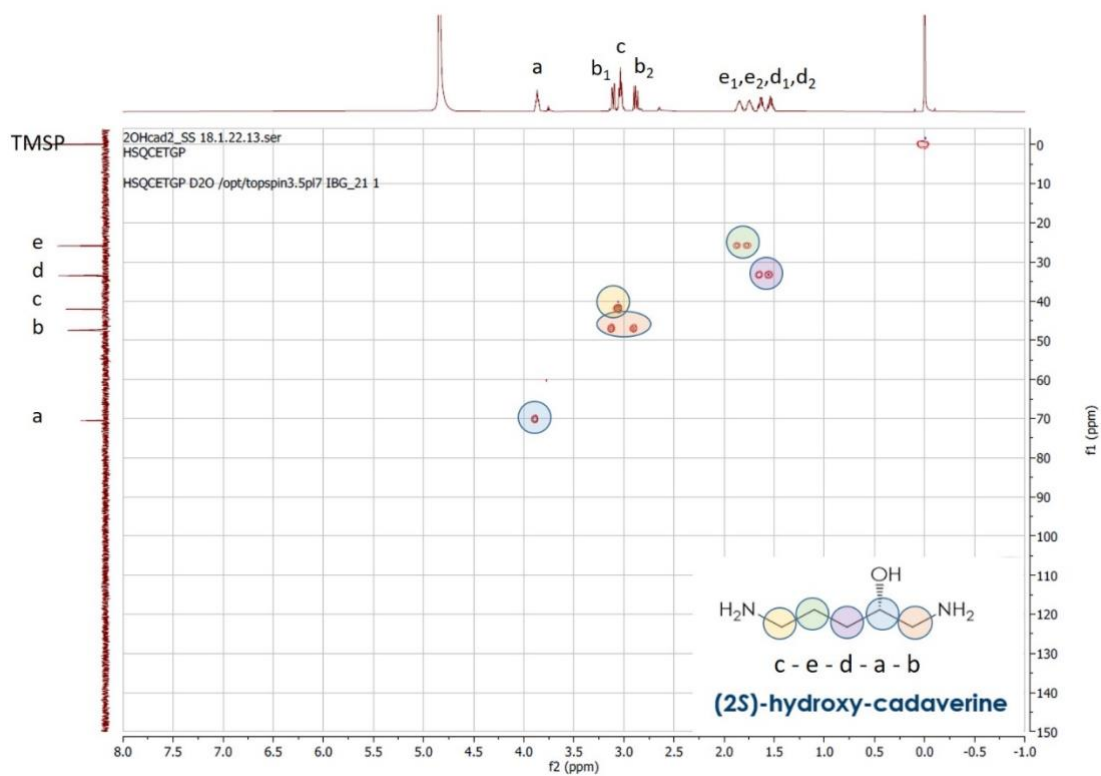


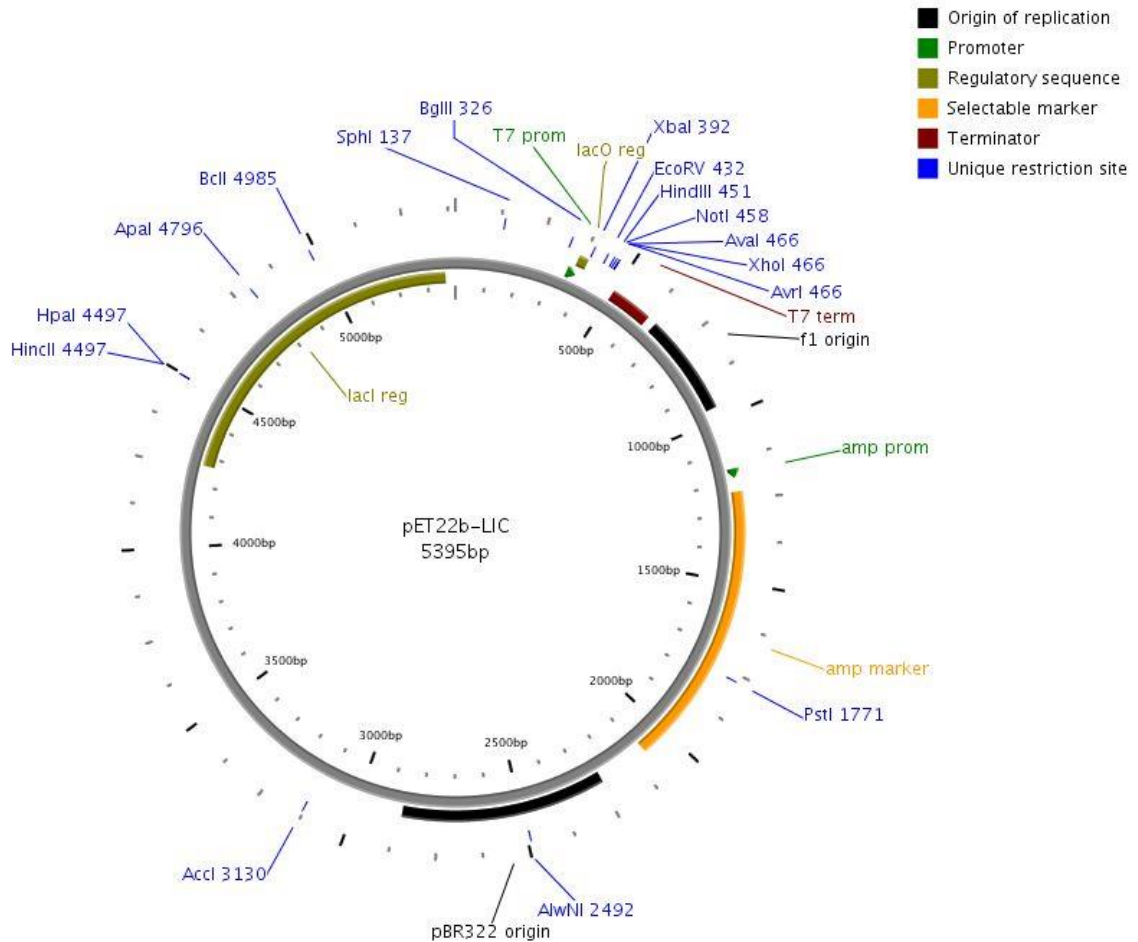
Figure S67: 2D HSQC NMR of (2S)-hydroxy-cadaverine.

## Results

### 2.2.13 Plasmid maps and sequences

#### 2.2.13.1 Free enzymes

Plasmids of the free KDOs correspond to the plasmids used by Baud et al.[2,5,7].



#### **CaKDO**

>sp|C7QJ42|LYS3O\_CATAD L-lysine 3-hydroxylase OS=Catenulispora acidiphila (strain DSM 44928 / NRRL B-24433 / NBRC 102108 / JCM 14897) OX=479433 GN=Caci\_0231 PE=1 SV=1

MHHHHHHK NLSAYEVYESP KTSGESRTEAVSEAAFESDPEVSAILVLTSS EASTLERVADLVT AHALY  
AAHDFCAQAQLAAAELPSRVVARLQEF AWGDMNEGHL LKGLPQVRS LPPTPTSNVHAVAATTPMSR  
YQALINECVGRMIA YEAEGHGHTFQDMVPSAMSAHSQTS LGS AVELE LHTEQAFSPLR PDFVSLACLRG  
DPRALTYLFSARQLVATLTTQEIAMLR EPMWTTTVD ESFLAEGRTFLLGFERGPI PILSGADDDP FIVFDQ  
DLMRGISAPAQELQQT VIRAYYAERVSHCLAPGEMLLIDNRR AVHGRSIFAPRFDGADRFLSR SFIVADG  
SRSRHARSSFG RVVSARFS

## Results

>C7QJ42

ATGCATCATCACCATCACCATAAGAACCTGTCTGCGTATGAAGTGTATGAATCGCCGAAGACCAG  
CGGAGAGTCACGTACCGAAGCCGTTTCGGAGGCCGCCTTCGAATCCGACCCCGAAGTGAGCGCAA  
TCCTAGTCCTGACCTCCTCCGAAGCCTCGACGCTGGAGCGCGTTCGCCGACCTCGTGACCGCGCACG  
CGCTGTATGCCGCTACGATTTCTGTGCCAGGCCAGCTGGCCGCCGCGAACTGCCGTCGCGGG  
TCGTTGCCCGGTTGCAGGAGTTCGCCTGGGGCGACATGAACGAGGGCCACCTTCTGATAAAAGGCC  
TGCCGCAGGTCCGCTCCCTGCCACCGACACCGACGTCCAACGTGCACGCCGTCGCCGCGACGACGC  
CGATGTCGCGCTACCAGGCCCTCATCAATGAGTGCCTGGGGCGCATGATTGCCTACGAGGCCGAGG  
GGCACGGCCACACCTTCCAGGACATGGTCCCAGCGCC  
ATGAGCGCGCACTCGCAGACCAGTCTCGGCTCGGCGGTTGAGCTCGAACTGCACACCGAGCAGGC  
CTTCAGTCCGCTGCGTCCGGACTTCGTCAGCCTGGCCTGTCTTCGCGGCGATCCACGAGCCCTGACT  
TACCTGTTCTCGGCCCGGCAACTGGTCGCGACGCTGACGACACAGGAAATCGCCATGCTGCGCGAG  
CCCATGTGGACCACCACCGTCGACGAGTCTTCTGGCGGAGGGGCGTACGTTCTGCTCGGCTTC  
GAGCGCGGTCCGATCCCGATATTGAGCGGTGCCGACGACGATCCGTTTCATCGTCTTCGACCAGGAT  
CTGATGCGGGGGATCTCGGCGCCCGCGCAGGAACTCCAACAGACTGTGATCCGCGCCTACTATGCC  
GAGCGCGTCAGCCACTGCCTCGCACCCGGTGAGATGCTCCTCATCGACAACCGGCGCGCCGTCCAC  
GGCAGGTCGATCTTCGCCCCGCGTTTCGACGGCGCTGACCGGTTCTTTCCAGAAGCTTCATCGTGG  
CCGACGGATCGCGCAGTCGGCACGCGGTTCTTCTTCGGCCGCGTCTCTGCGAGGTTTCAGCT  
AA

### CpKDO

>sp|C7PLM6|LYS4O\_CHIPD L-lysine 4-hydroxylase OS=Chitinophaga pinensis (strain ATCC 43595 / DSM 2588 / NCIB 11800 / UQM 2034) OX=485918 GN=Cpin\_2834 PE=1 SV=1

MHHHHHHRPLDVPTISPQAQDLPRTMHFAEPLQLIIDITEEEKLEITYIGKKLKRKYKSYDDPGFIS  
MLHLNAYTLLPERIAKVLSNFGTDFSDQYGA VVLRGLIEIGQDELGPTPRSWQETDHEKIMEYGFISL  
LHGAVPSKPVEYFAQRKGGGLMHAIIPDENMSFTQTGSGSRTDLFVHTEDAFLHNAADFLSFLRNEE  
RVPSTLYSIRSHGRPDAILQELFKPIYKCPKDANYASEEALGDDIRTSVLYGSRSAFMRFDAAEQIYNED  
ANQDPEALHNLKRFWEARKLIYNDFVPESGDLIFVNNHLCAHGRNAFLAGFREENGQLVKCERRMLL  
RMMSKTSLINIREVTHPENPYLIMEEHYGVYSAHLANL

>C7PLM6

ATGCATCATCACCATCACCATAGACCCTTAGACGTGACACCCACAATTAGCCCAGGAGCCCAGGA  
CCTTCCGCGCACTATGCATTTTGCTGCTGAACCTCCTTTACAGCCTTTGATAATAGATATTACTGAA  
GAAGAAAAACTGGAAATTACCTATATCGGGAAAAAGCTAAAAAGAAAGTATAAAAGCTATGATGA  
TCCCGGTTTTATTTCAATGCTGCACTTAAATGCCTATACGCTGCTACCGGAGCGTATAGCAAAGGTG  
CTGAGTAATTTCCGTACAGACTTTTCCGACCAGCAATACGGAGCTGTCGTATTGCGTGGACTGATA  
GAAATAGGTCAGGATGAATTAGGCCCAACCCACGTTCTGGCAGGAAACCGACCATGAAAAGAT  
TATGGAATATGGCTTCATTTCTCCTTATTACATGGCGCTGTACCATCCAAACCCGTCGAGTATTT  
GCGCAGCGAAAAGGTGGTGGCTTAATGCACGCGATTATTCCTGATGAGAATATGAGCTTTACACAA  
ACAGGCTCAGGTTCCCGTACAGATCTTTTTGTACATACAGAAGATGCTTTCCTGCATAATGCGGCTG

## Results

ATTTTCTGAGTTTTCTTTTCCTGCGGAATGAAGAACGTGTGCCTTCCACCTTATATTCTATCCGCTCT  
CATGGCAGACCGGATGCGATATTACAGGAGCTTTTCAAGCCTATCTATAAGTGTCCGAAGGATGCG  
AACTATGCTTCCGAAGAAGCCCTGGGAGATGACATCCGTACTIONTCTGTTTTATATGGTAGCAGATCC  
GCTCCCTTCATGCGCTTTGATGCTGCGGAACAGATTTATAATGAAGACGCCAATCAGGATCCTGAA  
GCTTTACATAATCTGAAAAGATTCTGGGAAGAGGCGCGCAAACCTGATATATAATGACTTCGTTCT  
GAGTCAGGTGACCTGATCTTTGTGAATAATCATCTTTGTGCCATGGCCGGAATGCTTTCCTGGCAG  
GCTTCAGAGAGGAAAATGGTCAGCTGGTAAAATGCGAACGCCGTCTTATGTTACGTATGATGAGCA  
AAACCAGCTGATTAACATCCGTGAAGTAACCCACCCGAAAACCCTTATCTCATCATGGAAGAGC  
ACTACGGAAAAGTATATAGCGCTCACCTGGCAAACCTTAA

### **FjKDO**

>sp|A5FF23|LYS4O\_FLAJ1 L-lysine 4-hydroxylase OS=Flavobacterium johnsoniae (strain ATCC 17061 / DSM  
2064 / UW101) OX=376686 GN=Fjoh\_3169 PE=1 SV=1

MHHHHHHSQSLIEDEIPVKENYAYQIPTSLIVEVTPQERNILSNVGALLEKAFKSYENPDYIEALHLY  
SFQLLPERIARILSRFGTDFADQYGAIFRGLLEVDQDHLGPTPANWQSADYSKLNKYGFICSL LHGAVP  
SKPVQYYAQRKGGGILHAVIPDEKMAATQTGSGSKTNLYVHTEDAFLLHQADFLSFLYLRNEERVSTL  
YSVRSHGKVNKIMEKLFDPYQCPKDANYQEEINDGPLASVLYGNKLPFIRFDAAEQIFNENAGQTPE  
ALYNLTEFWNEAKELINSYIPDSGDVIFVNNHLCAHGRSAFTAGQKEENGKLVPCERRQMLRMMSKT  
SLIHRSMTHTDDPYFVMEHLGKVFDDQA

>A5FF23

ATGCATCATCACCATCACCATAAATCACAATCATTAAATTGAAGATGAGATACCAGTAAAAGAAAA  
CTATGCTTATCAAATCCTACAAGCCCGCTGATAGTGGAGGTTACGCCTCAGGAAAGAAACATTTT  
GTCTAATGTGGGCGCTCTGCTGGAAAAGGCATTTAAGAGCTATGAAAACCCAGATTATATAGAAGC  
GCTTCATCTGTATTCTTTTCAGCTTCTCCAGAAAGAATAGCCAGAATTTTAAGCCGTTTTGGAACA  
GATTTCTCAGCTGATCAGTATGGCGCTATTATTTTTAGAGGTCTTCTTGAAGTTGATCAGGATCATC  
TGGGACCAACTCCTGCGAATTGGCAGAGCGCTGATTACTCAAAACTC  
AATAAATACGGCTTTATTTGTTCTTGCTGCATGGTGCAGTTCCTTCAAACCAGTACAATATTATG  
CGCAGAGAAAGGGCGGGGAATTCTTCATGCTGTTATTCCAGATGAGAAAATGGCAGCTACGCAA  
ACAGGTTCCGGATCAAAAACAAATTTGTATGTTCCATACAGAAGATGCTTTTTCTTTTACATCAGGCTG  
ATTTTTTAAGTTTTCTATATCTGCGAAATGAAGAAAGAGTTCCTTCTACACTTACTCAGTAAGGTC  
GCATGGTAAGGTGAATAAGATAATGGAAAAGCTTTTTGATCCAATTTATCAATGTCCTAAAGATGC  
TAATTATCAGGAAGAAATTAATGATGGTCCGCTGGCTTCTGTTTTATATGGAAATAAAAAGCTGCC  
TTTTATTAGATTTGATGCAGCAGAGCAGATATTTAATGAAAACGCCGACAGACTCCCGAAGCTCT  
TTACAATTTAACTGAATTTTGAATGAAGCTAAAGAGTTGATTAATAGTGATTATATCCCAGATTCT  
GGTGATGTTATATTTGTAAATAATCATTTGTGTGCTCACGGAAGAAGTGCTTTTACAGCAGGGCAG  
AAAGAGGAGAATGGTAAGCTTGTGCCATGTGAGAGACGACAAATGTTAAGAATGATGAGCAAAAC  
CAGTCTAATTCATATAAGATCAATGACACATACCGATGATCCGTATTTTGTATGGAAGAACATTTA  
GGAAAAGTTTTGATCAGGCTTAA

## Results

### ***SrLDC***

#### **O50657-like**

MHHHHHHKFNRLSEKEVKTLAERFPTPFLVASLDKVEENYQFMRRHLPRAGVFYAMKANPT  
PEILSLLAGLGSHFDVASAGEMEILHELGVDSQMIYANPVKDERGLKAAAAYNVRRFTFDD  
PSEIDKMAKAVPGADVLVRIAVRNNKALVDLNTKFGAPVEEALDLLKAAQEAGLHAMGICF  
HVGSQSLSTAAYEEALLVARKLFDEAEAMGMHLTDLDIGGGFPVPAKGLNVDLAAMMEAI  
NKQIDRLFPDTAVWTEPGRYMCGTAVNLVTSVIGTKTRGPQPWYILDEGIYGCFSGIMYDHW  
TYPLHCFGKGTKKPSTFGGPPSCDGIDVLYRDFMAPELKIGDKVLVTEMGSYTSVSA TRFNQFY  
LAPTHIFEDQPEYAARLTEDDVKKKAAV

#### **SrLDC pET22b+**

TGGCGAATGGGACGCGCCCTGTAGCGGCGCATTAAAGCGGCGGGGTGTGGTGGTTACGCGCAGCG  
TGACCGCTACACTTGCCAGCGCCCTAGCGCCCGCTCCTTTTCGCTTCTTCCCTTCTTCTCGCCACG  
TTCGCCGGCTTTCCCGTCAAGCTCTAAATCGGGGCTCCCTTTAGGGTTCGATTTAGTGCTTTAC  
GGCACCTCGACCCCAAAAACTTGATTAGGGTGATGGTTCACGTAGTGGGCCATCGCCCTGATAGA  
CGTTTTTCGCCCTTTGACGTTGGAGTCCACGTTCTTTAATAGTGGACTCTTGTTCCAAACTGGAAC  
AACACTCAACCCTATCTCGGTCTATTCTTTTGATTTATAAGGGATTTTGCCGATTTGCGCCTATTGGT  
TAAAAAATGAGCTGATTTAACAAAAATTTAACGCGAATTTAACAAAATATTAACGTTTACAATTT  
CAGGTGGCACTTTTCGGGGAAATGTGCGCGGAACCCCTATTTGTTTATTTTTCTAAATACATTCAA  
TATGTATCCGCTCATGAGACAATAACCCTGATAAATGCTTCAATAATATTGAAAAAGGAAGATAT  
GAGTATTCAACATTTCCGTGTCGCCCTTATCCCTTTTTTGCGGCATTTTGCCTTCTGTTTTTGCTCA  
CCCAGAAACGCTGGTGAAAGTAAAAGATGCTGAAGATCAGTTGGGTGCACGAGTGGGTACATCG  
AACTGGATCTCAACAGCGGTAAGATCCTTGAGAGTTTTCGCCCCGAAGAAGCTTTTCCAATGATGA  
GCACTTTTAAAGTTCTGCTATGTGGCGCGGTATTATCCCGTATTGACGCCGGGCAAGAGCAACTCG  
GTCGCCGCATACACTATTCTCAGAATGACTTGGTTGAGTACTACCAGTCACAGAAAAGCATCTTA  
CGGATGGCATGACAGTAAGAGAATTATGCAGTGCTGCCATAACCATGAGTGATAAACTGCGGCC  
AACTTACTTCTGACAACGATCGGAGGACCGAAGGAGCTAACCGCTTTTTTGCACAACATGGGGGAT  
CATGTAACCTCGCCTTGATCGTTGGGAACCGGAGCTGAATGAAGCCATACCAAACGACGAGCGTGA  
CACCACGATGCCTGCAGCAATGGCAACAACGTTGCGCAAACCTATTAACCTGGCGAACTACTTACTCT  
AGCTTCCCGCAACAATTAATAGACTGGATGGAGGCGGATAAAGTTGCAGGACCACTTCTGCGCTC  
GGCCCTTCCGGCTGGCTGGTTTATTGCTGATAAATCTGGAGCCGGTGAGCGTGGGTCTCGCGGTAT  
CATTGCAGCACTGGGGCCAGATGGTAAGCCCTCCCGTATCGTAGTTATCTACACGACGGGGAGTCA  
GGCAACTATGGATGAACGAAATAGACAGATCGCTGAGATAGGTGCCTCACTGATTAAGCATTGGT  
AACTGTCAGACCAAGTTTACTCATATATACTTTAGATTGATTTAAAACCTCATTTTTAAATTTAAAAG  
GATCTAGGTGAAGATCCTTTTTGATAATCTCATGACCAAAAATCCCTAACGTGAGTTTTCGTTCCAC  
TGAGCGTCAGACCCCGTAGAAAAGATCAAAGGATCTTCTTGAGATCCTTTTTTCTGCGCGTAATCT  
GCTGCTTGCAAACAAAAAACCACCGCTACCAGCGGTGGTTTTGTTGCCGGATCAAGAGCTACCAA  
CTTTTTTCCGAAGGTAACCTGGCTTCAGCAGAGCGCAGATACCAAATACTGTCTTCTAGTGAGCC  
GTAGTTAGGCCACCACTTCAAGAACTCTGTAGCACCGCTACATAACCTCGCTCTGCTAATCCTGTTA

## Results

CCAGTGGCTGCTGCCAGTGGCGATAAGTCGTGTCTTACCGGGTTGGACTCAAGACGATAGTTACCG  
GATAAGGGCGCAGCGGTTCGGGCTGAACGGGGGGTTCGTGCACACAGCCCAGCTTGGAGCGAACGAC  
CTACACCGAACTGAGATACCTACAGCGTGAGCTATGAGAAAGCGCCACGCTTCCCGAAGGGAGAA  
AGGCGGACAGGTATCCGGTAAGCGGCAGGGTCGGAACAGGAGAGCGCACGAGGGAGCTTCCAGG  
GGGAAACGCCTGGTATCTTTATAGTCCTGTCTGGGTTTCGCCACCTCTGACTTGAGCGTCGATTTTTG  
TGATGCTCGTCAGGGGGGCGGAGCCTATGGAAAAACGCCAGCAACGCGGCCTTTTTACGGTTCCTG  
GCCTTTTGCTGGCCTTTTGCTCACATGTTCTTTCTGCGTTATCCCCTGATTCTGTGGATAACCGTAT  
TACCGCCTTTGAGTGAGCTGATACCGCTCGCCGACGCCGAACGACCGAGCGCAGCGAGTCAGTGA  
GCGAGGAAGCGGAAGAGCGCCTGATGCGGTATTTTCTCCTTACGCATCTGTGCGGTATTTACACC  
GCATATATGGTGCACCTCTCAGTACAATCTGCTCTGATGCCGCATAGTTAAGCCAGTATACACTCCGC  
TATCGCTACGTGACTGGGTCATGGCTGCGCCCCGACACCCGCCAACACCCGCTGACGCGCCCTGAC  
GGGCTTGTCTGCTCCCGGCATCCGCTTACAGACAAGCTGTGACCGTCTCCGGGAGCTGCATGTGTC  
AGAGGTTTTACCGTCATCACCGAAACGCGGAGGCAGCTGCGGTAAAGCTCATCAGCGTGGTCGT  
GAAGCGATTCACAGATGTCTGCCTGTTTCATCCGCGTCCAGCTCGTTGAGTTTCTCCAGAAGCGTTAA  
TGTCTGGCTTCTGATAAAGCGGGCCATGTTAAGGGCGGTTTTTCTGTTTGGTCACTGATGCCTCC  
GTGTAAGGGGGATTTCTGTTTCATGGGGTAATGATACCGATGAAACGAGAGAGGATGCTCACGAT  
ACGGGTTACTGATGATGAACATGCCCGGTTACTGGAACGTTGTGAGGGTAAACAACCTGGCGGTATG  
GATGCGGGCGGGACCAGAGAAAAATCACTCAGGGTCAATGCCAGCGCTTCGTTAATACAGATGTAG  
GTGTTCCACAGGGTAGCCAGCAGCATCCTGCGATGCAGATCCGGAACATAATGGTGCAGGGCGCT  
GACTTCCGCGTTTTCCAGACTTTACGAAACACGGAAACCGAAGACCATTTCATGTTGTTGCTCAGGTC  
GCAGACGTTTTGCAGCAGCAGTCGTTTACGTTTCGCTCGCGTATCGGTGATTCATTCTGCTAACCAG  
TAAGGCAACCCCGCCAGCCTAGCCGGTCTCAACGACAGGAGCACGATCATGCGCACCCGTGGG  
GCCGCCATGCCGGCGATAATGGCCTGCTTCTCGCCGAAACGTTTTGGTGGCGGGACCAGTGACGAAG  
GCTTGAGCGAGGGCGTGCAAGATTCCGAATACCGCAAGCGACAGGCCGATCATCGTCGCGCTCCA  
GCGAAAGCGGTCCTCGCCGAAAATGACCCAGAGCGCTGCCGGCACCTGTCCTACGAGTTGCATGAT  
AAAGAAGACAGTCATAAGTGCGGCGACGATAGTCATGCCCCGCGCCCACCCGAAGGAGCTGACTG  
GGTTGAAGGCTCTCAAGGGCATCGGTGAGATCCCGTGCCTAATGAGTGAGCTAACTTACATTAA  
TTGCGTTGCGCTCACTGCCCGTTTTCCAGTCGGGAAACCTGTCGTGCCAGCTGCATTAATGAATCGG  
CCAACGCGCGGGGAGAGGCGGTTTTGCGTATTGGGCGCCAGGGTGGTTTTTTCTTTTACCAGTGAGA  
CGGGCAACAGCTGATTGCCCTTACCGCCTGGCCCTGAGAGAGTTGCAGCAAGCGGTCCACGCTGG  
TTTGCCCCAGCAGGCGAAAATCCTGTTTGATGGTGGTTAACGGCGGGATATAACATGAGCTGTCTT  
CGGTATCGTCGTATCCCACTACCGAGATATCCGCACCAACGCGCAGCCCAGCTCGGTAATGGCGC  
GCATTGCGCCCAGCGCCATCTGATCGTTGGCAACCAGCATCGCAGTGGGAACGATGCCCTCATTCA  
GCATTTGCATGGTTTGTGAAAACCGGACATGGCACTCCAGTCGCTTCCCGTTCCGCTATCGGCTG  
AATTTGATTGCGAGTGAGATATTTATGCCAGCCAGCCAGACGCAGACGCGCCGAGACAGAACTTA  
ATGGGCCCCGCTAACAGCGCGATTTGCTGGTGACCCAATGCGACCAGATGCTCCACGCCAGTCGCG  
TACCGTCTTCATGGGAGAAAATAATACTGTTGATGGGTGTCTGGTCAGAGACATCAAGAAATAACG  
CCGGAACATTAGTGACGGCAGCTTCCACAGCAATGGCATCCTGGTCATCCAGCGGATAGTTAATGA  
TCAGCCCCTGACGCGTTGCGCGAGAAGATTGTGCACCGCCGCTTTACAGGCTTCGACGCCGCTTC  
GTTCTACCATCGACACCACCACGCTGGCACCCAGTTGATCGGCGCGAGATTTAATCGCCGCGACAA

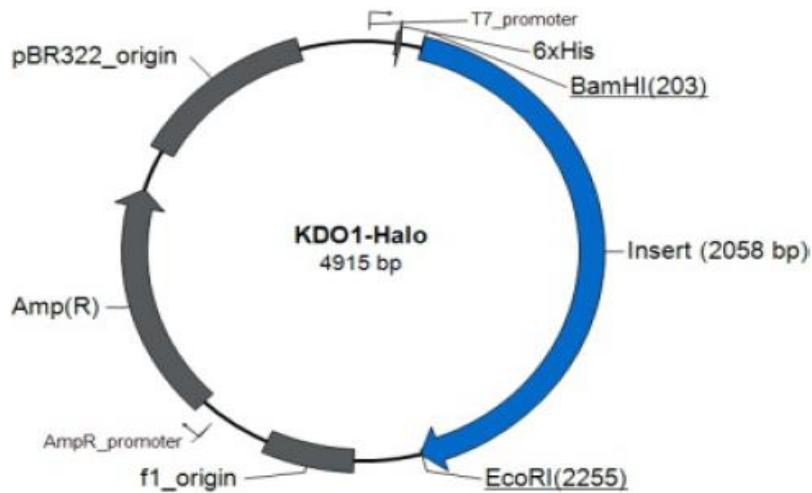
## Results

TTTGCACGGCGCGTGCAGGGCCAGACTGGAGGTGGCAACGCCAATCAGCAACGACTGTTTGCCC  
GCCAGTTGTTGTGCCACGCGGTTGGGAATGTAATTCAGCTCCGCCATCGCCGCTTCCACTTTTTCCC  
GCGTTTTTCGCAGAAACGTGGCTGGCCTGGTTCACCACGCGGAAACGGTCTGATAAGAGACACCG  
GCATACTCTGCGACATCGTATAACGTTACTGGTTTCACATTCACCACCCTGAATTGACTCTCTCCG  
GGCGCTATCATGCCATAACGCGAAAGGTTTTGCGCCATTCGATGGTGTCCGGGATCTCGACGCTCT  
CCCTTATGCGACTCCTGCATTAGGAAGCAGCCAGTAGTAGGTTGAGGCCGTTGAGCACCGCCGCC  
GCAAGGAATGGTGCATGCAAGGAGATGGCGCCCAACAGTCCCCCGGCCACGGGGCCTGCCACCAT  
ACCCACGCCGAAACAAGCGCTCATGAGCCCGAAGTGGCGAGCCCGATCTTCCCCATCGGTGATGT  
GGCGATATAGGCGCCAGCAACCGCACCTGTGGCGCCGGTATGCCGGCCACGATGCGTCCGGCGT  
AGAGGATCGAGATCTCGATCCCGCGAAATTAATACGACTCACTATAGGGGAATTGTGAGCGGATA  
ACAATTCCCCTCTAGAAATAATTTTTGTTTAATTCAAAGGAGATAGGAT  
ATGCATCATCACCATCACCATAAAAATTTACAGACTTAGCGAAAAAGAAGTAAAAACGCTTGCGGA  
GCGTTTTCCCAACGCCCTTTTTGGTGGCATCACTGGACAAAGTTGAGGAGA ACTACCAGTTTATGCG  
TCGTCATTTGCCGCGGGCGGGAGTGTTTTATGCGATGAAGGCGAACCCGACACCCGAGATTTTATC  
TCTGCTGGCGGGCCTTGGTCCATTTTATGATGTGGCCTCGGCCGGTGAAGTGGAAATTCTCCATGAA  
TTAGGCGTAGATGGTTCGCAGATGATATATGCCAATCCGGTAAAGGATGAGCGCGGGCTTAAGGCT  
GCGGCTGCATATAATGTACGCCGTTTTACCTTTGATGACCCGTCGGAATCGACAAGATGGCCAAG  
GCTGTGCCTGGTGCAGATGTGCTCGTGCGTATTGCTGTGCGCAACAACAAGGCCTTGGTAGACCTC  
AATACGAAGTTCGGCGCACCTGTGGAAGAGGCGCTGGATTTACTGAAAGCTGCGCAGGAGGCCGG  
CCTTCATGCCATGGGCATCTGCTTCCATGTGGGCAGCCAGTCGTTGTCCACGGCGGCTTATGAGGA  
AGCCCTGCTGGTGGCCCGCAAGCTTTTTGATGAAGCGGAAGCGATGGGTATGCACCTGACGGATTT  
GGATATCGGTGGCGGTTTTCCCCGTTCCCGATGCCAAGGGGTTGAATGTGGATTTGGCGGCCATGAT  
GGAAGCCATCAACAAGCAGATTGACCGCTTGTTCGCCGATACGGCTGTTTGGACGGAGCCGGGGCG  
CTATATGTGCGGTACGGCGGTGAACCTTGTGACCTCTGTTATCGGCACCAAGACCCGCGGCCCGCA  
GCCCTGGTATATTTGGATGAAGGTATCTATGGTTGCTTCTCTGGCATCATGTACGACCATTTGGACG  
TACCCTTTGCACTGCTTTGGCAAGGGCACCAAGAAGCCTTCGACCTTTGGCGGTCCCAGCTGCGAT  
GGTATCGATGTGCTCTATCGCGACTTTATGGCGCCGGAGCTCAAAAATCGGCGACAAGGTGCTCGTG  
ACGGAAATGGGTTCTTATACCAGCGTCAGCGCTACCCGCTTCAATGGTTTCTATCTGGCACCCACCA  
TTATCTTCGAGGACCAGCCGGAGTACGCGGCGCGGCTCACGGAGGATGATGTGAAGAAAAAGGCG  
GCTGTATAAATCACTATCCATTACACGAAGCTTGGCGCCGCACTCGAGCACCACCACCACCAC  
TGAGATCCGGCTGCTAACAAGCCCGAAAGGAAGCTGAGTTGGCTGCTGCCACCGCTGAGCAATA  
ACTAGCATAACCCCTTGGGGCCTCTAAACGGGTCTTGAGGGGTTTTTTGCTGAAAGGAGGAACTAT  
ATCCGGAT

## Results

### 2.2.13.2 HaloTag® variants

KDO HaloTag® plasmids contain an N-Terminal HaloTag® connected to the target enzyme via a peptide linker. Plasmids were codon optimized and produced by ThermoFisher Scientific. HaloTag® = underlined, linker= italic, enzyme= bold



### ***Ca*KDO-HaloTag®**

GATCTCGATCCCGCAAATTAATACGACTCACTATAGGGAGACCACAACGGTTTCCCTCTAGAAAT  
AATTTTGTTTAACTTTAAGAAGGAGATATACATATGCGGGGTTCTCATCATCATCATCATGGTA  
TGGCTAGCATGACTGGTGGACAGCAAATGGGTCCGGATCTGTACGACGATGACGATAAGGATCGA  
TGGGGATCCATGATTGGCACC GGTTTCCGTTTGATCCGCATTATGTTGAAGTTCTGGGTGAACGTA  
TGCATTATGTGGATGTTGGTCCGCGTGATGGTACACCGGTTCTGTTTCTGCATGGTAATCCGACCAG  
CAGCTATGTTTGGCGTAACATTATTCCGCATGTTGCACCGACACATCGTTGTATTGCACCGGATCTG  
ATTGGTATGGGTAAAAGCGATAAACTGATCTGGGCTATTTTTTCGATGATCATGTGCGTTTTATGG  
ACGCCTTTATTGAAGCACTGGGTTTAGAAGAAGTTGTGCTGGTTATTCATGATTGGGGTAGTGCCCT  
GGTTTTTCATTGGGCAAACGTAATCCGGAACGTGTTAAAGGTATTGCCTTCATGGAATTTATTCGT  
CCGATTCCGACCTGGGATGAATGGCCTGAATTTGCACGTGAAACCTTTCAGGCATTTTCGTACCACC  
GATGTGGGTCGTAAACTGATTATTGATCAGAACGTTTTTATCGAAGGCACCCTGCCGATGGGTGTT  
GTTTCGTCGCTGACCGAAGTTGAAATGGATCATTATCGTGAACCGTTTCTGAATCCGGTTGATCGCG  
AACCGCTGTGGCGTTTTCCGAATGAACTGCCGATTGCCGGTGAACCTGCAAATATTGTTGCACTGG  
TTGAAGAGTATATGGATTGGCTGCATCAGAGTCCGGTTCGAAACTGCTGTTTTGGGGCACACCGG  
GTGTTCTGATTCCGCCTGCAGAAGCAGCACGTCTGGCAAAAAGCCTGCCGAATTGTAAAGCAGTTGATAT  
TGGTCCGGTCTGAATCTGCTGCAAGAAGATAATCCAGATCTGATCGGTAGCGAAATTGCACGTTGGCTG  
AGCACCTGGAAATTAGCGGTCTGGCAGAAGCCGACGCAAAAAGAAGCAGCTGCCAAAGAAGCGGCAGCG  
AAAGAGGCTGCAGCAAAGGCAGCAGCAGCCGAGTCGACAAAAAATCTGAGCGCATATGAAG  
TTTATGAGAGCCCGAAAACCAGCGGTGAAAGCCGTACCGAAGCAGTTAGCGAAGCAGCATT  
GAAAGCGATCCGGAAGTTAGCGCAATTCTGGTTCTGACCAGCAGTGAAGCAAGTACCCTGGA

## Results

ACGTGTGGCAGATCTGGTTACCGCACATGCACTGTATGCAGCACATGATTTTTGTGCACAGG  
CACAGCTGGCAGCCGCAGAAGTCCCGTCACGTGTTGTTGCACGTCTGCAAGAA  
TTTGCATGGGGTGATATGAATGAAGGTCATCTGCTGATTAAGGTCCTGCCGAGGTTTCGTAG  
CCTGCCTCCGACACCGACCAGTAATGTTTCATGCAGTTGCAGCAACCACACCGATGAGCCGTT  
ATCAGGCACTGATTAATGAATGTGTTGGTCGCATGATTGCCTATGAAGCCGAAGGTCATGGT  
CATACATTTAGGATATGGTTCCGAGCGCAATGAGCGCACATAGCCAGACCAGCCTGGGTAG  
CGCAGTTGAACTGGAAGTGCATACCGAACAGGCATTTAGTCCGCTGCGTCCGGATTTTGTTA  
GCCTGGCATGTCTGCGTGGTGATCCGCGTGCCTGACCTACCTGTTTAGCGCACGTGAGCTG  
GTTGCGACCCTGACCACACAAGAAATTGCAATGCTGCGTGAACCTATGTGGACCACCACCGT  
TGATGAAAGTTTTCTGGCGGAAGGTCGTACCTTTCTGCTGGGTTTTGAACGTGGTCCTATTCC  
GATTCTGAGCGGTGCAGATGATGATCCGTTTATTGTTTTGATCAGGATCTGATGCGTGGTAT  
TAGCGCACCGGCACAAGAAGTGCAGCAGACCCTTATTCTGTCATATTATGCAGAACGTGTGA  
GCCATTGTCTGGCACCAGGTTGAGATGCTGCTGATTGATAATCGTCGTGCAGTTCATGGTCGT  
AGCATTTTTGCACCGCGTTTTGATGGTGCAGATCGTTTTCTGAGCCGTAGCTTTATTGTTGCC  
GATGGTAGCCGTAGCCGTCATGCACGTAGCAGCTTTGGTTCGTGTTGTGAGCGCACGTTTTAG  
CTAAGAATTCGAAGCTTGATCCGGCTGCTAACAAAGCCCGAAAGGAAGCTGAGTTGGCTGCTGCC  
ACCGCTGAGCAATAACTAGCATAACCCCTTGGGGCCTCTAAACGGGTCTTGAGGGGTTTTTTGCTG  
AAAGGAGGAACTATATCCGGATCTGGCGTAATAGCGAAGAGGCCCGCACCGATCGCCCTCCCAA  
CAGTTGCGCAGCCTGAATGGCGAATGGGACGCGCCCTGTAGCGGCGCATTAAAGCGCGGGGGTGT  
GGTGGTTACGCGCAGCGTGACCGCTACACTTGCCAGCGCCCTAGCGCCCGCTCCTTTTCGCTTTCTTC  
CCTTCCTTTCTCGCCACGTTCCGCGGCTTTCCCGTCAAGCTCTAAATCGGGGGCTCCCTTTAGGGT  
TCCGATTTAGTGCTTTACGGCACCTCGACCCCAAAAACTTGATTAGGGTGATGGTTCACGTAGTG  
GGCCATCGCCCTGATAGACGGTTTTTCGCCCTTTGACGTTGGAGTCCACGTTCTTTAATAGTGGACT  
CTTGTTCCAAACTGGAACAACACTCAACCCTATCTCGGTCTATTCTTTTGATTTATAAGGGATTTTG  
CCGATTTCCGGCCTATTGGTTAAAAAATGAGCTGATTTAACAAAAATTAACCGGAATTTTAACAAA  
ATATTAACGCTTACAATTTAGGTGGCACTTTTCGGGGAAATGTGCGCGGAACCCCTATTTGTTTATT  
TTTCTAAATACATTCAAATATGTATCCGCTCATGAGACAATAACCCTGATAAATGCTTCAATAATAT  
TGAAAAAGGAAGAGTATGAGTATTCAACATTTCCGTGTCGCCCTTATCCCTTTTTTGCGGCATTTT  
GCCTTCCTGTTTTTGGCTACCCAGAAACGCTGGTGAAAGTAAAAGATGCTGAAGATCAGTTGGGTG  
CACGAGTGGGTTACATCGAACTGGATCTCAACAGCGGTAAGATCCTTGAGAGTTTTCGCCCCGAAG  
AACGTTTTCCAATGATGAGCACTTTTAAAGTTCTGCTATGTGGCGCGGTATTATCCCGTATTGACGC  
CGGGCAAGAGCAACTCGGTCGCCGCATACACTATTCTCAGAATGACTTGGTTGAGTACTCACCAGT  
CACAGAAAAGCATCTTACGGATGGCATGACAGTAAGAGAATTATGCAGTGCTGCCATAACCATGA  
GTGATAAACAAGTGCAGCAACTTACTTCTGACAACGATCGGAGGACCGAAGGAGCTAACCGCTTTTT  
TGCACAACATGGGGGATCATGTAACCTGCCTTGATCGTTGGGAACCGGAGCTGAATGAAGCCATAC  
CAAACGACGAGCGTGACACCAGATGCCTGTAGCAATGGCAACAACGTTGCGCAAACCTATTAACCT  
GGCGAACTACTTACTCTAGCTTCCCGGCAACAATTAATAGACTGGATGGAGGCGGATAAAGTTGCA  
GGACCACTTCTGCGCTCGGCCCTTCCGGTGGCTGGTTTTATTGCTGATAAATCTGGAGCCGGTGAGC  
GTGGGTCTCGCGGTATCATTGCAGCACTGGGGCCAGATGGTAAGCCCTCCCGTATCGTAGTTATCT  
ACACGACGGGGAGTCAGGCAACTATGGATGAACGAAATAGACAGATCGCTGAGATAGGTGCCT

## Results

CACTGATTAAGCATTGGTAACTGTCAGACCAAGTTTACTCATATATACTTTAGATTGATTTAAACT  
TCATTTTAAATTTAAAAGGATCTAGGTGAAGATCCTTTTTGATAATCTCATGACCAAATCCCTTAA  
CGTGAGTTTTTCGTTCCACTGAGCGTCAGACCCCGTAGAAAAGATCAAAGGATCTTCTTGAGATCCT  
TTTTTCTGCGCGTAATCTGCTGCTTGCAAACAAAAAACCCGCTACCAGCGGTGGTTTGTTCG  
CGGATCAAGAGCTACCAACTCTTTTTCCGAAGGTAAGTGGCTTCAGCAGAGCGCAGATACCAAATA  
CTGTTCTTCTAGTGTAGCCGTAGTTAGGCCACCACTTCAAGAACTCTGTAGCACCCGCTACATACCT  
CGCTCTGCTAATCCTGTTACCAGTGGCTGCTGCCAGTGGCGATAAGTCGTGTCTTACCGGGTTGGAC  
TCAAGACGATAGTTACCGGATAAGGCGCAGCGGTGCGGGCTGAACGGGGGGTTCGTGCACACAGCC  
CAGCTTGGAGCGAACGACCTACACCGAACTGAGATACCTACAGCGTGAGCTATGAGAAAGCGCCA  
CGTTCCCGAAGGGAGAAAGGCGGACAGGTATCCGGTAAGCGGCAGGGTTCGGAACAGGAGAGCG  
CACGAGGGAGCTTCCAGGGGAAACGCCTGGTATCTTTATAGTCCTGTGCGGTTTCGCCACCTCTG  
ACTTGAGCGTCGATTTTTGTGATGCTCGTCAGGGGGCGGAGCCTATGGAAAAACGCCAGCAACGC  
GGCCTTTTTACGGTTCCTGGCCTTTTGCTGGCCTTTTGCTCACATGTTCTTTCCTGCGTTATCCCCTG  
ATTCTGTGGATAACCGTATTACCGCCTTTGAGTGAGCTGATACCGCTCGCCGCAGCCGAACGACCG  
AGCGCAGCGAGTCAGTGAGCGAGGAAGCGGAAGAGCGCCAATACGCAAACCGCCTCTCCCCGCG  
CGTTGGCCGATTCATTAATGCAG

### ***CpKDO-HaloTag®***

GATCTCGATCCCGCGAAATTAATACGACTCACTATAGGGAGACCACAACGGTTTCCCTCTAGAAAT  
AATTTTGTAACTTTAAGAAGGAGATATACATATGCGGGGTTCTCATCATCATCATCATGTTA  
TGGCTAGCATGACTGGTGGACAGCAAATGGGTGCGGATCTGTACGACGATGACGATAAGGATCGA  
TGGGATCCATGATTGGCACCGGTTTTCCGTTTGATCCGCATTATGTTGAAGTTCTGGGTGAACGTA  
TGCATTATGTGGATGTTGGTCCGCGTGATGGTACACCGGTTCTGTTTCTGCATGGTAATCCGACCAG  
CAGCTATGTTTGGCGTAACATTATTCCGCATGTTGCACCGACACATCGTTGTATTGCACCGGATCTG  
ATTGGTATGGGTAAGCGATAAACCTGATCTGGGCTATTTTTTCGATGATCATGTGCGTTTTATGG  
ACGCCTTTATTGAAGCACTGGGTTTTAGAAGAAGTTGTGCTGGTTATTCATGATTGGGGTAGTGCCT  
GGTTTTTCATTGGGCAAACGTAATCCGGAACGTGTTAAAGGTATTGCCTTCATGGAATTTATTCGT  
CCGATTCCGACCTGGGATGAATGGCCTGAATTTGCACGTGAAACCTTTCAGGCATTTTCGTACCACC  
GATGTGGGTCGTAAACTGATTATTGATCAGAACGTTTTTATCGAAGGCACCCTGCCGATGGGTGTT  
GTTTCGTCGCTGACCGAAGTTGAAATGGATCATTATCGTGAACCGTTTCTGAATCCGGTTGATCGCG  
AACCGCTGTGGCGTTTTCCGAATGAACTGCCGATTGCCGGTGAACCTGCAAATATTGTTGCACTGG  
TTGAAGAGTATATGGATTGGCTGCATCAGAGTCCGGTTCGAAACTGCTGTTTTGGGGCACACCGG  
GTGTTCTGATTCCGCCTGCAGAAGCAGCACGTCTGGCAAAAAGCCTGCCGAATTGAAAAGCAGTTGATAT  
TGGTCCGGGTCTGAATCTGCTGCAAGAAGATAATCCAGATCTGATCGGTAGCGAAATTGCACGTTGGCTG  
AGCACCTGGAAATTAGCGGTCTGGCAGAAGCCGCAGCAAAAAGAAGCAGCTGCCAAAGAAGCGGCAGC  
GAAAGAGGCTGCAGCAAAGGCAGCAGCAGCCGAGTCGACAAAAAATCTGAGCGCATATGAA  
GTTTATGAGAGCCCCGAAAACCAGCGGTGAAAGCCGTACCGAAGCAGTTAGCGAAGCAGCATT  
TGAAAGCGATCCGGAAGTTAGCGCAATTCTGGTTCTGACCAGCAGTGAAGCAAGTACCCTGG  
AACGTGTGGCAGATCTGGTTACCGCACATGCACTGTATGCAGCACATGATTTTTGTGCACAG

## Results

GCACAGCTGGCAGCCGCAGAACTGCCGTCACGTGTTGTTGCACGTCTGCAAGAATTTGCATG  
GGGTGATATGAATGAAGGTCATCTGCTGATTAAAGGTCTGCCGCAGGTTTCGTAGCCTGCCTC  
CGACACCGACCAGTAATGTTTCATGCAGTTGCAGCAACCACACCGATGAGCCGTTATCAGGCA  
CTGATTAATGAATGTGTTGGTCGCATGATTGCCTATGAAGCCGAAGGTCATGGTCATACATTT  
CAGGATATGGTTCCGAGCGCAATGAGCGCACATAGCCAGACCAGCCTGGGTAGCGCAGTTGA  
ACTGGAAGTGCATACCGAACAGGCATTTAGTCCGCTGCGTCCGGATTTTGTAGCCTGGCAT  
GTCTGCGTGGTGATCCGCGTGCACTGACCTACCTGTTTAGCGCACGTGAGCTGGTTGCGACC  
CTGACCACACAAGAAATTGCAATGCTGCGTGAACCTATGTGGACCACCACCGTTGATGAAAG  
TTTTCTGGCGGAAGGTCGTACCTTTCTGCTGGGTTTTGAACGTGGTCCTATTCCGATTCTGAG  
CGGTGCAGATGATGATCCGTTTATTGTTTTGATCAGGATCTGATGCGTGGTATTAGCGCACC  
GGCACAAGAACTGCAGCAGACCGTTATTCGTGCATATTATGCAGAACGTGTGAGCCATTGTC  
TGGCACCGGGTGAGATGCTGCTGATTGATAATCGTCGTGCAGTTCATGGTCGTAGCATTTTT  
GCACCGCGTTTTGATGGTGCAGATCGTTTTCTGAGCCGTAGCTTTATTGTTGCCGATGGTAGC  
CGTAGCCGTCATGCACGTAGCAGCTTTGGTCTGTGTTGTGAGCGCACGTTTTAGCTAAGAATT  
CGAAGCTTGATCCGGCTGCTAACAAAGCCCGAAAGGAAGCTGAGTTGGCTGCTGCCACCGCTGAG  
CAATAACTAGCATAACCCCTTGGGGCCTCTAACCGGTCTTGAGGGGTTTTTGTGAAAGGAGGA  
ACTATATCCGGATCTGGCGTAATAGCGAAGAGGCCCGCACCGATCGCCCTTCCCAACAGTTGCGCA  
GCCTGAATGGCGAATGGGACGCGCCCTGTAGCGGCGCATTAAAGCGCGGCGGGTGTGGTGGTTACG  
CGCAGCGTGACCGCTACACTTGCCAGCGCCCTAGCGCCCGCTCCTTTCGCTTCTTCCCTTCCTTCT  
CGCCACGTTCCGCGGCTTTCCCGTCAAGCTCTAAATCGGGGGCTCCCTTAGGGTCCGATTTAGT  
GCTTTACGGCACCTCGACCCCAAAAACTTGATTAGGGTGATGGTTCACGTAGTGGGCCATCGCCC  
TGATAGACGGTTTTTTCGCCCTTGGACGTTGGAGTCCACGTTCTTTAATAGTGGACTCTTGTCCAAA  
CTGGAACAACACTCAACCCTATCTCGGTCTATTCTTTGATTTATAAGGGATTTTGCCGATTTCCGC  
CTATTGGTTAAAAAATGAGCTGATTTAACAAAAATTTAACGCGAATTTTAACAAAATATTAACGCT  
TACAATTTAGGTGGCACTTTTCGGGGAAATGTGCGCGGAACCCCTATTGTTTATTTTTCTAAATAC  
ATTCAAATATGTATCCGCTCATGAGACAATAACCCTGATAAATGCTTCAATAATATTGAAAAAGGA  
AGAGTATGAGTATTCAACATTTCCGTGTCGCCCTTATTCCCTTTTTTGCGGCATTTTGCCTTCTGTT  
TTTGCTCACCCAGAAACGCTGGTGAAAGTAAAAGATGCTGAAGATCAGTTGGGTGCACGAGTGGG  
TTACATCGAACTGGATCTCAACAGCGGTAAGATCCTTGAGAGTTTTTCGCCCCGAAGAACGTTTTCC  
AATGATGAGCACTTTTAAAGTTCTGCTATGTGGCGCGGTATTATCCCGTATTGACGCCGGGCAAGA  
GCAACTCGGTGCGCCGCATACACTATTCTCAGAATGACTTGGTTGAGTACTACCAGTACACAGAAAA  
GCATCTTACGGATGGCATGACAGTAAGAGAATTATGCAGTGTGCCATAACCATGAGTGATAACAC  
TGCGGCCAACTTACTTCTGACAACGATCGGAGGACCGAAGGAGCTAACCGCTTTTTTGACAACAT  
GGGGGATCATGTAACCTGCCTTGATCGTTGGGAACCGGAGCTGAATGAAGCCATAACCAAACGACG  
AGCGTGACACCACGATGCCTGTAGCAATGGCAACAACGTTGCGCAAACCTATTAACCTGGCGAACTAC  
TACTCTAGCTTCCCGCAACAATTAATAGACTGGATGGAGGCGGATAAAGTTGCAGGACCACTTC  
TGCGCTCGGCCCTTCCGGCTGGCTGGTTTATTGCTGATAAATCTGGAGCCGGTGAGCGTGGGTCTCG  
CGGTATCATTGCAGCACTGGGGCCAGATGGTAAGCCCTCCCGTATCGTAGTTATCTACACGACGGG  
GAGTCAGGCAACTATGGATGAACGAAATAGACAGATCGCTGAGATAGGTGCCTCACTGATTAAGC  
ATTGGTAACTGTCAGACCAAGTTTACTCATATATACTTTAGATTGATTTAAAACCTTCATTTTAATTT

## Results

AAAAGGATCTAGGTGAAGATCCTTTTTGATAATCTCATGACCAAATCCCTTAACGTGAGTTTTTCGT  
TCCACTGAGCGTCAGACCCCGTAGAAAAGATCAAAGGATCTTCTTGAGATCCTTTTTTTCTGCGCGT  
AATCTGCTGCTTGCAAACAAAAAACCACCGCTACCAGCGGTGGTTTTGTTTGCCGGATCAAGAGCT  
ACCAACTCTTTTTCCGAAGGTAAGTGGCTTCAGCAGAGCGCAGATACCAAATACTGTTCTTCTAGTG  
TAGCCGTAGTTAGGCCACCACTTCAAGAACTCTGTAGCACCGCTACATACTCGCTCTGCTAATCC  
TGTTACCAGTGGCTGCTGCCAGTGGCGATAAGTCGTGTCTTACCGGGTTGGACTCAAGACGATAGT  
TACCGGATAAGGCGCAGCGGTGGGCTGAACGGGGGGTTCGTGCACACAGCCAGCTTGGAGCGA  
ACGACCTACACCGAACTGAGATACCTACAGCGTGAGCTATGAGAAAGCGCCACGCTTCCCGAAGG  
GAGAAAGGCGGACAGGTATCCGGTAAGCGGCAGGGTCGGAACAGGAGAGCGCACGAGGGAGCTT  
CCAGGGGGAAACGCCTGGTATCTTTATAGTCTGTCCGGTTTCGCCACCTCTGACTTGAGCGTCGAT  
TTTTGTGATGCTCGTCAGGGGGGCGGAGCCTATGGAAAAACGCCAGCAACGCGGCCTTTTTACGGT  
TCCTGGCCTTTTGCTGGCCTTTTGCTCACATGTTCTTTCCTGCGTTATCCCCTGATTCTGTGGATAAC  
CGTATTACCGCCTTTGAGTGAGCTGATACCGCTCGCCGACGCCGACCGAGCGCAGCGAGTCAG  
TGAGCGAGGAAGCGGAAGAGCGCCCAATACGCAAACCGCCTCTCCCCGCGCGTTGGCCGATTCAAT  
AATGCAG

### ***FjKDO-HaloTag®***

GATCTCGATCCCGCGAAATTAATACGACTCACTATAGGGAGACCACAACGGTTTTCCCTCTAGAAAT  
AATTTTGTAACTTTAAGAAGGAGATATACATATGCGGGGTTCTCATCATCATCATCATGTTA  
TGGCTAGCATGACTGGTGGACAGCAAATGGGTTCGGGATCTGTACGACGATGACGATAAAGGATCGA  
TGGGGATCCATGATTGGCACCCGGTTTTCCGTTTGATCCGCATTATGTTGAAGTTCTGGGTGAACGTA  
TGCATTATGTGGATGTTGGTCCGCGTGATGGTACACCCGGTCTGTTTCTGCATGGTAATCCGACCAG  
CAGCTATGTTTGGCGTAACATTATTCCGCATGTTGCACCGACACATCGTTGTATTGCACCCGATCTG  
ATTGGTATGGGTAAGCGATAAACCTGATCTGGGCTATTTTTTCGATGATCATGTGCGTTTTATGG  
ACGCCTTTATTGAAGCACTGGGTTTAGAAGAAGTTGTGCTGGTTATTCATGATTGGGGTAGTGCCCT  
GGTTTTTCATTGGGCAAACGTAATCCGGAACGTGTTAAAGGTATTGCCTTCATGGAATTTATTCGT  
CCGATTCCGACCTGGGATGAATGGCCTGAATTTGCACGTGAAACCTTTCAGGCATTTTCGTACCACC  
GATGTGGGTCGTAAACTGATTATTGATCAGAACGTTTTTATCGAAGGCACCCTGCCGATGGGTGTT  
GTTTCGTCCGCTGACCGAAGTTGAAAATGGATCATTATCGTGAACCGTTTTCTGAATCCGGTTGATCGCG  
AACCGCTGTGGCGTTTTCCGAATGAACTGCCGATTGCCGGTGAACCTGCAAATATTGTTGCACTGG  
TTGAAGAGTATATGGATTGGCTGCATCAGAGTCCGGTTCGGAACTGCTGTTTTGGGGCACACCGGGT  
GTTCTGATTCCGCCTGCAGAAGCAGCACGTCTGGCAAAAAGCCTGCCGAATTGAAAAGCAGTTGATATTG  
GTCCGGGTCTGAATCTGCTGCAAGAAGATAATCCAGATCTGATCGGTAGCGAAATTGCACGTTGGCTGAG  
CACCCTGGAATTAGCGGTCTGGCAGAAGCCGACGAAAAGAAGCAGCTGCCAAAGAAGCGGCAGCGAA  
AGAGGCTGCAGCAAAGGCAGCAGCCGAGTCGACAAAAAGCCAGAGCCTGATTGAAGATGAA  
ATTCGGTGAAAAGAACTATGCCTATCAGATTCCGACAAGTCCGCTGATTGTTGAAGTGAC  
ACCGCAAGAACGTAATATTCTGAGCAATGTTGGTGCCTGCTGGAAAAAGCATTAAAAGCT  
ATGAGAACCCGATTATATTGAAGCCCTGCATCTGTATAGCTTTCAGCTGCTGCCGGAACGT  
ATTGCACGTATTCTGAGTCGTTTTGGTACAGATTTTAGCGCAGATCAGTATGGTGCAATTATC

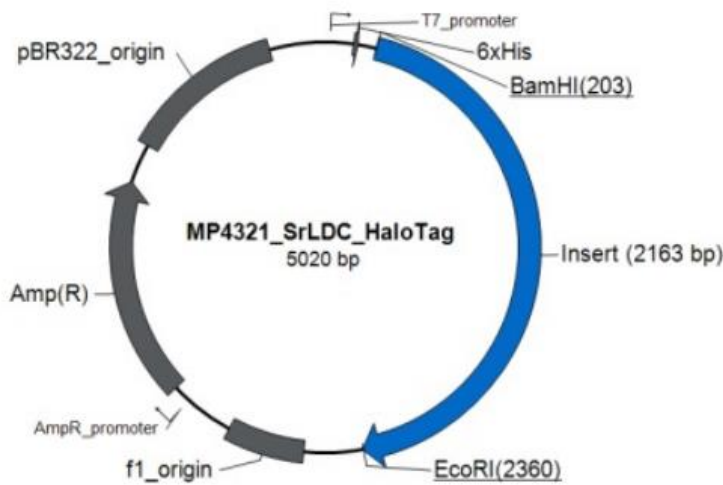
## Results

TTTCGTGGTCTGCTGGAAGTTGATCAGGATCATCTGGGTCCGACACCCGGCAAATTGGCAGAG  
CGCAGATTATAGCAAACCTGAACAAATATGGCTTTATCTGCAGCCTGCTGCATGGTGCAGTTCC  
GAGCAAACCGGTTCAAGTATTATGCACAGCGTAAAGGTGGTGGTATTCTGCATGCCGTTATTC  
CGGATGAAAAAATGGCAGCAACCCAGACCGGTAGCGGTAGCAAAACCAATCTGTATGTTTCAT  
ACCGAAGATGCCTTTCTGCTGCACCAGGCAGATTTTCTGAGCTTTCTGTATCTGCGTAATGAA  
GAACGTGTGCCGAGCACACTGTATAGCGTTCGTAGCCATGGTAAAGTGAACAAGATTATGGA  
AAAACCTGTTTCGACCCGATTTATCAGTGTCCGAAAGATGCCAATTATCAAGAAGAAATTAACGA  
CGGTCCGCTGGCAAGCGTTCTGTATGGTAACAAAAAACTGCCGTTTATTTCGTTTTGATGCAGC  
GGAGCAGATTTTAAACGAAAATGCAGGTCAGACACCCGGAAGCACTGTATAATCTGACCGAAT  
TTTGGAACGAAGCCAAAGAACTGATCAACAGCGATTACATTCGGATAGCGGTGATGTGATT  
TTTGTGAATAATCATCTGTGTGCACATGGTCGTAGCGCATTACCCGAGGCCAGAAAGAAGA  
AAACGGTAAACTGGTTCCGTGTGAACGTCGTCAGATGCTGCGTATGATGAGCAAAACCTCAC  
TGATTCATATTCGTAGCATGACCATACCGATGATCCGTAATTCGTTATGGAAGAACATCTGG  
GCAAAGTTTTTTCGATCAGGCCTAAGAATTCGAAGCTTGATCCGGCTGCTAACAAAGCCCGAAAGG  
AAGCTGAGTTGGCTGCTGCCACCGCTGAGCAATAACTAGCATAACCCCTTGGGGCCTCTAAACGGG  
TCTTGAGGGGTTTTTTGCTGAAAGGAGGAACTATATCCGGATCTGGCGTAATAGCGAAGAGGCCCG  
CACCGATCGCCCTCCCAACAGTTGCGCAGCCTGAATGGCGAATGGGACGCGCCCTGTAGCGGGCGC  
ATTAAGCGCGGGCGGGTGTGGTGGTTACGCGCAGCGTGACCGCTACACTTGCCAGCGCCCTAGCGCC  
CGCTCCTTTCGCTTTCTTCCCTTCTTCTCGCCACGTTCCGCGGCTTCCCCCGTCAAGCTCTAAATC  
GGGGGCTCCCTTAGGGTTCCGATTTAGTGCTTTACGGCACCTCGACCCCAAAAACTTGATTAGG  
GTGATGGTTCACGTAGTGGGCCATCGCCCTGATAGACGGTTTTTCGCCCTTGACGTTGGAGTCCAC  
GTTCTTTAATAGTGGACTCTTGTTCAAACTGGAACAACACTCAACCCTATCTCGGTCTATTCTTTT  
GATTTATAAGGGATTTTGCCGATTTTCGGCCTATTGGTTAAAAAATGAGCTGATTTAACAAAAATTTA  
ACGCGAATTTTAAACAAAATATTAACGCTTACAATTTAGGTGGCACTTTTCGGGGAAATGTGCGCGG  
AACCCCTATTTGTTTATTTTTCTAAATACATTCAAATATGTATCCGCTCATGAGACAATAACCCTGA  
TAAATGCTTCAATAATATTGAAAAAGGAAGAGTATGAGTATTCAACATTTCCGTGTCCGCTTATTC  
CCTTTTTTTCGCGCATTTTGCCTTCTGTTTTTGTCTACCCAGAAACGCTGGTGAAAGTAAAAGATGC  
TGAAGATCAGTTGGGTGCACGAGTGGGTTACATCGAACTGGATCTCAACAGCGGTAAGATCCTTGA  
GAGTTTTTCGCCCCGAAGAACGTTTTTCCAATGATGAGCACTTTTAAAGTTCTGCTATGTGGCGCGGTA  
TTATCCCGTATTGACGCCGGGCAAGAGCAACTCGGTCCGCGCATACTACTTCTCAGAATGACTTG  
GTTGAGTACTCACCAGTCACAGAAAAGCATCTTACGGATGGCATGACAGTAAGAGAATTATGCAGT  
GCTGCCATAACCATGAGTGATAAACAACACTGCGGCCAACTTACTTCTGACAACGATCGGAGGACCGAAG  
GAGCTAACCGCTTTTTTGCACAACATGGGGGATCATGTAACCTCGCCTTGATCGTTGGGAACCGGAG  
CTGAATGAAGCCATAACCAAACGACGAGCGTGACACCACGATGCCTGTAGCAATGGCAACAACGTT  
GCGCAAACCTATTAACCTGGCGAACTACTTACTCTAGCTTCCCGGCAACAATTAATAGACTGGATGGA  
GGCGGATAAAGTTGCAGGACCACTTCTGCGCTCGGCCCTCCGGCTGGCTGGTTTATTGCTGATAA  
ATCTGGAGCCGGTGAGCGTGGGTCTCGCGGTATCATTGCAGCACTGGGGCCAGATGGTAAGCCCTC  
CCGTATCGTAGTTATCTACACGACGGGGAGTCAGGCAACTATGGATGAACGAAATAGACAGATCG  
CTGAGATAGGTGCCTCACTGATTAAGCATTGGTAACTGTCAGACCAAGTTTACTCATATATACTTTA  
GATTGATTTAAAACCTTCATTTTTAATTTAAAAGGATCTAGGTGAAGATCCTTTTTGATAATCTCATG

## Results

ACCAAAATCCCTTAACGTGAGTTTTTCGTTCCACTGAGCGTCAGACCCCGTAGAAAAGATCAAAGGA  
TCTTCTTGAGATCCTTTTTTTCTGCGCGTAATCTGCTGCTTGCAAACAAAAAACACCGCTACCAG  
CGGTGGTTTTGTTTGCCGGATCAAGAGCTACCAACTCTTTTTCCGAAGGTAAGTGGCTTCAGCAGAG  
CGCAGATACCAAATACTGTTCTTCTAGTGTAGCCGTAGTTAGGCCACCACTTCAAGAACTCTGTAG  
CACCGCCTACATACCTCGCTCTGCTAATCCTGTTACCAGTGGCTGCTGCCAGTGGCGATAAGTCGTG  
TCTTACCGGGTTGGACTCAAGACGATAGTTACCGGATAAAGGCGCAGCGGTCGGGCTGAACGGGGG  
GTTTCGTGCACACAGCCCAGCTTGGAGCGAACGACCTACACCGAACTGAGATACTACAGCGTGAG  
CTATGAGAAAGCGCCACGCTTCCCGAAGGGAGAAAGGCGGACAGGTATCCGTAAGCGGCAGGGT  
CGGAACAGGAGAGCGCACGAGGGAGCTTCCAGGGGAAACGCCTGGTATCTTTATAGTCCTGTGCG  
GGTTTCGCCACCTCTGACTTGAGCGTCGATTTTTGTGATGCTCGTCAGGGGGCGGAGCCTATGGA  
AAAACGCCAGCAACGCGGCCTTTTTACGGTTCCTGGCCTTTTGTGCTGGCCTTTTGTGCTCACATGTTCTTT  
CCTGCGTTATCCCCTGATTCTGTGGATAACCGTATTACCGCCTTTGAGTGAGCTGATACCGCTCGCC  
GCAGCCGAACGACCGAGCGCAGCGAGTCAGTGAGCGAGGAAGCGGAAGAGCGCCCAATACGCAA  
ACCGCCTCTCCCCGCGCGTTGGCCGATTCATTAATGCAG

### **SrLDC-HaloTag®**



GATCTCGATCCCGCGAAATTAATACGACTCACTATAGGGAGACCACAACGGTTTTCCCTCTAGAAAT  
AATTTTGTTTAACTTTAAGAAGGAGATATACATATGCGGGGTTCTCATCATCATCATCATGGTA  
TGGCTAGCATGACTGGTGGACAGCAAATGGGTCCGGATCTGTACGACGATGACGATAAGGATCGA  
TGGGGATCCATGATTGGCACCGGTTTTCCGTTTGATCCGCATTATGTTGAAGTTCTGGGTGAACGTA  
TGCATTATGTGGATGTTGGTCCGCGTGATGGTACACCGGTTCTGTTTCTGCATGGTAATCCGACCAG  
CAGCTATGTTTGGCGTAACATTATTCCGCATGTTGCACCGACACATCGTTGTATTGCACCGGATCTG  
ATTGGTATGGGTAAGCGATAAACCTGATCTGGGCTATTTTTTCGATGATCATGTGCGTTTTATGG  
ACGCCTTTATTGAAGCACTGGGTTTAGAAGAAGTTGTGCTGGTTATTCATGATTGGGGTAGTGCCTT

## Results

GGGTTTTTCATTGGGCAAACGTAATCCGGAACGTGTTAAAGGTATTGCCTTCATGGAATTTATTTCGT  
CCGATTCCGACCTGGGATGAATGGCCTGAATTTGCACGTGAAACCTTTCAGGCATTTTCGTACCACC  
GATGTGGGTCGTAAACTGATTATTGATCAGAACGTTTTTATCGAAGGCACCCTGCCGATGGGTGTT  
GTTTCGTCCGCTGACCGAAGTTGAAATGGATCATTATCGTGAACCGTTTTCTGAATCCGGTTGATCGCG  
AACCGCTGTGGCGTTTTCCGAATGAACTGCCGATTGCCGGTGAACCTGCAAATATTGTTGCACTGG  
TTGAAGAGTATATGGATTGGCTGCATCAGAGTCCGGTCCGAAACTGCTGTTTTGGGGCACACCGG  
GTGTTCTGATTCCGCCTGCAGAAGCAGCACGTCTGGCAAAAAGCCTGCCGAATTGTAAAGCAGTTG  
ATATTGGTCCGGGTCTGAATCTGCTGCAAGAAGATAATCCAGATCTGATCGGTAGCGAAATTGCAC  
GTTGGCTGAGCACCTGGAAATTAGCGGTCTGGCAGAAGCCGCAGCAAAAAGAAGCAGCTGCCAAA  
GAAGCGGCAGCGAAAGAGGCTGCAGCAAAGGCAGCAGCAGCCGAAGTCGACAAAAACTTTCGTCT  
GAGCGAAAAAGAAGTTAAAACCCTGGCCAAACGTATTCCGACGCCGTTTTCTGGTTGCAAGCCTGGA  
TAAAGTTGAAGAGAACTATCAGTTTATGCGTCGTATCTGCCTCGTGCCGGTGTTTTTTATGCAATG  
AAAGCAAATCCGACACCGGAAATTCTGAGCCTGCTGGCAGGTCTGGGTAGCCATTTTATGTTGCA  
TCAGCCGGTGAAATGGAAATCCTGCATGAACTGGGTGTTGATGGTAGCCAGATGATTTATGCAAAT  
CCGGTTAAAGATGCACGTGGTCTGAAAGCAGCCGCAGATTATAATGTTTCGTCGTTTTACCTTTGATG  
ATCCGAGCGAAATCGATAAAATGGCAAAAAGCAGTTCCGGGTGCAGATGTTCTGGTTCGTATTGCAG  
TTCGTAATAACAAAGCCCTGGTTGATCTGAATACGAAATTTGGTGCACCGGTGGAAGAAGCCCTGG  
ATCTGCTGAAAGCCGCACAGGATGCAGGTCTGCATGCAATGGGTATTTGTTTTTCATGTTGGTAGTC  
AGAGCCTGAGCACCGCAGCATATGAAGAAGCACTGCTGGTTGCACGTCGTCTGTTTATGAAAGCCG  
AAGAAATGGGTATGCATCTGACCGATCTGGATATTGGTGGTGGTTTTCCGGTTCCTGATGCAAAAAG  
GTCTGAATGTTGATCTGGCAGCAATGATGGAAGCCATTAATAAGCAGATTGATCGCCTGTTTCCGG  
ATACCGCAGTTTGGACCGAACC GGTCGTTATATGTGTGGCACCGCAGTTAATCTGGTTACCAGCG  
TTATTGGTACAAAAACCCGTGGTGAACAGCCGTGGTATATTCTGGATGAAGGTATTTATGGTTGCTT  
CAGCGGCATCATGTATGATCATTGGACCTATCCGCTGCATTGTTTTGGTAAAGGTAACAAAAAACC  
GAGCACCTTTGGTGGTCCGAGTTGTGATGGTATTGATGTTCTGTATCGTGATTTTATGGCACCGGAA  
CTGAAAATTGGTGATAAAGTTCTGGTGACCGAAATGGGTTTCATATACCAGCGTGAGCGCAACCCGT  
TTAATGGTTTTTATCTGGCACCGACCATCATCTTTGAAGATCAGCCGGAAATATGCAGCCCGTCTGA  
CGGAAGATGATGATGTTAAAAAGAAAGCAGCGGTGTAAGAATTCGAAGCTTGATCCGGCTGCTAA  
CAAAGCCCGAAAGGAAGCTGAGTTGGCTGCTGCCACCGCTGAGCAATAACTAGCATAACCCCTTG  
GGCCTCTAAACGGGTCTTGAGGGGTTTTTTGCTGAAAGGAGGAACTATATCCGGATCTGGCGTAA  
TAGCGAAGAGGCCCGCACCGATCGCCCTCCCAACAGTTGCGCAGCCTGAATGGCGAATGGGACG  
CGCCCTGTAGCGGCGCATTAAAGCGCGGCGGGTGTGGTGGTTACGCGCAGCGTGACCGCTACACTTG  
CCAGCGCCCTAGCGCCCGCTCCTTTTCGCTTTCTCCCTTCCTTTCTCGCCACGTTTCGCCGGCTTTCCC  
CGTCAAGCTCTAAATCGGGGGCTCCCTTTAGGGTTCAGATTTAGTGCTTTACGGCACCTCGACCCCA  
AAAACTTGATTAGGGTGATGGTTCACGTAGTGGGCCATCGCCCTGATAGACGGTTTTTTCGCCCTTT  
GACGTTGGAGTCCACGTTCTTTAATAGTGGACTCTTGTTCCAAACTGGAACAACACTCAACCCTATC  
TCGGTCTATTCTTTTGATTTATAAGGGATTTTGCCGATTTTCGGCCTATTGGTTAAAAAATGAGCTGA  
TTTAACAAAAATTTAACGCGAATTTTAACAAAATATTAACGCTTACAATTTAGGTGGCACTTTTCGG  
GGAAATGTGCGCGGAACCCCTATTTGTTTATTTTTCTAAATACATTCAAATATGTATCCGCTCATGA  
GACAATAACCCTGATAAATGCTTCAATAATATTGAAAAAGGAAGAGTATGAGTATTCAACATTTCC

## Results

GTGTCGCCCTTATTCCCTTTTTGCGGCATTTTGCCTTCCTGTTTTGCTCACCCAGAAACGCTGGTG  
AAAGTAAAAGATGCTGAAGATCAGTTGGGTGCACGAGTGGGTACATCGAACTGGATCTCAACAG  
CGGTAAGATCCTTGAGAGTTTTCGCCCCGAAGAAGCTTTTCCAATGATGAGCACTTTTAAAGTTCTG  
CTATGTGGCGCGGTATTATCCCGTATTGACGCCGGGCAAGAGCAACTCGGTCGCCGCATACACTAT  
TCTCAGAATGACTTGGTTGAGTACTCACCAGTCACAGAAAAGCATCTTACGGATGGCATGACAGTA  
AGAGAATTATGCAGTGCTGCCATAACCATGAGTGATAACACTGCGGCCAACTTACTTCTGACAACG  
ATCGGAGGACCGAAGGAGCTAACCGCTTTTTTGCACAACATGGGGGATCATGTAACCTGCCTTGAT  
CGTTGGGAACCGGAGCTGAATGAAGCCATACCAAACGACGAGCGTGACACCACGATGCCTGTAGC  
AATGGCAACAACGTTGCGCAAACCTATTAACCTGGCGAACTACTTACTCTAGCTTCCCGGCAACAATT  
AATAGACTGGATGGAGGCGGATAAAGTTGCAGGACCACTTCTGCGCTCGGCCCTTCCGGCTGGCTG  
GTTTTATTGCTGATAAATCTGGAGCCGGTGAGCGTGGGTCTCGCGGTATCATTGCAGCACTGGGGCC  
AGATGGTAAGCCCTCCCGTATCGTAGTTATCTACACGACGGGGAGTCAGGCAACTATGGATGAACG  
AAATAGACAGATCGCTGAGATAGGTGCCTCACTGATTAAGCATTGGTAACTGTCAGACCAAGTTTA  
CTCATATATACTTTAGATTGATTTAAACTTCATTTTTAATTTAAAAGGATCTAGGTGAAGATCCTT  
TTTGATAATCTCATGACCAAATCCCTAACGTGAGTTTTCGTTCCACTGAGCGTCAGACCCCGTAG  
AAAAGATCAAAGGATCTTCTTGAGATCCTTTTTTCTGCGCGTAATCTGCTGCTTGCAAACAAAAAA  
ACCACCGCTACCAGCGGTGGTTTTGTTTGCCGGATCAAGAGCTACCAACTCTTTTTCCGAAGGTAAC  
GGCTTCAGCAGAGCGCAGATAACCAAATACTGTTCTTCTAGTGTAGCCGTAGTTAGGCCACCACTTC  
AAGAACTCTGTAGCACCGCCTACATACCTCGCTCTGCTAATCCTGTTACCAGTGGCTGCTGCCAGTG  
GCGATAAGTCGTGTCTTACCGGGTTGGACTCAAGACGATAGTTACCGGATAAGGCGCAGCGGTCGG  
GCTGAACGGGGGGTTCGTGCACACAGCCCAGCTTGGAGCGAACGACCTACACCGAACTGAGATAC  
CTACAGCGTGAGCTATGAGAAAGCGCCACGCTTCCCGAAGGGAGAAAGGCGGACAGGTATCCGGT  
AAGCGGCAGGGTCGGAACAGGAGAGCGCACGAGGGAGCTTCCAGGGGGAAACGCCTGGTATCTTT  
ATAGTCCTGTGCGGTTTTCGCCACCTCTGACTTGAGCGTTCGATTTTTGTGATGCTCGTCAGGGGGGCG  
GAGCCTATGGAAAACGCCAGCAACGCGGCCTTTTTACGGTTCCTGGCCTTTTGCTGGCCTTTTGCT  
CACATGTTCTTTCCTGCGTTATCCCTGATTCTGTGGATAACCGTATTACCGCCTTTGAGTGAGCTG  
ATACCGCTCGCCGCAGCCGAACGACCGAGCGCAGCGAGTCAGTGAGCGAGGAAGCGGAAGAGCG  
CCCAATACGCAAACCGCCTCTCCCCGCGCGTTGGCCGATTCATTAATGCAG

### 2.2.14 References

1. Zhang, X.; King-Smith, E.; Renata, H. Total Synthesis of Tambromycin by Combining Chemocatalytic and Biocatalytic C–H Functionalization. *Angew. Chemie - Int. Ed.* **2018**, *57*, 5037–5041, doi:10.1002/anie.201801165.
2. Baud, D.; Saaidi, P.-L.L.; Monfleur, A.; Harari, M.; Cuccaro, J.; Fossey, A.A.; Besnard, M.; Debard, A.; Mariage, A.; Pellouin, V.; et al. Synthesis of Mono- and Dihydroxylated Amino Acids with New  $\alpha$ -Ketoglutarate-Dependent Dioxygenases: Biocatalytic Oxidation of C-H Bonds. *ChemCatChem* **2014**, *6*, 3012–3017, doi:10.1002/cctc.201402498.
3. Baud, D.; Peruch, O.; Saaidi, P.L.; Fossey, A.; Mariage, A.; Petit, J.L.; Salanoubat, M.; Vergne-Vaxelaire, C.; de Berardinis, V.; Zaparucha, A. Biocatalytic Approaches towards the Synthesis of Chiral Amino Alcohols from Lysine: Cascade Reactions Combining  $\alpha$ -Keto Acid Oxygenase Hydroxylation with Pyridoxal Phosphate- Dependent Decarboxylation. *Adv. Synth. Catal.* **2017**, *359*, 1563–1569.
4. Bradford, M.M. A Rapid and Sensitive Method for the Quantitation Microgram Quantities of Protein Utilizing the Principle of Protein-Dye Binding. *Anal. Biochem.* **1976**, 248–254, doi:10.1016/j.cj.2017.04.003.
5. Bastard, K.; Isabet, T.; Stura, E.A.; Legrand, P.; Zaparucha, A. Structural Studies based on two Lysine Dioxygenases with Distinct Regioselectivity Brings Insights Into Enzyme Specificity within the Clavaminate Synthase-Like Family. *Sci. Rep.* **2018**, *8*, 8–18, doi:10.1038/s41598-018-34795-9.
6. Chen, R.F.; Scott, C.; Trepman, E. Fluorescence properties of o-phthaldialdehyde derivatives of amino acids. *BBA - Protein Struct.* **1979**, *576*, 440–455, doi:10.1016/0005-2795(79)90419-7.
7. Hara, R.; Yamagata, K.; Miyake, R.; Kawabata, H.; Uehara, H.; Kino, K.; Baud, D.; Saaidi, P.L.; Monfleur, A.; Harari, M.; et al. Discovery of Lysine Hydroxylases in the Clavaminate Acid Synthase-Like Superfamily for Efficient Hydroxylysine Bioproduction. *Appl. Environ. Microbiol.* **2017**, *83*, 1–14, doi:10.1128/AEM.00693-17.
8. Prell, C.; Vonderbank, S.-A.; Meyer, F.; Pérez-García, F.; Wendisch, V.F. Metabolic engineering of *Corynebacterium glutamicum* for de novo production of 3-hydroxycadaverine. *Curr. Res. Biotechnol.* **2021**, *4*, 32–46, doi:10.1016/j.crbiot.2021.12.004.
9. Paczia, N.; Nilgen, A.; Lehmann, T.; Gätgens, J.; Wiechert, W.; Noack, S. Extensive exometabolome analysis reveals extended overflow metabolism in various microorganisms. *Microb. Cell Fact.* **2012**, *11*, 1–14, doi:10.1186/1475-2859-11-122.

### 3 Discussion

The biocatalytic (cascade) process employing KDOs and *Sr*LDC is still in an early development stage. Therefore, further bottlenecks of the overall (cascade) process were identified, which will be discussed in detail together with the development of corresponding optimization strategies. To this end, the results presented in Chapter 2 are discussed in more detail and supplemented with additional unpublished results where appropriate. The discussion will address the following aspects:

- I. **Biocatalyst production:** Expression systems and suitable enzyme purification strategies.
- II. **KDO reaction system:** Optimization of the reaction system, including evaluation of suitable assays.
- III. **Biocatalyst formulation:** strategies including enzyme immobilization, reaction engineering, and process engineering.
- IV. **Application of immobilized KDOs in analytical- and preparative scale biotransformations:** Including repetitive batch studies, development of a KDO regeneration system, and KDO application in different preparative lab scales with different substrate concentrations.
- V. **Cascade reaction towards (2*S*)-hydroxy-cadaverine:** Development and evaluation of cascade reactions towards hydroxy-cadaverine using HaloTag® immobilized *Ca*KDO and *Sr*LDC in preparative lab scale.
- VI. ***Sr*LDC as an alternative enzyme for the production of biopolymer precursors:** Evaluation of *Sr*LDC as a suitable catalyst for the production of cadaverine, putrescine, and hydroxylated-cadaverine.
- VII. **Product isolation and purification:** Identification of bottlenecks and discussion of purification or reaction engineering strategies for the optimization of the purification of hydroxy-L-lysine and hydroxy-cadaverine
- VIII. **Economic and ecological process evaluation**

### 3.1 Biocatalyst Production

#### 3.1.1 Soluble KDO production

KDOs are specifically complex enzymes. They require Fe(II) as a cofactor, which must be kept in the reduced state to enable activity. Further,  $\alpha$ -ketoglutarate is required as a cosubstrate. Both additives are probably also needed for the stability of these enzymes and to enable proper folding. Additionally, *Ca*KDO shows hydrophobic patches on its surface (Chapter 3.3.3). Taken together, the frequently observed formation of inactive inclusion bodies upon recombinant expression in *E. coli* [78] is not surprising. To improve the soluble production of these enzymes, even vertebrate expression systems in CHO cells were used for the human lysyl hydroxylase LH2 [165]. In this work, a screening of suitable production conditions in *E. coli* BL21 (DE3), but also in different *E. coli* strains like Tuner BL21 (DE3) for uniform IPTG distribution and Rosetta2 BL21 (DE3) to overcome *E. coli*'s codon bias (Chapter 1.6.1), was performed (Table 12).

Many other groups working with KDOs use different Rosetta strains (Chapter 1.6.1) for the production of diverse KDOs. This was demonstrated by Dann et al. [55] and Hara et al. [83,166,167] who produced an asparaginyl hydroxylase (FIH-1), different lysine hydroxylases [83], a proline hydroxylase (*cis*-3Hyp) [167], and an ectoin hydroxylase (EctD) [166] in different Rosetta strains, respectively. Although *E. coli* has a remarkable capacity to produce large quantities of recombinant protein, there are limits when the codon usage in the mRNA for the recombinant gene differs from that of the *E. coli* host, therefore Rosetta BL21 expression hosts contain extra copies of the *E. coli* tRNA genes with rare codons (Chapter 1.6.1) [121–123]. However, in our case, expression in Rosetta2 BL21 (DE3) did not lead to an increase in soluble protein production, but we achieved an increase in soluble KDO production for all three KDOs when the genes were co-expressed with the GroEL/ES chaperones (Chapter 1.6.1) by applying a protocol from Zhang et al. [82] (SI, Chapter 2.2.1.1, Figure S24). Without co-expression of chaperones, the KDOs were barely active and precipitated already from the cell-free extract. Especially for *Fj*KDO soluble enzyme production was significantly increased (SI, Chapter 2.2.1.1, Figure S24). The production protocol was also successfully applied to the KDO-HaloTag® fusion variants (SI, Chapter 2.2.1.1, Figure S25).

During the course of this work also other groups successfully applied GroEL/ES for KDO co-expression [79,89]. Rolf & Nerke developed a cell-free protein synthesis system including chaperones for the initial screening of different lysine hydroxylases [80]. Surprisingly, co-

## Discussion

expression of chaperones showed an increase in enzyme concentration in only a few variants and a decrease in soluble protein production in others. Rolf & Nerke postulated that some chaperones (DnaJ, DnaK, and GrpE) can be inhibitory for the production of some proteins, probably due to enhanced proteolysis, as earlier published by Nishihara et al. [168]. This could also explain why in our case, co-expression of DnaK-DnaJ-GrpE-GroES-GroEL did not increase soluble protein production (Table 12). While oxygen supply is an important point during the biotransformation (Chapter 1.6.1), cultivation in the lab cultivation system (DASGIP) with controlled aeration did not increase soluble protein production. Also, supplementation of the cofactor, Fe(II), and reducing agent, L-ascorbic acid, which was crucial for the purification of active KDOs (Chapter 3.1.2), did not increase soluble protein production. The addition of  $\alpha$ -ketoglutarate was not tested, because we assumed that sufficient  $\alpha$ -ketoglutarate was present in the cells.

Table 12: Strategies tested to increase soluble KDO production. Some results are part of the bachelor thesis of Max Torkler [169].

Strategy	Conditions*	Enzyme	Increase in soluble protein production
<b>Different production media</b>	Lb-medium	<i>CpKDO</i>	no
	AI-medium		
	TB-medium		
	TB-medium + betaine & sorbitol		
	Wilms-MOPS		
	Brain Heart Broth		
<b>Controlled Aeration</b>	DASGIP cultivation in Wilms-MOPS medium	<i>CpKDO</i>	no
<b>IPTG Concentration</b>	0 - 0.5 mM	<i>CpKDO</i>	no
<b>Homogeneous IPTG distribution</b>	<i>E. coli</i> Tuner BL21 DE3	<i>CpKDO</i>	no
<b>Induction temperature</b> [169]	20 °C, 30 °C,	<i>CpKDO</i>	no

## Discussion

<b>Additional amount of tRNAs</b> [169]	<i>E. coli</i> Rosetta 2 BL21	<i>Ca</i> KDO	no
	DE3	<i>Cp</i> KDO	
<b>Addition of Cofactor/ Reducing Agent</b> [169]	Ammonium iron(II) sulfate (FeII), L-ascorbic acid, Dithiotreitol (in different concentrations)	<i>Cp</i> KDO	no
	DnaK-DnaJ-GrpE GroES-GroEL	<i>Cp</i> KDO	no
<b>Co-expression of chaperones</b>	GroEL/GroES	<i>Ca</i> KDO, <i>Cp</i> KDO, <i>Fj</i> KDO	Yes

\*If not explicitly stated, production was performed in *E. coli* BL21 DE3

### 3.1.2 Optimization of KDO purification

Next, we investigated under which purification conditions KDOs were most stable and precipitation could be prevented. As earlier reported [29], we also observed the loss of activity after elution from IMAC, when we tried to purify *Cp*KDO in TRIS buffer (SI, Figure S29). It is assumed that KDOs might lose the iron ion from the active site upon IMAC purification and therefore become instable [29]. Bastard et al. [66] reported that *Ca*KDO likely lost its iron upon purification for crystallization studies [66], which might support this hypothesis. It is also likely that KDOs become instable due to oxidative damage upon loss of the cellular environment, as discussed in Chapter 3.2. We presumed a positive effect on the enzyme stability upon the addition of these cofactors since *Ca*KDO and *Fs*KDO showed a higher degree of ordered structure in structural investigations upon binding of Fe(II) and  $\alpha$ -ketoglutarate [66]. *Ca*KDO was shown to be the most instable enzyme among the three tested KDOs in this work. Therefore, we first tested purification with additives on this enzyme. Purification was done in HEPES buffer, because the enzyme shows the highest activity in this buffer, but also sodium phosphate buffer was tested. Low concentrations of the cosubstrate  $\alpha$ -ketoglutarate (5 mM) and

## Discussion

dithiothreitol (DTT) (0.1 mM) as reducing agents were added to the equilibration, washing, and elution buffers. Directly after elution 2.5 mM L-ascorbic acid and 1 mM ammoniumiron(II)sulfate was added to the eluted enzyme and the desalting buffer, which successfully prevented precipitation during purification. While *Ca*KDO purified in HEPES buffer with 10 vol% glycerol showed the highest activity directly after purification, enzyme activity was rapidly lost after a few days of storage at different temperatures (Figure 68). However, HEPES buffer and glycerol both prevent lyophilization of the enzyme. Purification with sodium phosphate buffer (SI, Chapter 2.2.2.1.2) prevented precipitation and inactivation of all three KDOs successfully and lyophilization was achieved, leading to slightly prolonged enzyme activity during storage (Figure 68). Purification of *Ca*KDO produced with chaperones (SI, Chapter 2.2.1.1, Figure S27) yielded about 3.5 times more lyophilizate compared to expression without chaperones (Table 13), possibly, because more enzyme molecules were correctly folded when co-expressed with chaperones. SDS-PAGE demonstrates that after purification and immobilization, chaperones are still present (SI, Figure S24, and Figure S31), demonstrating the strong binding to the target enzyme, which was described previously for several other proteins [170].

However, as can be seen in Table 13, the enzyme yield is still low and purification of these enzymes is laborious and costly as well. In addition, all components from the desalting step accumulate in the lyophilizate, reducing the protein content to 10-40% (Table 13). This results in the need to use large amounts of lyophilizate, making the enzyme difficult to handle. In addition, precipitation of *Ca*KDO during biotransformations remained an issue (SI, Figure S30).

## Discussion

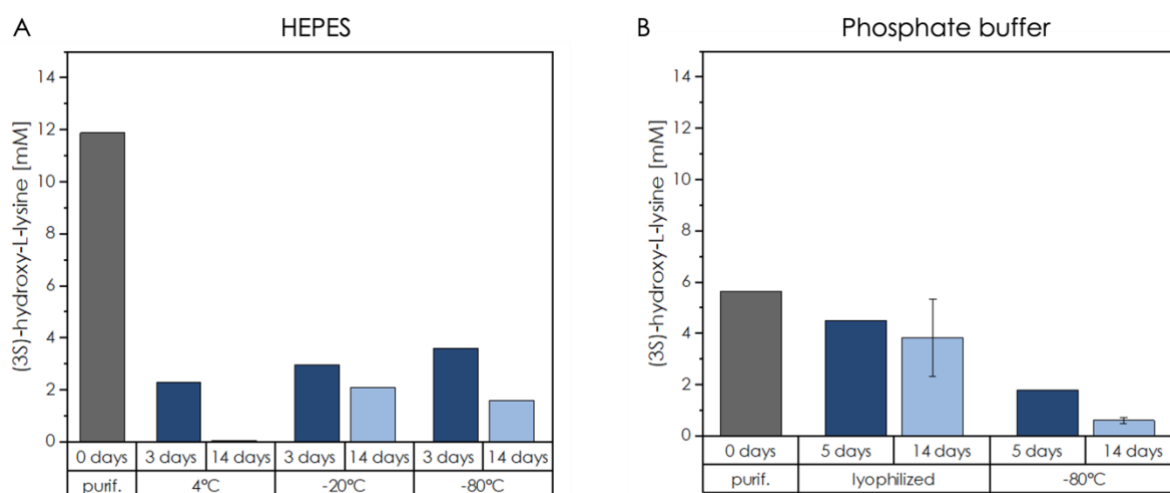


Figure 68: Storage stability of CaKDO after purification in A) HEPES buffer+10 vol% glycerol and B) Phosphate buffer. Day 0 corresponds to the day of purification. Afterward, enzymes were stored at the corresponding temperatures for the given time with the addition of 10 vol% glycerol. Enzymes purified in phosphate buffer were lyophilized on day 1 and tested after storage at -20 °C or 10 vol% glycerol was added for storage of the soluble enzyme at -80 °C. Reaction conditions for the determination of residual activity: 1 ml stock solution of 10 mM L-lysine, 15 mM  $\alpha$ -ketoglutarate, 2.5 mM L-ascorbic acid, 1 mM  $(\text{NH}_4)_2\text{Fe}(\text{SO}_4)_2$  in 50 mM HEPES, pH 7.5, was transferred into a 2 ml reaction tube. The reaction was started with the corresponding amount of enzyme (0.08 mg ml<sup>-1</sup> for purification in phosphate buffer or 0.06 mg ml<sup>-1</sup> for purification in HEPES buffer) at 300 rpm, room temperature, and an open lid for aeration. Samples were taken after 120 min, quenched at 80 °C for 5 min, and transferred to HPLC analytics. Technical duplicates in A were measured only for storage of the lyophilizate after 14 days. All the other data correspond to single measurements.

Table 13: Lyophilizate yield and protein content of different KDOs produced with and without chaperones after purification and lyophilization as described in the SI, Chapters 2.2.1.1 and 2.2.2.1.2.

Enzyme	mg lyophilizate per g wet cells	Protein content in lyophilizate [%]
<b>CaKDO with chaperones</b>	3.3	10
<b>CaKDO without chaperones</b>	11.4	20
<b>CpKDO without chaperones</b>	9.8	40
<b>FjKDO without chaperones</b>	5	37

### 3.2 KDO reaction system

KDOs depend on Fe(II) for the activation of oxygen. At the same time, the free Fe(II) cofactor can easily be oxidized by molecular oxygen. Since both are available in the reaction mix, oxidation of the iron occurs, leading to the Fenton reaction [171,172] and thus to the formation of reactive oxygen species. Reactive oxygen species can affect the enzyme stability by attacking amino acids on the enzyme's surface [173], which in the worst case can lead to the loss of

## Discussion

quaternary structure and inactivation of the enzyme, and has a particularly large impact when working with isolated enzymes. Fe(II)/ $\alpha$ -ketoglutarate dependent dioxygenases show an increased sensitivity towards oxygen and its radicals. Hassett et al. [174] investigated the sensitivity of catechol-2,3-dioxygenase towards  $\text{H}_2\text{O}_2$  and the underlying mechanism. Upon exposure to stoichiometric amounts of  $\text{H}_2\text{O}_2$ , the Fe(II) in the active site is oxidized. Thereby, it is either lost from the enzyme or the environment of the iron becomes highly disordered, resulting in a loss of enzyme activity [174]. To keep Fe(II) in its reduced state, L-ascorbic acid is added to the reaction mixture as an oxygen scavenger. Additionally,  $\alpha$ -ketoglutarate can work as a ROS scavenger. Upon reaction of  $\alpha$ -ketoglutarate with  $\text{H}_2\text{O}_2$  and water,  $\text{CO}_2$  and succinate are formed [175]. This could be the reason why  $\alpha$ -ketoglutarate is used in a 1.5 excess over the substrate in most KDO reactions. Indeed, in control reactions where no enzyme was present, we could always detect succinate in the background (data not shown).

Because most studies employing KDOs use cell-free extracts, whole cells, or perform reactions in analytical scale, there is little literature available that examines or discusses the design of an *in vitro* KDO reaction system in terms of ROS generation, the influence of other redox-active small molecules or metal chelating compound. The generation of ROS in combination with the increased sensitivity of KDOs could be another reason why hardly any large-scale applications of KDOs are known so far, despite their potential for industrial applications [64]. However, an in-depth investigation of the reaction system was beyond the scope of this dissertation. Nevertheless, we investigated optimal reaction parameters and additives concerning ROS and iron-chelating effects, which are discussed below.

Since CaKDO is the most unstable enzyme among the three tested KDOs, we suspected that optimization of the reaction parameters would have the greatest effect here. Because the detection of different ROS would have led to a high experimental effort, only the influence of different parameters on the total conversion was investigated. The influence of Fe(II) concentration, the pH, the buffer type, and the temperature was tested, followed by the addition of other ROS scavenging additives.

While phosphate buffer was used for the purification of the enzymes (Chapter 3.1.2), HEPES buffer was found to be better suited for biotransformations (Figure 69). This is in line with previous findings where the amount of ROS formed correlates with the buffer used and is lower in HEPES buffer compared to other buffers [176–179]. Moreover, buffers such as HEPES and MOPS are more suitable for reaction systems containing metal ions due to their lower metal-binding affinity compared to, for example, phosphate buffers [178]. Interestingly, in TRIS

## Discussion

buffer, which also has higher metal binding constants, *CaKDO* showed similar conversions at pH 7.0 to HEPES at 7.5 (Figure 69A). Since the buffer capacity of TRIS buffer ranges from 7.0-9.2 and the reaction would occur in the lower buffer range, HEPES at pH 7.5 was chosen as the buffer for the reaction, which is consistent with the previous results of Baud et al. [90]. One way to eliminate potential ROS is to add catalase to the reaction [180]. Here, we also tested other components that can act on ROS scavenging and degradation (mannitol, sorbitol, BSA, catalase) (Figure 69B). Of all tested additives, catalase appeared to have the best effect on conversion and initial rate activity when applied in low concentrations of 0.1 mg mL<sup>-1</sup> (Figure 69B). When applied in the relatively high concentration of 1 mg mL<sup>-1</sup> (Figure 69C/D) conversion could be further increased (Figure 69C). Considering that catalase is a very active enzyme and small amounts are usually sufficient to eliminate H<sub>2</sub>O<sub>2</sub>, the observed effects with 1 mg mL<sup>-1</sup> catalase hint towards further effects besides removal of H<sub>2</sub>O<sub>2</sub>. As will be discussed in the following chapters (Chapter 3.3.3) and was also previously discussed in the results part of this thesis (Chapter 2.1), *CaKDO* is an aggregation-sensitive enzyme. Foreign proteins like BSA or large-size subunit catalases can protect aggregation-prone enzymes similarly to chaperones or heat shock proteins when applied in sufficient concentrations [181,182]. We used the catalase from bovine liver, which does not have a large size subunit, and was not found to show effects on aggregation-prone enzymes before [182]. Nevertheless, it has to be considered, that working with aggregation-prone proteins is complex and while the catalase from bovine liver might not have shown chaperone like shielding effects on other enzymes, it might be an entirely different case for *CaKDO* [183]. Nonetheless, further research is needed to explain the protection mechanism of the catalase toward *CaKDO*.

The optimal reaction temperature was found at 20 °C for *CaKDO* and 25 °C for *FjKDO* (Figure 70), which is also in agreement with the results published by Baud et al. [90]. The low reaction temperature could be a result of higher stability of the enzyme at lower temperatures or the dissolved oxygen concentration, which is higher in aqueous solutions at a lower temperature. Overall, we identified the *in vitro* KDO reaction system as one of the most important but under-researched elements for a successful application of KDOs in biotransformations, which urgently requires further mechanistic understanding for the application of isolated KDOs [64].

## Discussion

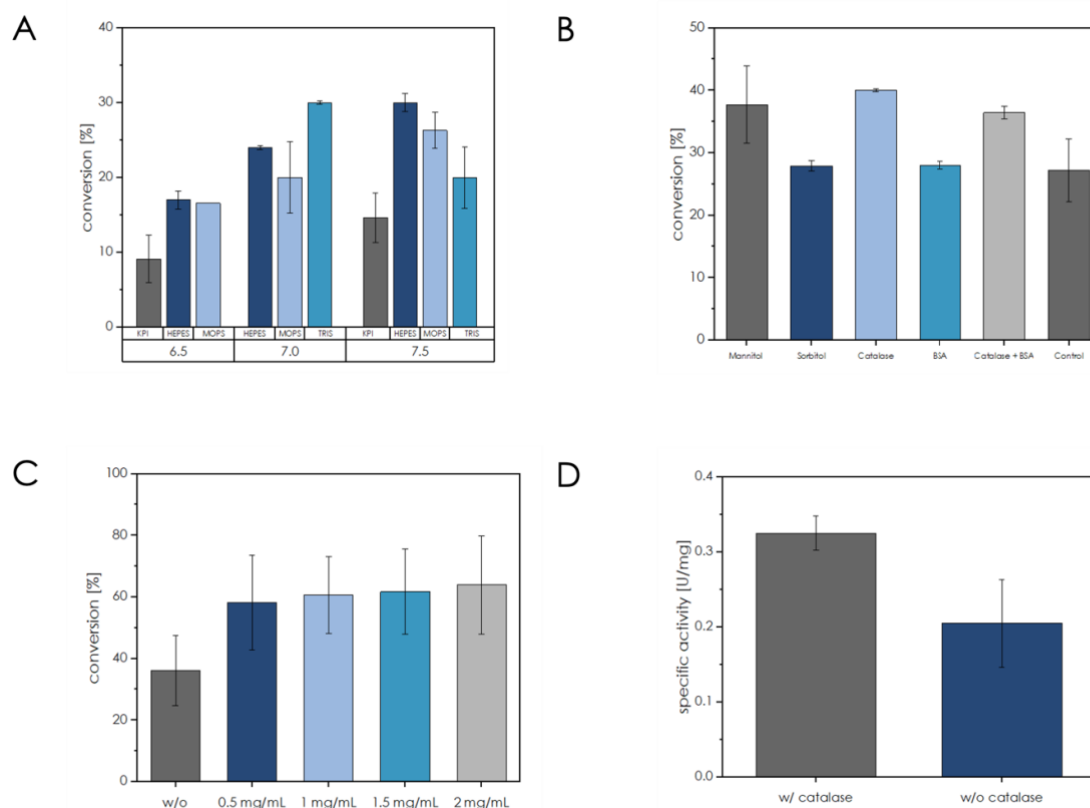


**Figure 69:** Influence of different reaction parameters on CaKDO. A) pH and buffer, B) Additives for scavenging and degradation of ROS, C) Addition of catalase in different concentrations, D) specific activity with and without the addition of catalase (0.5–2 mg mL<sup>-1</sup>). Reaction conditions: 1 ml stock solution containing 10 mM L-lysine, 15 mM  $\alpha$ -ketoglutarate, 2.5 mM L-ascorbic acid, 1 mM (NH<sub>4</sub>)<sub>2</sub>Fe(SO<sub>4</sub>)<sub>2</sub> in 50 mM HEPES, pH 7.5 was transferred into a 2 ml reaction tube. The reaction was started with the corresponding amount of catalyst (0.03 mg mL<sup>-1</sup> supplement screening and 0.05 mg mL<sup>-1</sup> for initial rate activity measurements) at 300 rpm, room temperature, and an open lid for aeration. Additive concentrations: 5 mM mannitol, 5 mM sorbitol, 0.1 mg mL<sup>-1</sup> catalase, 0.2 mg mL<sup>-1</sup> BSA. Samples for additive screening and optimization of catalase concentration were taken after 24 h and quenched at 80 °C for 5 min. Samples for initial rate activity measurements were taken every 2 minutes over a total reaction time of 10 min. These samples were horizontally attached to a thermo shaker with a closed lid and shaken at 500 rpm. Samples were then analyzed by HPLC (Chapter 2.1, Section 3.6). Error bars correspond to data from two independent reactions, respectively.

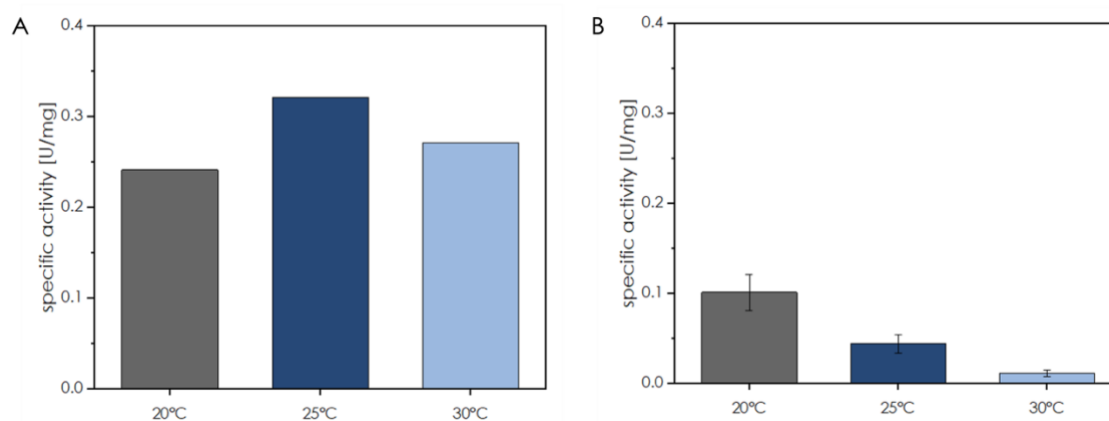


**Figure 70:** Enzyme activity at different temperatures. A) free FjKDO and B) free CaKDO. Reaction conditions: 100 mM L-lysine, 150 mM  $\alpha$ -ketoglutarate, 2.5 mM L-ascorbic acid, 1 mM (NH<sub>4</sub>)<sub>2</sub>Fe(SO<sub>4</sub>)<sub>2</sub>, 0.01 mM DTT, 200 mM HEPES, pH 7.5, 750 rpm, 0.5 mg mL<sup>-1</sup> free enzyme, 1 ml reaction volume, measured by HPLC (Chapter 2.1, Section 3.6). Reactions in A were performed as single reactions. Error bars in B correspond to data from two independent reactions.

### 3.2.1 Evaluation of KDO activity assays

There are several assays available to measure the activity of KDOs, but they all have certain limitations. Assays based on isotope detection of  $^{14}\text{CO}_2$  release during the reaction or detection of isotope labeled  $\alpha$ -ketoglutarate and succinate [180,184] are tedious because they contain radioactive reagents, laborious protocols, and are not easily adaptable to high throughput screenings [185]. Other assays include the spectrophotometric measurement of  $\alpha$ -ketoglutarate, e.g. by fluorescent labeling [186]. Here, the cross-reactivity of the L-ascorbic acid with the reagent is disadvantageous [185]. Coupled enzyme assays detect the co-product succinate using either luciferase [165] or NAD(P)H-dependent enzymes [185]. However, none of these assays detects the main substrate L-lysine or the hydroxy-L-lysine products. As discussed above (Chapter 3.2),  $\alpha$ -ketoglutarate can react with  $\text{H}_2\text{O}_2$  to succinate also in absence of the enzyme. Further, succinate and  $\alpha$ -ketoglutarate are also present in the metabolic background when working with cell-free extract or whole cells. Therefore, assays based on the detection of  $\alpha$ -ketoglutarate and succinate should be used with caution. They are certainly useful for initial high throughput assays, but not for a detailed characterization of enzymes or biotransformations.

In the case of lysine hydroxylases, substrate (L-lysine) and products (hydroxy-L-lysines) should be determined by LC/MS [80,82] or HPLC [83,90]. Analysis by HPLC after modification with *o*-phthalaldehyde (OPA) [83,101] or Fluorenylmethoxycarbonyl (FMOC) [69,90] is the most common application, using DAD detection [69,90] or fluorescence detection (FLD) [83,101]. Although HPLC-based methods are much more accurate than the previously mentioned assays, there are also some issues to consider regarding the detection of (hydroxylated) lysines: When L-lysine is quantified by FLD, the fluorescence signal is generally lower compared to other amino acids. This is due to the derivatization of the two amino groups and the proximity of the two OPA groups (Figure 71), which causes quenching of the fluorescence signal [187]. We, therefore, tested the detection of L-lysine, hydroxy-L-lysines, and cadaverine by DAD detection and FLD detection (SI, Chapter 2.2.9). Since (3*S*)-hydroxy-L-lysine and (4*R*)-hydroxy-L-lysine are not commercially available and also chemically difficult to synthesize, HPLC calibration was performed with 5-hydroxy-D, L-lysine, which is commercially available and has been used in other publications for LC/MS or HPLC calibrations [80,101]. However, in our case, DAD detection and FLD detection of the same samples gave different hydroxy-L-lysine concentrations (SI, Figure S42), most likely due to intermolecular quenching of the

## Discussion

fluorescence signal resulting from the position of the hydroxy group. Therefore, calibration with 5-hydroxy-DL-lysine will give different concentrations, because the OH group is at a different position compared to the actual products (3*S*)-hydroxy-L-lysine and (4*R*)-hydroxy-L-lysine (Figure 71), which affects the extent of quenching. Unlike fluorescence measurements, quenching effects do not affect absorbance measurements with a DAD detector. Still, OPA-modification of the  $\alpha$ - and  $\epsilon$ -amino groups (Figure 71) occurs with different reaction rates, most likely due to steric hindrance of the  $\alpha$ -amino group by the carboxy group and different pKa values. Therefore, different concentrations of mono- or di-derivatized (hydroxy-) lysines are formed during each derivatization, leading to an error in the measured concentration. This generally occurs during OPA derivatization of L-lysine derivatives and is independent of the detection method [187]. By normalizing the substrate and product peaks to the weighed substrate concentrations and calculating the resulting conversion based on the product peak area (%), the conversion can be more accurately determined (SI, Chapter 2.2.9). Since selectively immobilized or isolated enzymes were used in this work, no side reactions were expected that could lead to a decrease of the L-lysine concentration by the formation of products other than the expected hydroxyl-L-lysine derivatives. Therefore, we chose OPA derivatization in combination with DAD detection for our studies. In our specific case, using the normalized values is more accurate than using actual measured concentrations based on a calibration with the product surrogate 5-hydroxy-D,L-lysine.

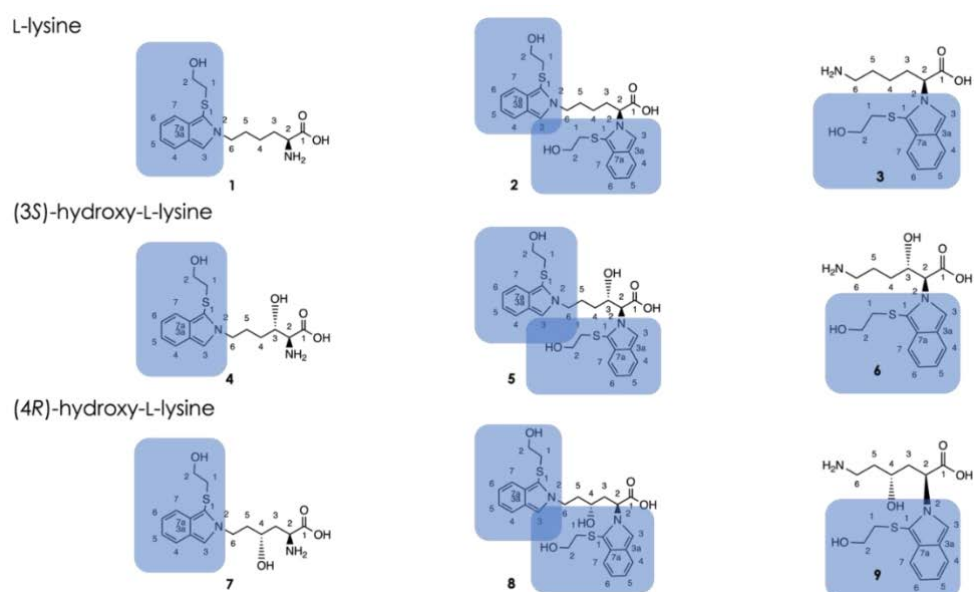


Figure 71: OPA derivatives of L-lysine and mono- and di-hydroxylated L-lysine derivatives.

### 3.3 Biocatalyst formulation - KDO immobilization studies

The enzyme is usually the most significant cost factor in enzyme-catalyzed syntheses [37]. Therefore, efficient immobilization techniques are critical to increase process economy, specifically for challenging enzymes such as KDOs that are difficult to produce and have low activity. We tested two in situ immobilization techniques: HaloTag® and EziG™ (Chapter 1.6.2.1), to increase the enzymes' stability and avoid laborious purification.

#### 3.3.1 EziG™ vs HaloTag® - Binding capacities and specific activities

To compare the different immobilization strategies, we compared the binding capacities and specific activities as shown and discussed in Chapter 2. While the amount of enzyme bound to the HaloLink™ resin was in line with the manufacturer notes of at least 7 mg protein per mL resin [188], EziG™ binding capacities of 3-16% were under or in the lower range of the manufacturers' notes of 15-60% w/w [189]. Similar low binding capacities for EziG™ beads were also found for different transaminases (unpublished results, Kevin Mack, Laura Grabowski, IBG-1, Forschungszentrum Jülich GmbH) and *Sr*LDC (SI, Chapter 2.2.3.3.1, Table S7). Low binding capacities could be a result of a rapid binding of the enzyme to the carrier surface, thereby blocking further binding sites in the porous material. In addition, surface modifications of the carrier can act to attract or repel protons or polar interactions on the enzyme surface, thus reducing overall binding [155]. The amount of enzyme bound to the carrier also determines the process economy.

Furthermore, when comparing the specific activities of the different immobilized enzymes to the purified enzyme (with His-tag), two of the three tested KDOs (*Ca*KDO and *Cp*KDO) showed higher activity upon HaloTag® immobilization compared to the EziG™ immobilizates (Chapter 2.1, Figure 17, see Section 2.2, for a detailed discussion of the results). Surprisingly, in the case of *Ca*KDO, the initial rate activity increased upon immobilization (Chapter 2.1, Figure 17), which is most likely an artifact due to an increase in enzyme stability, as discussed in the next chapter (Chapter 3.3.2). Overall, these results demonstrate the different performance of immobilization methods again, even with highly similar enzymes.

HaloTag®-immobilized enzymes were chosen for further investigation for the following reasons: Two out of three KDOs performed best with HaloTag®-based immobilization. Furthermore, HaloLink™ resin is commercially available and shows better binding capacities.

The HaloTag® fusion can be attached to any substrate carrying the specific HaloLinker™; consequently, this immobilization technique can be tailored to meet particular cost or sustainability demands (Chapter 3.8). Another advantage is covalent immobilization, which prevents enzyme leakage compared to non-covalent immobilization. Commonly, covalent immobilization involves crosslinking reagents like glutaraldehyde, which are supposed to link the functional groups of an enzyme and the functional groups of a carrier, which is often accompanied by a significant loss of activity. Such reactions typically lead to random immobilization sites of the enzyme with the carrier and additional intra- and intermolecular crosslinks on the enzyme surface. Consequently, such methods are difficult to reproduce. In contrast, site-specific immobilizations mediated by a fusion tag show increased reproducibility. The HaloTag® system is one of the few techniques that maintain high residual activity and require only short immobilization times (< 30 min) under gentle conditions [130]. Covalent immobilization is especially advantageous for KDO reactions. The demand for molecular oxygen requires proper aeration of the reaction, which can be achieved in open vessels like shaking flasks and fast orbital shaking (>150 rpm), open vessels using a stirrer, or closed vessels with aeration via spargers. These techniques lead to strong shear forces between the particles, making enzyme leakage more likely for non-covalent immobilizations. On the other hand, these shear forces might also destroy the Sepharose beads of the HaloLink™ resin, while glass beads, as used with the EziG technology, might be more resistant. Nevertheless, the HaloTag® is also a solubility tag, which might also help prevent enzyme aggregation [151].

### **3.3.2 Stability and activity of *Ca*KDO under reaction conditions upon HaloTag® immobilization**

As described in Chapter 2, HaloTag®-based immobilization enables conversions of > 200 mM L-lysine in analytical scale reactions for all three KDOs (Chapter 2.1, Figure 19). Especially for *Ca*KDO activity and stability were significantly improved upon HaloTag® immobilization (Figure 18). While an increase in stability is common for immobilized enzymes, specific activity usually decreases. In general, the fixation of an enzyme to a carrier can prevent aggregation, which increases operational stability [190]. Also, by creating a protective microenvironment for the enzyme, it is shielded from mechanical stress, oxygen, hydrogen peroxide, dissolved gases, and organic solvents [191–194]. In contrast to an immobilized enzyme, the free enzyme might not retain enzyme activity if it is sensitive to the reaction

## Discussion

conditions. Consequently, an increase in specific activity is usually an artifact caused by changes in the stability of the immobilized enzyme or incorrect protein determination of the immobilizate, compared to the free enzyme [191,194].

In case of the increase of initial rate activity of *CaKDO*, we propose that the increase in activity is most likely an artifact due to the low stability of the free enzyme. As soon as the protective cell environment is disrupted by cell lysis, the enzyme starts to aggregate, probably due to hydrophobic patches on the enzyme surface (Chapter 3.3.3, Figure 75, and Figure 76). Although we could purify *CaKDO* successfully, without any visible precipitation, the application in biotransformation still led to rapid precipitation of the enzyme (SI, Figure S30). Upon IMAC purification, the enzyme is exposed to oxidative conditions for several hours, which might lead to a loss of active enzyme, consequently reducing the activity of the lyophilizate. In addition, loss of iron from the active site due to oxidation or enzyme inactivation might occur due to a ROS-induced loss of secondary structure. This theory is supported by the results of Bastard et al. who found that *CaKDO* lost its active site iron when purified for crystallization studies [66]. In the cell and the crude extract, protein concentrations are higher than in diluted solutions of the cell-free extract; on the IMAC and in the eluate, protein concentrations are even lower. In addition, foreign proteins can protect aggregation-sensitive proteins (e.g., chaperones and heat shock proteins), but when they are removed e.g. by protein purification via IMAC, these “protein shields” no longer exist. In contrast, HaloTag® immobilization directly from the cell-free extract can be achieved in less than 40 minutes after cell lysis, which decreases exposure to oxygen and resulting inactivation. Likewise, the HaloTag immobilizes the KDO directly from the crude extract to the carrier. By keeping the enzyme molecules apart and stabilizing their conformation, they are prevented from aggregating via hydrophobic interactions (Chapter 3.3.3). Consequently, they are not left without the protecting environment of other proteins or, in this case, the immobilizate for as long as they are upon IMAC purification. Furthermore, the addition of catalase to a reaction with the immobilized *CaKDO* did not lead to an increase in turnover, whereas it led to a 1.7-fold increase in activity for the soluble enzyme (Chapter 2.1, Figure 17B). This could indicate that the immobilized *CaKDO* is protected from ROS or aggregation by similar means as the free *CaKDO* by the addition of catalase, as discussed in Chapter 3.2.

To summarize, increased activity and stability of immobilized *CaKDO* might be due to (i) shielding from enzyme aggregation, (ii) protection of the active site iron from oxidation, and (iii) protection of the enzyme against ROS.

### 3.3.3 Comparison of the stabilities of *CaKDO*, *CpKDO*, and *FjKDO* based on their structure

As demonstrated in Chapter 2.1, Figure 18, the purified *CpKDO* and *FjKDO* show much higher stability under reaction conditions than *CaKDO*. As outlined above, *CaKDO* shows a comparatively strong tendency to precipitate in its free form (SI, Figure S30), which suggests a higher tendency towards aggregation compared to the other tested KDOs. One reason for the precipitation of proteins in aqueous media could be their isoelectric point (IP). As the net charge of a protein is zero at the IP, protein solubility reaches a minimum, due to the missing charge repulsion of the protein molecules. However, the IPs of KDOs investigated in this work are highly similar (*CaKDO*: 5.77, *FjKDO*: 5.82; *CpKDO*: 5.85) [195] thus, IP does not explain the observed differences.

For further clarification, we compared the primary and quaternary structures concerning their quaternary structure in solution versus the crystal as well as concerning surface features such as exposed cysteine residues or hydrophobic patches, since these are the main factors contributing to enzyme aggregation. The sequence alignment in Figure S37 clearly shows that *CpKDO*, *FjKDO*, and *FsKDO* as members of the same subfamily and have high sequence similarity. In contrast, the sequence of *CaKDO* differs significantly [66]. The primary structures contain three (*CpKDO*) to four (*CaKDO*, *FjKDO*, *FsKDO*) cysteine residues, three of which are conserved between members of the same subfamily (*CpKDO*, *FjKDO*, and *FsKDO*), whereas there is no conserved cysteine to *CaKDO*. Since there are no crystal structures for *CpKDO* and *FjKDO* available, we used the structure of the related *FsKDO* for comparison with the crystal structure of *CaKDO* (Figure S37) [66]. The crystal structures show that one cysteine residue is accessible on the enzyme surface in both enzymes, respectively (Figure 72 and Figure 73), which makes precipitation caused by intermolecular disulfide bonds in both cases similarly likely and does not explain the different behavior of *CaKDO* relative to *CpKDO* and *FjKDO* (Figure 18).

Hydrophobic patches on the enzyme surface are a further indication of an increased aggregation tendency. In the unit cell of the crystal, both enzymes appear as tetramers (Figure 72 and 73CD) and the overall number of hydrophobic residues on the tetrameric enzyme surface does not differ between *CaKDO* and *FsKDO* (Figure 74). However, size-exclusion studies revealed that *CaKDO* is dimeric, whereas *FsKDO* retains its tetrameric structure also in solution (Figure 73

## Discussion

and Figure 75) [66]. These results hint toward a less stable dimer-dimer interface in *CaKDO* relative to *FsKDO*. A closer look at the *CaKDO* tetramer reveals its non-symmetrical structure, which is in contrast to the highly symmetric structure of *FsKDO* (Figure 75). Specifically, monomer 3 and 4 of dimer 2 have an interface only with one monomer in dimer 1 (Figure 75B). The interface of the single dimers contains hydrophobic patches, which are partly covered by the formation of the tetramer (Figure 76 and Figure 77). Of course, the enzyme concentration required for crystallization is far higher (*CaKDO*: 9.3 mg mL<sup>-1</sup>) than in biotransformations (0.5 mg mL<sup>-1</sup>, Figure 18), therefore this aggregation behavior might not be the same during biotransformations. As can be seen in Figure 77, further hydrophobic patches on the surface of the single dimer exist, which might lead to the formation of larger enzyme aggregates. These hydrophobic patches might be an indication of why *CaKDO* tends to rapidly precipitate in solution and why immobilization prevents said aggregation and leads to higher activities and stabilities, as explained in Chapter 3.3.2. However, further studies are needed to prove that this is the reason for the higher stability of *CaKDO* compared to *FjKDO* and *CpKDO*.

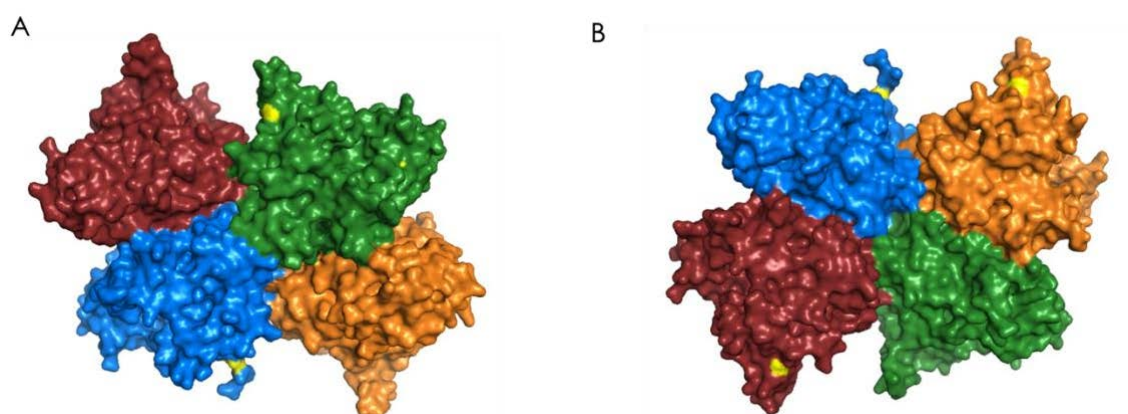


Figure 72: Surface representation of the *FsKDO* tetramer. A) Front side. B) Rear side. Different colors indicate different monomers; yellow patches mark cysteine residues on the surface. Based on PDB code 6EUR [66].

## Discussion

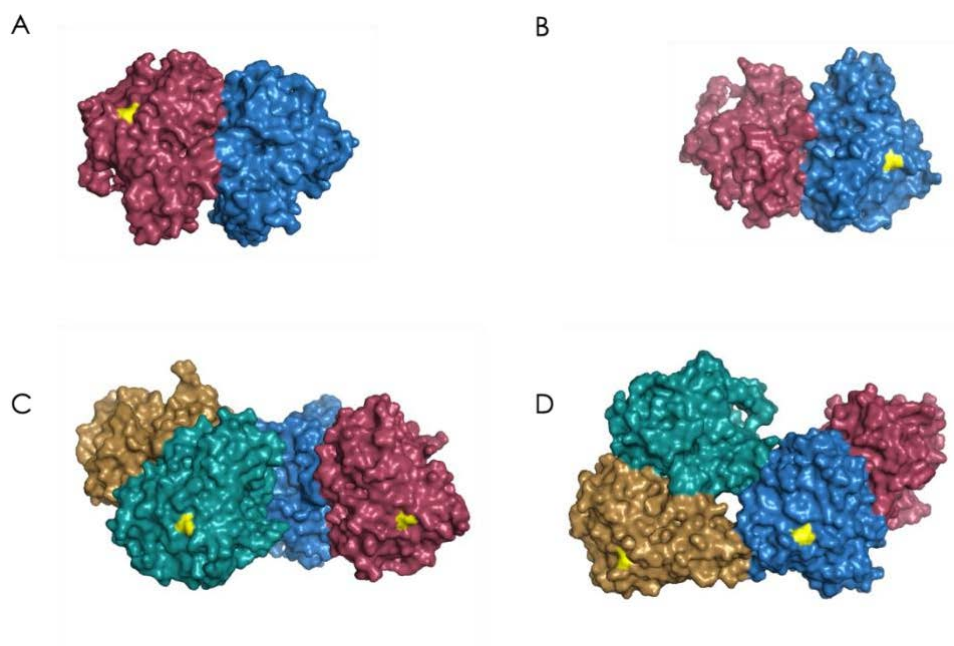


Figure 73: Surface representation of the CaKDO dimer (native structure in solution), and the tetramer (observed in crystals). A) Dimer front side. B) Dimer rear side. C) Tetramer front side. D) Tetramer rear side. Different colors indicate single monomers. Yellow patches mark cysteine residues on the enzyme's surface. Representation based on PDB code 6F2B [66].

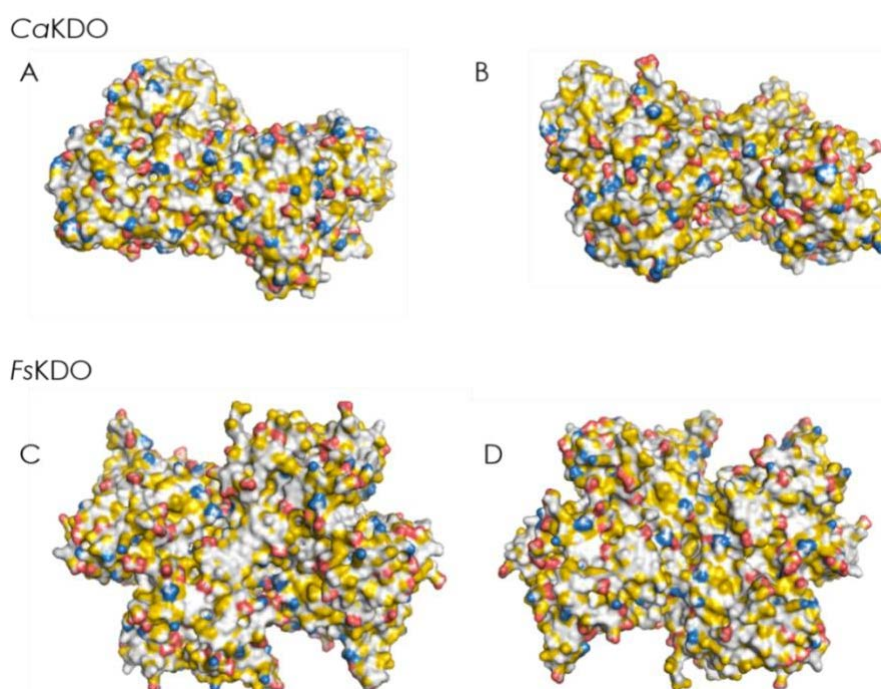


Figure 74: Representation of surface areas in terms of polar (white), non-polar (yellow), negatively (red), and positively (blue) charged residues. A) CaKDO tetramer front side B) CaKDO tetramer rearview C) FsKDO tetramer front side D) FsKDO tetramer rear side. The picture was generated with PyMOL using a published Python script (YRB) from Hagemans et al. [196] for the visualization of the respective residues. Described as followed: "Functional groups are colored according to the YRB highlighting scheme (hydrocarbon groups without polar substitutions, yellow; negatively charged oxygens of glutamate and aspartate, red; nitrogens of positively charged functional groups of lysine and arginine, blue; all remaining atoms including the polar backbone, white)" [196]. Structures according to PDB codes 6EUR and 6F2B [66].

## Discussion

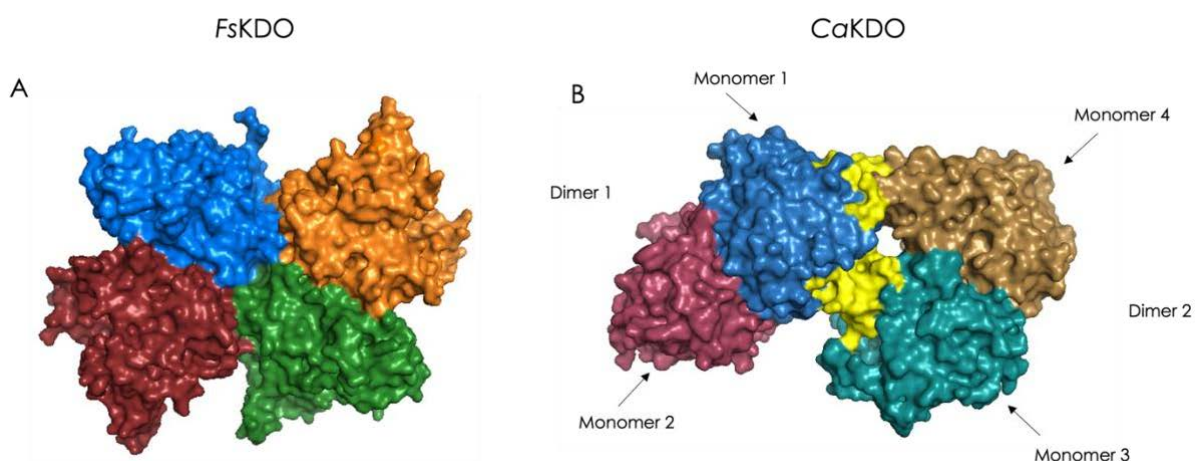


Figure 75: A) FskKDO Tetramer and B) CaKDO tetramer according to PDB codes 6EUR and 6F2B, respectively. Different colors represent the single monomers. In contrast to FskKDO, CaKDO tetramer is not formed via a dimer-dimer interface, but rather through hydrophobic patches between monomer 1 of dimer 1, and monomer 3 and 4 of dimer 2, indicated by yellow patches. Hydrophobic interfaces are presented in Figure 76 in detail. Structures according to PDB codes 6EUR and 6F2B [66].

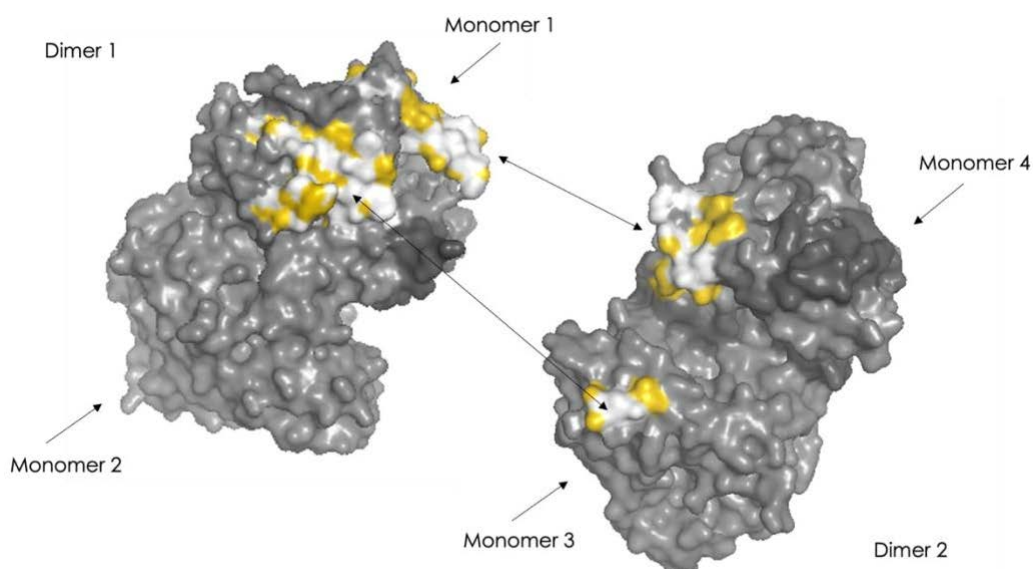


Figure 76: CaKDO dimers. As can be seen, dimer interfaces indicated in yellow in Figure 75 are generated most likely by hydrophobic patches. Hydrophobic patches of the dimer interfaces were generated by PyMOL using Python script (YRB) from Hagemans et al. [196]. Described as followed: “Functional groups are colored according to the YRB highlighting scheme (hydrocarbon groups without polar substitutions, yellow; negatively charged oxygens of glutamate and aspartate, red; nitrogens of positively charged functional groups of lysine and arginine, blue; all remaining atoms including the polar backbone, white)” [196]. Structures according to [66], PDB code 6F2B.

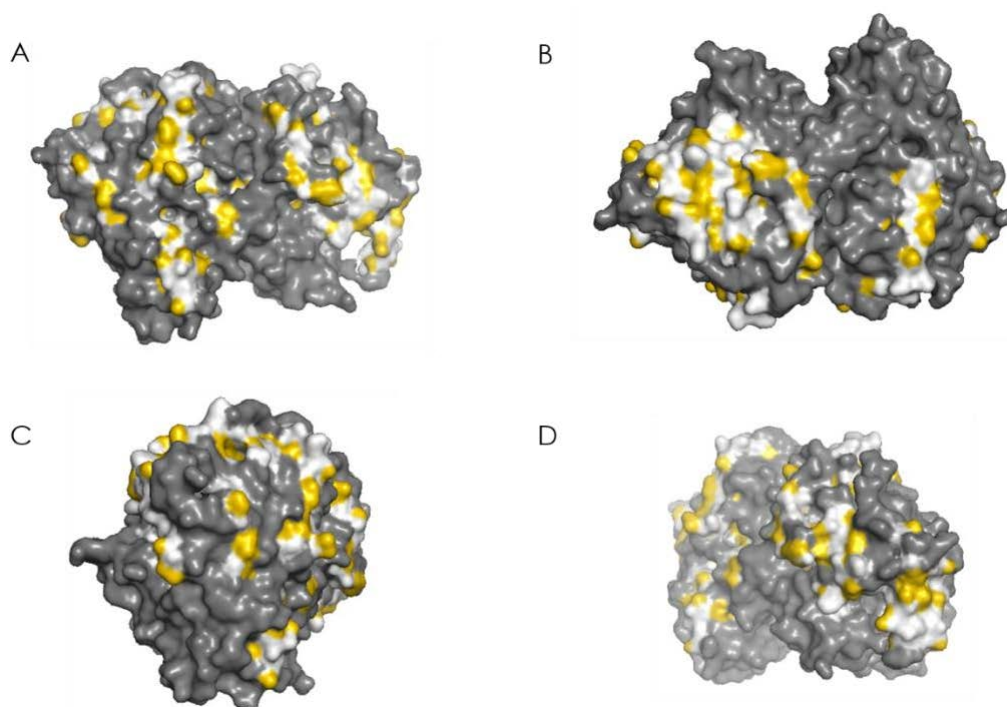


Figure 77: CaKDO dimer with all hydrophobic patches. A) Front side. B) Rear side. C) Site view: left. D) Site view: right. Hydrophobic patches were generated by PyMOL using Python script (YRB) from Hagemans et al. [196]. Described as followed: “Functional groups are colored according to the YRB highlighting scheme (hydrocarbon groups without polar substitutions, yellow; negatively charged oxygens of glutamate and aspartate, red; nitrogens of positively charged functional groups of lysine and arginine, blue; all remaining atoms including the polar backbone, white)” [196]. Structures according to [66], PDB code 6F2B.

### 3.4 Application of immobilized KDOs in biotransformations

#### 3.4.1 Recyclability of immobilized KDOs

A significant advantage of immobilized enzymes is their recyclability [37]. At the analytical scale (1 mL), *Cp*KDO- and *Fj*KDO HaloTag® were recycled up to four times with 84% and 100% conversion in 4 h, respectively. After seven batches, 27% conversion in 4 h was achieved with immobilized *Fj*KDO (Chapter 2.1, Figure 20). Inactivation of the enzyme is most likely the result of constant shaking, friction between the beads, and partial loss of the immobilisate during the inter-batch wash steps. As discussed above, KDOs are sensitive to oxygen or ROS exposure, which might contribute to enzyme inactivation. Nevertheless, the little loss of activity after four batches for *Fj*KDO-HaloTag® and after seven batches for *Cp*KDO-HaloTag® was surprising, since KDO stability has always been a significant concern anyway. Previous experiments with SadA immobilized on EziG™ Amber by the Kourist group [81] showed only 10% of the initial reaction rate after the first reaction cycle. Additionally, our experiments were performed over four days (*Cp*KDO) or seven days (*Fj*KDO), including storage of the enzyme

## Discussion

overnight at 4 °C, indicating that these KDOs are stable at least for several days in their immobilized form.

Compared to the single reactions, the specific space-time yields could be increased almost threefold for the *Cp*KDO-HaloTag®-catalyzed reaction and 4.4-fold for the *Fj*KDO-HaloTag®-catalyzed reaction, demonstrating that a recycling approach can effectively improve the reaction productivity (Table 14).

Table 14: Comparison of specific space-time yields of single- and repetitive batch reactions catalyzed by three different KDOs in analytical scale (1 mL). For reaction conditions, see 2.1, Section 3.3.3.

Enzyme	Specific space-time-yields [g <sub>product</sub> L <sup>-1</sup> h <sup>-1</sup> per g <sub>immobilized enzyme</sub> ]				
	Single reaction	Repetitive batch	Number of batches	Conversion of last batch [%]	STY increase
<b><i>Ca</i>KDO</b>	1622	2219*	2	71	1.4 x
<b><i>Cp</i>KDO</b>	795	2333	4	84	3 x
<b><i>Fj</i>KDO</b>	1081	4803	7	27	4.4 x

\*Upon recycling with EDTA and dithionite

Unfortunately, the recycling of *Ca*KDO-HaloTag® was not as effective. As described and discussed in Chapter 2, the enzyme lost most of its activity after the first batch, which was accompanied by a blue color change of the reaction supernatant (Figure 20). Upon treatment with EDTA and dithionite, the enzyme could be reactivated at least once (SI, Chapter 2.2.4, Figure S35, Table 14). Similar results have also been observed for other KDOs and may be caused by oxidation of an active site residue, probably induced by iron or ROS [78]. The oxidation observed for some KDOs that show color shifts occurs at aromatic residues [49,197,198]; for *Ca*KDO, however, there are no aromatic amino acids nearby. In other cases, other residues in the active site, like lysine, but further away from the iron were oxidized [199]. It is still not completely clear what causes this oxidation of active site residues, as well as how it affects KDOs in biotransformations [78].

There could also be some unidentified interactions between reaction components since in our case not the immobilisate but the reaction supernatant turns blue (SI, Figure S34). However, the interaction of different components in the reaction, including the generation of ROS as well as *Ca*KDO's intrinsic instability are poorly understood, as discussed in Chapter 3.2 and Chapter 3.3.3. Whatever the underlying mechanism, it is only found to this extent in *Ca*KDO and not in *Cp*KDO or *Fj*KDO. A detailed mechanistic analysis is required to investigate these

## Discussion

phenomena, which was beyond the scope of this thesis. However, in case of *CaKDO* inactivation can be strongly reduced by applying a fed-batch mode. The reaction supernatant did not change color as long as L-lysine was present and conversion of 200 mM L-lysine was possible (Figure 78).

Summarizing: As long as L-lysine is present in the reaction mixture, the immobilized *CaKDO* remains active. Therefore, instead of *CaKDO* regeneration, other reaction setups, like fed-batch or continuous mode, can be considered where the full conversion of L-lysine is prevented. It has to be tested, which minimal concentration of L-lysine would be sufficient to maintain the enzyme activity.

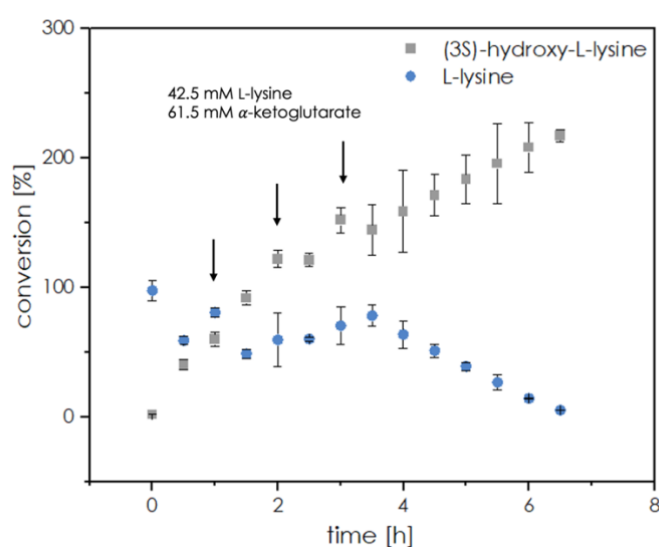


Figure 78: *CaKDO*-HaloTag®-catalyzed hydroxylation of L-lysine in a fed-batch mode. Reaction conditions: 1 mL scale in 200 mM HEPES, pH 7.5, with 5 mg mL<sup>-1</sup> immobilized enzyme, 100 mM L-lysine, 150 mM  $\alpha$ -ketoglutarate, 2.5 mM L-ascorbic acid, 0.01 mM DTT, and 1 mM (NH<sub>4</sub>)<sub>2</sub>Fe(SO<sub>4</sub>)<sub>2</sub> for 24 h at 25 °C in an overhead shaker. The arrows indicate the addition of 42.5 mM L-lysine and 61.5 mM  $\alpha$ -ketoglutarate. Error bars are the result of two independent immobilizations.

### 3.4.2 Application of immobilized KDOs in preparative lab scale

Most groups working on the synthesis of hydroxy-L-lysines by KDOs, use cell-free extracts or whole cells, except Baud et al. [69,90], who applied purified enzymes for some of their reactions. When working with isolated KDOs, low titers and yields (1.6 g L<sup>-1</sup> or 0.016 g total yield) were observed [69,90]. A summary of published hydroxy-L-lysine syntheses with KDO is shown in Table 2 and was already discussed in chapter 2.1, Section 2.4. Application in a 15 mL scale, with the full conversion of 100 mM substrate and product titers of 16 g L<sup>-1</sup> could be

## Discussion

demonstrated for *Ca*KDO and *Fj*KDO immobilized with HaloTag® (Chapter 2.1, Figure 21). Additionally, we demonstrated that a larger concentration of substrate (200 mM) or scale (50 mL) was in general feasible for the *Ca*KDO-catalyzed reaction (Chapter 2.2.6, Figure S38). Still, there is little research on a preparative KDO reaction setup, especially for immobilized KDOs. Using immobilized KDOs, we found that aeration must be carefully balanced: Too much oxygen can oxidize the Fe(II) cofactor, rendering the cofactor unavailable for the enzyme and decreasing its stability by increasing ROS production. As long as adequate oxygen concentration is maintained, shaking flasks can be a simple and effective setting in many laboratory-scale experimental setups [69,90]. Our results show that an increase in scale and substrate concentration can be realized with immobilized enzymes in combination with an open reaction system for oxygenation.

For KDO-catalyzed reactions up to 1 L, shaking flasks are easy to handle; however, for a larger scale, it is not sufficient, so further studies should focus on developing suitable reaction modes and reactor designs. Important factors to consider are sufficient mixing of the beads thereby avoiding strong shear forces and a controllable aeration system. Simultaneous mixing of the beads and aeration might be achieved by spargers, for example, by airlift reactors. However, even if ROS generation could be minimized, enzymes could be inactivated at the gas interface. Furthermore, continuous titration of the reaction mixture is obligatory, since the pH decreases during the reaction, due to the generation of CO<sub>2</sub>. We operated at high buffer concentrations (200 mM HEPES) to keep the pH constant, which was rather counterproductive for the purification of the hydroxy lysines. As explained in chapter 3.8., HEPES buffer does not only complicate product purification but is also much too expensive for a larger scale. In general, buffer systems can cause problems when used with KDOs since they interfere with product purification and require constant monitoring of metal complexation. For technical applications, buffers are generally disadvantageous because of the costs and wastewater contamination. By continuous titration, the pH can be controlled, and the buffer can be minimized or even eliminated. However, temporal pH hot spots could result during titration, which would negatively affect the enzyme. To avoid such hot spots, a vigorous stirring of the solution is mandatory, which is also a challenge for enzymes. For this case, a reaction set up with two reactors and a cyclic pumping of the reaction solution between both compartments could prevent enzyme inactivation by pH hot spots (Figure 79). The pH would be measured in the first compartment containing the enzyme, while the second is only used for titration and could

be vigorously stirred. A filter could retain the enzyme in the first vessel. Consequently, possible pH hot spots would occur only in the second vessel.

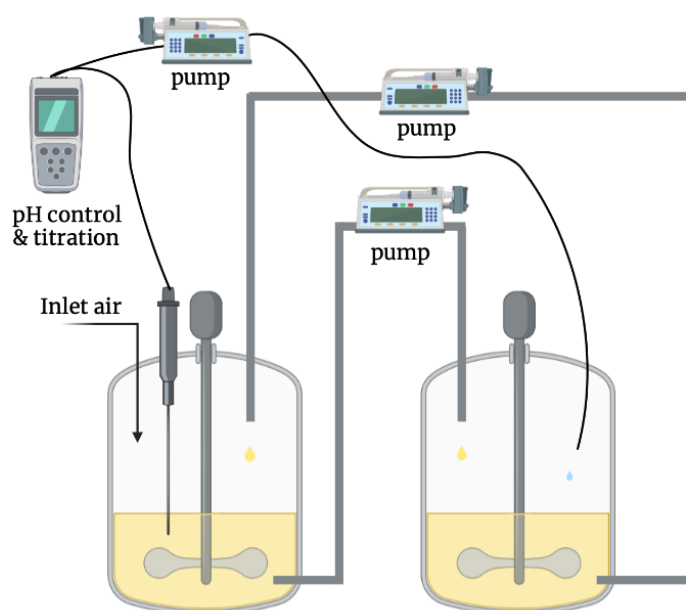


*Figure 79: Schematic representation of an alternative reaction setup aiming for easier product purification, by using a buffer-free reaction system with continuous titration. By cyclic pumping of the reaction solution between two compartments, the inactivation of the enzyme by pH hot spots could be prevented. The pH is measured in the first compartment containing the enzyme that is retained there by a filter, while the second compartment is enzyme-free and only used for slow titration. Consequently, possible pH hot spots would occur only in the second vessel. Figure created with BioRender.com.*

Summarizing: The application of KDOs in preparative laboratory-scale reactions works best in simple open reaction setups with shaking flasks. To further increase the scale or reaction performance, it is vital to investigate further reaction engineering, reactor design, and reaction mode strategies.

### 3.5 Cascade Reaction towards (2S)-hydroxy-cadaverine

As previously shown by Baud et al. [69], a combination of the KDO reaction with a second step incorporating different (lysine) decarboxylases in an enzymatic cascade process provides access to valuable hydroxy-cadaverines (Figure 8). This two-step cascade reaction was limited to a substrate concentration of 10 mM at a 10 mL scale, with the KDO reaction being the limiting step [69]. Direct hydroxylation of cadaverine by KDOs is not possible, probably due to a conserved arginine residue in the active site. Upon interaction with the  $\alpha$ -amino group of L-lysine with the arginine residue, the lid of the active site closes [66,69,90]. Because the chemical production of (2S)-hydroxy-cadaverine is more challenging compared to 3-hydroxy-cadaverine, due to its chiral center, we concentrated on this cascade. Starting from 100 mM

## Discussion

L-lysine in a 15 mL scale we used *CaKDO* in the first step and lysine decarboxylase from *Selenomonas ruminantium* (*SrLDC*) in the second reaction step, both immobilized on HaloLink™ resin [69,96,106,200,201]. Before application in the cascade reaction, *SrLDC* immobilization studies [202], and optimization of the reaction in preparative lab-scale [203] were performed in the Bachelor thesis of Solange Wetzels [202] and the Master thesis of Mariela Bregu [203]. These studies used L-lysine as the substrate since hydroxy-L-lysines are not commercially available and difficult to synthesize chemically.

The cascade reaction was successfully performed with 97% conversion within a total reaction time of 47 h (Chapter 2.1, Figure 23) without intermediate product purification, corresponding to a specific space-time yield of 6.5 g<sub>product</sub> L<sup>-1</sup> h<sup>-1</sup> per immobilized *SrLDC* and a product titer of 11.6 g L<sup>-1</sup> (2*S*)-hydroxy cadaverine. Since *SrLDC*'s natural substrate is L-lysine and *SrLDC* is more active towards L-lysine than (3*S*)-hydroxy-L-lysine, the reaction was performed in a sequential mode to avoid cross-reactivity. As both reaction steps use immobilized enzymes, recycling and reuse of the enzymes in a further reaction are principally possible upon *CaKDO* regeneration (Chapters 2.1, 2.2.4, and 3.4.1). For the decarboxylation of L-lysine to cadaverine in preparative lab-scale, *SrLDC*-HaloTag® could be recycled five times in 1 h batch reactions with 94% conversion (Chapter 2.1, Figure 23). Further research is required to determine whether similar recyclability approaches are feasible with (3*S*)-hydroxy-L-lysine as a substrate. It has already been shown that increasing the substrate concentration to at least 200 mM is possible for the *CaKDO* reaction (Chapter 2.1, Figure 19), suggesting that this could also apply to the cascade reaction. Nevertheless, previous studies suggest inhibition of *SrLDC* by higher concentrations of L-lysine (SI, Figure S39). Although it has not been tested yet if substrate inhibition also occurs with (3*S*)-hydroxy-L-lysine, a fed-batch approach might be a suitable reaction mode for the second cascade step.

Overall, our experiments represent a solid starting point for further optimization of the cascade reaction, e.g., for an increase in scale, recycling approaches, different reaction modes, and an increase in substrate concentration to optimize the specific space-time yields further. Previous studies revealed that *CpDC*, *SrLDC*, and *EcLDC* show activity towards (4*R*)-hydroxy-L-lysine, however, with different conversions in whole-cell systems [83,101]. A similar preparative reaction cascade with immobilized *FjKDO* or *CpKDO* to produce (4*R*)-hydroxy-L-lysine and subsequent decarboxylation catalyzed by *EcLDC*, *CpDC*, or *SrLDC* could also be suitable for the production of 3-hydroxy-cadaverine.

### 3.6 *Sr*LDC as an alternative enzyme for the production of biopolymer precursors

#### 3.6.1 Process evaluation

As our preliminary studies with *Sr*LDC have demonstrated, this enzyme can also be used for the production of cadaverine, which is a precursor for (fully-) bio-based polyamides as outlined in Chapter 1.5.1. So far, cadaverine is produced by fermentation, whole-cell catalysis, or immobilized lysine decarboxylases [92]. To the best of my knowledge, *Sr*LDC was never tested as an enzyme for cadaverine production at the preparative lab scale.

Upon HaloTag® immobilization of *Sr*LDC, we demonstrated the conversion of 100 mM L-lysine in a 15 mL repetitive batch within 1 h reaction time. After six batches, the conversion was only a little impaired, probably due to a loss of immobilisate during the washing steps between the reaction cycles (Chapter 2.1, Figure 23B). Surprisingly, recycling of HaloTag® immobilized *Sr*LDC led to a high space-time yield of 15,680 g<sub>product</sub> L<sup>-1</sup> d<sup>-1</sup> g<sub>immobilized *Sr*LDC</sub>.

Most processes employing immobilized enzymes use the constitutive (*Ec*LDCc) or the inducible (*CadA*) LDCs from *E. coli* [92]. Thereby, these enzymes were applied as *E. coli* whole cells or immobilized on poly(3-hydroxybutyrate) (P(3HB)) biopolymers [204], chitin [205], via different carrier-free immobilization methods like catalytically active inclusion bodies (CatIBs) [136], and as cross-linked enzyme aggregates (CLEAS) [206].

Parameters of different literature-known processes employing immobilized cells or enzymes are summarized in Table 15. Notably, most parameters were calculated based on the values given in the respective publications, which were often not complete. Therefore, only a general comparison was possible.

Overall, cadaverine titers of 8.47-221 g L<sup>-1</sup> and total yields of 2.65-540 g could be achieved, where the highest titers of 221 g L<sup>-1</sup> correspond to an *E. coli* fed-batch process overexpressing *CadA* and *CadB* [207].

Through a repetitive batch process of immobilized *CadA* on chitin [205], yields of 540 g cadaverine were obtained from a 4 L scale reaction by reusing the enzyme for 4 cycles. In comparison, immobilized *Sr*LDC on HaloLink™ resin gave access to product titers of 58.4 g L<sup>-1</sup> and total yields of 5.3 g cadaverine due to the smaller scale of 15 mL. Space-time yields ranged from 2.9-454.8 g L<sup>-1</sup> d<sup>-1</sup>, where the highest value was reported by Bhatia et al. [208] using immobilized *E. coli* whole cells in barium alginate beads with overexpressed *CadA*. Among the processes compared in Table 15, our STY of 235.2 g L<sup>-1</sup> d<sup>-1</sup> is the third-highest. However, many other publications lack information on the amount of enzyme needed to calculate the specific

## Discussion

space-time yields. Other processes use (immobilized) whole cells, where the determination of the active LDC concentration is not possible. However, studies in which these values can be compared are the immobilization of LDCc as CatIBs [138] and the immobilization of CadA on chitin [205], which gave specific space-time yields ranging from 16-477  $\text{g}_{\text{product}} \text{L}^{-1} \text{d}^{-1} \text{g}^{-1}_{\text{enzyme}}$  (or CatIBs). Surprisingly, recycling of HaloTag®-immobilized *SrLDC* led to significantly higher specific space-time yields of 15,680  $\text{g}_{\text{product}} \text{L}^{-1} \text{d}^{-1} \text{g}^{-1}_{\text{immobilized } SrLDC}$ . The reason for this is probably the minimal loss of activity upon immobilization (Figure 22) [202,203] and during the six reaction cycles (Chapter 2.1, Figure 23B) [203]. Compared to other strategies employing whole cells, alginate beads, chitin, or CatIBs, the directed immobilization on the HaloLink™ resin scores with lower mass transfer limitations and a higher concentration of active enzyme molecules on the beads. In addition, *SrLDC* might have several advantages over the most commonly used CadA and LDCc from *E. coli* as discussed in the next chapter (Chapters 3.6.1 and 0).

Further process intensification of the *SrLDC* reaction from L-lysine to cadaverine should focus on reaction mode engineering. Because of the decarboxylation reaction, CO<sub>2</sub> is produced causing the pH to become acidic. At the same time, protons are consumed from the medium during the reaction, and the diamine forms. Consequently, the pH will drift into the basic pH range. As we have shown, higher pH results in a decrease in activity for *SrLDC* (SI, Chapter 2.2.7, Figure S39). Similar to the KDO reaction (Chapter 3.4.2) we used a high concentration of HEPES (100-200 mM), to keep the pH constant. As previously discussed, the downside is that HEPES is expensive and complicates downstream processing of the diamine (Chapter 3.7). As for the KDO reaction, changing to a different buffer or reducing buffer concentration is another objective. In contrast to the KDO reaction, *SrLDC* does not need oxygen or metal ion cofactors for the decarboxylation reaction. In this case, *SrLDC* activity in cheaper and less complicated buffers concerning downstream processing approaches should be tested. As previously discussed, phosphate buffer is a good alternative since it is cheap and is unlikely to interfere with downstream processing (Chapters 3.4.2 and 3.7.4). The reaction could be run by combining continuous titration with a fed-batch approach, to target the substrate inhibition and pH adjustment. Another approach would be an enzyme membrane reactor (EMR) or a plug-flow reactor. The continuous mode of such approaches would be advantageous in overcoming substrate inhibition or potential product inhibition. In an EMR, operating under continuous conditions, substrate concentrations are low, but the product concentrations are constantly high. This could create problems if the diamines have an inhibitory effect. In contrast to an EMR, the

## Discussion

substrate concentration and product concentration change over the length of a plug-flow reactor. However, pH control via titration in plug flow reactors is not possible, therefore high buffer concentration would need to be applied. Currently, we have not detected any signs of product inhibition. All the approaches have advantages and disadvantages; therefore, a further experimental investigation is necessary.

Summarizing, recycling *SrLDC* immobilized on Halolink™resin is comparable to previously reported cadaverine production methods and is a good starting point for further investigation and process intensification.

## Discussion

Table 15: Productivity measures for the production of cadaverine in this thesis compared to literature values. Table adapted from [209]. (Specific) Space-time yields were calculated based on the parameters given in the respective publications.

Reference	Seo et al. [204]	Zhou et al. [205]	Ma et al. [207]	Oh et al. [211]	Park et al. [200]	Kim et al. [210]	Bhatia et al. [208]	Kloss et al. [138]	This thesis
Reaction mode	Repetitive batch	Repetitive batch	Fed-batch	batch	Repetitive batch	continuous	batch	batch	Repetitive batch
Immobilization	Intracellular PHA	Chitin	<i>E. coli</i> whole cells	<i>E. coli</i> whole cells	CLEAS	alginate beads with <i>E. coli</i> whole cells	Barium alginate beads (with <i>E. coli</i> whole cells)	CatIBs	HaloTag® immobilization
Enzyme	CadA	CadA	CadA CadB	LdcC	CadA	CadA	CadA	LdcC	SrLDC
Total reaction time [h]	5x1	10	16	120	No data	123	4	24	6x1
Conversion [%]	75-80	95-97%	92	95.6	100	91-94 (for 48 h)	84	87	94-100
Reusability of immobilisate	5	4	-	-	10	-	-	-	> 6
L-lysine concentration [M]	0.1	0.2	1.95	1.37	0.1	0.91	1	1	0.6
Cadaverine [g L <sup>-1</sup> ]	n.d.	135	221	134	n.d.	83.7	75.8	88.4	59
Scale [mL]	0.2	4000	50	n.d.	5	5500	50	30	6 x 15 mL (90 mL)
Total cadaverine [g]	n.d.	540 (4 L)	11.1	n.d.	n.d.	466.5	3.79	2.65	5.3
Enzymatic productivity [g <sub>cadaverine</sub> g <sup>-1</sup> <sub>biocatalyst</sub> ]	n.d.	794	n.d.	n.d.	n.d.	n.d.	n.d.	8.8	353.3
STY [g L <sup>-1</sup> d <sup>-1</sup> ]	No data	324.24	331	26.7	No data	16.3	455	89	236
sSTY [g <sub>product</sub> L <sup>-1</sup> d <sup>-1</sup> g <sup>-1</sup> <sub>enzyme</sub> ]	No data	476.82	No data	No data	No data	No data	No data	296	15,730

### 3.6.2 Potential of *SrLDC* as a suitable enzyme for the production of polyamide precursors

As previously mentioned, most published processes towards cadaverine with immobilized LDCs use the constitutive (*EcLDCc*) or inducible (*CadA*) LDCs, which belong to the aspartate amino-transferase superfamily [105,212]. While *CadA* is active in a pH range between 5.0-6.0, it is rapidly inhibited above pH 8.0 [213], and further by higher concentrations of L-lysine (> 6 mM) [214] and cadaverine [215]. In contrast, the constitutive *EcLDCc* is active in a broader pH range (pH 5.0-9.0) [216] and does not show substrate inhibition at substrate concentrations up to 10 mM L-lysine [214]. Both LDCs form identical homo-decameric structures, resolved for both enzymes by X-ray crystallography [217] and cryo-electron microscopy [218]. By association of five symmetric dimers, *EcLDC* oligomers are formed, which results in a homodecameric enzyme [217–219]. Upon dimerization, the active site is formed, which can be found between two dimers [217,218]. *CadA* forms decamers at a pH of 5, and disintegrates into inactive dimers at pH > 7.5 [92,220].

In contrast, *SrLDC* is active in a broader pH range between 5.0-8.0 [201] than *CadA* and is more stable upon pH shifts. Our studies indicate that *SrLDC* is a reasonably stable enzyme but probably inhibited by higher L-lysine concentrations (> 100 mM) [203] (SI, Figure S39), whereas there is currently no hint towards product inhibition by cadaverine. In this case, fed-batch or repetitive batch processes and a continuous enzyme membrane reactor could be more efficient in gaining high product concentrations, as already discussed previously (Chapter 3.6.1).

Furthermore, all mentioned LDCs are PLP-dependent enzymes. PLP quickly degrades upon illumination to the main photoproducts, 4-pyridoxic acid-5'-phosphate, and a benzoin-like PLP dimer [221–223]. Degradation seems to be oxygen-dependent and can irreversibly inactivate enzymes. When bound as internal aldimine and exposed to light, PLP might act as a specific photosensitizer and destroy histidine residues in the active site [224]. Gerlach et al. [223] tested the sensitivity toward light for two LDCs. Compared to handling in the dark, illumination with blue light induced an activity loss of 85% for *EcLDCc*, whereas *SrLDC* lost only 45% of activity under the same conditions. It is, therefore, advisable to exclude light during handling and reaction to maintain the enzyme stability. Normal laboratory lighting conditions resulted in *SrLDC* being 50% more active and *EcLDCc* only 10% more active than when illuminated with blue light [223]. Therefore, *SrLDC* might be less prone to light-induced enzyme inactivation

than *EcLDC*, which might be due to its flexible binding site [103,109]. *SrLDC* exhibits a comparably low binding affinity towards PLP, which could facilitate the exchange of degraded PLP for fresh PLP from the reaction mixture [223]. Since *SrLDC* may remain active when fresh PLP is added, it could be an ideal enzyme for prolonged use over several days.

Furthermore, *SrLDC* is a bifunctional lysine/ornithine decarboxylase [105], which is even more attractive as putrescin, the decarboxylation product of L-ornithine, is another building block for biopolymers. Indeed, the total conversion of 100 mM L-ornithine in a 15 mL preparative lab reaction was catalyzed with HaloTag®-immobilized *SrLDC* (SI, Figure S40), yielding 8.8 g L<sup>-1</sup> 1,4-diaminobutane (putrescine). These results show that *SrLDC* should be considered as an alternative enzyme to produce cadaverine (and putrescin) either in its immobilized form or as a heterologously expressed enzyme in fermentative processes, employing e.g. *Corynebacterium glutamicum* or *Escherichia coli*.

### **3.7 Downstream processing of hydroxy-L-lysine and hydroxy-cadaverine**

#### **3.7.1 Purification of hydroxy-L-lysines and hydroxy-cadaverines from the reaction mixture**

When synthesis is accomplished by fermentation or whole cells with recombinant enzymes, the final product may contain a mixture of different components such as cell debris, metabolites, buffer salts, or fermentation media. Therefore, product purification can be expensive and complex. In particular, separating water-soluble products like amino acids (derivatives) and diamines from the fermentation broth can be challenging, and isolation of hydroxy-L-lysines and hydroxy-cadaverines is much easier from less complex reaction mixtures containing only the target product without residual substrate or by-products. Regarding the hydroxylation of L-lysine, the separation of hydroxy-L-lysines from the remaining L-lysines is a challenge, due to their chemical and physical similarity. By HPLC and GC-ToF-MS analyses, we demonstrated that L-lysine was completely converted to the respective hydroxy-L-lysine and contained no by-products other than  $\alpha$ -ketoglutarate, succinate, and HEPES (Chapter 2.2.12). Nevertheless, the isolated product yields of (3*S*)-hydroxy-L-lysine, (4*R*)-hydroxy-L-lysine, and (2*S*)-hydroxy-cadaverine were low. (3*S*)-hydroxy-L-lysine and (2*S*)-hydroxy-cadaverine were purified by a two-step purification procedure according to a protocol of Fossey-Jouenne et al. [225] (Figure 80A). The first step employs a strong cation exchange resin. While Fossey-Jouenne et al. used flash chromatography, we used a Büchner funnel with the cation exchange

## Discussion

resin to speed up the chromatographic procedure by applying vacuum. The second step is a solid-mixed mode (strong cation exchanger and reversed-phase separation) phase extraction using Oasis MCX6cc cartridges. This step is necessary to remove HEPES from the final product, as HEPES is chemically similar to the hydroxy-L-lysines and the 2-hydroxy-cadaverine. Phosphate buffer or buffer-free systems would be beneficial to simplify the downstream processing, as discussed above (Chapters 3.4.2 and 3.6.1). By using a different buffer or a buffer-free system during the biotransformation, the second purification step could be omitted (Figure 80B).

Another bottleneck of the purification is the elution of the products (hydroxy-L-lysines and hydroxy-cadaverines) from the cation exchange resin by large volumes of ammonia. The protocol [225] uses an ammonium hydroxide gradient ranging from 4% to 28%. However, most of the products (hydroxy-L-lysines and hydroxy-cadaverines) were found in the 4% or 10% fractions. Thus, optimizing the gradient could also reduce the amount of ammonium hydroxide used in the process.

Therefore, optimizing the purification procedure along with changing the buffer system or using buffer-free systems during the biotransformation will most likely result in a higher isolated yield.

In addition, succinate is also an interesting precursor for biopolymers or pharmaceuticals, so a simultaneous purification of succinate would be desirable. Succinate and  $\alpha$ -ketoglutarate can be found in their uncharged state at acidic pH (pH 1-2) in the flow-through after the first cation exchange step, as the latter is supplied in 1.5-fold excess. Additionally, the flow-through contains residuals of ascorbic acid and ammonium iron(II) sulfate. By adding  $H_2O_2$ , the remaining  $\alpha$ -ketoglutarate can be converted to succinate with the release of carbon dioxide and water. The succinate could then be isolated from a basic solution using an anion exchanger (Figure 80C).

## Discussion

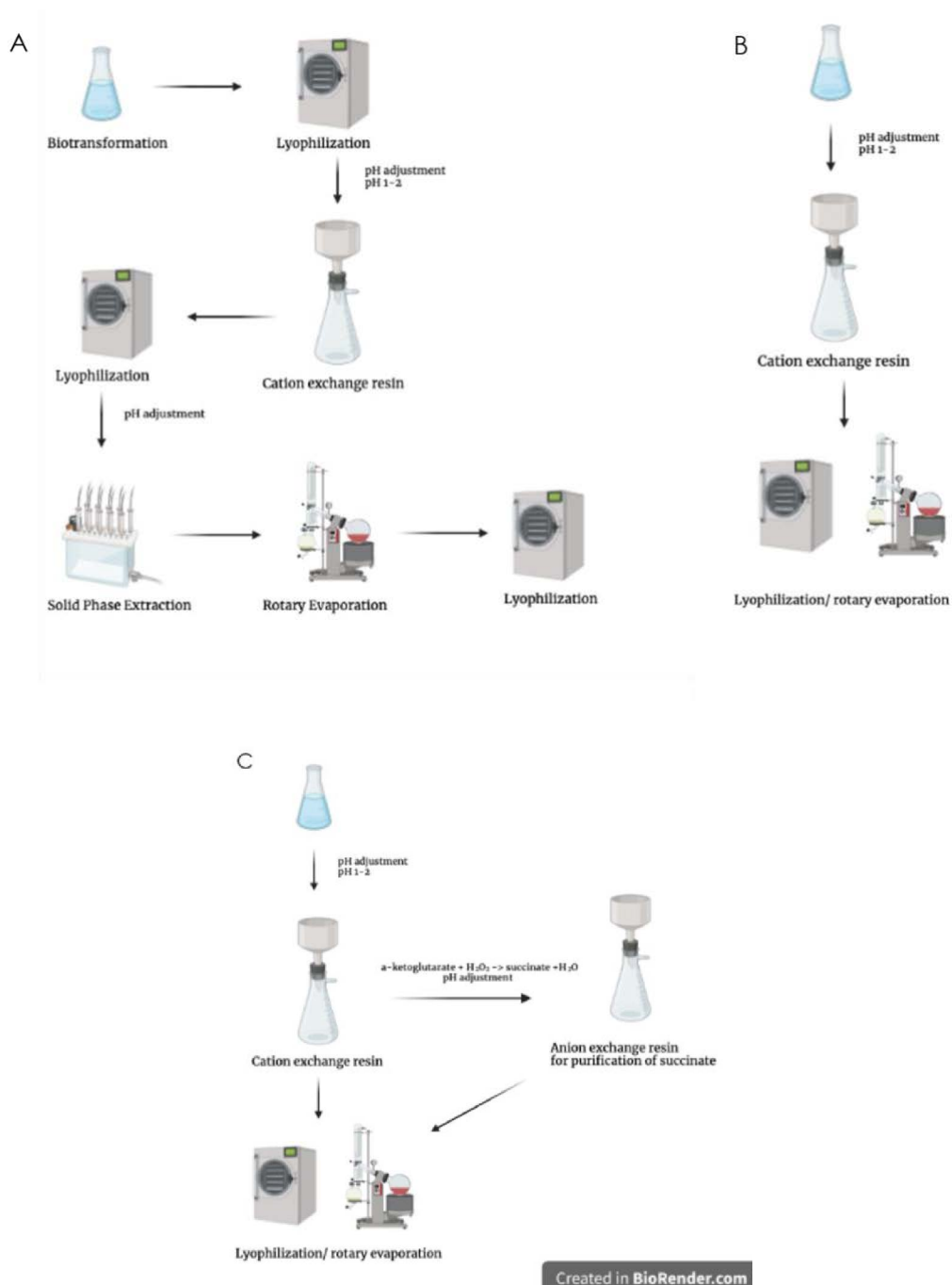


Figure 80: A) Schematic representation of the modified product purification based on the protocol by Fossey-Jouenne [225]. B) Theoretically optimized purification protocol without HEPES. C) Schematic representation of simultaneous purification of succinate. Figure created in BioRender.com.

### 3.7.2 Alternative purification strategies for hydroxy-L-lysines

Considering there are no alternative strategies for hydroxy-L-lysines purification exists, a closer look at amino acid and in particular, L-lysine purification strategies, might provide some useful

insights. As amino acids dissociate in an aqueous solution and form different ionic species as a function of pH, their solubility in nonpolar solvents is very low. Therefore, the purification of amino acids is generally based on chromatographic purification using ion-exchange materials or crystallization at the isoelectric point. Liquid-liquid extraction of amino acids is only possible by adding extractants to the organic phase, like phosphoric acid derivatives, high molecular weight quaternary aliphatic amines, or crown-ethers [226], which would negatively influence step economy or at least increase the E-factor due to higher amounts of waste. Reactive extraction of L-lysine was done with di-(2-ethylhexyl)phosphoric acid (D2EHPA); however, the separation yield was only 68% [226]. For the lack of alternatives, L-lysine is still commonly purified by chromatographic procedures with strong cation exchangers, followed by evaporation, crystallization, and (spray) drying [227–229]. To find effective alternative purification strategies for hydroxy-L-lysines, further research is needed. Nevertheless, as discussed above (Chapter 3.7.1), the existing protocol can be optimized and after the separation of the immobilized enzyme, the cation exchange resin could be easily applied to the supernatant, so that purification via a column can be eliminated.

### **3.7.3 Alternative purification strategies for hydroxy-cadaverine**

Cadaverine is a colorless viscous fuming liquid with a boiling point of 178-180 °C. Isolation and purification methods include evaporation, distillation, and solvent extraction. The raw production mixture can include inorganic or organic impurities, which may interfere with evaporation or distillation and increase energy consumption as well as equipment costs. Therefore, solvent extraction has become the most popular and economic separation method and has mostly replaced distillation [92,230]. Yun-Gi Hong et al. used methyl ethyl ketone as an extractant with an extraction efficiency of more than 70% [231]. Krzyzaniak et al. screened di-2-ethylhexyl phosphoric acid (D2EHPA), 4-nonylphenol, 3,4-bis((2-ethylhexyl)oxy) phenol, versatic acid 1019, 4-octylbenzaldehyde and di-nonyl-naphthalene-sulfonic acid (DNNSA) as extractants, and found 4-nonylphenol to be the most efficient extractant for purification from aqueous media [232]. However, these organic solvents are highly toxic and can easily cause environmental pollution [230]. Meanwhile, Lui et al. developed a solvent extraction method consisting of deprotonation-evaporation, pH adjustment-deprotonation-evaporation, deprotonation-extraction-evaporation, and

deprotonation-extraction-rectification, with the latter being the most effective method enabling the recovery of 99% cadaverine [230] (Figure 80).

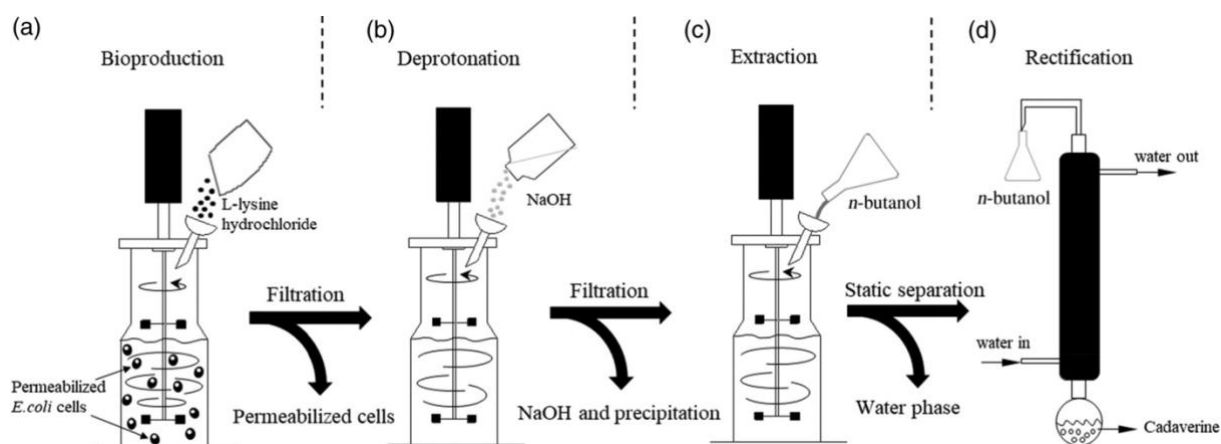


Figure 81: Solvent extraction method for cadaverine developed by Liu et al. [230]. Figure reprinted with permission from John Wiley and Sons.

Kind et al. found n-butanol as the best extractant for cadaverine [233]. A combination of different approaches, also including cation exchange resins, is also possible, as was reviewed by Huang et al. [92].

Similar extraction methods could also be possible for the purification of hydroxy-cadaverine. However, the additional hydroxy group could lower the solubility of the hydroxy-cadaverine in organic solvents; therefore, a solvent screening would be necessary to identify the best extractant.

### 3.8 Economic and ecologic process evaluation

While the current biocatalytic process is still far from a technical scale, an assessment of the sustainability or greenness of a process in the early development stage is necessary to identify further bottlenecks and optimization approaches. Some aspects have already been discussed in previous chapters, but are re-examined for an overall assessment of the process. Furthermore, it should be noted that the calculated values in the following discussion are based on scale-independent values [162]. Obviously, costs can vary between a large-scale and small-scale process, as the environmental impact of different types of waste can vary with different scales. Additionally, evaluation of the industrial potential cannot seriously be reflected in an academic study. Since the presented process for the production of hydroxylated lysines and hydroxylated

cadaverine is still at an early development stage, no information about actual industrial product demands, product prices, process layouts, and labor costs are known. Furthermore, no information about an actual existing industrial process is available.

At the actual early stage of process development it is not critical to discuss the details, including all the parameters, such as those mentioned by Tufvesson and Lima-Ramos [19,37,128,162], so only the atom economy and the E-factor (Chapter 1.6.5), two factors to predict process greenness, were selected. This first general assessment should guide further optimization strategies.

### ***Atom economy***

A significant advantage of KDOs is that they are self-sufficient and do not need expensive cofactors or cofactor regeneration systems. However, the overall atom economy of the process is at 50% and can thus only be described as moderate. This is a consequence of  $\alpha$ -ketoglutarate as a cosubstrate, which is decarboxylated to succinate. As mentioned by Busch et al., this will be similar for every reaction using KDOs. Therefore, Busch et al. have worked on strategies for a cosubstrate generation cascade [81]. However, succinate is interesting as well, because it can be used as a precursor for fully bio-based polymers or pharmaceuticals (Chapter 1.5.1) and could be purified instead. As discussed in chapter 3.7, succinate could be isolated from the reaction mixture by chromatographic purification. Isolation of both, the hydroxy-L-lysines and the succinate can increase the atom economy to 86.4%. Still, a higher atom economy cannot be reached as  $\text{CO}_2$  is released by the decarboxylation of  $\alpha$ -ketoglutarate to succinate. Due to the additional  $\text{CO}_2$  released during the decarboxylation of the hydroxy-L-lysine (second reaction step) to hydroxy-cadaverine, the atom economy decreases to 72.9 % for the overall cascade process (Table 16). For the *Sr*LDC-catalyzed production of cadaverine, the atom economy is even lower at 69.9%.

### ***E-factor***

The atom economy only considers mol% of the substrates and products, but not the step economy, which, amongst others, also impacts waste streams (Chapter 1.6.5). Therefore, the E-factor was also calculated (Table 16). Notably, for the calculations, only the components for the biotransformation were included, since product purification is not yet optimized. The E-factor of the KDO processes is at 4.44 without purification of succinate and at 1.56 including succinate isolation.

## Discussion

The cascade reaction to 2-hydroxy-cadaverine shows an E-factor of 1.95 with the inclusion of the isolation of succinate. If succinate is not isolated, the E-factor is 5.72. For the single reaction of L-lysine towards cadaverine, the E-factor is at 2.78. The E-factors of all processes would profit from a reduction or a replacement of the HEPES buffer (concentration) as proposed in Chapter 3.7.3. The E-factor of the *Sr*LDC-catalyzed reaction could also profit from a reduced PLP concentration. Because PLP is unstable upon light exposure [223] (Chapter 0), the reaction should typically be carried out without light exposure, as was done in this thesis. Additionally, lower initial concentration and a supplementation strategy with fresh PLP could also reduce the overall PLP waste. It should also be noted that the produced (hydroxy) diamines are precursors not only for bulk chemicals like biopolymers but also for fine chemicals and potential active pharmaceutical ingredients. Here, the accepted E-factor and product values are higher than for bulk chemicals. While E-factors of 5 to 50 are acceptable for fine chemicals, E-factors tolerated for pharmaceutical precursors range between 25 to >100 (Table 1).

### ***E-factor calculation including wastewater***

However, considerable amounts of water are consumed, especially during biotransformations in aqueous media. The production of biocatalysts also accounts for a large part of wastewater generation. Wastewater treatment is energy-intensive and accounts for a large part of the process costs; the inclusion of water into the E-factor calculation leads to high values (Table 16). Therefore, it can make a comparison of process parameters difficult. It should also be remembered that the E-factor does not take into account the environmental impact of waste. Therefore, the enzyme preparation itself and the water are often not considered waste, as enzymes are naturally biodegradable, and water is considered inheritably sustainable. In this regard, none of the substances used for the biocatalyst production or the biotransformation in this thesis is ecologically problematic.

Furthermore, L-lysine,  $\alpha$ -ketoglutarate, and L-ascorbic acid can theoretically even be obtained by fermentation from biomass, which is often more environmentally friendly than petroleum-based raw materials. Nevertheless, the E-factor in Table 16 was calculated including the amount of water used for the cultivation process, immobilization, and biotransformation. It should be noted that additional waste generated during cell cultivation, e.g. from the medium components were ignored. Of course, the E-factor increases drastically with the amount of wastewater (Table 16). Notably, the values shown in Table 16 already represent the optimized process. In this thesis, several optimization steps lead to the reduction of wastewater in the overall process.

## Discussion

Especially, the water consumption for the preparation of the biocatalyst could be decreased by increasing soluble protein production through the co-expression of chaperones (Chapter 3.1.1). In addition, the use of an in-situ immobilization technique decreases the amount of water used compared to a chromatographic purification procedure (Chapter 3.3). In addition, the second step of the cascade process could be started directly from the reaction supernatant of the first step without intermediate product purification (Chapter 3.5), which decreases the E-factor further. Generally, the whole process and process alternatives up to the actual end product must be considered for a full assessment. As the chemical regio- and stereoselective C-H oxidation involves extensive protection group chemistry, and suffers from low yields, high amount of by-products, and elaborate product purification, a biocatalytic approach might generally be competitive.

Table 16: Ecologic benchmarks for the production of hydroxy-L-lysines, hydroxy-cadaverine, and cadaverine.

Process	Atom economy [%]	E-factor	w/o	E-factor w/ water****
		water [kg product]	waste/kg	
Production of hydroxy-L-lysines by KDOs	50.0**	1.56*		CaKDO 915.64*- 1916.85**
	86.4*	4.44**		FjKDO 1068.68*- 2237.02**
Production of hydroxy-cadaverine via cascade process***	72.86	1.95*		1959.71*
		5.72**		4898.66**
Production of cadaverine by SrLDC	69.9	2.78		1161.44

\*with succinate recovery

\*\* without succinate recovery

\*\*\* values based on the overall cascade process, not the second reaction step

\*\*\*\* Including fermentation, immobilization, and biotransformation

### CO<sub>2</sub> generation

The generation of CO<sub>2</sub> in both the KDO reaction and the LDC reaction is an essential aspect related to this reaction. While CO<sub>2</sub> generation can be neglected at the preparative laboratory scale, as the process scales up, CO<sub>2</sub> becomes a concern for the process's environmental impact and will increase costs due to taxes on CO<sub>2</sub>. One way to deal with the produced CO<sub>2</sub> is to look into the net CO<sub>2</sub> production of these processes. Like L-lysine, which is a platform chemical produced from renewable resources (e.g. fermentation based on glucose or glycerin),  $\alpha$ -ketoglutarate and L-ascorbic acid can also be obtained through fermentation. Since glucose and glycerol are produced plant-based, the overall CO<sub>2</sub> release will be balanced by the CO<sub>2</sub>

consumption of said plants. Even though actual conventional processes probably release more CO<sub>2</sub> than bio-based processes, future processes should preferably be CO<sub>2</sub> neutral. In contrast to CO<sub>2</sub> generated by many chemical processes, the CO<sub>2</sub> from enzymatic or fermentation processes is often highly pure (99%). Hence, the carbon could easily be captured, compressed, and fed into (photo)-bioreactors, where microorganisms could produce value-added products by CO<sub>2</sub> assimilation. Other industrial-relevant products like ethanol, oils, or carotenoids can be generated by CO<sub>2</sub> fixation using algae [234]. Also, succinic acid can be produced, e.g. by *Actinobacillus succinogenes*, which can also use CO<sub>2</sub> as a C-source [235–237].

### ***Influence of the enzyme formulation and -immobilization***

Finally, the enzyme formulation plays a crucial role in these processes. For the single KDO reaction, the cascade reaction, and the *Sr*LDC reaction towards cadaverine, L-lysine is used as a substrate. In processes with whole cells, L-lysine is partly lost by competing pathways in the cells. As already pointed out earlier, clean product streams are necessary or at least advantageous for the efficient purification of hydroxy-L-lysine, hydroxy-cadaverine, and cadaverine (Chapter 3.7). In this regard, purified enzymes are most suitable. However, the production of purified enzymes is expensive due to the usual chromatographic purification. In situ HaloTag®-based immobilization is therefore advantageous as it requires little additional labor, time, and equipment. Especially for KDOs, which are difficult to prepare and purify and are unstable in their purified form, immobilization is essential for their application in biotransformations (Chapters 3.3 and 3.4). Immobilization facilitates easy concentration of the pure enzyme and enables enzyme recycling (Chapter 3.5). For cadaverine production with immobilized *Sr*LDC, recycling of the enzyme for at least six batches is possible, thereby specific space-time yields are significantly increased (Chapter 3.6). Consequently, the carrier, which is sold by Promega, will mainly determine additional costs. A major application of the HaloTag® technology is cell imaging, the identification of protein-protein interactions [238], and laboratory-scale enzyme immobilization [130,149,150]. The result is a high price due to the relatively small market targeted. Still, product prices are correlated to scale [37], so a larger scale production might result in lower carrier costs. The HaloTag® recognizes respective terminal chloroalkane residues on any carrier and forms a covalent ester bond. Consequently, binding to any carrier with this surface modification is possible. Different HaloTag® ligand building blocks are available, which enable the modification of any potential carrier, with activated carboxylic acids, sulfonyl halide, isocyanate, or amine groups on the surface [239].

## Discussion

Therefore, any material can be modified with these ligands, meeting different sustainability demands or costs by choosing cheap and abundant materials. Reusing the carrier material when the enzyme is exhausted, which is possible with the EziG™ technology, would also be advantageous. However, with the current technology, process costs would strongly increase. The inactive enzyme can be cleaved from the HaloLink™resin upon saponification with SDS and NaOH, leaving a terminal hydroxyl group exposed on the HaloLink™resin, preventing carrier recycling. However, strategies to reinstall terminal chlorine without harming the carrier material is in principle possible. Yet, these modification reagents are expensive and the arising chemical waste must also be considered. On the other hand, Sepharose is biologically degradable; consequently discarding the carrier after use is not connected to challenging or hazardous disposal strategies. Therefore, carrier recycling is, at present, not a realistic option. Furthermore, the HaloTag® technology is patented by the Promega Corporation [240], which restricts its commercial application. Additional investments need to be taken into account to acquire respective licenses. Furthermore, the respective KDOs are also patented [76], and a commercial application would require respective licenses, too.

In summary, it should be remembered that the biotransformations described in this thesis are still at an early stage of laboratory development. Nevertheless, for the preparative laboratory scale, the concepts described here provide a good solution for using individual KDOs. Whether the KDO-catalyzed reactions, in particular, have a chance of technical implementation ultimately depends on how high-priced the related products are, how high the demand is, and what alternative reactions are available to obtain these products [12].

## 4 Conclusion, summary, and outlook

In this thesis, the biocatalytic process for the production of hydroxy-L-lysines and hydroxy-cadaverine [69,90] was developed for preparative application at a laboratory scale.

KDOs are interesting enzymes because they catalyze the stereo- and regioselective hydroxylation of non-activated C-H bonds, a chemically challenging reaction. Especially, the stereoselective hydroxylation of amino acids can give access to many precursors for active pharmaceutical ingredients or fine chemicals. Compared to other enzymes that catalyze the hydroxylation of C-H bonds, such as P450 monooxygenases, there is little research on the identification of bottlenecks or optimizing KDOs for their application in biotransformations. Only a few preparative scale applications with these enzymes in their purified form are known, most likely because they are difficult to produce and unstable under reaction conditions. As a result, KDOs are difficult to handle and are only applicable in analytical scale reactions or laboratory preparative scale reactions up to now. This instability seems, at least partly, to be caused by the reaction system where reactive oxygen species impair enzyme stability and the oxidation of the iron cofactor leads to enzyme inactivation.

In this thesis, the production of the KDOs (*Ca*KDO, *Cp*KDO, and *Fj*KDO) as inactive inclusion bodies and their instability after purification and under reaction conditions were identified as significant bottlenecks. By co-expression of chaperones [82], the soluble protein production could be significantly improved. The HaloTag®-based immobilization of KDOs directly from the cell-free extract increased enzyme activity and stability for *Ca*KDO, probably by protecting the enzyme from the reactive oxygen species and preventing enzyme aggregation. Immobilization enabled simple recyclability of *Cp*KDO and *Fj*KDO but not for *Ca*KDO, which required a reactivation with dithionite and EDTA. The immobilized enzymes enabled the full conversion of 100 mM L-lysine to (3*S*)-hydroxy-L-lysine and (4*R*)-hydroxy-L-lysine, respectively, in a 15 mL scale reaction. An increase in substrate concentration to at least 200 mM L-lysine upon further optimization of the reaction set-up is highly likely since we could not identify any substrate or product inhibition at these concentrations.

In comparison to reactions using whole-cell biocatalysis or fermentative processes, for example, to produce amino acids, our reaction set-up with isolated, immobilized enzymes leads to much cleaner product streams, which simplifies product purification. However, purification of hydroxy-L-lysine from HEPES buffer used in the reaction via cation exchange resins was identified as another bottleneck of the overall process. Due to its high similarity to the

## Conclusion, summary, and outlook

hydroxy-L-lysines and its high concentration in the reaction supernatant, HEPES impurities impair the purity of the final product. Therefore, further process intensification should aim for a cleaner product stream without HEPES and alternative buffers like phosphate buffers or buffer-free systems.

After the bottlenecks of the first step of the cascade reaction towards hydroxy-cadaverine were solved, the decarboxylation of 100 mM (3*S*)-hydroxy-L-lysine catalyzed by *Sr*LDC could easily be implemented. Likewise, *Sr*LDC was immobilized via the HaloTag® for easier separation from the reaction supernatant. In addition, the catalyst for the reaction of 100 mM L-lysine to cadaverine could be recycled for at least six batches with minimal activity loss. Using immobilized enzymes, this process is also competitive with other cadaverine production processes; therefore, *Sr*LDC might be an excellent alternative to commonly used LDCs from *E. coli* for cadaverine production. While the purification of 2-hydroxy-cadaverine could be successfully achieved by a two-step chromatographic purification, optimization of the purification might increase product yield and reduce product purification to one-step purification via cation exchange resins. Since removing HEPES is a challenge here, the factors that have the greatest impact are again the change to phosphate buffer or a buffer-free system. The development of integrated product purification strategies in further studies, e.g. development of organic phase extraction, might enhance the overall process economics and ecologic benchmarks.

In conclusion, the major bottlenecks of the process were identified and eliminated, which enabled a preparative scale reaction. However, new bottlenecks like the KDO reaction system or product purification were identified, which should be addressed in additional studies.

To explore the potential of KDOs in preparative applications further, additional research should focus on the characterization of the reaction system, aiming for a decrease of reactive oxygen species. Also, further knowledge about the oxidative inactivation of the enzyme by oxidation of active site residues or the Fe(II) and subsequent loss of Fe(III) from the active site is needed. With this knowledge, other strategies to prevent oxidative damage can be developed. Protein engineering for KDOs has received less attention than that for P450 monooxygenases. By improving the iron-binding in the active site or identifying and exchanging active site residues that are susceptible to oxidative damage, protein engineering could lead to variants with increased process stability.

Furthermore, the investigation of alternative in situ immobilization techniques could help to develop KDO-catalyzed biotransformations further. Therefore, combining protein engineering

## Conclusion, summary, and outlook

strategies with in-situ immobilization can result in robust processes with stable KDO variants and recycling methods. The strategies developed here enable the application of KDOs for L-lysine conversion up to concentrations of 200 mM at a preparative laboratory scale, allowing yields of up to 0.8 g (16-32 g L<sup>-1</sup>). Consequently, KDOs could now be used to develop new synthesis routes for bioorganic synthesis. With the implementation of further process intensification strategies robust preparative scale processes with the potential for industrial application would be possible even for these highly sensitive enzymes.

## 5 References

1. Kamm, B. Biomasse-Wirtschaft Und Bioraffinerie-Systeme. *J. Chem. Inf. Model.* **2008**, *53*, 287.
2. Min, F. *Bioeconomy in Germany Translation*; 2015;
3. De Jong, E.; Stichnothe, H.; Bell, G.; Jorgensen, H. *Bio-Based Chemicals: A 2020 Update*; 2020; ISBN 9781910154694.
4. Chandel, A.K.; Garlapati, V.K.; Singh, A.K.; Antunes, F.A.F.; da Silva, S.S. The Path Forward for Lignocellulose Biorefineries: Bottlenecks, Solutions, and Perspective on Commercialization. *Bioresour. Technol.* **2018**, *264*, 370–381, doi:10.1016/j.biortech.2018.06.004.
5. Werpy, T.; Petersen, G. Top Value Added Chemicals from Biomass Volume I — Results of Screening for Potential Candidates from Sugars and Synthesis Gas Top Value Added Chemicals From Biomass Volume I: Results of Screening for Potential Candidates. *Other Inf. PBD 1 Aug 2004* **2004**, Medium: ED; Size: 76 pp. pages, doi:10.2172/15008859.
6. Anastas, P.T.; Williamson, T.C. Green Chemistry: Designing Chemistry for the Environment. *J. Am. Chem. Soc.* **1996**, *118*, 10945–10945, doi:10.1021/ja9656917.
7. Anastas, P.; Eghbali, N. Green Chemistry: Principles and Practice. *Chem. Soc. Rev.* **2010**, *39*, 301–312, doi:10.1039/b918763b.
8. Tang, S.L.Y.Y.; Smith, R.L.; Poliakoff, M. Principles of Green Chemistry: Productively. *Green Chem.* **2005**, *7*, 761–762, doi:10.1039/b513020b.
9. Tang, S.Y.; Bourne, R.A.; Smith, R.L.; Poliakoff, M. The 24 Principles of Green Engineering and Green Chemistry: “IMPROVEMENTS PRODUCTIVELY.” *Green Chem.* **2008**, *10*, 268–26, doi:10.1039/b719469m.
10. Lindström, B.; Pettersson, L.J. A Brief History of Catalysis. *Cattech* **2003**, *7*, 130–138, doi:10.1023/A:1025001809516.
11. Wiley, A.J. Enzymes. A Practical Introduction to Structure, Mechanism, and Data Analysis, Second Ed. Robert A. Copeland. *Anal. Biochem.* **2001**, *291*, 172, doi:10.1006/abio.2001.5023.
12. Straathof, A.J.J.; Panke, S.; Schmid, A. The Production of Fine Chemicals by Biotransformations. *Curr. Opin. Biotechnol.* **2002**, *13*, 548–556, doi:10.1016/S0958-1669(02)00360-9.
13. Wohlgemuth, R. Asymmetric Biocatalysis with Microbial Enzymes and Cells. *Curr. Opin. Microbiol.* **2010**, *13*, 283–292, doi:10.1016/j.mib.2010.04.001.
14. Breuer, M.; Stürmer, R. Chemie Und Biologie Hand in Hand. Enzyme Als Katalysatoren. *Chemie unserer Zeit* **2006**, *40*, 104–111, doi:10.1002/ciuz.200600379.
15. Wu, S.; Li, Z. Whole-Cell Cascade Biotransformations for One-Pot Multistep Organic Synthesis. *ChemCatChem* **2018**, 1–16, doi:10.1002/cctc.201701669.
16. Sheldon, R.A. Green Solvents for Sustainable Organic Synthesis: State of the Art. *Green Chem.* **2005**, *7*, 267, doi:10.1039/b418069k.
17. Wohlgemuth, R. The Locks and Keys to Industrial Biotechnology. *N. Biotechnol.* **2009**, *25*, 204–213, doi:10.1016/j.nbt.2009.01.002.
18. Patel, R.; Hanson, R.; Goswami, A.; Nanduri, V.; Banerjee, A.; Donovan, M.-J.; Goldberg, S.; Johnston, R.; Brzozowski, D.; Tully, T. et al. Enzymatic Synthesis of Chiral Intermediates for Pharmaceuticals. *J. Ind. Microbiol. Biotechnol.* **2003**, *30*, 252–259, doi:10.1007/s10295-003-0032-6.
19. Lima-Ramos, J.; Tufvesson, P.; Woodley, J.M. Application of Environmental and Economic Metrics to Guide the Development of Biocatalytic Processes. *Green Process. Synth.* **2014**, *3*, 195–213, doi:10.1515/gps-2013-0094.
20. Sheldon, R.A. The E Factor 25 Years on: The Rise of Green Chemistry and Sustainability. *Green Chem.* **2017**, *19*, 18–43, doi:10.1039/C6GC02157C.
21. de María, P.D.; Hollmann, F. On the (Un)Greenness of Biocatalysis: Some Challenging Figures and Some Promising Options. *Front. Microbiol.* **2015**, *6*, 6–10, doi:10.3389/fmicb.2015.01257.
22. Kuhn, D.; Kholiq, M.A.; Heinzle, E.; Bühler, B.; Schmid, A. Intensification and Economic and Ecological Assessment of a Biocatalytic Oxyfunctionalization Process. *Green Chem.* **2010**, *12*, 815–882, doi:10.1039/b921896c.
23. Jegannathan, K.R.; Nielsen, P.H. Environmental Assessment of Enzyme Use in Industrial Production—a Literature Review. *J. Clean. Prod.* **2013**, *42*, 228–240, doi:10.1016/j.jclepro.2012.11.005.
24. van Schie, M.M.C.H.; Spöring, J.D.; Bocola, M.; Domínguez de María, P.; Rother, D. Applied Biocatalysis beyond Just Buffers - From Aqueous to Unconventional Media. Options and Guidelines. *Green Chem.* **2021**, *23*, 3191–3206, doi:10.1039/d1gc00561h.
25. Faber, K. *Biotransformations in Organic Chemistry*; ChemInform.; Springer Berlin Heidelberg: Berlin, Heidelberg, 2011; ISBN 978-3-642-17392-9.

## References

26. Smith, S.W. Chiral Toxicology: It's the Same Thing Only Different. *Toxicol. Sci.* **2009**, *110*, 4–30, doi:10.1093/toxsci/kfp097.
27. Beck, G. Synthesis of Chiral Drug Substances. *Synlett* **2002**, 837–850, doi:10.1055/s-2002-31890.
28. Kocienski, P.J. *Protecting Groups 3rd Edition*; Thieme: New York, 2005;
29. MA, M.S.; de la Torre *Dead Ends and Detours*; WILEY-VCH Verlag GmbH & Co. KGaA: Weinheim, Germany, 2004;
30. Arora, B.; Mukherjee, J.; Gupta, M.N. Enzyme Promiscuity: Using the Dark Side of Enzyme Specificity in White Biotechnology. *Sustain. Chem. Process.* **2014**, *2*, 1–9, doi:10.1186/s40508-014-0025-y.
31. Gröger, H.; Hummel, W. Combining the “two Worlds” of Chemocatalysis and Biocatalysis towards Multi-Step One-Pot Processes in Aqueous Media. *Curr. Opin. Chem. Biol.* **2014**, *19*, 171–179, doi:10.1016/j.cbpa.2014.03.002.
32. Kroutil, W.; Rueping, M. Introduction to ACS Catalysis Virtual Special Issue on Cascade Catalysis. *ACS Catal.* **2014**, *4*, 2086–2087, doi:doi.org/10.1021/cs500622h.
33. Siedentop, R.; Claaßen, C.; Rother, D.; Lütz, S.; Rosenthal, K. Getting the Most out of Enzyme Cascades: Strategies to Optimize in Vitro Multi-enzymatic Reactions. *Catalysts* **2021**, *11*, 1–24, doi:10.3390/catal11101183.
34. Ricca, E.; Brucher, B.; Schrittwieser, J.H. Multi-Enzymatic Cascade Reactions: Overview and Perspectives. *Adv. Synth. Catal.* **2011**, *353*, 2239–2262, doi:10.1002/adsc.201100256.
35. Schrittwieser, J.H.; Velikogne, S.; Hall, M.; Kroutil, W. Artificial Biocatalytic Linear Cascades for Preparation of Organic Molecules. *Chem. Rev.* **2018**, *118*, 270–348, doi:10.1021/acs.chemrev.7b00033.
36. Sheldon, R.A.; van Pelt, S. Enzyme Immobilisation in Biocatalysis: Why, What and How. *Chem. Soc. Rev.* **2013**, *42*, 6223–6235, doi:10.1039/C3CS60075K.
37. Tufvesson, P.; Lima-Ramos, J.; Nordblad, M.; Woodley, J.M. Guidelines and Cost Analysis for Catalyst Production in Biocatalytic Processes. *Org. Process Res. Dev.* **2011**, *15*, 266–274, doi:10.1021/op1002165.
38. Woodley, J.M. Integrating Protein Engineering with Process Design for Biocatalysis. *Philos. Trans. R. Soc. A Math. Phys. Eng. Sci.* **2018**, *376*, doi:10.1098/rsta.2017.0062.
39. Burek, B.O.; Dawood, A.W.H.; Hollmann, F.; Liese, A.; Holtmann, D. Process Intensification as Game Changer in Enzyme Catalysis. **2022**, *2*, 1–18, doi:10.3389/fctls.2022.858706.
40. Hauer, B. Embracing Nature's Catalysts: A Viewpoint on the Future of Biocatalysis. *ACS Catal.* **2020**, *10*, 8418–8427, doi:10.1021/acscatal.0c01708.
41. Dong, J.J.; Fernández-Fueyo, E.; Hollmann, F.; Paul, C.E.; Pesic, M.; Schmidt, S.; Wang, Y.; Younes, S.; Zhang, W. Biocatalytic Oxidation Reactions: A Chemist's Perspective. *Angew. Chemie - Int. Ed.* **2018**, *57*, 9238–9261, doi:10.1002/anie.201800343.
42. Peters, C.; Buller, R.M. Industrial Application of 2-Oxoglutarate-Dependent Oxygenases. *Catalysts* **2019**, *9*.
43. Blank, L.M.; Ebert, B.E.; Buehler, K.; Bühler, B. Redox Biocatalysis and Metabolism: Molecular Mechanisms and Metabolic Network Analysis. *Antioxidants Redox Signal.* **2010**, *13*, 349–394, doi:10.1089/ars.2009.2931.
44. Roper, L.; Grogan, G. *Biocatalysis for Organic Chemists: Hydroxylations*; Elsevier Inc., 2016; ISBN 9780124115422.
45. Zhang, R.K.; Huang, X.; Arnold, F.H. Selective C-H Bond Functionalization with Engineered Heme Proteins: New Tools to Generate Complexity. *Curr. Opin. Chem. Biol.* **2019**, *49*, 67–75, doi:10.1016/j.cbpa.2018.10.004.
46. Bormann, S.; Gomez Baraibar, A.; Ni, Y.; Holtmann, D.; Hollmann, F. Specific Oxyfunctionalisations Catalysed by Peroxygenases: Opportunities, Challenges and Solutions. *Catal. Sci. Technol.* **2015**, *5*, 2038–2052, doi:10.1039/c4cy01477d.
47. Fernández-Fueyo, E.; Ni, Y.; Gomez Baraibar, A.; Alcalde, M.; van Langen, L.M.; Hollmann, F. Towards Preparative Peroxygenase-Catalyzed Oxyfunctionalization Reactions in Organic Media. *J. Mol. Catal. B Enzym.* **2016**, *134*, 347–352, doi:10.1016/j.molcatb.2016.09.013.
48. Chakrabarty, S.; Wang, Y.; Perkins, J.C.; Narayan, A.R.H. Scalable Biocatalytic C-H Oxyfunctionalization Reactions. *Chem. Soc. Rev.* **2020**, *49*, 8137–8155, doi:10.1039/d0cs00440e.
49. Clifton, I.J.; McDonough, M.A.; Ehrismann, D.; Kershaw, N.J.; Granatino, N.; Schofield, C.J. Structural Studies on 2-Oxoglutarate Oxygenases and Related Double-Stranded  $\beta$ -Helix Fold Proteins. *J. Inorg. Biochem.* **2006**, *100*, 644–669, doi:10.1016/j.jinorgbio.2006.01.024.
50. Gao, S.S.; Naowarajna, N.; Cheng, R.; Liu, X.; Liu, P. Recent Examples of  $\alpha$ -Ketoglutarate-Dependent Mononuclear Non-Haem Iron Enzymes in Natural Product Biosyntheses. *Nat. Prod. Rep.* **2018**, *35*, 792–837, doi:10.1039/c7np00067g.
51. Martinez, S.; Hausinger, R.P. Catalytic Mechanisms of Fe(II)- and 2-Oxoglutarate-Dependent Oxygenases. *J. Biol. Chem.* **2015**, *290*, 20702–20711, doi:10.1074/jbc.R115.648691.
52. Schofield, C.; Hausinger, R. *2-Oxoglutarate-Dependent Oxygenases*; Schofield, C., Hausinger, R., Eds.;

## References

- Metallobiology; The Royal Society of Chemistry, 2015; ISBN 978-1-84973-950-4.
53. Hibi, M.; Ogawa, J. Characteristics and Biotechnology Applications of Aliphatic Amino Acid Hydroxylases Belonging to the Fe(II)/ $\alpha$ -Ketoglutarate-Dependent Dioxygenase Superfamily. *Appl. Microbiol. Biotechnol.* **2014**, *98*, 3869–3876, doi:10.1007/s00253-014-5620-z.
  54. Sedgwick, B. Repairing DNA-Methylation Damage. *Nat. Rev. Mol. Cell Biol.* **2004**, *5*, 148–157, doi:10.1038/nrm1312.
  55. Dann, C.E.; Bruick, R.K.; Deisenhofer, J. Structure of Factor-Inhibiting Hypoxia-Inducible Factor 1: An Asparaginyl Hydroxylase Involved in the Hypoxic Response Pathway. *Proc. Natl. Acad. Sci. U. S. A.* **2002**, *99*, 15351–15356, doi:10.1073/pnas.202614999.
  56. Hirota, K.; Semenza, G.L. Regulation of Hypoxia-Inducible Factor 1 by Prolyl and Asparaginyl Hydroxylases. *Biochem. Biophys. Res. Commun.* **2005**, *338*, 610–616, doi:10.1016/j.bbrc.2005.08.193.
  57. Kaelin, W.G. How Oxygen Makes Its Presence Felt. *Genes Dev.* **2002**, *16*, 1441–1445.
  58. Schofield, C.J.; Ratcliffe, P.J. Oxygen Sensing by HIF Hydroxylases. *Nat. Rev. Mol. Cell Biol.* **2004**, *5*, 343–354, doi:10.1038/nrm1366.
  59. Hewitson, K.S.; Schofield, C.J. The HIF Pathway as a Therapeutic Target. *Drug Discov. Today* **2004**, *9*, 704–711, doi:10.1016/S1359-6446(04)03202-7.
  60. Hausinger, R.P.; Hausinger, R.P. *Fe (II)/ $\alpha$ -Ketoglutarate-Dependent Hydroxylases and Related Enzymes Fe ( II ) /  $\alpha$ -Ketoglutarate-Dependent Hydroxylases and Related Enzymes*; 2008; Vol. 9238; ISBN 1040923049044.
  61. Prescott, A.G.; Lloyd, M.D. The Iron(II) and 2-Oxoacid-Dependent Dioxygenases and Their Role in Metabolism. *Nat. Prod. Rep.* **2000**, *17*, 367–383, doi:10.1039/a902197c.
  62. Kershaw, N.J.; Caines, M.E.C.; Sleeman, M.C.; Schofield, C.J. The Enzymology of Clavam and Carbapenem Biosynthesis. *Chem. Commun.* **2005**, 4251–4263, doi:10.1039/b505964j.
  63. Zwick, C.R.; Renata, H. Remote C-H Hydroxylation by an  $\alpha$ -Ketoglutarate-Dependent Dioxygenase Enables Efficient Chemoenzymatic Synthesis of Manzacidin C and Proline Analogs. *J. Am. Chem. Soc.* **2018**, *140*, 1165–1169, doi:10.1021/jacs.7b12918.
  64. Islam, S.; Leissing, T.M.; Chowdhury, R.; Hopkinson, R.J.; Schofield, C.J. 2-Oxoglutarate-Dependent Oxygenases. *Annu. Rev. Biochem.* **2018**, *87*, 585–620, doi:https://doi.org/10.1146/annurev-biochem-061516-044724.
  65. Purpero, V.; Moran, G.R. The Diverse and Pervasive Chemistries of the  $\alpha$ -Keto Acid Dependent Enzymes. *J. Biol. Inorg. Chem.* **2007**, *12*, 587–601, doi:10.1007/s00775-007-0231-0.
  66. Bastard, K.; Isabet, T.; Stura, E.A.; Legrand, P.; Zapparucha, A. Structural Studies Based on Two Lysine Dioxygenases with Distinct Regioselectivity Brings Insights Into Enzyme Specificity within the Clavaminate Synthase-Like Family. *Sci. Rep.* **2018**, *8*, 8–18, doi:10.1038/s41598-018-34795-9.
  67. Welford, R.W.D.; Kirkpatrick, J.M.; McNeill, L.A.; Puri, M.; Oldham, N.J.; Schofield, C.J. Incorporation of Oxygen into the Succinate Co-Product of Iron(II) and 2-Oxoglutarate Dependent Oxygenases from Bacteria, Plants and Humans. *FEBS Lett.* **2005**, *579*, 5170–5174, doi:10.1016/j.febslet.2005.08.033.
  68. Aik, W.; McDonough, M.A.; Thalhammer, A.; Chowdhury, R.; Schofield, C.J. Role of the Jelly-Roll Fold in Substrate Binding by 2-Oxoglutarate Oxygenases. *Curr. Opin. Struct. Biol.* **2012**, *22*, 691–700, doi:10.1016/j.sbi.2012.10.001.
  69. Baud, D.; Peruch, O.; Saaidi, P.-L.; Fossey, A.; Mariage, A.; Petit, J.-L.; Salanoubat, M.; Vergne-Vaxelaire, C.; de Berardinis, V.; Zapparucha, A. Biocatalytic Approaches towards the Synthesis of Chiral Amino Alcohols from Lysine: Cascade Reactions Combining Alpha-Keto Acid Oxygenase Hydroxylation with Pyridoxal Phosphate- Dependent Decarboxylation. *Adv. Synth. Catal.* **2017**, *359*, 1563–1569, doi:10.1002/adsc.201600934.
  70. Abiko, A.; Masamune, S. An Improved, Convenient Procedure for Reduction of Amino Acids to Aminoalcohols: Use of NaBH<sub>4</sub>-H<sub>2</sub>SO<sub>4</sub>. *Tetrahedron Lett.* **1992**, *33*, 5517–5518, doi:10.1016/S0040-4039(00)61133-4.
  71. Chen, H.; Bong, Y.K.; Cabirol, F.; Gohel, A.; Li, T.; Moore, J.C.; Quintanar-Audelo, M.; Yang, H.; Collier, S.J.; Smith, D. Biocatalysts and Methods for Hydroxylation of Chemical Compounds.
  72. Miyake, R.; Dekishima, Y. Method for Manufacturing Cis-5-Hydroxy-L-Pipecolic Acid.
  73. Ozaki, A.; Mori, H.; Shibasaki, T.; Ando, K.; Chiba, S. Process for Producing Trans-4-Hydroxy-L-Proline.
  74. Ozaki, A.; Mori, H.; Shibasaki, T.; Ando, K.; Ochiai, K.; Chiba, S.; Uosaki, Y. Process for Producing Cis-3-Hydroxy-L-Proline.
  75. Kino, K.; Hara, R. L-Proline Cis-4-Hydroxylase and Use Thereof to Produce Cis-4-Hydroxy-L-Proline.
  76. Kino, K.; Hara, R.; Miyake, R.; Kawabata, H. Method for Producing Hydroxy-L-Lysine Employing an L-Lysine Hydroxylase and Method for Producing Hydroxy-L-Pipecolic Acid.
  77. Kodera, T.; Smirnov, S.V.; Samsonova, N.N.; Kotliarova, V.A.; Rushkevich, N.Y.; Kozlov, Y.I.; Shimizu, S.; Ogawa, J.; Hibi, M. Method for Producing 4-Hydroxy-L-Isoleucine.
  78. Mantri, M.; Zhang, Z.; McDonough, M.A.; Schofield, C.J. Autocatalysed Oxidative Modifications to 2-

## References

- Oxoglutarate Dependent Oxygenases. *FEBS J.* **2012**, *279*, 1563–1575, doi:10.1111/j.1742-4658.2012.08496.x.
79. Amatuni, A.; Renata, H. Identification of a Lysine 4-Hydroxylase from the Glidobactin Biosynthesis and Evaluation of Its Biocatalytic Potential. *Org. Biomol. Chem.* **2019**, *17*, 1736–1739, doi:10.1039/c8ob02054j.
  80. Rolf, J.; Nerke, P.; Britner, A.; Krick, S.; Lütz, S.; Rosenthal, K. From Cell-Free Protein Synthesis to Whole-Cell Biotransformation: Screening and Identification of Novel  $\alpha$ -Ketoglutarate-Dependent Dioxygenases for Preparative-Scale Synthesis of Hydroxy-L-Lysine. *Catalysts* **2021**, *11*, doi:10.3390/catal11091038.
  81. Busch, F.; Brummund, J.; Calderini, E.; Schürmann, M.; Kourist, R. Cofactor Generation Cascade for  $\alpha$ -Ketoglutarate and Fe(II)-Dependent Dioxygenases. *ACS Sustain. Chem. Eng.* **2020**, *8*, 8604–8612, doi:10.1021/acssuschemeng.0c01122.
  82. Zhang, X.; King-Smith, E.; Renata, H. Total Synthesis of Tambromycin by Combining Chemocatalytic and Biocatalytic C–H Functionalization. *Angew. Chemie Int. Ed.* **2018**, *57*, 5037–5041, doi:10.1002/anie.201801165.
  83. Hara, R.; Yamagata, K.; Miyake, R.; Kawabata, H.; Uehara, H.; Kino, K.; Baud, D.; Saaidi, P.L.; Monfleur, A.; Harari, M. et al. Discovery of Lysine Hydroxylases in the Clavamincic Acid Synthase-Like Superfamily for Efficient Hydroxylysine Bioproduction. *Appl. Environ. Microbiol.* **2017**, *83*, 1–14, doi:10.1128/AEM.00693-17.
  84. Strieker, M.; Essen, L.O.; Walsh, C.T.; Marahiel, M.A. Non-Heme Hydroxylase Engineering for Simple Enzymatic Synthesis of L-Threo-Hydroxyaspartic Acid. *ChemBioChem* **2008**, *9*, 374–376, doi:10.1002/cbic.200700557.
  85. Qiao, Z.; Xu, M.; Shao, M.; Zhao, Y.; Long, M.; Yang, T.; Zhang, X.; Yang, S.; Nakanishi, H.; Rao, Z. Engineered Disulfide Bonds Improve Thermostability and Activity of L-isoleucine Hydroxylase for Efficient 4-HIL Production in *Bacillus Subtilis* 168. *Eng. Life Sci.* **2020**, *20*, 7–16, doi:10.1002/elsc.201900090.
  86. Wang, F.; Zhu, M.; Song, Z.; Li, C.; Wang, Y.; Zhu, Z.; Sun, D.; Lu, F.; Qin, H.M. Reshaping the Binding Pocket of Lysine Hydroxylase for Enhanced Activity. *ACS Catal.* **2020**, *10*, 13946–13956, doi:10.1021/acscatal.0c03841.
  87. Marin, J.; Didierjean, C.; Aubry, A.; Casimir, J.; Briand, J.; Guichard, G.; Poincare, H. Synthesis of Enantiopure 4-Hydroxypipicolate and 4-Hydroxylysine Derivatives from a Common 4, 6-Dioxopiperidinecarboxylate Precursor. **2004**, 130–141, doi:10.1021/jo0353886.
  88. Lampe, J.W.; Hughes, P.F.; Biggers, C.K.; Smith, S.H.; Hu, H. Total Synthesis of (–)- and (+)-Balanol. *Synthesis (Stuttg.)* **1996**, *3263*, 4572–4581.
  89. Amatuni, A.; Shuster, A.; Adibekian, A.; Renata, H. Concise Chemoenzymatic Total Synthesis and Identification of Cellular Targets of Cepafungin I. *Cell Chem. Biol.* **2020**, *27*, 1318–1326.e18, doi:10.1016/j.chembiol.2020.07.012.
  90. Baud, D.; Saaidi, P.-L.; Monfleur, A.; Harari, M.; Cuccaro, J.; Fossey, A.; Besnard, M.; Debard, A.; Mariage, A.; Pellouin, V. et al. Synthesis of Mono- and Dihydroxylated Amino Acids with New  $\alpha$ -Ketoglutarate-Dependent Dioxygenases: Biocatalytic Oxidation of C-H Bonds. *ChemCatChem* **2014**, *6*, 3012–3017, doi:10.1002/cctc.201402498.
  91. McDonough, M.A.; Loenarz, C.; Chowdhury, R.; Clifton, I.J.; Schofield, C.J. Structural Studies on Human 2-Oxoglutarate Dependent Oxygenases. *Curr. Opin. Struct. Biol.* **2010**, *20*, 659–672, doi:10.1016/j.sbi.2010.08.006.
  92. Huang, Y.; Ji, X.; Ma, Z.; Łężyk, M.; Huang, Y.; Zhao, H. Green Chemical and Biological Synthesis of Cadaverine: Recent Development and Challenges. *RSC Adv.* **2021**, *11*, 23922–23942, doi:10.1039/d1ra02764f.
  93. Nanda, S.; Patra, B.R.; Patel, R.; Bakos, J.; Dalai, A.K. Innovations in Applications and Prospects of Bioplastics and Biopolymers: A Review. *Environ. Chem. Lett.* **2022**, *20*, 379–395, doi:10.1007/s10311-021-01334-4.
  94. Kind, S.; Wittmann, C. Bio-Based Production of the Platform Chemical 1,5-Diaminopentane. *Appl. Microbiol. Biotechnol.* **2011**, *91*, 1287–1296, doi:10.1007/s00253-011-3457-2.
  95. Becker, J.; Wittmann, C. *Industrial Biotechnology*; Wittmann, C., Liao, J.C., Eds.; Wiley 2010; VCH Verlag GmbH & Co. KGaA: Weinheim, Germany, 2017; ISBN 9783527807833.
  96. Kikuchi, Y.; Kojima, H.; Tanaka, T.; Takatsuka, Y.; Kamio, Y. Characterization of a Second Lysine Decarboxylase Isolated from *Escherichia Coli*. *J. Bacteriol.* **1997**, *179*, 4486–4492, doi:10.1128/jb.179.14.4486-4492.1997.
  97. Yamamoto, Y.; Miwa, Y.; Miyoshi, K.; Furuyama, J.I.; Ohmori, H. The *Escherichia Coli* LdcC Gene Encodes Another Lysine Decarboxylase, Probably a Constitutive Enzyme. *Genes Genet. Syst.* **1997**, *72*, 167–172, doi:10.1266/ggs.72.167.

## References

98. Scott, E.; Peter, F.; Sanders, J. Biomass in the Manufacture of Industrial Products-the Use of Proteins and Amino Acids. *Appl. Microbiol. Biotechnol.* **2007**, *75*, 751–762, doi:10.1007/s00253-007-0932-x.
99. Gómez, R. V.; Varela, O. Synthesis of Regioisomeric, Stereoregular AABB-Type Polyamides from Chiral Diamines and Diacids Derived from Natural Amino Acids. *Tetrahedron Asymmetry* **2007**, *18*, 2190–2196, doi:10.1016/j.tetasy.2007.09.010.
100. Kakwere, H.; Perrier, S. Design of Complex Polymeric Architectures and Nanostructured Materials/Hybrids by Living Radical Polymerization of Hydroxylated Monomers. *Polym. Chem.* **2011**, *2*, 270–288, doi:10.1039/c0py00160k.
101. Prell, C.; Vonderbank, S.-A.A.; Meyer, F.; Pérez-García, F.; Wendisch, V.F. Metabolic Engineering of *Corynebacterium glutamicum* for de Novo Production of 3-Hydroxycadaverine. *Curr. Res. Biotechnol.* **2022**, *4*, 32–46, doi:10.1016/j.crbiot.2021.12.004.
102. Orgueira, H.A.; Erra-Balsells, R.; Nonami, H.; Varela, O. Synthesis of Chiral Polyhydroxy Polyamides Having Chains of Defined Regio and Stereoregularity. *Macromolecules* **2001**, *34*, 687–695, doi:10.1021/ma000016+.
103. Sagong, H.; Son, H.F.; Kim, S.; Kim, Y.; Kim, K.; Kim, K. Crystal Structure and Pyridoxal 5-Phosphate Binding Property of Lysine Decarboxylase from *Selenomonas Ruminantium*. **2016**, 1–15, doi:10.1371/journal.pone.0166667.
104. Terawaki, Y. Purification and Properties of *Selenomonas Ruminantium* Lysine Decarboxylase. **1983**, *153*, 658–664.
105. Michael, A.J. Evolution of Biosynthetic Diversity. *Biochem. J.* **2017**, *474*, 2277–2299, doi:10.1042/BCJ20160823.
106. Takatsuka, Y.; Yamaguchi, Y.; Ono, M.; Kamio, Y. Gene Cloning and Molecular Characterization of Lysine Decarboxylase from *Selenomonas Ruminantium* Delineate Its Evolutionary Relationship to Ornithine Decarboxylases from Eukaryotes. **2000**, *182*, 6732–6741.
107. Ojima, S.K.; Amio, Y.K. Molecular Basis for the Maintenance of Envelope Integrity in *Selenomonas Ruminantium*: Cadaverine Biosynthesis and Covalent Modification into the Peptidoglycan Play a Major Role. *J. Nutr. Sci. Vitaminol. (Tokyo)*. **2012**, *58*, 153–160, doi:10.3177/jnsv.58.153.
108. Takatsuka, Y.; Kamio, Y. Molecular Dissection of the *Selenomonas Ruminantium* Cell Envelope and Lysine Decarboxylase Involved in the Biosynthesis of a Polyamine Covalently Linked to the Cell Wall Peptidoglycan Layer. *Biosci. Biotechnol. Biochem.* **2004**, *68*, 1–19, doi:10.1271/bbb.68.1.
109. Sagong, H.; Kim, K. Lysine Decarboxylase with an Enhanced Affinity for Pyridoxal 5-Phosphate by Disulfide Bond-Mediated Spatial Reconstitution. **2017**, 1–16, doi:10.1371/journal.pone.0170163.
110. Rocha, J.F.; Pina, A.F.; Sousa, S.F.; Cerqueira, N.M.F.S.A. PLP-Dependent Enzymes as Important Biocatalysts for the Pharmaceutical, Chemical and Food Industries: A Structural and Mechanistic Perspective. *Catal. Sci. Technol.* **2019**, *9*, 4864–4876, doi:10.1039/C9CY01210A.
111. Fernandes, H.S.; Ramos, M.J.; Cerqueira, N.M.F.S.A. The Catalytic Mechanism of the Pyridoxal-5'-Phosphate-Dependent Enzyme, Histidine Decarboxylase: A Computational Study. *Chem. - A Eur. J.* **2017**, *23*, 9162–9173, doi:10.1002/chem.201701375.
112. Toney, M.D. Reaction Specificity in Pyridoxal Phosphate Enzymes. **2005**, *433*, 279–287, doi:10.1016/j.abb.2004.09.037.
113. Schneider, G.; Käck, H.; Lindqvist, Y. The Manifold of Vitamin B6 Dependent Enzymes. *Structure* **2000**, *8*, 1–6, doi:10.1016/S0969-2126(00)00085-X.
114. Jordan, F.; Patel, H. Catalysis in Enzymatic Decarboxylations: Comparison of Selected Cofactor-Dependent and Cofactor-Independent Examples. *ACS Catal.* **2013**, *3*, 1601–1617, doi:10.1021/cs400272x.
115. Packiam, K.A.R.; Ramanan, R.N.; Ooi, C.W.; Krishnaswamy, L.; Tey, B.T. Stepwise Optimization of Recombinant Protein Production in *Escherichia Coli* Utilizing Computational and Experimental Approaches. *Appl. Microbiol. Biotechnol.* **2020**, *104*, 3253–3266, doi:10.1007/s00253-020-10454-w.
116. Sørensen, H.P.; Mortensen, K.K. Soluble Expression of Recombinant Proteins in the Cytoplasm of *Escherichia Coli*. *Microb. Cell Fact.* **2005**, *4*, 1–8, doi:10.1186/1475-2859-4-1.
117. García-Fruitós, Elena; Aris Giralt, A. *Insoluble Proteins*; Springer Science+Business Media, LLC, part of Springer Nature 2022: Caldes de Montbui, Spain, 1959; Vol. 75; ISBN 9781071618585.
118. Kaur, J.; Kumar, A.; Kaur, J. Strategies for Optimization of Heterologous Protein Expression in *E. Coli*: Roadblocks and Reinforcements. *Int. J. Biol. Macromol.* **2018**, *106*, 803–822, doi:10.1016/j.ijbiomac.2017.08.080.
119. Novagen Competent Cells Manual.
120. Takara Bio Inc *Chaperone Plasmid Set, Product Manual*;
121. Chen, G.F.T.; Inouye, M. Role of the AGA/AGG Codons, the Rarest Codons in Global Gene Expression in *Escherichia Coli*. *Genes Dev.* **1994**, *8*, 2641–2652, doi:10.1101/gad.8.21.2641.
122. Kane, J.F. Effects of Rare Codon Clusters on High-Level Expression of Heterologous Proteins in *Escherichia Coli*. *Curr. Opin. Biotechnol.* **1995**, *6*, 494–500, doi:10.1016/0958-1669(95)80082-4.

## References

123. Hussain, H.A.; Ward, J.M. Enhanced Heterologous Expression of Two *Streptomyces Griseolus* Cytochrome P450s and *Streptomyces Coelicolor* Ferredoxin Reductase as Potentially Efficient Hydroxylation Catalysts. *Appl. Environ. Microbiol.* **2003**, *69*, 373–382, doi:10.1128/AEM.69.1.373-382.2003.
124. Bornscheuer, U.T.; Hauer, B.; Jaeger, K.E.; Schwaneberg, U. Directed Evolution Empowered Redesign of Natural Proteins for the Sustainable Production of Chemicals and Pharmaceuticals. *Angew. Chemie - Int. Ed.* **2019**, *58*, 36–40, doi:10.1002/anie.201812717.
125. Wachtmeister, J.; Rother, D. Recent Advances in Whole Cell Biocatalysis Techniques Bridging from Investigative to Industrial Scale. *Curr. Opin. Biotechnol.* **2016**, *42*, 169–177, doi:10.1016/j.copbio.2016.05.005.
126. Barbosa, O.; Ortiz, C.; Berenguer-Murcia, Á.; Torres, R.; Rodrigues, R.C.; Fernandez-Lafuente, R. Strategies for the One-Step Immobilization-Purification of Enzymes as Industrial Biocatalysts. *Biotechnol. Adv.* **2015**, *33*, 435–456, doi:10.1016/j.biotechadv.2015.03.006.
127. Fessner, W.D. Systems Biocatalysis: Development and Engineering of Cell-Free “Artificial Metabolisms” for Preparative Multi-Enzymatic Synthesis. *N. Biotechnol.* **2015**, *32*, 658–664, doi:10.1016/j.nbt.2014.11.007.
128. Lima-Ramos, J.; Neto, W.; Woodley, J.M. Engineering of Biocatalysts and Biocatalytic Processes. *Top. Catal.* **2014**, *57*, 301–320, doi:10.1007/s11244-013-0185-0.
129. Choi, J.M.; Han, S.S.; Kim, H.S. Industrial Applications of Enzyme Biocatalysis: Current Status and Future Aspects. *Biotechnol. Adv.* **2015**, *33*, 1443–1454, doi:10.1016/j.biotechadv.2015.02.014.
130. Döbber, J.; Pohl, M. HaloTag™: Evaluation of a Covalent One-Step Immobilization for Biocatalysis. *J. Biotechnol.* **2017**, *241*, 170–174, doi:10.1016/j.jbiotec.2016.12.004.
131. Sheldon, R.A.; Woodley, J.M. Role of Biocatalysis in Sustainable Chemistry. *Chem. Rev.* **2018**, *118*, 801–838, doi:10.1021/acs.chemrev.7b00203.
132. Sheldon, R.A. Characteristic Features and Biotechnological Applications of Cross-Linked Enzyme Aggregates (CLEAs). *Appl. Microbiol. Biotechnol.* **2011**, *92*, 467–477, doi:10.1007/s00253-011-3554-2.
133. Krauss, U.; Jäger, V.D.; Diener, M.; Pohl, M.; Jaeger, K.-E. Catalytically-Active Inclusion Bodies—Carrier-Free Protein Immobilizates for Application in Biotechnology and Biomedicine. *J. Biotechnol.* **2017**, *258*, 136–147, doi:10.1016/j.jbiotec.2017.04.033.
134. Carrió, M.; González-Montalbán, N.; Vera, A.; Villaverde, A.; Ventura, S. Amyloid-like Properties of Bacterial Inclusion Bodies. *J. Mol. Biol.* **2005**, *347*, 1025–1037, doi:10.1016/j.jmb.2005.02.030.
135. Diener, M.; Kopka, B.; Pohl, M.; Jaeger, K.-E.; Krauss, U. Fusion of a Coiled-Coil Domain Facilitates the High-Level Production of Catalytically Active Enzyme Inclusion Bodies. *ChemCatChem* **2016**, *8*, 142–152, doi:10.1002/cctc.201501001.
136. Küsters, K.; Pohl, M.; Krauss, U.; Ölçücü, G.; Albert, S.; Jaeger, K.E.; Wiechert, W.; Oldiges, M. Construction and Comprehensive Characterization of an *EcLDCc-CatIB* Set—varying Linkers and Aggregation Inducing Tags. *Microb. Cell Fact.* **2021**, *20*, 1–12, doi:10.1186/s12934-021-01539-w.
137. Jäger, V.D.; Kloss, R.; Grünberger, A.; Seide, S.; Hahn, D.; Karmainski, T.; Piqueray, M.; Embruch, J.; Longerich, S.; Mackfeld, U. et al. Tailoring the Properties of (Catalytically)-Active Inclusion Bodies. *Microb. Cell Fact.* **2019**, *18*, 1–20, doi:10.1186/s12934-019-1081-5.
138. Kloss, R.; Limberg, M.H.; Mackfeld, U.; Hahn, D.; Grünberger, A.; Jäger, V.D.; Krauss, U.; Oldiges, M.; Pohl, M. Catalytically Active Inclusion Bodies of L-Lysine Decarboxylase from *E. Coli* for 1,5-Diaminopentane Production. *Sci. Rep.* **2018**, *8*, 1–11, doi:10.1038/s41598-018-24070-2.
139. Jäger, V.D.; Piqueray, M.; Seide, S.; Pohl, M.; Wiechert, W.; Jaeger, K.E.; Krauss, U. An Enzymatic 2-Step Cofactor and Co-Product Recycling Cascade towards a Chiral 1,2-Diol. Part II: Catalytically Active Inclusion Bodies. *Adv. Synth. Catal.* **2019**, *361*, 2616–2626, doi:10.1002/adsc.201900189.
140. Cassimjee, K.E.; Federsel, H.-J. CHAPTER 13. EziG: A Universal Platform for Enzyme Immobilisation. In *RSC Catalysis Series*; The Royal Society of Chemistry, 2018; Vol. 2018, pp. 345–362 ISBN 9781782620907.
141. Brady, D.; Jordaan, J. Advances in Enzyme Immobilisation. *Biotechnol. Lett.* **2009**, *31*, 1639–1650, doi:10.1007/s10529-009-0076-4.
142. Schmidt, T.G.M.; Koepke, J.; Frank, R.; Skerra, A. Molecular Interaction between the Strep-Tag Affinity Peptide and Its Cognate Target, Streptavidin. *J. Mol. Biol.* **1996**, *255*, 753–766, doi:10.1006/jmbi.1996.0061.
143. Korndorfer, I. P.; Skerra, A. Improved Affinity of Engineered Streptavidin for the Strep-Tag II Peptide Is Due to a Fixed Open Conformation of the Lid-like Loop at the Binding Site. *Protein Sci.* **2002**, *11*, 883–893, doi:10.1110/ps.4150102.
144. Encell, L.P. Development of a Dehalogenase-Based Protein Fusion Tag Capable of Rapid, Selective and Covalent Attachment to Customizable Ligands. *Curr. Chem. Genomics* **2013**, *6*, 55–71, doi:10.2174/1875397301206010055.

## References

145. Keppler, A.; Gendreizig, S.; Gronemeyer, T.; Pick, H.; Vogel, H.; Johnsson, K. A General Method for the Covalent Labeling of Fusion Proteins with Small Molecules in Vivo. *Nat. Biotechnol.* **2003**, *21*, 86–89, doi:10.1038/nbt765.
146. Gautier, A.; Juillerat, A.; Heinis, C.; Corrêa, I.R.; Kindermann, M.; Beaufils, F.; Johnsson, K. An Engineered Protein Tag for Multiprotein Labeling in Living Cells. *Chem. Biol.* **2008**, *15*, 128–136, doi:10.1016/j.chembiol.2008.01.007.
147. Tian, J.; Jia, R.; Wenge, D.; Sun, H.; Wang, Y.; Chang, Y.; Luo, H. One-Step Purification and Immobilization of Recombinant Proteins Using SpyTag/SpyCatcher Chemistry. *Biotechnol. Lett.* **2021**, *43*, 1075–1087, doi:10.1007/s10529-021-03098-x.
148. Freitas, A.I.; Domingues, L.; Aguiar, T.Q. Tag-Mediated Single-Step Purification and Immobilization of Recombinant Proteins toward Protein-Engineered Advanced Materials. *J. Adv. Res.* **2022**, *36*, 249–264, doi:10.1016/j.jare.2021.06.010.
149. Döbber, J.; Pohl, M.; Ley, S. V.; Musio, B. Rapid, Selective and Stable HaloTag-LbADH Immobilization Directly from Crude Cell Extract for the Continuous Biocatalytic Production of Chiral Alcohols and Epoxides. *React. Chem. Eng.* **2018**, *3*, 8–12, doi:10.1039/C7RE00173H.
150. Döbber, J.; Gerlach, T.; Offermann, H.; Rother, D.; Pohl, M. Closing the Gap for Efficient Immobilization of Biocatalysts in Continuous Processes: HaloTag™ Fusion Enzymes for a Continuous Enzymatic Cascade towards a Vicinal Chiral Diol. *Green Chem.* **2018**, *20*, 544–552, doi:10.1039/C7GC03225K.
151. Sun, C.; Li, Y.; Taylor, S.E.; Mao, X.; Wilkinson, M.C.; Fernig, D.G. HaloTag Is an Effective Expression and Solubilisation Fusion Partner for a Range of Fibroblast Growth Factors. *PeerJ* **2015**, *2015*, 1–24, doi:10.7717/peerj.1060.
152. Hanefeld U, Gardossi L, M.E. Understanding Enzyme Immobilisation. *Chem Soc Rev. II* **2009**, *38*, 453–68.
153. Basso, A.; Serban, S. Industrial Applications of Immobilized Enzymes—A Review. *Mol. Catal.* **2019**, *479*, 110607, doi:10.1016/j.mcat.2019.110607.
154. Rios, G.M.; Belleville, M.P.; Paolucci, D.; Sanchez, J. Progress in Enzymatic Membrane Reactors - A Review. *J. Memb. Sci.* **2004**, *242*, 189–196, doi:10.1016/j.memsci.2003.06.004.
155. Liese, A.; Hilterhaus, L. Evaluation of Immobilized Enzymes for Industrial Applications. *Chem. Soc. Rev.* **2013**, *42*, 6236–6249, doi:10.1039/c3cs35511j.
156. Plutschack, M.B.; Pieber, B.; Gilmore, K.; Seeberger, P.H. The Hitchhiker’s Guide to Flow Chemistry. *Chem. Rev.* **2017**, *117*, 11796–11893, doi:10.1021/acs.chemrev.7b00183.
157. Britton, J.; Majumdar, S.; Weiss, G.A. Continuous Flow Biocatalysis. *Chem. Soc. Rev.* **2018**, doi:10.1039/C7CS00906B.
158. Hülsewede, D.; Meyer, L.E.; von Langermann, J. Application of In Situ Product Crystallization and Related Techniques in Biocatalytic Processes. *Chem. - A Eur. J.* **2019**, *25*, 4871–4884, doi:10.1002/chem.201804970.
159. Wender, P.A.; Verma, V.A.; Paxton, T.J.; Pillow, T.H. Function-Oriented Synthesis, Step Economy, and Drug Design. **2008**, *41*.
160. Wender, P.A.; Miller, B.L. Synthesis at the Molecular Frontier. *Nature* **2009**, *460*, 197–201, doi:10.1038/460197a.
161. Newhouse, T.; Baran, P.S.; Hoffmann, R.W. The Economies of Synthesis. *Chem. Soc. Rev.* **2009**, *38*, 3010, doi:10.1039/b821200g.
162. Tufvesson, P.; Lima-Ramos, J.; Haque, N. Al; Gernaey, K. V.; Woodley, J.M. Advances in the Process Development of Biocatalytic Processes. *Org. Process Res. Dev.* **2013**, *17*, 1233–1238, doi:10.1021/op4001675.
163. Pollard, D.J.; Woodley, J.M. Biocatalysis for Pharmaceutical Intermediates: The Future Is Now. *Trends Biotechnol.* **2007**, *25*, 66–73, doi:10.1016/j.tibtech.2006.12.005.
164. Sheldon, R.A. Engineering a More Sustainable World through Catalysis and Green Chemistry. *J. R. Soc. Interface* **2016**, *13*, 1–7, doi:10.1098/rsif.2016.0087.
165. Guo, H.F.; Cho, E.J.; Devkota, A.K.; Chen, Y.; Russell, W.; Phillips, G.N.; Yamauchi, M.; Dalby, K.N.; Kurie, J.M.; Jeong, E. et al. A Scalable Lysyl Hydroxylase 2 Expression System and Luciferase-Based Enzymatic Activity Assay. *Arch. Biochem. Biophys.* **2017**, *618*, 45–51, doi:10.1016/j.abb.2017.02.003.
166. Hara, R.; Nishikawa, T.; Okuhara, T.; Koketsu, K.; Kino, K. Ectoine Hydroxylase Displays Selective Trans-3-Hydroxylation Activity towards l-Proline. *Appl. Microbiol. Biotechnol.* **2019**, *103*, 5689–5698, doi:10.1007/s00253-019-09868-y.
167. Hara, R.; Kitatsuji, S.; Yamagata, K.; Kino, K. Development of a Multi-Enzymatic Cascade Reaction for the Synthesis of Trans-3-Hydroxy-l-Proline from l-Arginine. *Appl. Microbiol. Biotechnol.* **2016**, *100*, 243–253, doi:10.1007/s00253-015-6992-4.
168. Nishihara, K.; Kanemori, M.; Kitagawa, M.; Yanagi, H.; Yura, T. Chaperone Coexpression Plasmids: Differential and Synergistic Roles of DnaK-DnaJ-GrpE and GroEL-GroES in Assisting Folding of an

## References

- Allergen of Japanese Cedar Pollen, Cryj2, in *Escherichia Coli*. *Appl. Environ. Microbiol.* **1998**, *64*, 1694–1699, doi:10.1128/aem.64.5.1694-1699.1998.
169. Torkler, M.-H. Charakterisierung Der  $\alpha$ -Ketoglutarat Abhängigen Dioxygenasen Aus *Catenulispora Acidiphila*, *Chitinophaga Pinensis* Und Der L-Lysin-Decarboxylase Aus *Selenomonas Ruminantium*, Bachelor Thesis, University of Applied Sciences Aachen, Campus Jülich, 2020.
170. Rohman, M.; Harrison-Lavoie, K.J. Separation of Copurifying GroEL from Glutathione-S-Transferase Fusion Proteins. *Protein Expr. Purif.* **2000**, *20*, 45–47, doi:10.1006/prep.2000.1271.
171. Barbusiński, K. Controversy Over Fenton Mechanism. *Ecol. Chem. Eng. S.* **2009**, *16*, 347–358.
172. Goldstein, S.; Meyerstein, D.; Czapski, G. The Fenton Reagents. *Free Radic. Biol. Med.* **1993**, *15*, 435–445, doi:10.1016/0891-5849(93)90043-T.
173. Stadtman, E.R.; Levine, R.L. Free Radical-Mediated Oxidation of Free Amino Acids and Amino Acid Residues in Proteins. *Amino Acids* **2003**, *25*, 207–218, doi:10.1007/s00726-003-0011-2.
174. Hassett, D.J.; Ochsner, U.A.; Groce, S.L.; Parvatiyar, K.; Ma, J.F.; Lipscomb, J.D. Hydrogen Peroxide Sensitivity of Catechol-2,3-Dioxygenase: A Cautionary Note on Use of Xyle Reporter Fusions under Aerobic Conditions. *Appl. Environ. Microbiol.* **2000**, *66*, 4119–4123, doi:10.1128/AEM.66.9.4119-4123.2000.
175. Liu, S.; He, L.; Yao, K. The Antioxidative Function of Alpha-Ketoglutarate and Its Applications. *Biomed Res. Int.* **2018**, *2018*, doi:10.1155/2018/3408467.
176. Welch, K.D.; Davis, T.Z.; Aust, S.D. Iron Autoxidation and Free Radical Generation: Effects of Buffers, Ligands, and Chelators. *Arch. Biochem. Biophys.* **2002**, *397*, 360–369, doi:10.1006/abbi.2001.2694.
177. Tadolini, B. Iron Autoxidation in MOPS and HEPES Buffers. *Free Radic. Res. Commun.* **1987**, *4*, 149–160, doi:10.3109/10715768709088100.
178. Ferreira, C.M.H.; Pinto, I.S.S.; Soares, E. V.; Soares, H.M.V.M. (Un)Suitability of the Use of pH Buffers in Biological, Biochemical and Environmental Studies and Their Interaction with Metal Ions – A Review. *RSC Adv.* **2015**, *5*, 30989–31003, doi:10.1039/C4RA15453C.
179. Grady, J.K.; Chasteen, N.D.; Harris, D.C. Radicals from “Good’s” Buffers. *Anal. Biochem.* **1988**, *173*, 111–115, doi:10.1016/0003-2697(88)90167-4.
180. Kivirikko, K.I.; Prockop, D.J. Partial Purification and Characterization of Protocollagen Lysine Hydroxylase from Chick Embryos. *BBA - Enzymol.* **1972**, *258*, 366–379, doi:10.1016/0005-2744(72)90228-8.
181. Finn, T.E.; Nunez, A.C.; Sunde, M.; Easterbrook-Smith, S.B. Serum Albumin Prevents Protein Aggregation and Amyloid Formation and Retains Chaperone-like Activity in the Presence of Physiological Ligands. *J. Biol. Chem.* **2012**, *287*, 21530–21540, doi:10.1074/jbc.M112.372961.
182. Nava-Ramírez, T.; Hansberg, W. Chaperone Activity of Large-Size Subunit Catalases. *Free Radic. Biol. Med.* **2020**, *156*, 99–106, doi:10.1016/j.freeradbiomed.2020.05.020.
183. Wang, Wei; Nema, Sandeep; Teagarden, D. Protein Aggregation-Pathways and Influencing Factors. *Int. J. Pharm.* **2010**, doi:10.1016/j.iipharm.2010.02.025.
184. Wang, C.; Ristiluoma, M.M.; Salo, A.M.; Eskelinen, S.; Myllylä, R. Lysyl Hydroxylase 3 Is Secreted from Cells by Two Pathways. *J. Cell. Physiol.* **2012**, *227*, 668–675, doi:10.1002/jcp.22774.
185. Luo, L.; Pappalardi, M.B.; Tummino, P.J.; Copeland, R.A.; Fraser, M.E.; Grzyska, P.K.; Hausinger, R.P. An Assay for Fe(II)/2-Oxoglutarate-Dependent Dioxygenases by Enzyme-Coupled Detection of Succinate Formation. *Anal. Biochem.* **2006**, *353*, 69–74, doi:10.1016/j.ab.2006.03.033.
186. McNeill, L.A.; Bethge, L.; Hewitson, K.S.; Schofield, C.J. A Fluorescence-Based Assay for 2-Oxoglutarate-Dependent Oxygenases. *Anal. Biochem.* **2005**, *336*, 125–131, doi:10.1016/j.ab.2004.09.019.
187. Chen, R.F.; Scott, C.; Trepman, E. Fluorescence Properties of O-Phthaldialdehyde Derivatives of Amino Acids. *BBA - Protein Struct.* **1979**, *576*, 440–455, doi:10.1016/0005-2795(79)90419-7.
188. Promega HaloLink™ Resin Manual. **2016**, 17.
189. EnginZyme EziG™ Product Data Sheet. **2014**, 9137.
190. Singh, R.K.; Tiwari, M.K.; Singh, R.; Lee, J.K. From Protein Engineering to Immobilization: Promising Strategies for the Upgrade of Industrial Enzymes. *Int. J. Mol. Sci.* **2013**, *14*, 1232–1277, doi:10.3390/ijms14011232.
191. Rodrigues, R.C.; Ortiz, C.; Berenguer-Murcia, Á.; Torres, R.; Fernández-Lafuente, R. Modifying Enzyme Activity and Selectivity by Immobilization. *Chem. Soc. Rev.* **2013**, *42*, 6290–6307, doi:10.1039/c2cs35231a.
192. Bommarius, A.S.; Karau, A. Deactivation of Formate Dehydrogenase (FDH) in Solution and at Gas-Liquid Interfaces. *Biotechnol. Prog.* **2005**, *21*, 1663–1672, doi:10.1021/bp050249q.
193. Mateo, C.; Palomo, J.M.; Fernandez-Lorente, G.; Guisan, J.M.; Fernandez-Lafuente, R. Improvement of Enzyme Activity, Stability and Selectivity via Immobilization Techniques. *Enzyme Microb. Technol.* **2007**, *40*, 1451–1463, doi:10.1016/j.enzmictec.2007.01.018.
194. Wahab, R.A.; Elias, N.; Abdullah, F.; Ghoshal, S.K. On the Taught New Tricks of Enzymes

## References

- Immobilization: An All-Inclusive Overview. *React. Funct. Polym.* **2020**, *152*, 104613, doi:10.1016/j.reactfunctpolym.2020.104613.
195. Gasteiger E., Hoogland C., Gattiker A., Duvaud S., Wilkins M.R., Appel R.D., B.A. Protein Identification and Analysis Tools on the ExPASy Server. In *The proteomics protocols handbook*, John M. Walker, Ed.; Humana Press, 2005; pp. 571–607.
  196. Hagemans, D.; van Belzen, I.A.E.M.; Morán Luengo, T.; Rüdiger, S.G.D. A Script to Highlight Hydrophobicity and Charge on Protein Surfaces. *Front. Mol. Biosci.* **2015**, *2*, 1–11, doi:10.3389/fmolb.2015.00056.
  197. Henshaw, T.F.; Feig, M.; Hausinger, R.P. Aberrant Activity of the DNA Repair Enzyme AlkB. *J. Inorg. Biochem.* **2004**, *98*, 856–861, doi:10.1016/j.jinorgbio.2003.10.021.
  198. Koehntop, K.D.; Marimanikkuppam, S.; Ryle, M.J.; Hausinger, R.P.; Que, L. Self-Hydroxylation of Taurine/ $\alpha$ -Ketoglutarate Dioxygenase: Evidence for More than One Oxygen Activation Mechanism. *J. Biol. Inorg. Chem.* **2006**, *11*, 63–72, doi:10.1007/s00775-005-0059-4.
  199. Ge, Y.; Lawhorn, B.G.; ElNaggar, M.; Sze, S.K.; Begley, T.P.; McLafferty, F.W. Detection of Four Oxidation Sites in Viral Prolyl-4-Hydroxylase by Top-down Mass Spectrometry. *Protein Sci.* **2009**, *12*, 2320–2326, doi:10.1110/ps.03244403.
  200. Takatsuka, Y.; Tomita, T.; Kamio, Y. Identification of the Amino Acid Residues Conferring Substrate Specificity upon *Selenomonas Ruminantium* Lysine Decarboxylase. **2014**, *8451*, doi:10.1271/bbb.63.1843.
  201. Jeong, S.; Yeon, Y.J.; Choi, E.G.; Byun, S.; Cho, D.H.; Kim, I.K.; Kim, Y.H. Alkaliphilic Lysine Decarboxylases for Effective Synthesis of Cadaverine from L-Lysine. *Korean J. Chem. Eng.* **2016**, *33*, 1530–1533, doi:10.1007/s11814-016-0079-5.
  202. Wetzels, S. Untersuchung Zur Produktion Und Immobilisierung von PLP-Abhängigen Decarboxylasen, Bachelor Thesis, University of Applied Sciences Aachen, 2021.
  203. Bregu, M. Optimierung Der SrLDC-Katalysierten Cadaverinsynthese, Master Thesis, RWTH Aachen University, 2021.
  204. Seo, H.M.; Kim, J.H.; Jeon, J.M.; Song, H.S.; Bhatia, S.K.; Sathiyarayanan, G.; Park, K.; Kim, K.J.; Lee, S.H.; Kim, H.J. et al. In Situ Immobilization of Lysine Decarboxylase on a Biopolymer by Fusion with Phasin: Immobilization of CadA on Intracellular PHA. *Process Biochem.* **2016**, *51*, 1413–1419, doi:10.1016/j.procbio.2016.07.019.
  205. Zhou, N.; Zhang, A.; Wei, G.; Yang, S.; Xu, S.; Chen, K.; Ouyang, P. Cadaverine Production From L-Lysine With Chitin-Binding Protein-Mediated Lysine Decarboxylase Immobilization. *Front. Bioeng. Biotechnol.* **2020**, *8*, 1–11, doi:10.3389/fbioe.2020.00103.
  206. Park, S.H.; Soetyono, F.; Kim, H.K. Cadaverine Production by Using Cross-Linked Enzyme Aggregate of *Escherichia Coli* Lysine Decarboxylase. *J. Microbiol. Biotechnol.* **2017**, *27*, 289–296, doi:10.4014/jmb.1608.08033.
  207. Ma, W.; Cao, W.; Zhang, H.; Chen, K.; Li, Y.; Ouyang, P. Enhanced Cadaverine Production from L-Lysine Using Recombinant *Escherichia Coli* Co-Overexpressing CadA and CadB. *Biotechnol. Lett.* **2015**, *37*, 799–806, doi:10.1007/s10529-014-1753-5.
  208. Bhatia, S.K.; Kim, Y.H.; Kim, H.J.; Seo, H.M.; Kim, J.H.; Song, H.S.; Sathiyarayanan, G.; Park, S.H.; Park, K.; Yang, Y.H. Biotransformation of Lysine into Cadaverine Using Barium Alginate-Immobilized *Escherichia Coli* Overexpressing CadA. *Bioprocess Biosyst. Eng.* **2015**, *38*, 2315–2322, doi:10.1007/s00449-015-1465-9.
  209. Kloß, R. Catalytically Active Inclusion Bodies: A Novel Enzyme Immobilization Method for Biocatalysis. **2018**.
  210. Kim, J.H.; Seo, H.M.; Sathiyarayanan, G.; Bhatia, S.K.; Song, H.S.; Kim, J.; Jeon, J.M.; Yoon, J.J.; Kim, Y.G.; Park, K. et al. Development of a Continuous L-Lysine Bioconversion System for Cadaverine Production. *J. Ind. Eng. Chem.* **2017**, *46*, 44–48, doi:10.1016/j.jiec.2016.09.038.
  211. Oh, Y.H.; Kang, K.H.; Kwon, M.J.; Choi, J.W.; Joo, J.C.; Lee, S.H.; Yang, Y.H.; Song, B.K.; Kim, I.K.; Yoon, K.H. et al. Development of Engineered *Escherichia Coli* Whole-Cell Biocatalysts for High-Level Conversion of L-Lysine into Cadaverine. *J. Ind. Microbiol. Biotechnol.* **2015**, *42*, 1481–1491, doi:10.1007/s10295-015-1678-6.
  212. Li, B.; Liang, J.; Hanfrey, C.C.; Phillips, M.A.; Michael, A.J. Discovery of Ancestral L-Ornithine and L-Lysine Decarboxylases Reveals Parallel, Pseudoconvergent Evolution of Polyamine Biosynthesis. *J. Biol. Chem.* **2021**, *279*, 101219, doi:10.1016/j.jbc.2021.101219.
  213. Lemonnier, M.; Lane, D. Expression of the Second Lysine Decarboxylate Gene of *Escherichia Coli*. *Microbiology* **1998**, *144*, 751–760, doi:10.1099/00221287-144-3-751.
  214. Krithika, G.; Arunachalam, J.; Priyanka, H.; Indulekha, K. The Two Forms of Lysine Decarboxylase; Kinetics and Effect of Expression in Relation to Acid Tolerance Response in *E. Coli*. *J. Exp. Sci.* **2010**, *1*, 10–21.

## References

215. Sabo, D.L.; Boeker, E.A.; Byers, B.; Waron, H.; Fischer, E.H.; Byers, J.B.; Waron, H.; Fischer, E.H. Purification and Physical Properties of Inducible *Escherichia Coli* Lysine Decarboxylase. *Biochemistry* **1974**, *13*, 662–670, doi:10.1021/bi00701a005.
216. Kind, S.; Jeong, W.K.; Schröder, H.; Zelder, O.; Wittmann, C. Identification and Elimination of the Competing N-Acetyldiaminopentane Pathway for Improved Production of Diaminopentane by *Corynebacterium Glutamicum*. *Appl. Environ. Microbiol.* **2010**, *76*, 5175–5180, doi:10.1128/AEM.00834-10.
217. Kanjee, U.; Gutsche, I.; Alexopoulos, E.; Zhao, B.; El Bakkouri, M.; Thibault, G.; Liu, K.; Ramachandran, S.; Snider, J.; Pai, E.F. et al. Linkage between the Bacterial Acid Stress and Stringent Responses: The Structure of the Inducible Lysine Decarboxylase. *EMBO J.* **2011**, *30*, 931–944, doi:10.1038/emboj.2011.5.
218. Kandiah, E.; Carriel, D.; Perard, J.; Malet, H.; Bacia, M.; Liu, K.; Chan, S.W.S.; Houry, W.A.; De Choudens, S.O.; Elsen, S. et al. Structural Insights into the *Escherichia Coli* Lysine Decarboxylases and Molecular Determinants of Interaction with the AAA+ ATPase RavA. *Sci. Rep.* **2016**, *6*, 1–12, doi:10.1038/srep24601.
219. Alexopoulos, E.; Kanjee, U.; Snider, J.; Houry, W.A.; Pai, E.F. Crystallization and Preliminary X-Ray Analysis of the Inducible Lysine Decarboxylase from *Escherichia Coli*. *Acta Crystallogr. Sect. F Struct. Biol. Cryst. Commun.* **2008**, *64*, 700–706, doi:10.1107/S1744309108018757.
220. Snider, J.; Gutsche, I.; Lin, M.; Baby, S.; Cox, B.; Butland, G.; Greenblatt, J.; Emili, A.; Houry, W.A. Formation of a Distinctive Complex between the Inducible Bacterial Lysine Decarboxylase and a Novel AAA+ ATPase. *J. Biol. Chem.* **2006**, *281*, 1532–1546, doi:10.1074/jbc.M511172200.
221. Morrison, A.L.; Long, R.F. The Photolysis of Pyridoxal Phosphate. *J. Chem. Soc.* **1958**, 211, doi:10.1039/jr9580000211.
222. Reiber, H. Photochemical Reactions of Vitamin B6 Compounds, Isolation and Properties of Products. *BBA - Gen. Subj.* **1972**, *279*, 310–315, doi:10.1016/0304-4165(72)90148-1.
223. Gerlach, T.; Nugroho, D.L.; Rother, D. The Effect of Visible Light on the Catalytic Activity of PLP-Dependent Enzymes. *ChemCatChem* **2021**, *13*, 2398–2406, doi:10.1002/cctc.202100163.
224. Rippa, M.; Pontremoli, S. Pyridoxal 5'-Phosphate as a Specific Photosensitizer for Histidine Residue at the Active Site of 6-Phosphogluconate Dehydrogenase. *Arch. Biochem. Biophys.* **1969**, *133*, 112–118, doi:10.1016/0003-9861(69)90494-9.
225. Fossey-Jouenne, A.; Vergne-Vaxelaire, C.; Zaparucha, A. Enzymatic Cascade Reactions for the Synthesis of Chiral Amino Alcohols from L-Lysine. *J. Vis. Exp.* **2018**, *2018*, 1–9, doi:10.3791/56926.
226. Cascaval, D.; Oniscu, C.; Galaction, A.I. Selective Separation of Amino Acids by Reactive Extraction. *Biochem. Eng. J.* **2001**, *7*, 171–176, doi:10.1016/S1369-703X(00)00096-6.
227. Hermann, T. Industrial Production of Amino Acids by Coryneform Bacteria. *J. Biotechnol.* **2003**, *104*, 155–172, doi:10.1016/S0168-1656(03)00149-4.
228. Deischer, J.; Wolter, N.; Palkovits, R. Tailoring Activated Carbons for Efficient Downstream Processing: Selective Liquid-Phase Adsorption of Lysine. *ChemSusChem* **2020**, *13*, 3614–3621, doi:10.1002/cssc.202000885.
229. Anastassiadis, S. L-Lysine Fermentation. *Recent Pat. Biotechnol.* **2008**, *1*, 11–24, doi:10.2174/187220807779813947.
230. Liu, Y.; Zheng, Y.; Wu, H.; Zhang, W.; Ren, T.; You, S.; Qi, W.; Su, R.; He, Z. Development of an Integrated Process for the Production of High-Purity Cadaverine from Lysine Decarboxylase. *J. Chem. Technol. Biotechnol.* **2020**, *95*, 1542–1549, doi:10.1002/jctb.6348.
231. Hong, Y.G.; Kim, H.J.; Jeon, J.M.; Moon, Y.M.; Hong, J.W.; Joo, J.C.; Song, B.K.; Park, K.M.; Lee, S.H.; Yang, Y.H. Selective Recovery of Cadaverine from Lysine Decarboxylase Bioconversion Solution Using Methyl Ethyl Ketone. *J. Ind. Eng. Chem.* **2018**, *64*, 167–172, doi:10.1016/j.jiec.2018.03.013.
232. Krzyzaniak, A.; Schuur, B.; De Haan, A.B. Extractive Recovery of Aqueous Diamines for Bio-Based Plastics Production. *J. Chem. Technol. Biotechnol.* **2013**, *88*, 1937–1945, doi:10.1002/jctb.4058.
233. Kind, S.; Neubauer, S.; Becker, J.; Yamamoto, M.; Völkert, M.; Abendroth, G. von; Zelder, O.; Wittmann, C. From Zero to Hero – Production of Bio-Based Nylon from Renewable Resources Using Engineered *Corynebacterium Glutamicum*. *Metab. Eng.* **2014**, *25*, 113–123, doi:10.1016/j.ymben.2014.05.007.
234. Zhang, S.; Liu, Z. Advances in the Biological Fixation of Carbon Dioxide by Microalgae. *J. Chem. Technol. Biotechnol.* **2021**, *96*, 1475–1495, doi:10.1002/jctb.6714.
235. Zhang, Q.; Nurhayati; Cheng, C.L.; Nagarajan, D.; Chang, J.S.; Hu, J.; Lee, D.J. Carbon Capture and Utilization of Fermentation CO<sub>2</sub>: Integrated Ethanol Fermentation and Succinic Acid Production as an Efficient Platform. *Appl. Energy* **2017**, *206*, 364–371, doi:10.1016/j.apenergy.2017.08.193.
236. Pateraki, C.; Patsalou, M.; Vlysidis, A.; Kopsahelis, N.; Webb, C.; Koutinas, A.A.; Koutinas, M. *Actinobacillus Succinogenes*: Advances on Succinic Acid Production and Prospects for Development of Integrated Biorefineries. *Biochem. Eng. J.* **2016**, *112*, 285–303, doi:10.1016/j.bej.2016.04.005.
237. Sheldon, R.A.; Brady, D. Green Chemistry, Biocatalysis, and the Chemical Industry of the Future.

## References

- ChemSusChem* **2022**, 202102628, doi:10.1002/cssc.202102628.
238. Los, G. V.; Encell, L.P.; McDougall, M.G.; Hartzell, D.D.; Karassina, N.; Zimprich, C.; Wood, M.G.; Learish, R.; Ohana, R.F.; Urh, M. et al. HaloTag: A Novel Protein Labeling Technology for Cell Imaging and Protein Analysis. *ACS Chem. Biol.* **2008**, 3, 373–382, doi:10.1021/cb800025k.
239. Promega HaloTag® Ligand Building Blocks Available online: <https://www.promega.de/products/protein-detection/protein-labeling/halotag-iodoacetamide-ligand-buildingblocks/?catNum=P6711#specifications>.
240. Hitko, Carolyn W. and Kirkland, Thomas and Levin, Sergiy and Meisenheimer, Poncho and Ohana, Rachel Friedman and Uyeda, Harry Tetsuo and Zhu, J. Substrates for Covalent Thethering of Proteins to Functional Groups or Solid Surfaces 2021.

### 6 Danksagung

Eine Doktorarbeit alleine zu schreiben ist praktisch nicht machbar, daher möchte ich mich an dieser Stelle bei all den Menschen bedanken, die mir dabei geholfen haben:

Mein größter Dank geht dabei an Prof. Martina Pohl, für die Möglichkeit meine Doktorarbeit in einem unvergleichbar guten Arbeitsumfeld anfertigen zu dürfen. Dabei möchte ich mich vor allem für die außerordentlich gute Betreuung und anhaltende Unterstützung bei diesem herausfordernden Projekt bedanken. Auch für den Freiraum, der mir bei vielen Entscheidungen im Zuge dieses Projektes gewährt wurde, bin ich unendlich dankbar.

Genauso dankbar bin ich Prof. Jörg Pietruszka für die Bereitschaft, die Zweitbetreuung zu übernehmen und für die Zeit und Arbeit, die die Begutachtung und Prüfung dieser Arbeit kosten wird.

An dieser Stelle möchte ich mich auch grundsätzlich bei den Mitarbeitern des IBG-1 bedanken: Vielen Dank an Prof. Wolfgang Wiechert für das Ermöglichen dieser Dissertation und immerwährende Unterstützung, aber auch an Marianne Hess, alle Mitarbeiter:innen der Verwaltung, der Werkstatt und der IT, die dieses Institut am Laufen halten.

Generell möchte ich mich bei allen Mitgliedern der Biokatalyse Gruppe für die großartige, immer unterstützende und wertschätzende Arbeitsatmosphäre, selbst unter Lockdown Bedingungen, bedanken. Hier ein besonderer Dank nochmal an Prof. Martina Pohl und Prof. Dörte Rother, die durch viele Gedanken und Organisation diese Arbeitsatmosphäre maßgeblich aufrechterhalten. Besonders zu erwähnen sind auch Stephan Malzacher, Julia Tenhaef, Ramona Kloß, Laura Grabowski, Jan-Dirk Spöring, Matthias Rieb, Tim Gerlach, Douglas Weber und Kevin Mack, Lisa Seibt und Maria Allahham. Vielen Dank für die vielen Kaffee- und Mittagspausen, aus denen man stets mit guter Laune gekommen ist. Spezieller Dank geht hier auch an Christiane Claaßen: Danke, dass du dir trotz Zeitmangel und Corona-Infektion Zeit genommen hast, um mir bei der Auswertung der NMR Spektren zu helfen! In diesem Kontext auch ein großes Dankeschön an Jochem Gätgens, für die super enthusiastische Analyse meiner Produkte über GC-ToF. Durch deine Begeisterung hat die Zusammenarbeit wirklich sehr viel Spaß gemacht. Vielen Dank an Astrid Wirtz, die uns bei HPLC Problemen immer hilfreiche Ratschläge geben konnte und uns im Notfall sogar ihre HPLC zur Verfügung gestellt hat.

Mein Dank gilt auch meinen Studenten Max Torkler, Solange Wetzels und Mariela Bregu, die mit viel Engagement an diesem Projekt mitgewirkt haben, obwohl die Arbeit unter Corona Bedingungen nicht immer einfach war.

## Danksagung

Vor allem geht mein Dank an die Technikerinnen Heike Offermann, Doris Hahn, Ursula Mackfeld, Ilona Frindi-Wosch und Lilia Arnold die das Labor am Laufen halten und mit Ihrem schier unendlichen Knowhow eine riesige Hilfe waren. Vielen Dank auch für die vielen unterhaltsamen Gespräche während der Kaffeepause oder im Labor.

Insbesondere möchte ich Lilia Arnold danken: Ohne dich wäre dieses Projekt nicht möglich gewesen! Vielen Dank für deine immense Hilfe, Unterstützung und pragmatische Herangehensweise an Probleme. Danke für die vielen Gespräche im Labor über Gott und die Welt.

Danke auch an meinen Kooperationspartner Philipp Nerke, auch wenn es nicht zu einem gemeinsamen Projekt gekommen ist, bin ich sehr dankbar für die vielen konstruktiven Gespräche und den Austausch über KDOs.

Ein besonderer Dank gilt meiner Familie Jutta Seide, Erhard Seide und Larissa Seide und meinen Freunden, insbesondere Jana Kirschbaum, für das immer offene Ohr und die emotionale Unterstützung. Einen Riesen Dank auch an meinen Freund Joey Stimke. Für deine emotionale Unterstützung, Hilfe, deine Geduld und das Aushalten sämtlicher Launen bin ich unendlich dankbar. Danke, dass ihr mir immer wieder zeigt, dass beruflicher/akademischer Erfolg nur ein Teil des Lebens sind!

## **Eidesstattliche Erklärung**

Ich versichere an Eides Statt, dass die Dissertation von mir selbständig und ohne unzulässige fremde Hilfe unter Beachtung der „Grundsätze zur Sicherung guter wissenschaftlicher Praxis an der Heinrich- Heine-Universität Düsseldorf“ erstellt worden ist.

Bisher habe ich keine erfolglosen Promotionsversuche unternommen und diese Dissertation nicht an einer anderen Fakultät vorgelegt.

---

Ort, Datum

---

Selina Seide